

Mechanism of lung inflammation associated with inflammatory bowel disease

Sean W Mateer

The University of Newcastle, School of Biomedical Science and
Pharmacy

Thesis submitted in the fulfilment of the requirements for the
award of Doctor of Philosophy.

Sean Mateer
4-4-2017

Acknowledgements

As with all endeavours of this nature they cannot be achieved in isolation, therefore I have many people I need to thank for their help during my studies.

I would particularly like to thank my primary supervisor Dr. Simon Keely, who gave me the opportunity to come over to Australia and work in his lab. I am grateful for this opportunity and thankful for the all the support and advice I have received during this time. I would also like to thank my co-supervisors Dr. Jay Horvat and Prof. Philip Hansbro there knowledge during my studies has been invaluable.

Thank you to my colleagues in the gastrointestinal research group for their support in the lab and for being all round good people. I would like to express my thanks to lab members from collaborating research groups, in particular Dr. Steven Maltby, Dr. Hock Tay, Dr Max Plank and Dr. Andrew Jarnicki

A special thanks to family, who are always there regardless of how far way. I would also like to thank all the friends I have made during my studies in Newcastle. I wish I could think of something more insightful and philosophical to say but alas I cannot. I would just like to express my deep appreciated to all the staff and students at The University of Newcastle.

Table of contents

Abstract: 6

List of figures 7

List of tables 12

Abbreviations: 13

Chapter 1:	Inflammatory bowel disease	19
1.1	Background.....	19
1.2	IBD epidemiology and economic impact	20
1.3	Extra-intestinal manifestations of IBD	23
1.4	Respiratory pathologies associated with IBD.....	23
1.4.1	Subclinical respiratory pathologies	24
1.4.2	Active respiratory disease	26
1.5	Pathogenesis of IBD	27
1.5.1	Gastrointestinal pathophysiology	27
1.5.2	The genetics of IBD	28
1.5.3	Autophagy in IBD pathogenesis	30
1.5.4	Immune-microbiota homeostasis in IBD	30
1.5.5	Soluble mediators of inflammation	32
1.5.6	Intestinal barrier function in IBD	35
1.5.7	Immune responses in the gut	36
1.5.8	Immune responses in IBD	38
1.6	Systemic inflammation associated with IBD.....	39
1.7	Pathophysiology of IBD-induced respiratory disease	40
1.7.1	Immunopathology of IBD-induced respiratory disease	42
1.7.2	Potential mechanisms of IBD-induced respiratory disease	42
1.8	Murine models of IBD.....	44
1.8.1	Dextran sulfate sodium (DSS) colitis	44
1.8.2	2, 4, 6-trinitrobenzenesulfonic acid (TNBS) colitis	44
1.8.3	<i>Winnie</i> colitis	45
1.9	Study aim.....	45
Chapter 2:	Methods	47
2.1	Ethics statement.....	47
2.2	DSS murine model of colitis.....	47
2.3	TNBS murine model of colitis.....	48
2.4	<i>Winnie</i> spontaneous colitis	48
2.5	Colon histopathology.....	48

2.6	Pulmonary histopathology and alveolar enlargement.....	51
2.7	Immunohistochemistry for platelet activating factor receptor (PAFR).....	52
2.8	Lung function measurements.....	53
2.9	Airway inflammation, BAL fluid (BAL) collection.....	54
2.10	Differential leucocyte count BAL fluid.....	54
2.11	Cellular analysis of Lungs, blood and bone marrow.....	54
2.12	Bone marrow colony forming units (CFU) assay.....	57
2.13	Gene expression analysis.....	57
2.14	Cytokine analysis.....	59
2.15	Western blot analysis.....	59
2.16	Reagents and buffers.....	60
2.17	Statistics.....	61
Chapter 3: The effect of intestinal inflammation on the pulmonary system in murine models of colitis 62		
3.1	Introduction.....	62
3.1.1	Hypothesis	62
3.1.2	Aims	63
3.2	Methods.....	63
3.2.1	Characterisation of respiratory pathologies in murine models of colitis.	63
3.3	Results.....	64
3.3.1	Intestinal pathology in DSS colitis	64
3.3.2	Physiological effects of colitis on the respiratory system.	70
3.3.3	Immunological effects of colitis on the pulmonary system	76
3.3.4	Gene expression profile in the lungs of DSS colitis mice	81
3.3.5	Mediators of inflammation in DSS colitis-induced pulmonary inflammation	85
3.3.7	Myeloid cell production in DSS colitis	93
3.3.8	Colitis-induced pulmonary pathology in the TNBS model of colitis.	96
3.3.9	Colitis-induced pulmonary pathology in the <i>Winnie</i> model of colitis.	100
3.4	Discussion:.....	103
3.5	Conclusion.....	106
Chapter 4: The role of systemic IL-6 in the modulation of colitis-induced pulmonary inflammation. 107		
4.1	Introduction.....	107
4.1.1	Hypothesis	109
4.1.2	Aims	109
4.2	Methods.....	110
4.2.1	Anti-IL-6 intervention in acute DSS colitis	110
4.3	Results.....	112
4.3.1	Serum IL-6 levels in anti-IL-6 treated acute DSS colitis.	112
4.3.2	Intestinal pathology in anti-IL-6 treated acute DSS colitis.	114
4.3.3:	The influence of IL-6 on colitis-induced pulmonary pathology.	121
4.3.4:	The influence of IL-6 on colitis-induced pulmonary inflammation	125

4.3.5:	Gene expression profile in the lung of anti-IL-6 treated acute DSS colitis.	128
4.3.6	Cytokine and PAFR protein levels in the lung of anti-IL-6 treated acute DSS colitis.	132
4.3.7	Systemic inflammation in anti-IL-6 treated acute DSS colitis.	137
4.3.8	The effect of IL-6 on myeloid cell production in the bone marrow	140
4.4	Discussion.....	142
4.5	Conclusion.....	147
Chapter 5:	Platelet activating factor receptor (PAFR) signalling in the colitis-induced pulmonary inflammation.	148
5.1:	Introduction.....	148
5.1.1	Hypothesis	149
5.1.2	Aims	149
5.2	Methods	150
5.2.1	PAFR antagonist intervention in acute DSS colitis	150
5.3	Results	152
5.3.1	Intestinal pathology in CV-6209 treated acute DSS colitis.	152
5.3.2:	The influence of PAFR antagonism on colitis-induced pulmonary pathology.	160
5.3.3:	The role of PAFR signalling in colitis-induced pulmonary inflammation.	164
5.3.4:	Gene expression profile in the lung of CV-6209 treated acute DSS colitis.	168
5.3.5:	IL-1 β and CCL2 levels in the lung of CV-6209 treated acute DSS colitis.	170
5.3.6:	Systemic inflammation in CV-6209 treated acute DSS colitis.	172
5.4	Discussion.....	176
5.5	Conclusions	182
Chapter 6:	The role of PAFR signalling in the modulation of myeloid cells in colitis-induced pulmonary inflammation.	183
6.1	Introduction.....	183
6.1.1	Hypothesis:	184
6.1.2	Aims	184
6.2	Methods	185
6.2.1	Cell culture	185
6.2.2	DSS serum induced macrophage activation via PAFR signalling	185
6.2.3	CCL2 and LPS macrophage activation via PAFR signalling	186
6.2.4	PAF analysis	186
6.2.5	Bone Marrow neutrophil isolation	186
6.2.6	Assessment of Neutrophil activation via PAFR signalling from products of CCL2 and LPS activated macrophages.	187
6.2.7	Fluorescent <i>in situ</i> hybridisation analysis by flow cytometry (FISH-Flow)	188
6.2.8	Endotoxin assay	189
6.3	Results	190
6.3.1	PAFR expression in the lung of acute DSS colitis mice.	190

Error! Bookmark not defined.

6.3.2	Immunomodulatory factors in the serum of acute DSS colitis mice initiate inflammatory gene expression in macrophages via PAFR signalling. Error! Bookmark not defined.	
6.3.3	Bacterial load is increased in the lungs of acute DSS colitis mice	197
6.3.4	LPS-induced macrophage activation via PAFR signalling.	200
6.3.5	CCL2-induced macrophage activation via PAFR signalling.	204
6.3.6	PAF secretion from CCL2 treated macrophage.	208
6.3.7	The ability of CCL2 activated macrophages to induce the activation of neutrophils via PAFR signalling.	210
6.4	Discussion:.....	214
6.5	Conclusions	218
Chapter 7:	Final discussions	220
7.1	Study findings	220
7.1.1	Respiratory pathologies in murine models of colitis	220
7.1.2	IL-6 mediates systemic inflammation associated with colitis.	222
7.1.3	Cytokine signalling in colitis-induced pulmonary inflammation.	223
7.1.4	The role of PAFR signalling in the initiation of colitis-induced pulmonary inflammation.	225
7.2	Future directions:	227
7.3	Study limitations	227
7.4	Concluding remarks	229
8.0	Appendices	231
9.0	References	277

Abstract:

Inflammatory bowel disease (IBD) is associated with a number of immune-mediated pathologies in peripheral tissues termed extra-intestinal manifestations (EIM). The organs affected by EIM include the lung, liver, skin and eyes. IBD-induced respiratory pathologies are amongst the most prevalent comorbidities associated with IBD. Approximately 54% of IBD patients have some form of respiratory pathology. The respiratory pathologies associated with IBD range from subclinical respiratory inflammation to active respiratory disease. Bronchiectasis and chronic bronchitis are the most common respiratory diseases associated with IBD. The mechanism by which IBD can induce respiratory pathologies is unknown, this knowledge gap is partially due to a lack of basic science research in this field. Thus, the aim of this study was to utilize murine models of colitis to investigate the immunological mechanisms by which IBD can induce respiratory inflammation. In this study it was found that the DSS, TNBS and *Winnie* models of colitis develop pulmonary inflammation that is associated with leucocyte infiltration surrounding the pulmonary vasculature. Pulmonary inflammation in DSS colitis is characterised by neutrophil and monocyte recruitment to the lung. Systemic IL-6 levels were elevated in the DSS colitis model and IL-6 was identified to be a factor that contributes to neutrophil recruitment. It was found that systemic IL-6 mediates neutrophil development in the bone marrow thereby providing the cells required to perpetuate inflammation in the lung. Platelet activating factor receptor (PAFR), IL-1 β and CCL2 expression were increased in the lungs of DSS colitis mice. PAFR signalling in the lung induces the expression of IL-1 β and the recruitment of neutrophils, PAFR signalling did not induce CCL2 expression. It was found that immunomodulatory factors in the serum of DSS colitis induce IL-1 β production and CCL2 gene expression in alveolar macrophage through PAFR signalling. The results from this study identify a number of potential

pathogenic factors that may be involved in the development of IBD-induced respiratory pathologies.

List of figures

Chapter 1

Figure 1.2: Incidence and prevalence of IBD in the time interval 1980 – 2008

Figure 1.5.1: Factors that contribute the pathogenesis of IBD

Figure 1.5.7: T helper subsets, their differentiation factors and secreted cytokines

Figure 1.7: Pictorial illustration of the vicious cycle mode of bronchiectasis and chronic bronchitis pathogenesis.

Chapter 3

Figure 3.3.1A: Weight loss and colon shortening in acute DSS colitis.

Figure 3.3.1B: Histopathological scores in colon sections from acute DSS colitis.

Figure 3.3.1C: Colonic histopathology in acute DSS.

Figure 3.3.1.1A: Cytokine signalling in the colon of acute DSS colitis.

Figure 3.3.2A: Histopathological scores in lung sections from acute DSS colitis.

Figure 3.3.2B: Lung histopathology in acute DSS colitis.

Figure 3.3.2C: Physiological effects of acute DSS colitis on the pulmonary system.

Figure 3.3.2D: PAS-AB staining in lung sections from acute DSS colitis.

Figure 3.3.3A: Leucocyte phenotype in DSS colitis-induced pulmonary inflammation.

Figure 3.3.3B: Airway inflammation in acute DSS colitis.

Figure 3.3.4A: Gene expression profile in the lungs of DSS colitis.

Figure 3.3.4B: Gene expression profile in the lungs of DSS colitis continued.

Figure 3.3.5A: IL-1 β and CCL2 protein levels in the lungs of DSS acute colitis.

Figure 3.3.5B: PAFR protein level in the lungs of acute DSS colitis.

Figure 3.3.6A: Systemic inflammation in acute DSS colitis.

Figure 3.3.6B: Inflammatory cytokines in the circulatory system of acute DSS colitis.

Figure 3.3.7A: Myeloid progenitor cells in the bone marrow of acute DSS colitis.

Figure 3.3.7B: Mature myeloid cell populations in the bone marrow of acute DSS colitis.

Figure 3.3.8A: Histopathological scores in lung sections from TNBS colitis.

Figure 3.3.8B: Histopathology in lung sections from TNBS colitis.

Figure 3.3.8C: Pulmonary inflammation in TNBS colitis.

Figure 3.3.9A: Histopathological scores in lung sections from *Winnie* colitis.

Figure 3.3.8B: Pulmonary pathology in *Winnie* colitis continued

Chapter 4

Figure 4.2.1: Time course of anti-IL-6 interventions in DSS colitis.

Figure 4.3.1A: Weight loss and colon shortening in anti-IL-6 treated DSS colitis.

Figure 4.3.1B: Histopathological scores from colon sections in anti-IL-6 treated DSS colitis.

Figure 4.3.1C: Histopathology in colon sections from control and naïve DSS colitis

Figure 4.3.1D: Histopathology in colon sections from isotype and anti-IL-6 treated DSS colitis.

Figure 4.3.1E: Cytokine signalling in the colon of anti-IL-6 treated acute DSS colitis.

Figure 4.3.2: Histopathological scores in lung sections from anti-IL-6 treated DSS colitis.

Figure 4.3.2B: Histopathology in lung sections from control and naïve DSS colitis.

Figure 4.3.2C: Histopathology in lung sections from isotype and anti-IL-6 treated DSS colitis.

Figure 4.3.3A: Proportion of myeloid cells in the lung of anti-IL-6 treated acute DSS colitis.

Figure 4.3.3B: Proportion of neutrophils and monocytes in the lung of acute DSS colitis

Figure 4.3.4A: Gene expression profile in the lung of anti-IL-6 treated acute DSS colitis.

Figure 4.3.4B: Gene expression profile in the lung of anti-IL-6 treated acute DSS colitis continued.

Figure 4.3.5A: TNF and IFN- γ protein levels in the lung of anti-IL-6 treated acute DSS colitis.

Figure 4.3.5B: CCL2 and IL-1 β protein levels in the lungs of anti-IL-6 treated DSS colitis.

Figure 4.3.6C: PAFR protein levels in the lung of anti-IL-6 treated acute DSS colitis.

Figure 4.3.7A: Proportion of neutrophils and monocytes in the blood of anti-IL-6 treated acute DSS colitis.

Figure 4.3.7B: Systemic IL-6 levels in anti-IL-6 treated acute DSS colitis mice.

Figure: 4.3.7C: The influence of IL-6 on the differentiation of myeloid progenitor cells and the proportion of mature neutrophils in the bone marrow of acute DSS colitis mice.

Chapter 5

Figure 5.2.1 Time course of PAFR antagonist (CV-6209) interventions in acute DSS colitis.

Figure 5.3.1A: Weight loss and colon shortening in CV-6209 treated DSS colitis.

Figure 5.3.1B: Histopathological scores from colon sections in CV-209 treated DSS colitis.

Figure 5.3.1C: Histopathology in colon sections from control and vehicle treated DSS colitis.

Figure 5.3.1D: Histopathology in colon sections from I.N. and I.V. CV-6209 treated DSS colitis.

Figure 5.3.1E: Cytokine signalling in the colon of CV-6209 treated DSS colitis.

Figure 5.3.2A: Histopathological scores from lung sections of CV-6209 treated DSS colitis.

Figure 5.3.2B: Histopathology in lung sections from control and vehicle treated DSS colitis.

Figure 5.3.2C: Histopathology in lung sections from I.N. and I.V CV-6209 treated DSS colitis.

Figure 5.3.3A: Proportion of myeloid cells in the lung of DSS colitis.

Figure 5.3.3B: Proportion of neutrophils and monocytes in the lung of DSS colitis.

Figure 5.3.4 Gene expression profile in the lung of CV-6209 treated DSS colitis.

Figure 5.3.5: CCL2 and IL1 β levels in the lung of CV-6209 treated DSS colitis.

Figure 5.3.6A: Proportion of neutrophils and monocytes in the blood of CV-6209 treated DSS colitis.

Figure 5.3.6B: Systemic IL-6 levels in CV-6209 treated DSS colitis.

Chapter 6

Figure 6.3.1A: PAFR expression is localised to leucocytes in the lungs of DSS colitis.

Figure 6.3.1B: PAFR positive leucocytes are increased in the lung of acute DSS colitis.

Figure 6.3.2A: Gene expression in RAW 264.7 macrophages exposed to serum from DSS colitis and treated with CV-6209.

Figure 6.3.2B: IL-1 β secreted by RAW 264.7 macrophages exposed to serum from DSS colitis treated with CV-6209.

Figure 6.3.3A: Bacterial load in the lungs of acute DSS colitis.

Figure 6.3.4A Gene expression in RAW 264.7 macrophage treated with LPS and CV-6209.

Figure 6.3.4B: IL-1 β secreted by RAW 264.7 macrophage treated with LPS and CV-6209.

Figure 6.3.5A Gene expression in RAW 264.7 macrophage treated with CCL2 and CV-6209.

Figure 6.3.5B: IL-1 β secreted by RAW 264.7 macrophage treated with CCL2 and CV-6209.

Figure 6.3.6: PAF secreted by RAW 264.7 macrophage treated with CCL2 and LPS in the presence of CV-6209.

Figure 6.3.7A: The ability of secretory factors from CCL2 and LPS treated RAW 267.4 macrophage to induce CD11b expression on neutrophils via PAFR signalling.

Figure 6.3.7B: The ability of secretory factors from CCL2 and LPS treated RAW 267.4 macrophage to induce superoxide production from neutrophils via PAFR signalling.

Appendices

Figure 8.1.1A: Lymphoid populations in the lungs of control mice.

Figure 8.1.1B: Lymphoid populations in the lungs of acute DSS colitis mice.

Figure 8.1.2A: Myeloid cell populations in the lungs of control mice.

Figure 8.1.2B: Myeloid cell populations in the lungs of acute DSS colitis mice.

Figure 8.1.3A: Myeloid cell populations in the blood of control mice.

Figure 8.1.3B: Myeloid cell populations in the blood of acute DSS colitis mice.

Figure 8.1.4A: Hematopoietic stem and progenitor cells in the bone marrow of control mice.

Figure 8.1.4B: Hematopoietic stem and progenitor cells in the bone marrow of DSS colitis mice

Figure 8.1.5A: Mature myeloid populations in the bone marrow of control mice.

Figure 8.1.5B: Mature myeloid populations in the bone marrow of DSS colitis mice.

Figure 8.2.1A: Myeloid cell populations in the lungs control mice.

Figure 8.2.1B: Myeloid cell populations in the lungs of naïve DSS colitis mice.

Figure 8.2.1C: Myeloid cell populations in the lungs of isotype treated DSS colitis mice.

Figure 8.2.1D: Myeloid cell populations in the lungs of anti-IL-6 treated DSS colitis mice.

Figure 8.2.2A: Myeloid cell populations in the blood of control mice.

Figure 8.2.2B: Myeloid cell populations in the blood of naïve DSS colitis mice.

Figure 8.2.2C: Myeloid cell populations in the blood of isotype treated DSS colitis mice.

Figure 8.2.2D: Myeloid cell populations in the blood of anti-IL-6 treated DSS colitis mice.

Figure 8.3.1A: Myeloid cell populations in the lungs of control mice.

Figure 8.3.1B: Myeloid cell populations in the lungs of vehicle treated DSS colitis mice.

Figure 8.3.1C: Myeloid cell populations in the lungs of I.N. CV-6209 treated DSS colitis mice.

Figure 8.3.1D: Myeloid cell populations in the lungs of I.V. CV-6209 treated DSS colitis mice.

Figure 8.3.2A: Myeloid cell populations in the blood of control mice.

Figure 8.3.2B: Myeloid cell populations in the blood of vehicle treated DSS colitis mice.

Figure 8.3.2C: Myeloid cell populations in the blood of I.N. CV-6209 treated DSS colitis mice.

Figure 8.3.2D: Myeloid cell populations in the blood of I.V. CV-6209 treated DSS colitis mice.

Figure 8.4: Gating strategy utilized for the quantification of bacterial load by FISH-FLOW.

Figure 8.5A: CD11b expression on neutrophils incubated with supernatants

from vehicle stimulated macrophages in the presence and absence of CV-6209

Figure 8.5B: CD11b expression on neutrophils incubated with supernatants from CCL2 stimulated macrophages in the presence and absence of CV-6209.

Figure 8.5C: Superoxide levels in neutrophils incubated with supernatants from vehicle stimulated macrophages in the presence and absence of CV-6209.

Figure 8.5D: Superoxide levels in neutrophils incubated with supernatants from CCL2 stimulated macrophages in the presence and absence of CV-6209.

Figure 8.5E: CD11b expression on neutrophils treated directly with LPS in the absence of CV-6209

List of tables

Chapter 1

Table 1.4 Overview of the IBD-induced respiratory pathologies.

Chapter 2

Table 2.5 Gastrointestinal histopathological scoring system for DSS colitis.

Table 2.6 Histopathological scoring system for mouse lungs.

Table 2.10: Staining panel and gating strategy for immunophenotyping mouse tissues by flow cytometry.

Table 2.16: Composition and vendor of reagents used in experiments.

List of equations

Equation 3.3.1: Method utilized to calculate weight loss due to colitis.

Abbreviations:

2,4,6-trinitrobenzenesulfonic acid (TNBS)

3-diaminobenzidine (DAB)

4-(2-hydroxyethyl)-1-piperazineethanesulfonic acid (HEPES)

Alpha-1-antitrypsin (A1AT)

Bovine serum albumin (BSA)

Bronchial hyperresponsiveness (BHR)

Bronchoalveolar lavage (BAL)

Cadherin type-1 (CDH1)

Caspase recruitment domain-containing protein 15 (CARD15)

C-C chemokine receptor 2 (CCR2)

C-C chemokine receptor 9 (CCR9)

Centimetre of water (cmH₂O)

Central nervous system (CNS)

Chemokine (C-C) motif ligand 2 (CCL2)

Chronic obstructive pulmonary disease (COPD)

Ciliary neurotrophic factor (CNTF)

Colony forming units (CFU)

Crohn's disease (CD)

Cycle threshold (Ct)

Degrees Celsius ($^{\circ}\text{C}$)

Dextran sulfate sodium (DSS)

Diffusion capacity of the lung for carbon monoxide (DL_{co})

Dihydroethidium (DHE)

Dulbecco's modified eagle medium (DMEM)

Enzyme-linked immunosorbent assay (ELISA)

Ethylenediaminetetraacetic acid (EDTA)

Extracellular matrix protein-1 (ECM1)

Extraintestinal manifestations (EIM)

Forced expiratory flow (FEF)

Forced vital capacity (FVC)

Fraction of exhaled nitric oxide (FE_{No})

Gastrointestinal tract (GI)

Genome wide association studies (GWAS)

Glycoprotein 130 (Gp130)

Hanks buffered salt solution (HBSS)

Hematopoietic stem cells (HSC)

Hepatocyte nuclear factor-4 alpha (HNF4A)

High-resolution computer tomography (HRCT)

Horse radish peroxidase (HRP)

Human leucocyte antigen-B27 (HLA-B27)

Hypothalamic-pituitary adrenal (HPA)

Immunoglobulin G (IgG)

Inflammatory bowel diseases (IBD)

Interferon- γ (IFN- γ)

Interleukin IL-12 (IL-12)

Interleukin-1 beta (IL-1 β)

Interleukin-10 (IL-10)

Interleukin-11 (IL-11)

Interleukin-12B (IL-12B)

Interleukin-13 (IL-13)

Interleukin-17 (IL-17)

Interleukin-2 (IL-2)

Interleukin-22 (IL-22)

Interleukin-23 (IL-23)

Interleukin-23 receptor (IL-23R)

Interleukin-27 (IL-27)

Interleukin-4 (IL-4)

Interleukin-5 (IL-5)

Interleukin-6 (IL-6)

Interleukin-8 (IL-8)

Intraperitoneal (IP)

Janus kinase-2 (JAK2)

Laminin beta-1 (LAMB1)

Leukemia inhibitory factor (LIF)

Lipopolysaccharide (LPS)

Lipoteichoic acid (LTA)

Litre (L)

Major histocompatibility complex (MHC) class II

Matrix metalloproteases (MMP)

Mean linear intercept (L_M)

Medium-chain-fatty acids (MCFAs)

Membrane bound IL-6 receptor (IL-6R)

Mesenteric lymph nodes (MLN)

Microgram (μg)

Microlitre (μL)

Micrometre (μm)

Micromole (μM)

Millilitre (mL)

Millimole (mM)

Minutes (min)

Moloney murine leukemia virus reverse transcriptase (MMLV-RT)

Monocyte chemoattractant protein-1 (MCP-1)

Mucin 2 (MUC2)

Mucosal vascular addressin cell adhesion molecule 1(MAdCAM-1)

Multi-potent progenitor cells (MPP)

Muramyl dipeptide (MDP)

NACHT, LRR, and PYD domains-containing protein 3 (NALP3)

Nanogram (ng)

Natural killer cells (NK)

Nucleotide-binding oligomerization domain-containing protein 2 (NOD2)

Oncostatin M (OSM)

p38 mitogen-activated protein kinases pathway (p38 MAPK)

PAF acetylhydrolase (PAF-AH)

Paraformaldehyde (PFA)

Pattern recognition receptor (PRR)

Periodic acid–Schiff Alcian blue (PAS-AB)

Phosphate buffered saline (PBS)

Platelet activating factor (PAF)

Platelet activating factor receptor (PAFR).

Primary sclerosing cholangitis (PSC)

Potential hydrogen (pH)

Pulmonary parenchymal disease (PPD)

Quantitative polymerase chain reaction (qPCR)

Reactive oxygen species (ROS)

Revolutions per minute (RPM)

Ribonucleic acid (RNA)

Seconds (s)

Signal transducer and activator of transcription-3 (STAT3)

Soluble IL-6 receptor (sIL-6R)

T helper 1 (Th1)

T helper 17 (Th17)

T helper 2 (Th2)

T regulatory (Treg)

TBS (tris-buffered saline)

TBS-T (tris-buffered saline – 0.1% tween 20)

TBS-TX (tris-buffered saline – 0.1% triton X-100)

Toll-like receptor 2 (TLR2)

Toll-like receptor 4 (TLR4)

Toll-like receptors (TLR)

Transforming growth factor beta (TGF- β)

Tumor necrosis factor (TNF)

Ulcerative colitis (UC)

Vascular cell adhesion molecule 1 (VCAM1)

Chapter 1: Inflammatory bowel disease

1.1 Background

Inflammatory bowel disease (IBD) is the umbrella term for a number of chronic inflammatory conditions that predominately affect the gastrointestinal (GI) tract. The most prominent phenotypes of IBD are Crohn's disease (CD) and ulcerative colitis (UC) (Thoreson and Cullen 2007). While CD and UC have a number of similarities they are distinct conditions with different disease phenotypes. CD is characterised by transmural inflammation that can affect the entire gastrointestinal tract, however pathology generally manifests in the ileum and colon. The symptoms of CD include, diarrhoea, chronic abdominal pain, weight loss, colonic stenosis and fistulas (Walsh, Mabee et al. 2011). In contrast, UC is characterized by superficial inflammation that predominately affects the colon mucosa. Pathology manifests as ulceration and polyp formation. The symptoms of UC include, diarrhoea, chronic abdominal pain, weight loss and anaemia (Head and Jurenka 2003). In addition to pathology within the GI tract, IBD patients can also exhibit secondary organ pathologies, termed "extra-intestinal manifestations" (EIM). EIM develop as inflammatory responses in skin, eyes, joints, liver and lungs (Levine and Burakoff 2011). EIM are present in approximately 45% of IBD patients and can contribute to the morbidity associated with IBD (Danese, Semeraro et al. 2005).

The aetiology of IBD is unknown, the current paradigm is that the initiation of disease is a multifactorial process that involves genetic susceptibility, immuno-regulatory factors and environmental stimuli (Scharl and Rogler 2012). The current hypothesis to account for IBD states, that a dysfunctional immune system results in an inappropriate immune response to commensal enteric bacteria in a genetically susceptible host and that the onset and relapse of disease is triggered by environmental factors (Scharl and Rogler 2012). This hypothesis has been formed on the basis of considerable basic science and clinical research into the pathogenesis of IBD. In contrast, basic science research on the EIM of IBD has been limited, thus there is no current consensus hypothesis to account for the pathogenesis of these conditions. (Abraham and Sellin 2012)

1.2 IBD epidemiology and economic impact

IBD is largely a disease of the Western world, with industrialised nations in North America and Europe having the greatest prevalence and incidence rates (Molodecky, Soon et al. 2012) (Figure 1.2). Analysis of epidemiological data by Molodecky *et al.* reported annual incidence rates of 24.3 per 100,000 in Europe and 19.2 per 100,000 in North America. In addition, this study reported that in a time-trend analysis, 75% of CD studies and 60% of UC studies had a statistically significant increase in incidence rates, indicating that IBD is becoming more common and thus a significant public health issue (Molodecky, Soon et al. 2012). The incidence rates of IBD in Australia follow a similar trend to that seen in North American and Europe. In 2010 the annual incidence rates of CD and UC in Australia was reported as 29.3 per 100,000 and 11.2 per 100,000 respectively, amongst the highest in the world (Wilson, Hair et al. 2010).

The age of onset for IBD varies between 15 - 30 years of age, with 10% of cases occurring in patients under 18 years of age (Loftus 2004). As IBD is an incurable chronic disease that is most common in children and young adults, patients require clinical care for a large proportion of their life. The clinical care of IBD involves regular endoscopy and medication, thus the clinical care of IBD patients carries a substantial economic burden (Stone 2012).

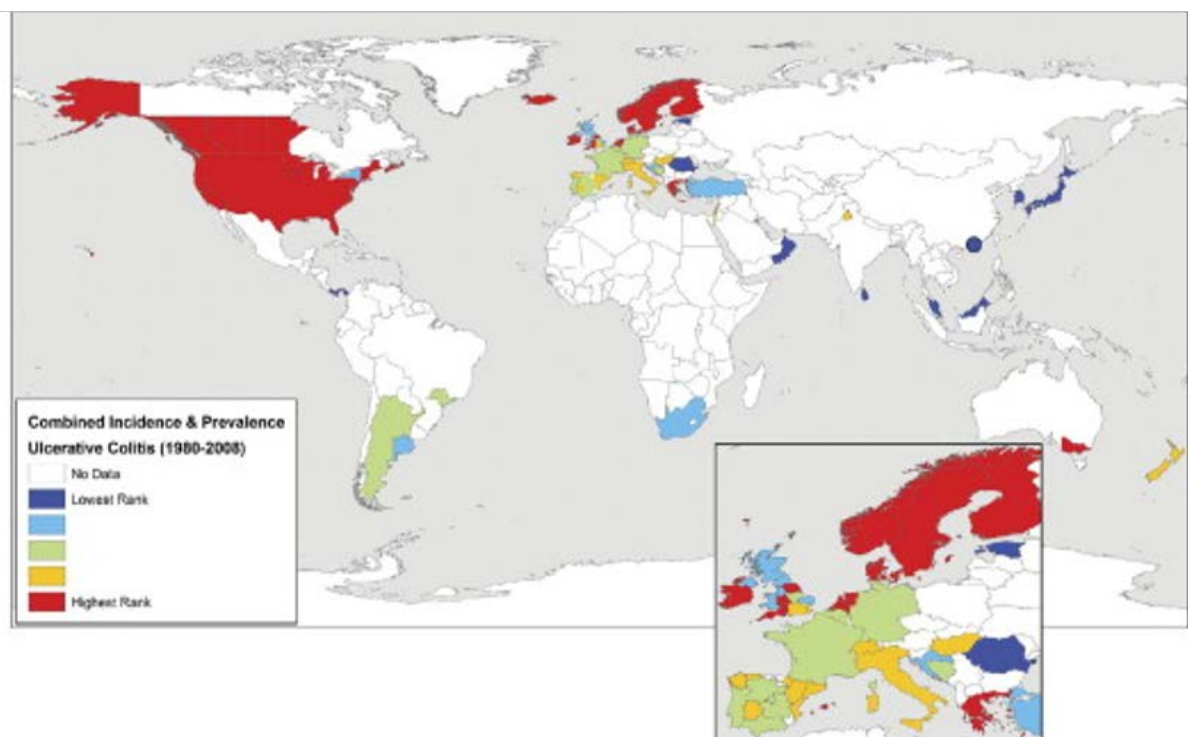
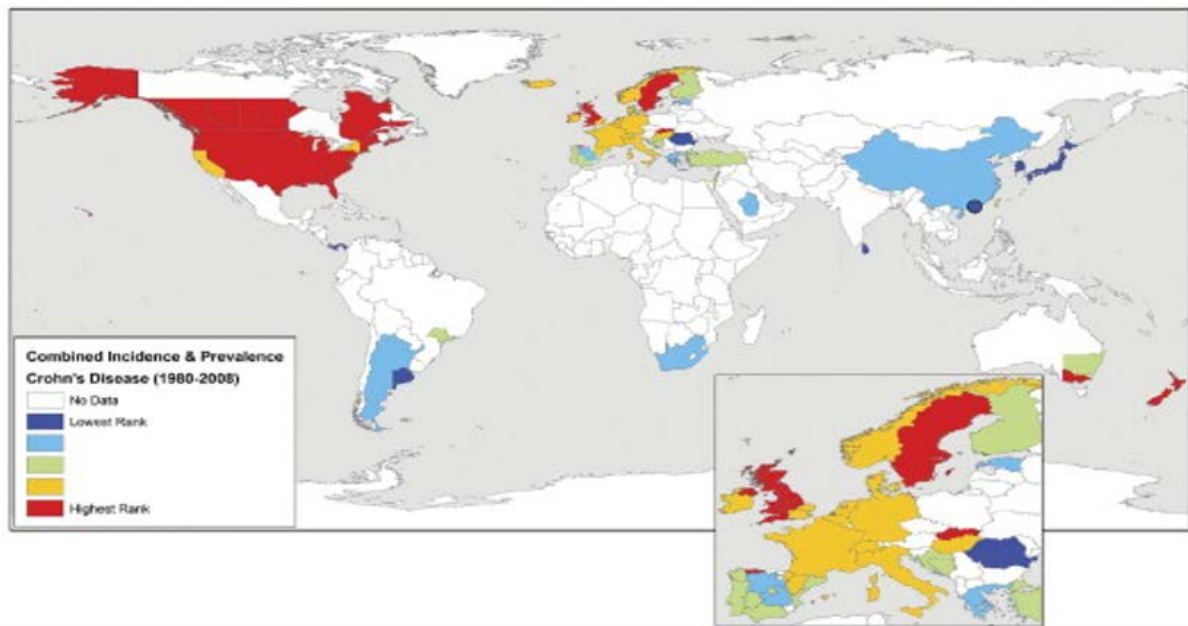


Figure 1.2: Incidence and prevalence of IBD in the time interval 1980 – 2008 (Molodecky, Soon et al. 2012).

1.3 Extra-intestinal manifestations of IBD

EIM are IBD-dependent immune mediated pathological events that occur outside the GI tract. EIM develop in approximately 45% of IBD patients. EIM can develop as primary sclerosing cholangitis (PSC) in the liver, erythema nodosum in the skin, arthropathies in the lower extremities, uveitis and episcleritis in the eye as well as a diverse range of respiratory pathologies (Orchard, Chua et al. 2002, Loftus, Harewood et al. 2005, Black, Mendoza et al. 2007, De Vos 2009, Ciccacci, Biancone et al. 2012).

1.4 Respiratory pathologies associated with IBD

The respiratory pathologies associated with IBD are extremely heterogeneous, ranging from subclinical abnormalities to irreversible respiratory disease (Table 1.4). As the respiratory pathologies associated with IBD are highly variable and often subclinical their true prevalence has been controversial. A systematic review of 1,400 case reports by Rogers *et al.* in 1971 reported only 3 cases of IBD-induced respiratory disease (0.4%). In contrast a more recent systematic review by Black *et al.* in 2007 reported 55 cases of respiratory disease in 155 IBD patients (35%) (Rogers, Clark et al. 1971, Black, Mendoza et al. 2007). The discrepancies between these two articles can be attributed to the vast advances in pulmonary diagnostics since the review by Rodgers *et al.* Thus a number of less severe cases may have gone undetected. This is important, especially since the majority of IBD-induced respiratory pathologies are subclinical. Studies that have aimed to directly assess the prevalence of subclinical respiratory pathologies in IBD patients report that 46 – 64% of IBD patients examined have some form of respiratory pathology (Eade, Smith et al. 1980, Bonniere, Wallaert et al. 1986, Tzanakis, Bouros et al. 1998, Marvisi, Borrello et al. 2000, Herrlinger, Noftz et al. 2002, Ates, Karıncaoglu et al. 2011). The strikingly high prevalence rates in these

studies demonstrate that the prevalence of respiratory pathologies in IBD patients is higher than currently appreciated by the scientific community.

IBD-induced respiratory pathologies	
Sub-clinical Manifestations	Clinical Manifestations
Altered pulmonary function	Bronchiectasis
Alveolar lymphocytosis	Chronic bronchitis
Asymptomatic physiological pulmonary abnormalities	Pulmonary parenchymal disease
Increase in exhaled reactive oxygen species	Sarcoidosis

Table 1.4 Overview of the IBD-induced respiratory pathologies.

1.4.1 Subclinical respiratory pathologies

The studies that have assessed subclinical respiratory pathologies in IBD patients have utilized spirometry, high-resolution computed tomography (HRCT) and measurements of airway inflammation (Bonniere, Wallaert et al. 1986, Songur, Songur et al. 2003). In spirometry assessments, a decrease in the diffusion capacity of the lung for carbon monoxide (DL_{CO}) and forced expiratory flow (FEF) are the most prevalent lung function abnormalities (Eade, Smith et al. 1980, Bonniere, Wallaert et al. 1986, Tzanakis, Bouros et al. 1998, Marvisi, Borrello et al. 2000, Herrlinger, Noftz et al. 2002, Mohamed-Hussein, Mohamed et al. 2007, Yilmaz, Demirci et al. 2010, Ates, Karıncaoglu et al. 2011). A decrease in DL_{CO} indicates a reduction in surface area for gaseous exchange due to a change in alveolar volume, which is a characteristic of the pathology associated with chronic obstructive

pulmonary disease (COPD) and interstitial lung disease (Ranu, Wilde et al. 2011). FEF is a measure of obstructive lung conditions and a reduction in FEF is reflective of airway obstruction, a characteristic of bronchiectasis and bronchitis (Ranu, Wilde et al. 2011). HRCT is a highly sensitive tool capable of visualizing lung morphology, studies that have utilized HRCT to assess respiratory pathologies in IBD report that 22 - 64% of IBD patients examined had a form of structural pathology (Songur, Songur et al. 2003, Mohamed-Hussein, Mohamed et al. 2007, Yilmaz 2010, Desai, Patil et al. 2011). These pathologies included peribronchial thickening, bronchiectasis and ground glass opacities (Songur, Songur et al. 2003, Mohamed-Hussein, Mohamed et al. 2007, Yilmaz 2010, Desai, Patil et al. 2011).

Subclinical respiratory inflammation is also associated with IBD. Bonniere *et al.* and Sarioglu *et al.* analyzed the cellular composition of bronchoalveolar lavage (BAL) fluid from IBD patients and reported that alveolar lymphocytosis was present in 54 and 46% of IBD patients respectively (Bonniere, Wallaert et al. 1986, Sarioglu, Turkel et al. 2006). Subclinical respiratory inflammation was also reported as an increase in reactive oxygen species (ROS), measured by the fraction of exhaled nitric oxide (FE_{N_o}) by Zyilmaz *et al.* and the production of superoxide anion from BAL macrophages by Bonniere *et al.* (Bonniere, Wallaert et al. 1986, Ozyilmaz, Yildirim et al. 2010). ROS are produced from neutrophils and classically activated macrophages and thus are utilized as markers of inflammation. Further evidence of respiratory inflammation in IBD patients is provided by Krenke *et al.*, this study found that the inflammatory cytokines interleukin-6 (IL-6), interleukin-8 (IL-8), interleukin-1 β (IL-1 β) and tumor necrosis factor (TNF) are elevated in the breath condensate of pediatric IBD patients (Krenke, Peradzynska et al. 2014). Taken together these studies demonstrate the high prevalence of subclinical respiratory inflammation associated with IBD. While these pathologies are asymptomatic they do demonstrate the high level of latent respiratory

pathology in IBD patients that has the potential to develop into irreversible respiratory disease if not managed appropriately.

1.4.2 Active respiratory disease

The clinically active respiratory diseases associated with IBD include, bronchiectasis, chronic bronchitis, and pulmonary parenchymal disease (PPD). Bronchiectasis and chronic bronchitis account for 66% of all respiratory diseases diagnosed in IBD (Camus, Piard et al. 1993, Black, Mendoza et al. 2007). The pathology and pathogenesis of these conditions is described in detail in section 1.7.2. Rarer respiratory diseases have also been reported in IBD these include tracheobronchitis, serositis and pulmonary parenchymal disease (Balestra, Balestra et al. 1988, Hotermans, Benard et al. 1996). As the prevalence of these diseases amongst IBD patients is low, this study focused on IBD-induced bronchiectasis and chronic bronchitis. Treatments such as sulfasalazine, a common IBD treatment can induce lung toxicity. However there has not been any clinical studies that have aimed to delineate the number of respiratory pathologies in IBD patients that are drug-induced. Physicians consider that drug-induced lung toxicity is a distinct issue that is not related to IBD-induced respiratory disease. This assumption comes from the observation that the symptoms of drug-induced lung toxicity is relieved by drug dechallenge (Black, Mendoza et al. 2007).

Smoking is a well-known environmental risk factor for the development of respiratory diseases. In contrast smoking as risk factor in the development of IBD is not as conclusive because smoking has diverging effects in IBD patients depending on disease phenotype (Lakatos, Szamosi et al. 2007). Smoking is detrimental to the progression of CD but has a beneficial effect on UC pathology (Lakatos, Szamosi et al. 2007). While the reasons for these diverging effects are unknown, a number of hypothesis have been postulated, these include the protective effect of nicotine on gastrointestinal

permeability and smoking-induced dysbiosis. However studies designed to test these hypothesis have been minimal (Parkes, Whelan et al. 2014). In regards to the role of cigarette smoke in IBD-induced respiratory disease the relationship is unclear, to my knowledge there is no scientific studies that have investigated this relationship. A clinical study by Globisch and Mohr *et al.* that investigated the respiratory pathologies of IBD also examined an association with smoking and found no correlation (Dierkes-Globisch and Mohr 2002). This study would suggest cigarette smoke is not a primary environmental risk factor associated with IBD-induced respiratory disease. However based on the knowledge of cigarette smoke in the development of chronic obstructive pulmonary diseases (Hogg 2004), it is fair to assume that smoking would also exacerbate IBD-induced respiratory disease.

1.5 Pathogenesis of IBD

1.5.1 Gastrointestinal pathophysiology

Gastrointestinal pathology in IBD arises due to a series of interactions between, susceptibility genes, the microbiome, the environment and the immune system (Sartor 2006). Genome wide association studies (GWAS) have identified a number of susceptibility loci that predispose to the development of IBD. These genes are involved in the maintenance of epithelial barrier function, microbial recognition and modulation of the mucosal immune system. The host microbiome has been identified as an important factor in the aetiology of IBD through the modulation of mucosal immune responses. Endpoint GI pathology is mediated by components of the immune system, thus cell-signalling factors that modulate leucocyte function in the mucosa also play an important role in IBD pathogenesis. An overview of how these factors lead to the development of GI pathology in IBD is described below.

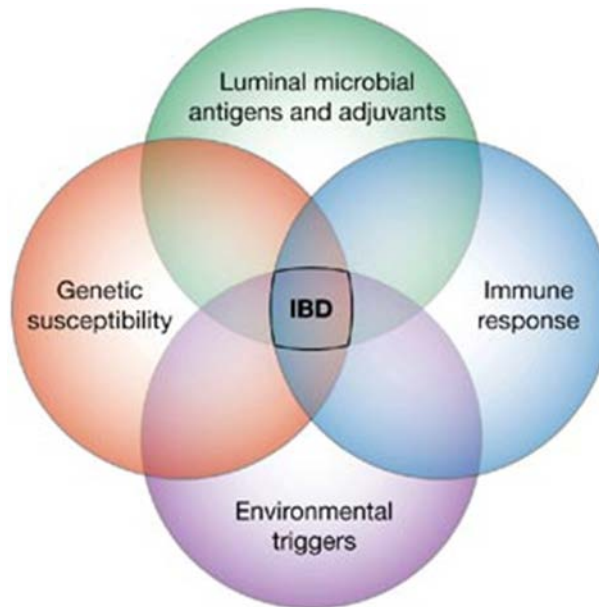


Figure 1.5.1: Factors that contribute to the pathogenesis of IBD (Sartor 2006).

1.5.2 The genetics of IBD

GWAS have identified have identified 200 risk loci in IBD (Franke, McGovern et al. 2010, Anderson, Boucher et al. 2011, Liu, van Sommeren et al. 2015). These genes are involved in a range of functions that contribute to intestinal homeostasis, such as, epithelial cell function, immune responses and microbial recognition (Cho 2008). The most prominent gene associated with IBD is nucleotide-binding oligomerization domain-containing protein 2 (NOD2) also known as caspase recruitment domain-containing protein 15 (CARD15). Mutations in this gene are present in 25 – 35% of CD patients (Economou, Trikalinos et al. 2004). The biological function of NOD2 is to regulate microbial recognition, thus mutations in this gene can result in aberrant immune responses to enteric bacteria (Economou, Trikalinos et al. 2004, Barnich, Hisamatsu et al. 2005). A meta-analysis by Anderson *et al.* revealed that mutations in the genes encoding hepatocyte nuclear factor-4 alpha (HNF4A), extracellular matrix protein-1 (ECM1), cadherin type-1 (CDH1) and laminin beta-1 (LAMB1) are associated with epithelial barrier dysfunction (Anderson, Boucher et al. 2011).

This study also identified mutations in the genes encoding the interleukin-23 receptor (IL-23R), janus kinase-2 (JAK2), signal transducer and activator of transcription-3 (STAT3) and interleukin-12B (IL-12B) to be involved in aberrant immune responses. While genetic factors do predispose to the development of IBD, the association between risk allele and IBD is not absolute (Cho 2008). Furthermore twin studies have reported concordance rates of 30.3% in monozygotic twins vs 3.6% in dizygotic twins in CD and 15.4% vs 3.9% in UC (Cho and Brant 2011). Thus genetic susceptibility is a risk factor associated with IBD, but not the primary contributing factor. In regards to EIM, genetic risk factors have been identified for the development of the cutaneous and arthritic manifestations of IBD (Ciccacci, Biancone et al. 2013) (Arvikar and Fisher 2011). Variants in the *TRAF3IP2* gene are associated with the development of erythema nodosum in IBD patients. *TRAF3IP2* encodes adapter protein CIKS; this protein modulates IL-17 signalling and thus plays a role innate and adaptive immune responses (Qian, Liu et al. 2007). HLA-B27 is a major histocompatibility complex (MHC) class I protein and thus is involved in modulating immune responses (Lopez de Castro 2007). The human leucocyte antigen-B27 (HLA-B27) haplotype is associated with the arthropathies induced by IBD (Arvikar and Fisher 2011). . However the role of HLA-B27 in the EIM of IBD is only limited to a sub-section of patients that carry this polymorphism. In regards to PSC 15 risk loci has been associated with the condition, half of these risk loci have also been associated with IBD (Liu, Hov et al. 2013). 72% of patients in this study had a diagnosis of concomitant IBD, therefore while genetic risk loci are an overlapping feature of IBD and PSC they are unlikely to be the primary pathological feature that accounts for the causation of these two diseases (Liu, Hov et al. 2013). In respect to the IBD-induced respiratory diseases there has not been any genetic associated identified that predispose to the development IBD-induced respiratory disease.

1.5.3 Autophagy in IBD pathogenesis

Autophagy is a process used by cells to destroy misfolded proteins, damaged cellular machinery and intracellular pathogens (Glick, Barth et al. 2010). The process of Autophagy utilizes lysosomal acid proteases to destroy cellular debris/pathogens that have been engulfed in autophagosomes (Glick, Barth et al. 2010). As autophagy provides has an essential role in cellular function and anti-microbial processes aberrant autophagy has been hypothesized to be involved in IBD pathogenesis (Scharl and Rogler 2012). Polymorphisms in genes that regulate autophagy such as, autophagy-related 16-like 1 (ATG16L1) and immunity-related GTPase family M (IRGM) are known risk factors for the development of IBD. Polymorphisms in these genes are thought to contribute to IBD through inducing aberrant autophagy which results in impaired intestinal epithelial barrier function and subsequent gut inflammation (Scharl and Rogler 2012).

1.5.4 Immune-microbiota homeostasis in IBD

The gut microbiota is the collection of bacterial species that inhabit the gastrointestinal tract. These microorganisms have a symbiotic role with the host, conferring numerous biological functions that contribute to the maintenance of intestinal homeostasis. These biological functions include immune regulation, maintaining epithelial barrier function and metabolizing dietary carbohydrates (Sartor and Mazmanian 2012). The microbiota contributes to intestinal homeostasis by promoting the differentiation of T-cell subsets with protective functions. (Hooper, Littman et al. 2012). Furthermore the microbiota provides energy for the host epithelium through the production of the short chain fatty acids (Kelly, Zheng et al. 2015). Cells of the innate immune system contribute to the maintenance of this symbiotic relationship through the induction of immunological tolerance (Mowat 2003). Immunological tolerance is induced in part by the unique phenotype of intestinal

macrophages. Intestinal macrophages are highly phagocytic, express high levels of major histocompatibility complex (MHC) class II and display anergic responses to pattern recognition receptor (PRR) signalling (Smythies, Sellers et al. 2005). This phenotype allows intestinal macrophages to sample the components of the microbiota without inducing exaggerated immune responses to commensal bacteria (Smythies, Sellers et al. 2005). Dendritic cells (DC) also play a pivotal role in the maintenance of intestinal homeostasis. DC continuously sample antigens in the mucosa, in the role DC can induce tolerance to commensal bacteria and mount proinflammatory responses to pathogens. DC induces these responses through the direct cell-cell interactions with T cells and B cells as well as the secretion of cytokines. Intestinal epithelial cells contribute to immunological tolerance by providing a physical barrier to the lumen, secreting mucins and sensing pathogens via toll-like receptors (TLR) (Mowat 2003).

In IBD it is hypothesized that this symbiotic relationship between commensal enteric bacteria and the mucosal immune system is comprised, resulting in enhanced immune reactivity to enteric bacteria. Indeed serum antibodies against microbial antigens have been identified in CD patients (Quinton, Sendid et al. 1998, Mow, Vasiliauskas et al. 2004). The disruption of host-microbiota homeostasis is hypothesized to be induced by pathogenic microbes such as *Mycobacterium avium paratuberculosis*, which are frequently detected in CD patients (Autschbach, Eisold et al. 2005). An alternative hypothesis is that a shift in the composition of bacterial species in the microbiota, termed dysbiosis, induces aberrant immune responses (Marteau and Chaput 2011). Dysbiosis is a feature of both phenotypes of IBD, thus a reduction in the bacterial species with anti-inflammatory properties may induce aberrant immune responses in the gut and initiate inflammation (Marteau and Chaput 2011). There have been many advances in our understanding of the interactions between the microbiota

and the host in the context of IBD, however the exact role of the microbiota in the pathogenesis of IBD is still unknown.

1.5.5 Soluble mediators of inflammation

A large number of compounds that initiate and maintain inflammation are produced by leucocytes. An understanding of the function and cellular source of these compounds is critical for understanding the immunopathogenesis of IBD. Soluble mediators of inflammation come in the form of cytokines and phospholipids. A brief description of these compounds and their role in IBD pathogenesis is described below.

Tumour necrosis factor (TNF): TNF is an inflammatory cytokine that is primarily produced by activated macrophages, although it can also be produced by many other leucocytes such as neutrophils, natural killer (NK) cells and CD4⁺ T helper (Winsauer, Kruglov et al. 2014). TNF activates the inflammatory functions of neutrophils and macrophages resulting in the production of an array of proteins involved in inflammation. TNF mediates the extravasation of leucocytes to sites of inflammation through the activation of endothelial cells. Endothelial cells stimulated with TNF express the adhesion molecules and chemokines required for leucocyte extravasation. Through these functions TNF has been implicated in mediating the pathogenesis of IBD, in fact anti-TNF therapy has been shown to be an efficacious treatment for IBD (Barreiro-de-Acosta, Lorenzo et al. 2012).

Interferon- γ (IFN- γ): IFN- γ is a cytokine involved in modulating a number of immunological functions. In the context of IBD, IFN- γ mediates T helper 1 (Th1) responses. IFN- γ secreted by Th1 cells results in the activation of macrophages and the differentiation of

naïve T cells into Th1 cells (Strober and Fuss 2011). IFN- γ macrophage activation induces the production of ROS and inflammatory cytokines. ROS released by IFN- γ activated macrophages damages structural tissue in the intestinal mucosa (Neurath 2014).

Interleukin-6 (IL-6); IL-6 is a pleiotropic cytokine involved in the regulation of a number of physiological processes. In immunology, IL-6 is involved in controlling humoral immunity, chronic inflammation, hematopoiesis and innate immunity (Scheller, Chalaris et al. 2011). In the context of IBD pathology, IL-6 is secreted by macrophages and epithelial cells in response to immunomodulatory factors. IL-6 released in this manner results in the chemotaxis of leucocytes and activation of the acute phase response (Borish, Rosenbaum et al. 1989, Parker, Cheng et al. 2011). The acute phase response is a systemic reaction to tissue injury. Activation of the acute phase response results in the release of acute phase proteins into the bloodstream. These proteins are involved in the chemotaxis of leucocytes and anti-microbial responses. IL-6 also plays a role in the differentiation of T helper 17 (Th17) cells a subset of T cells that are involved in the pathogenesis of IBD (Neurath and Finotto 2011).

IL-1 β ; IL-1 β is a potent inflammatory cytokine that modulates acute inflammation. IL-1 β activates the cytotoxic effects of neutrophils and macrophages. IL-1 β also induces the expression of adhesion molecules and chemokines in endothelial cells which facilitates leucocyte extravasation (Huang, Wu et al. 2015). IL-1 β production is regulated by multimeric protein complexes called inflammasomes. Inflammasome formation is induced by PRR signaling. IL-1 β is consistently elevated in mucosal tissues of IBD patients and correlates with disease activity (Coccia, Harrison et al. 2012). In IBD macrophages, neutrophils and the intestinal epithelium are the most prominent producers of IL-1 β (Neurath 2014).

Chemokine (C-C) motif ligand 2 (CCL2); CCL2 is a chemokine that recruits monocytes, memory T cells and dendritic cells to sites of inflammation. CCL2 can also indirectly recruit neutrophils to sites of inflammation via the expression of leukotrienes and platelet activating factor (PAF) (Reichel, Rehberg et al. 2009). CCL2 expression is highly expressed in the intestinal mucosa of CD and UC patients (de Souza and Fiocchi 2016). In IBD, the endothelium and monocytes are the most prevalent producers of CCL2 (Neurath 2014).

Interleukin-23 (IL-23), IL-23 is a cytokine that regulates the function of a subset of T helper lymphocytes termed Th17 cells (Sarra, Pallone et al. 2010). Th17 cells regulate the recruitment of effector leucocytes to sites of inflammation in autoimmune diseases. IL-23 is secreted by activated macrophages and dendritic cells. In IBD it is hypothesized that IL-23 mediates gut inflammation through the activation and proliferation of Th17 cells (Sarra, Pallone et al. 2010).

Interleukin-17 (IL-17); IL-17 is a cytokine produced by the Th17 subset of T helper lymphocytes. The biological function of IL-17 under physiological conditions is to aid in host defence against extracellular bacterial and fungal infections (Gaffen 2008). IL-17 fulfils this role through mediating the recruitment of neutrophils and monocytes to sites of inflammation. Aberrant IL-17 production has been implicated in the pathogenesis of IBD (Sarra, Pallone et al. 2010). In IBD it is thought that IL-17 produced by Th17 cells induces the expression of IL-8, IL-6 and IL-1 β from epithelial cells perpetuating chronic inflammation (Sarra, Pallone et al. 2010). However IL-17 has also been reported to be essential in maintaining intestinal epithelial barrier integrity and restitution of gut

inflammation. Thus whether IL-17 plays a positive or negative role in IBD pathology is controversial (Lee, Tato et al. 2015).

Platelet activating factor (PAF); PAF is a phospholipid mediator of inflammation, the biological function of PAF is largely confined to the activation and migration of leucocytes, particularly neutrophils. The effect of PAF on neutrophils include, chemotaxis, expression of reactive oxygen species and adhesion molecule expression that facilitates extravasation (Montrucchio, Alloatti et al. 2000). The biological effect of PAF is mediated by the G-protein coupled receptor (GPCR) platelet activating factor receptor (PAFR). PAF can induce the expression of cytokines in intestinal epithelial cells and thus has been implicated in the pathogenesis of IBD (Borthakur, Bhattacharyya et al. 2010). In IBD PAF is produced by monocytes, neutrophils and endothelial cells (Edwards and Constantinescu 2009).

1.5.6 Intestinal barrier function in IBD

The intestinal mucosa is protected from the pathogenic microorganisms in the lumen of the GI tract by the intestinal barrier. The defensive properties of the intestinal barrier include physical barriers, such as the epithelium and mucins as well as antimicrobial peptides and cytokine secretion from epithelial cells (Antoni, Nuding et al. 2014). In IBD patients aberrant function of the intestinal barrier results in exposure of the intestinal mucosa to the gut lumen. A number of mechanisms have been hypothesized to cause intestinal barrier dysfunction in IBD patients. These hypotheses are based around an increase in epithelial permeability (Hering, Fromm et al. 2012). Epithelial permeability is thought to result from a combination of aberrant mucin production, abnormal autophagy in epithelial cells as well as inappropriate signalling from pattern recognition receptors. Defects in these processes allow

microorganisms to penetrate the intestinal epithelial barrier which stimulates host immune responses and ultimately results in chronic intestinal inflammation (Antoni, Nuding et al. 2014).

1.5.7 Immune responses in the gut

In the gut innate immune responses are regulated in part by epithelial cells. Epithelial cells provide a physical defensive barrier and initiate innate immune responses via cytokine/chemokine signalling following PRR activation (Eri, Adams et al. 2011). Myeloid cells such as neutrophils and monocytes are recruited from the vasculature in response to cytokine/chemokine signalling. Upon activation neutrophils/macrophages release cytotoxic agents and inflammatory cytokines. These inflammatory cytokines assist in the further chemoattraction and activation of myeloid cells (Danese 2005). Inflammatory cytokines secreted by epithelial cells also induce the activation of tissue resident macrophages (Mosser 2003). Macrophages in conjunction with dendritic cells phagocytose invading pathogens for antigen presentation to lymphocytes at peripheral lymphoid tissues, initiating the adaptive immune response (Karlinger, Gyorke et al. 2000). The adaptive immune response is comprised of lymphocytes (T and B cells) that when activated, generate effector responses. The effector responses of T cells involve cytokine production for CD4⁺ T helper subsets and cytotoxic cell death by CD8⁺ T cells. The cytokine secretory profile of the adaptive response is dependent on the T cell subset, which itself is based upon the cytokines present in the lymph node tissue microenvironment during antigen presentation (figure 1.5.7). Interleukin IL-12 (IL-12) induces the differentiation of Th1 cells, IL-6/interleukin-23 (IL-23)/(transforming growth factor beta) TGF- β induce Th17 cells, interleukin-4 (IL-4) induce T helper 2 (Th2) cells and interleukin-2 (IL-2)/TGF- β induce Treg cells (Zenewicz, Antov et al. 2009). Th1, Th2 and Th17 subsets are involved in inflammatory responses. T helper subsets

induce their response through the secretion of cytokines that activate effector cells, the cytokines secreted by Th1, Th2 and Th17 cells is described in figure 1.5.7. Th1 cells are involved in the removal of tumour cells and intracellular pathogens and these cells produce the cytokines IFN- γ and TNF. Th2 cells are involved in the removal of extracellular pathogens and allergy; these cells secrete the cytokines IL-4, interleukin-5 (IL-5) and interleukin-13 (IL-13). Th17 cells are involved in the elimination of extracellular bacteria and produce the cytokines interleukin-17 (IL-17) and interleukin-22 (IL-22) (Bailey, Nelson et al. 2014). Treg cells mediate the attenuation of proinflammatory responses via the suppression of effector T cells and the production of interleukin-10 (IL-10) (Strobel and Mowat 1998).

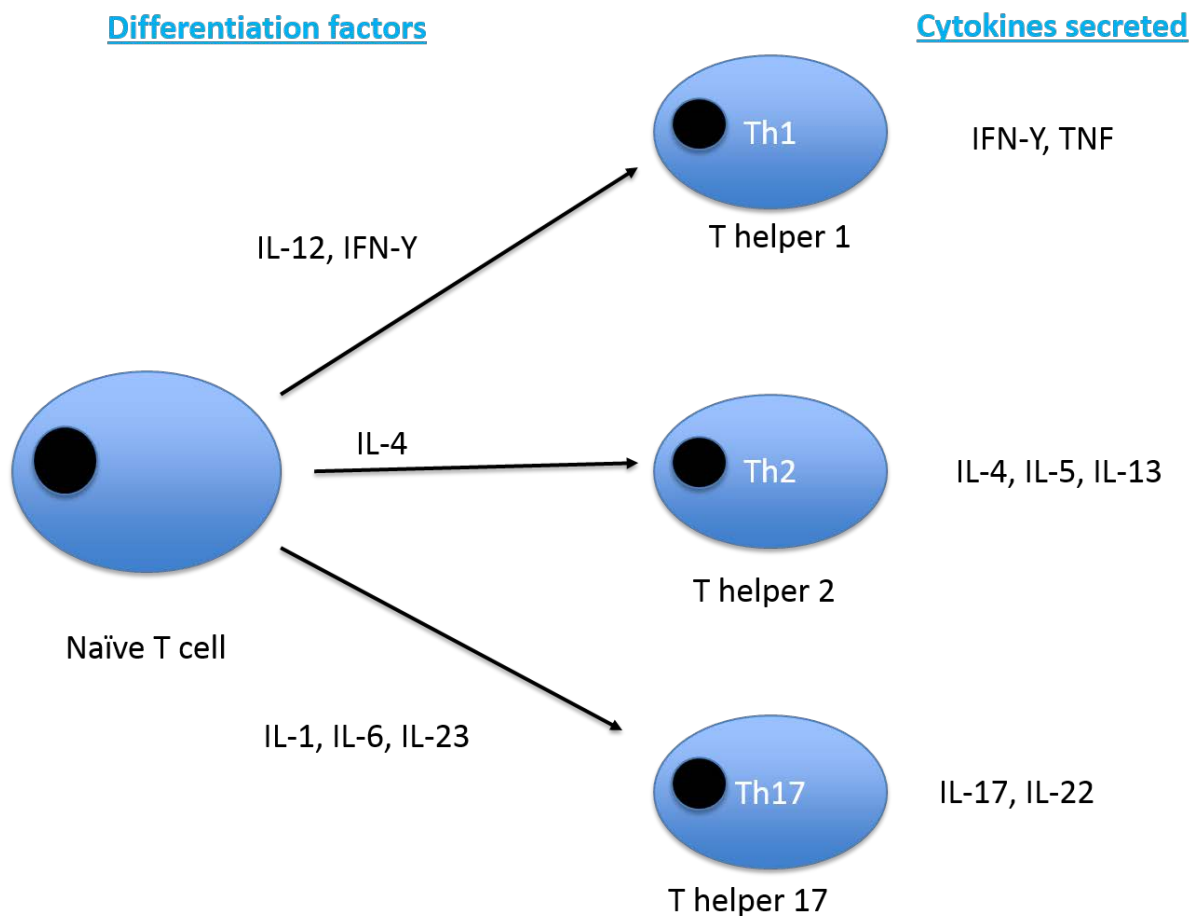


Figure 1.5.7: T helper subsets, their differentiation factors and secreted cytokines

1.5.8 Immune responses in IBD

In IBD it is hypothesized that a loss of tolerance to commensal enteric bacteria results in aberrant immune responses from epithelial cells and tissue resident leucocytes. These aberrant immune responses damage the intestinal epithelial barrier allowing translocation of bacteria into the lamina propria. Dendritic cells in the lamina propria sample bacterial antigens and migrate to the mesenteric lymph nodes where they interact with naïve T cells to generate effector T cell subsets. CD is associated with Th1 and Th17 differentiation (Eastaff-Leung, Mabarrack et al. 2010); while the T cell phenotype associated with UC is not as conclusive. UC is considered to have a Th2 profile, but the concentrations of IL-4 and IL-5, which are elevated in Th2 responses, have been variable in UC tissues. Thus UC is considered that have an atypical Th2 profile (Fuss, Neurath et al. 1996). Post-differentiation, Th1/Th17/Th2 cells migrate from the mesenteric lymph node (MLN) to the intestinal mucosa where they induce their effector functions via cytokine secretion. Cytokine secretion by effector T cell subsets results in the chemoattraction and activation of myeloid cells (Baumgart and Carding 2007). IFN- γ and TNF secreted by Th1 cells results in the activation of macrophage (Clark, Hoare et al. 2005). IL-17 produced by Th17 cells results in neutrophil recruitment and sequential expression of TNF, IL-6 and IL-1 β (Eastaff-Leung, Mabarrack et al. 2010). Myeloid cells activated in this manner, express a number of chemokines and lipid mediators of inflammation, such as CCL2 and PAF that perpetuate the inflammatory milieu at the intestinal mucosa. Furthermore activated myeloid cells, release cytotoxic compounds that induce damage to structural cells in the intestinal mucosa. These compounds include ROS and matrix metalloproteinases (MMP) (Chandran, Sathaporn et al. 2003, Ajuebor, Kunkel et al. 2004).

In summary the immunopathology of IBD is mediated by innate and adaptive immune responses. Inflammation is propagated by cell mediated responses involving the differentiation of Th1/Th2/Th17 cells. Cytokines secreted by effector lymphocytes recruit and subsequently activate myeloid cells in the intestinal mucosa. The proinflammatory properties of myeloid cells activated in this manner induce the clinical symptoms of IBD (de Souza and Fiocchi 2016).

1.6 Systemic inflammation associated with IBD.

Systemic inflammation associated with IBD is characterised by active circulatory CD4⁺ and CD8⁺ T cell populations and neutrophilia (McCarthy, Rampton et al. 1991, Funderburg, Stubblefield Park et al. 2013). In addition, systemic inflammation is driven by elevated systemic IL-6 and C-reactive proteins levels as well as bacteraemia (Funderburg, Stubblefield Park et al. 2013, Keely, Campbell et al. 2014). IBD-induced systemic inflammation is hypothesized to occur due to the loss of epithelial barrier function and concurrent vasodilation that is associated with colitis. Intestinal permeability induced by colitis may allow microbial products to enter the lamina propria and translocate into the circulatory system. In addition elevated cytokine levels and vasodilation occur in parallel in the intestinal mucosa, potentially allowing inflammatory cytokines access to the circulatory system (Hatoum, Gauthier et al. 2005). Microbial products and cytokines in the circulatory system can activate leucocytes and endothelial cells to express adhesion molecules and chemokines, therefore the presence of these immunomodulatory factors in the circulatory system of IBD patients may present a possible mechanism by which inflammation can occur at extra-intestinal sites.

1.7 Pathophysiology of IBD-induced respiratory disease

As mentioned previously (1.4.2) bronchiectasis and chronic bronchitis are the most prevalent respiratory diseases associated with IBD. Bronchiectasis is a chronic idiopathic disease of the upper airways, defined as permanent dilation of the bronchial tree. Clinically bronchiectasis manifests as progressive cough, purulent sputum, dyspnea, fatigue and mild to moderate airflow obstruction (Whitwell 1952). The current opinion on bronchiectasis pathogenesis is that stimulation of the respiratory mucosal immune system, leads to an exaggerated immune response that can damage the structural components of the airway wall (Fuschillo, De Felice et al. 2008). This inflammatory damage to the airway wall has a detrimental effect on the physical defensive barriers of the lung allowing opportunistic infections to colonise the lower respiratory tract and initiate a “vicious cycle” of infection and inflammation (Sepper, Kontinen et al. 1995) (Figure 1.7). Chronic bronchitis is a respiratory disease similar to bronchiectasis with respect to a pathology induced by a “vicious cycle” of infection and inflammation, however permanent enlargement of the bronchi is not observed. Rather, pathology manifests as bronchial gland hyperplasia, excessive mucous secretions, pulmonary edema and peribronchiolar fibrosis (Hoidal 1994, Hill, Bayley et al. 2000). Another aspect in which chronic bronchitis differs from bronchiectasis is the initial stimulation of the respiratory mucosal immune system. In chronic bronchitis this trigger is considered to be environmental pollutants such as cigarette smoke, as opposed to a bacterial/viral infection in bronchiectasis. However, it is important to note that both bronchiectasis and chronic bronchitis are idiopathic diseases, thus a range of stimuli can initiate pathogenesis, including infection, environmental pollutants and of course IBD (Fuschillo, De Felice et al. 2008).

Genetic risk factors also contribute the development of bronchiectasis and chronic bronchitis. The genetic disorders alpha-1-antitrypsin (A1AT) deficiency and cystic fibrosis are

associated with the risk of developing both these conditions (Hill, Bayley et al. 2000, Zielenski 2000). In regards to IBD-induced respiratory disease there are no identified genetic risk factors identified that predispose to the development of these conditions. For this reason, the immunological factors involved in the pathogenesis of IBD-induced respiratory disease are the focus of this study (Ardizzone, Puttini et al. 2008).

Vicious cycle hypothesis of Bronchiectasis & chronic bronchitis pathogenesis

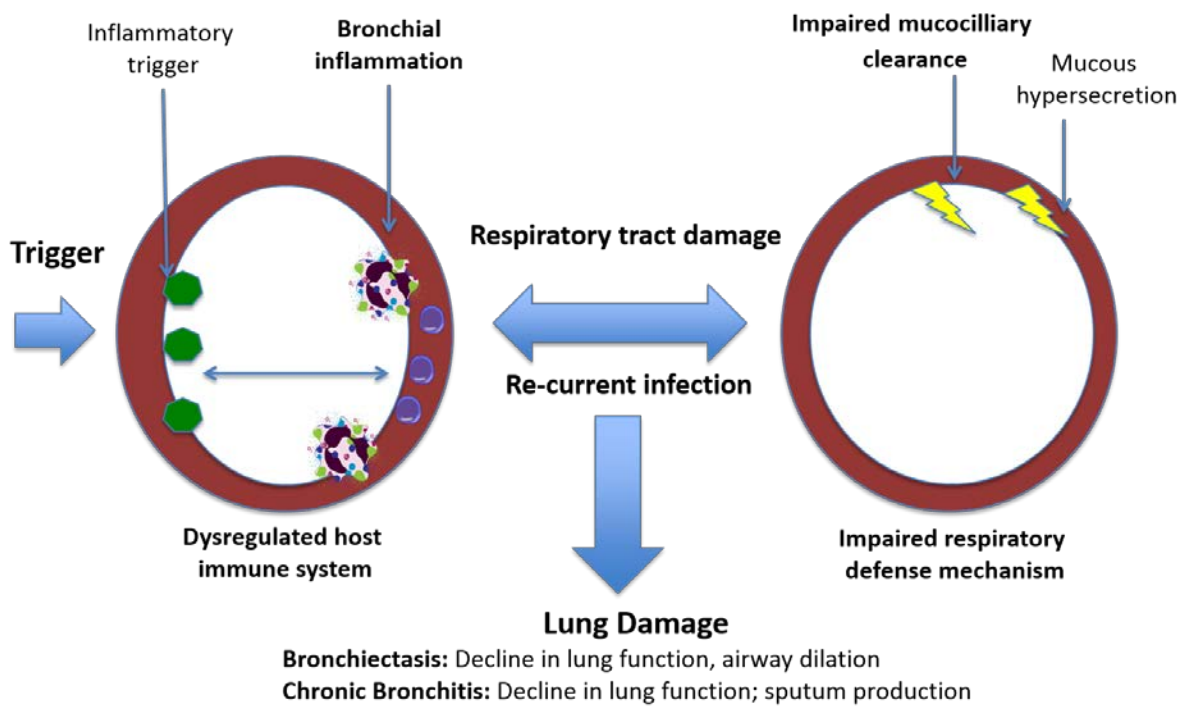


Figure 1.7: Pictorial illustration of the vicious cycle mode of bronchiectasis and chronic bronchitis pathogenesis.

1.7.1 Immunopathology of IBD-induced respiratory disease

The immunopathology of bronchiectasis and chronic bronchitis is comparable in respect to inflammatory phenotype. In both diseases stimulation of the respiratory mucosal immune system results in elevated levels of IL-1 β , IL-8, and TNF which mediate extravasation of neutrophils from the circulatory system into the airway mucosa and lumen (Eller, Lapa e Silva et al. 1994, Loukides, Horvath et al. 1998). Upon activation, infiltrating neutrophils release proteolytic enzymes such as MMP, resulting in the destruction of elastin and collagen which comprises the structural integrity of the lung (Sepper, Kontinen et al. 1995). In addition to innate immune cells, cells of the adaptive immune response have been implicated in the pathogenesis of both conditions, with infiltrating T cell populations present in the airway mucosa (Fournier, Lebargy et al. 1989, Silva, Jones et al. 1989). T cell infiltration in bronchiectasis is generally observed as T cell follicles in the bronchial wall, the phenotype of these lymphocytes remains controversial with conflicting reports regarding CD4⁺/CD8⁺ T cell ratios (Eller, Lapa e Silva et al. 1994). The phenotype of T cells involved in the pathogenesis of chronic bronchitis is more conclusive with CD8⁺ T cells isolated from the airways of chronic bronchitis patients (Saetta, Di Stefano et al. 1998). Thus innate and adaptive immune responses play a role in bronchiectasis and chronic bronchitis pathology. Pathology is driven by the infiltration of active neutrophils into the airway lumen, initiated by an idiopathic trigger, or initiated/sustained by cell-mediated process involving monocytes and T-cells.

1.7.2 Potential mechanisms of IBD-induced respiratory disease

Neutrophilic inflammation is a common feature of the immunopathology observed in the gut and lung of IBD patients. To postulate about the mechanism by which IBD can induce neutrophilic inflammation in the lung, knowledge of the factors that mediate neutrophil

recruitment is required. Neutrophil extravasation is a multistep process that involves cytokine activation of neutrophils and the vascular endothelium (Jagels and Hugli 1992). Cytokine signalling induces the expression of selectins and chemokines on the microvascular endothelium. Selectins mediate the rolling of neutrophils on the endothelium, enabling chemokine signalling to occur. Chemokine signalling promotes cytoskeletal rearrangement, integrin expression and subsequent extravasation of neutrophils into target tissue (Yoshida, Kondo et al. 2006). The cytokines that activate the microvasculature include TNF, IL-1 β and IL-6; these cytokines are elevated in the intestinal mucosa and circulatory system of IBD patients (Neurath 2014). It is possible that gut derived cytokines enter the systemic blood through either evading the filtering effect of the liver on splanchnic blood and/or by inducing cytokine production from liver resident immune cells which then enter the systemic blood. Thus it is possible that systemic inflammatory cytokines originating either directly or indirectly from the intestinal mucosa can activate the pulmonary endothelium and induce the extravasation of neutrophils into the respiratory system. This concept of systemic cytokines mediating gut-lung crosstalk is demonstrated in a model of eosinophil-associated gastrointestinal disease (EGID) associated bronchial hyperresponsiveness (BHR) (Forbes, Smart et al. 2004). In this study Forbes *et al.* demonstrated that intestinal inflammation results in BHR due to increased systemic cytokine levels of GI origin (Forbes, Smart et al. 2004). Furthermore as the lung is highly vascularised and receives the entire cardiac output, the respiratory system is highly vulnerable to the effects of systemic inflammation. This property of the lung is best seen with the high occurrence of acute lung injury in sepsis patients (Schuster, Metzler et al. 2003). Based on this knowledge it is fair to hypothesize that the aberrant mucosal immune responses induced by IBD results in dysregulated systemic cytokine signalling, enabling the dissemination of neutrophilic inflammation to the lung.

There is currently no published experimental evidence to directly support these hypotheses; therefore further research focusing on these pathways is required.

1.8 Murine models of IBD

A number of animal models of IBD have been developed to investigate the pathogenesis of IBD and test the efficacy of new therapeutics. These models include chemically induced models of colitis and transgenic models of spontaneous colitis.

1.8.1 Dextran sulfate sodium (DSS) colitis

DSS colitis is a murine model of chemically induced-colitis. DSS is a sulphated polysaccharide that is toxic to intestinal epithelial cells. DSS forms complexes with medium-chain-fatty acids (MCFAs) to form nanometer sized vesicles that fuse with the membrane of colonocytes. The presence of these vesicles in the cytoplasm of colonocytes affects epithelial function, resulting in epithelial permeability and subsequent intestinal inflammation (Laroui, Ingersoll et al. 2012). Upon administration of DSS mice develop GI pathology that is akin to UC. Histological characteristics of DSS include, epithelial damage, distortion of colonic crypt architecture and severe inflammatory infiltrate within the lamina propria (Kim, Shajib et al. 2012).

1.8.2 2, 4, 6-trinitrobenzenesulfonic acid (TNBS) colitis

TNBS colitis is a chemically induced model of colitis induced by rectal administration of the hapten TNBS. TNBS renders autologous colonic proteins immunogenic resulting in Th1 driven inflammation, autologous to the inflammatory phenotype of CD. Histologically TNBS is characterised by epithelial injury and distortion of crypt architecture (Scheiffele and Fuss

2002). The development of TNBS varies with mouse strain, C57BL/6 mice are relatively resistant to TNBS colitis, whereas BALB/c are highly susceptible. For this reason, BALB/c mice were utilized for TNBS experiments in this study.

1.8.3 Winnie colitis

The *Winnie* mouse strain has a missense mutation in the mucin *Muc2* gene. This mutation results in aberrant mucin 2 (MUC2) biosynthesis culminating in endoplasmic reticulum stress, mucus layer depletion, increased intestinal permeability and intestinal inflammation (Eri, Adams et al. 2011). Intestinal inflammation in *Winnie* colitis is associated with a Th17 mediated mechanism. Histologically *Winnie* colitis manifests as epithelial cell degradation and distortion of crypt architecture akin to the pathology observed in UC (Eri, Adams et al. 2011).

1.9 Study aim

The lung in IBD was the focus of this study because of the high prevalence of respiratory pathologies in IBD patients approximately 40% (Black, Mendoza et al. 2007). While the majority of these pathologies are subclinical, even mild respiratory inflammation can lead to loss of pulmonary function, as is illustrate by the prevalence of dysfunctional spirometry in IBD patients. These respiratory pathologies can lead to substantial morbidity, for this reason the respiratory EIM of IBD were considered a healthcare issue that warranted investigation.

An understanding of the factors that mediate the pathogenesis of these conditions is essential for developing therapeutic strategies, managing diagnosis and predicting the course of disease. For these reasons the overall aim of this study was to understand the mechanism by

which IBD can induce respiratory pathologies. To fulfil this aim the more specific aims were employed;

- 1) To characterize the functional, histological and immunological effects of colitis on the respiratory system in murine models of colitis.
- 2) Identification of pathogenic factors associated with colitis-induced respiratory inflammation through the phenotyping of leucocytes and cytokines involved in colitis-induced respiratory inflammation.
- 3) The completion of intervention based experiments to delineate the function of cytokine signalling in the development of colitis-induced pulmonary inflammation.

Together these aim will provide insight into the immunological mechanism that are involved in the respiratory pathologies associated with IBD

Chapter 2: Methods

2.1 Ethics statement

This study was performed in accordance with the recommendations in the Australian code of practice for the care and use of animals for scientific purposes issued by the National Health and Medical Research Council of Australia. The Animal Care and Ethics Committee of The University of Newcastle, Australia approved all experimental protocols.

2.2 DSS murine model of colitis

Six-week-old female WT C57BL/6 mice were used in experiments. Mice were sex matched, breed and housed in specific pathogen free conditions (SPF) and supplied by Australian bioresources Ltd. To induce colitis mice were given 4% DSS *ad libitum* in drinking water. Acute DSS colitis mice model received DSS for 6 days and were sacrificed at day 7. Age matched controls received drinking water for the duration of the experiment time course. Animals were weighed daily for the duration of the colitis model. At the experimental end-point the colon, lungs, bone marrow and blood were collected.

2.3 TNBS murine model of colitis

Six-week-old female BALB/c mice were used in experiments. Mice were supplied by Australian Bioresources Ltd, breed and housed under SPF conditions. Sex matched controls were used for all experiments. To induce colitis mice were first sensitized to TNBS by epicutaneous application of 1% TNBS in acetone/olive oil solution (4:1). After seven days, mice were anesthetised with isoflourane and intrarectally administered 5 microlitre (μL)/gram (g) body weight of a 2.5% TNBS solution as previously described (Scheiffele and Fuss 2002). TNBS was diluted in a 50% ethanol solution in PBS. Vehicle treated control animals received an equivalent volume of 50% ethanol alone. Mice were sacrificed 7 days post-intrarectal TNBS administration. Mice were weighed for the duration of the experiment, colon and lung tissue was collected at the experiment end-point.

2.4 Winnie spontaneous colitis

Winnie (Win/Win) mice were housed in specific-pathogen-free conditions for 16 weeks. After 16 weeks spontaneous colitis developed and mice were sacrificed. 16-week old litter-matched C57/BL6 mice were used as controls for these experiments.

2.5 Colon histopathology

For subsets of experiments, the colon was excised, measured, cut longitudinally and washed in phosphate buffered saline (PBS). Colons were then rolled, starting at the distal end and running to the proximal end, so that the distal portion of the colon is in the centre and the structure resembles a “Swiss roll”. “Swiss rolls” were immersed in 4 millilitre (mL) of 10% buffered formalin for 24 hours and stored in 70% ethanol thereafter. Colons were embedded

in paraffin and cut longitudinally into 5 micrometre (μm) Sections. Sections were stained with hematoxylin and eosin and histopathology was assessed by light microscopy. Histopathology was scored according to the criteria in Table 2.5 (Marks, Goggins et al. 2015). Histopathology was scored by the PhD student. To mitigate the risk of unconscious bias the PhD student was blinded to treatments/interventions.

Gastrointestinal histopathological scoring system**Score 1 – Inflammatory score**

0 =	No evidence for inflammation
1	Low level of inflammation with scattered infiltrating mononuclear cells (1–2 foci only)
2	Moderate inflammation with multiple foci
3	High level of inflammation with increased vascular density and marked wall thickening
4	Maximal severity of inflammation with transmural leukocyte infiltration and loss of goblet cells.

Score 2 – Tissue injury

0	No epithelial injury
1	Occasional epithelial lesion
2	1–2 foci of ulcerations
3	Extensive ulcerations.

Score 3 – Colitis activity

Colitis activity scored on a scale of 0 – 3, based on the properties below, where 0 = no colitis and 3 = maximal colitis

Hypervascularization

Presence of mononuclear cells

Epithelial hyperplasia

Epithelial injury

Presence of neutrophils

Score 4 – Lymphoid aggregates

Lymphoid aggregates; scored on a scale of 0 – 3

Total score = (score 1 + score 2 + score 3 + score 4)/13

Table 2.5: Gastrointestinal histopathological scoring system for DSS colitis (Marks, Goggins et al. 2015).

2.6 Pulmonary histopathology and alveolar enlargement.

A ventral midline incision from the groin to the chin was performed to expose the thoracic cavity. The diaphragm was cut to collapse the lungs and the ribcage was removed. Lungs were perfused with 0.9% saline by cardiac puncture with a 19-gauge needle. Lungs were fixed by intratracheal inflation with 1.5mL of 10% buffered formalin. The lungs were then excised and immersed in 4mL of 10% buffered formalin for 24 hours and subsequently stored in 70% ethanol. Lungs were embedded in paraffin, cut longitudinally into 5 μ m Sections and stained with hematoxylin and eosin. Histopathology was assessed by light microscopy. Histopathology was scored according to the criteria in Table 2.6 (Horvat, Beagley et al. 2007). Histopathology was scored by the PhD student. To mitigate the risk of unconscious bias the PhD student was blinded to treatments/interventions. Lungs were also stained with periodic acid–Schiff Alcian blue (PAS-AB) for quantification of mucous-secreting cells. Structural damage to alveoli and lung parenchyma was calculated using the mean linear intercept (L_M) method. The L_M method is based on calculating alveoli diameter, when alveoli and parenchymal tissues are damaged; there is an increase in alveoli size. Therefore, alveoli diameter was calculated as a measurement of lung structural damage. To calculate alveoli diameter, 40 images of hematoxylin and eosin stained lung Sections were captured per lung ($\times 40$ magnification). The first 10 images that did not contain airways and/or blood vessels were overlaid with an 11–horizontal line template. Intercepts of alveolar walls with lines were enumerated and the alveolar diameter calculated by dividing the total length of the 11 lines by the average number of intercepts per lung Section.

Histopathological scoring system for mouse lungs**Score 1 - Airways inflammation****0 = Lack of inflammatory cells around airways – Absent****1 = Some airways have small number of cells – Mild****2 = Some airways have significant inflammation – Moderate****3 = Majority of airways have some inflammation – Marked****4 = Majority of airways are significantly inflamed – Severe****Score 2 -Vascular inflammation****0 = Lack of inflammatory cells around vessels – Absent****1 = Some vessels have small number of cells – Mild****2 = Some vessels have significant inflammation – Moderate****3 = Majority of vessels have some inflammation – Marked****4 = Majority of vessels are significantly inflamed – Severe****Score 3 - Parenchymal inflammation (10x magnification)****0 = <1% affected****1 = 1-9% affected****2 = 10-29% affected****3 = 30-49% affected****4 = >50% affected****Total score = (score 1 + score 2 + score 3)/12****Table 2.6: Histopathological scoring system for mouse lungs (Horvat, Beagley et al. 2007)****2.7 Immunohistochemistry for platelet activating factor receptor (PAFR).**

Lung Sections were prepared as described in Section 2.6; paraffin was removed from lung sections by incubation in two changes of xylene and sections hydrated by incubation in decreasing concentrations of ethanol. An antigen retrieval step was conducted after hydration. Sections were incubated in sodium citrate buffer (10mM sodium citrate, 0.05% Tween 20, potential hydrogen (pH) 6.0) for 20 minutes (min) at 100 degrees Celsius (⁰C). After antigen retrieval slides were washed in three changes of tris-buffered saline (TBS). Endogenous

peroxidases were quenched by incubation in TBS containing 1% hydrogen peroxide for 15min at room temperature. After this incubation slides were washed in three changes of TBS containing 0.01% triton X-100 (TBS-TX), blocked in TBS containing 5% bovine serum albumin (BSA) for 1 hour at room temperature. Following blocking, tissue sections were incubated with 50 μ L of anti-PAFR 1:50 (Santa-Cruz Biotech) overnight at 4⁰C. Anti-PAFR antibody was diluted 1:50 in 1% BSA/TBS. Slides were washed with TBS-TX and sections incubated with 50 μ L anti-goat immunoglobulin (IgG) with conjugated with horse radish peroxidase (HRP) for 1 hour at room temperature (R&D Systems). Secondary antibody was diluted 1:100 in 1% BSA/TBS. Antibody isotype controls were not used. Antibody binding was visualised by incubation with the HRP substrate 3–diaminobenzidine (DAB) for 5 minutes. Lung sections were counterstained with hematoxylin, dehydrated in increasing concentrations of ethanol and slides mounted. PAFR staining was determined by the presence of DAB staining in lung sections by light microscopy. PAFR⁺ cells were enumerated by counting the number of cells in a 10mm² microscope reticle at 60x magnification. 10 random fields from each section was counted and the average number of PAFR⁺ positive cells calculated.

2.8 Lung function measurements

Lung function was measured using a forced manoeuvres system (Buxco). Mice were anaesthetized with medetomidine (10mg/kg) and ketamine (100mg/kg) by intraperitoneal injection (IP) and a 2.5cm 20 gauge cannula inserted in the trachea. The tracheal cannula was connected up to a manifold and a volume history manoeuvre performed three times. After this, three fast flow manoeuvres were performed with one-minute intervals between them. This manoeuvre involved inflating the animal's lungs to a tracheal pressure of 25 cmH₂O, holding this pressure for 2 seconds (s) and then exhaling as quickly as possible, until the

respiratory flow declined to 5 mL/s, forced vital capacity (FVC) were calculated from this manoeuvre.

2.9 Airway inflammation, BAL fluid (BAL) collection

Airway inflammation was determined by enumerating leucocytes in BAL fluid. BAL fluid was collected by intratracheal lavage with PBS (two washes, 1mL per wash). The collected fluid was centrifuged (1250 revolutions per minute (RPM), 10min, 4°C) and the cell pellet resuspended in 250µL of PBS and leucocytes enumerated by haemocytometer count.

2.10 Differential leucocyte count BAL fluid

The number of cells in BAL fluid was enumerated and 100,000 cells were spun down onto the centre of a microscope slide using the Cytospin 4 cytocentrifuge (800g, 5min, RT) (ThermoFisher). After spinning the slides were air dried and May-Grunwald Giemsa staining conducted for differential leucocyte cell counts. Slides were incubated in May-Grunwald solution for 5mins, rinsed in H₂O for 1min, incubated in Giemsa stain for 20mins and rinsed twice in H₂O for 5min. After staining slides were left to air dry and coverslipped. All reagents obtained from Sigma Aldrich. The proportion of monocytes/macrophages, neutrophils, lymphocytes and eosinophils were identified based upon their morphological characteristics by light microscopy. 200 cells were counted from each slide at 10x and the percentage monocytes/macrophages, neutrophils, lymphocytes and eosinophils on each slide calculated. Slides were blinded for counting.

2.11 Cellular analysis of Lungs, blood and bone marrow

Single cell suspensions of lungs were prepared by mechanical disruption and enzymatic digestion. Lungs were excised cut into 5 millimeter (mm) pieces and suspended in 1mL of 1

micromole (μM) 4-(2-hydroxyethyl)-1-piperazineethanesulfonic acid (HEPES) buffer supplemented with collagenase and DNAase and incubated for 45 minutes at 35°C . Digested samples were then passed through a $70\mu\text{m}$ cell strainer, the cells centrifuged (1250 RPM, 10min, 4°C), resuspended in 1mL of red blood cell lysis buffer and incubated on ice for 5min. Following incubation, the cells were pelleted and resuspended in 1mL of PBS/2% foetal calf serum (FCS)/15mM EDTA. Pilot studies to validate this method of enzymatic digestion for the analysis of leucocyte phenotypes in murine lungs under inflammation conditions have been conducted previously by colleagues in the Hunter Medical Research Institute and published in The Journal of Immunology (Maltby, Hansbro et al. 2014). Furthermore intra-experimental validation of cell yield and viability was conducted for each experiment. $10\mu\text{L}$ was taken from each sample and cell yield/viability was assessed by trypan blue exclusion count using a haemocytometer.

Blood was collected in an EDTA coated syringe via cardiac puncture and transferred to an EDTA coated tube. Blood was centrifuged (1250RPM, 10min, 4°C), serum removed and the cell pellet subjected to two cycles of red blood cell lysis buffer incubations. Following incubations cells were pelleted and resuspended in $250\mu\text{L}$ of PBS/2% FCS/15mM EDTA and enumerated with a haemocytometer for staining with flow cytometry antibodies. Bone marrow was collected by dissection of the femur and tibia followed by flushing of these bone with PBS/2% FCS/15mM EDTA through a 28-gauge needle. Cell suspension was then centrifuged (1250RPM, 10min, 4°C), resuspended in 1mL of PBS/2% FCS/15mM EDTA and cells enumerated with a haemocytometer for staining with flow cytometry antibodies.

After generation of single cell suspensions, cells were treated with the FC block anti-FcγRIII/II (BD bioscience) in PBS/15mM EDTA for 20min, following this, cells were incubated with fixable viability dye eFlour® 506 (Ebiosciences) for 20min. The cells were then stained with combinations of fluorochrome-conjugated antibodies, for 45min. Lung and blood cells were stained with FITC-conjugated Ly6G, APC-conjugated Gr-1, PerCP-Cy5.5-conjugated CD11b, PE-Cy7-conjugated CD45, PE-conjugated Siglec-F, FITC-conjugated CD4, APC-Cy7-conjugated CD3 and PercP-conjugated CD8. Bone marrow cells were stained with FITC-conjugated Ly6G, APC-conjugated Gr-1, PerCP-Cy5.5-conjugated CD11b, APC-Cy7-conjugated CD45, PE-conjugated Siglec-F, PE-Cy7-conjugated Sca-1, PerCP-Cy5.5-conjugated c-kit, PE-conjugated CD150, FITC-conjugated CD48 and APC-conjugated lineage mixture containing (CD3e, CD11b, B220, Ly-76, & Gr-1). All antibodies supplied from BD biosciences. Following antibody/dye incubations, the cells were washed in PBS/2% FCS/15mM EDTA and fixed for 30min in PBS/2% FCS/0.1% paraformaldehyde (PFA). Cells were analysed on the BD FACSCanto II flow cytometer, using FACS Diva software (BD biosciences). Cell phenotype was resolved utilizing the gating strategy in Table 2.10.

Phenotype	Staining panel/gating strategy
Myeloid cells	CD45 ⁺ CD11b ⁺ Gr1 ⁺
Neutrophils	CD45 ⁺ Gr1 ⁺ CD11b ⁺ Ly6G ⁺ SSChi
Monocytes	CD45 ⁺ Gr1 ⁺ CD11b ⁺ Ly6G ⁻ SSClo
Eosinophil	CD45 ⁺ SiglecF ⁺
Lymphocytes	CD45 ⁺ CD3 ⁺
CD4⁺ T lymphocytes	CD45 ⁺ CD3 ⁺ CD4 ⁺
CD8⁺ T lymphocytes	CD45 ⁺ CD3 ⁺ CD8 ⁺
B lymphocytes	CD45 ⁺ B220 ⁺
Lineage negative stem cells	Lin ⁻ (CD3e ⁻ CD11b ⁻ B220 ⁻ Ly-76 ⁻ Gr-1 ⁻)

	ScaI ⁺ c-kit ⁺
Hematopoietic stem cell (HSC)	Lin ⁻ CD48 ⁻ CD150 ⁺
Multi potent progenitor cells (MPP)	Lin ⁻ CD48 ⁺ CD150 ⁻

Table 2.10: Staining panel and gating strategy for immunophenotyping mouse tissues by flow cytometry.

2.12 Bone marrow colony forming units (CFU) assay

Bone marrow isolate was processed to a single cell suspension as described previously (Section 2.10); cells were plated at 2×10^4 cells/plate in Methocult GF3534 (Stem Cell Technologies). Plates were cultured for 7 days and myeloid colonies (CFU-granulocyte [CFU-G]/CFU-monocyte [CFU-M]/CFU-granulocyte/macrophage [CFU-GM]) were counted by light microscopy, according to manufacturer's instructions.

2.13 Gene expression analysis

Tissue was harvested placed in TRIzol reagent (Invitrogen) and stored at -80°C until analysis. Total ribonucleic acid (RNA) was extracted by phenol-chloroform separation and isopropanol precipitation. Phenol-chloroform extraction is a liquid-liquid extraction technique used to isolated nucleic acids. Through this technique nucleic acids can be isolated from proteins. The phenol-chloroform extraction separates solutions into two phases an organic phase and an aqueous phase. Nucleic acids will dissolve into the aqueous layer and protein/lipids will enter the organic phase. In this way nucleic acids can be resolved from tissue homogenates and cell lysates. Nucleic acids can then be extracted from the aqueous solution through isopropanol precipitation.

Complementary deoxyribonucleic acid (cDNA) was prepared by reverse transcriptase – polymerase chain reaction using a Moloney murine leukemia virus reverse transcriptase

(MMLV-RT) called iScript (Biorad). Quantitative polymerase chain reaction (qPCR) was performed on a ViiA7 real-time PCR machine (Life Technologies) using SYBR green reagents (Biorad). Gene expression was normalized to the reference gene beta-actin utilizing the primer sets described in Table 2.12. Primer sets were designed to cross exon boundaries to specifically amplify messenger RNA products.

Primer	Nucleotide sequence
<i>Il-6</i> forward	5'-CTA CCC CAA TTT CCA ATG CT-3'
<i>Il-6</i> reverse	5'-ACC ACA GTG AGG AAT GTC CA-3'
<i>Il-1β</i> forward	5'- CCC AAC TGG TAC ATC AGC AC-3'
<i>Il-1β</i> reverse	5'- TCT GGT CAT TCA GGA AAA GG-3'
<i>Ccl2</i> forward	5'- TGC TAC TCA TTC ACC AGC AA-3'
<i>Ccl2</i> reverse	5'- GTC TGG ACC CAT TCC TTC TT-3'
<i>Ifn-γ</i> forward	5'- CAA AAG GAT GGT GAC ATG AA-3'
<i>Ifn-γ</i> reverse	5'-TTG GCA ATA CTC ATG AAT GC-3'
<i>Tnf</i> forward	5'- CAA TCA GGG CTT CGT AGG TA-3'
<i>Tnf</i> reverse	5'- GGC CCT GGT TTC TTA TCA AT-3'
<i>Ptafr</i> forward	5'- TTT CGA TAC ACG CTC TTT CC-3'
<i>Ptafr</i> reverse	5'- AGC AGG TCA GCC ATA GTG AG-3'
<i>mACTB</i> forward	5'- GGA GAA AAT CTG GCA CCA CA-3'
<i>mACTB</i> reverse	5'- AGA GGC GTA CAG GGA TAG CA-3'
<i>Tlr4</i> forward	5'- CCT GAT GAC ATT CCT TCT-3'
<i>Tlr4</i> reverse	5'- AGC CAC CAG ATT CTC TAA-3'
<i>Tlr2</i> forward	5'- CGC CCT TTA AGC TGT GTC-3'
<i>Tlr2</i> reverse	5'- CGA TGG AAT CGA TGA TGT-3'

Table 2.12: Oligonucleotide sequences for qPCR assays

2.14 Cytokine analysis

Lung tissue was dissected and placed in radio immunoprecipitation assay buffer (RIPA) (Sigma-Aldrich) and supplemented with halt protease and phosphatase inhibitor cocktail (Thermo, Scientific). To isolate total lung protein, tissue was homogenised and centrifuged (12,000 RPM, 10min, 4⁰C), the supernatant was removed and stored at -80⁰C. Blood was collected by cardiac puncture and centrifuged (12,000 RPM, 10min, 4⁰C); plasma was removed and stored at -80⁰C. Cytokine levels of IL-6, IL-10, CCL2, IFN- γ , TNF- α and IL-12p70 were measured using the mouse inflammation cytometric bead array kit (BD biosciences) according to manufacturer's specifications on a BD FACS Canto II flow cytometer and analysed using the FCAP array software (BD biosciences). IL-1 β cytokine levels were measured using the IL-1 β DuoSet sandwich enzyme-linked immunosorbent assay (ELISA) (R&D systems) according to manufacturer's instructions. Cytokine levels were normalized to total protein concentration, measured using the Pierce BCA Protein Assay Kit (Thermo Fisher Scientific).

2.15 Western blot analysis

Total lung protein was isolated and quantified as described previously, proteins were resolved on 9.5% Mini-Protean TGX stain free polyacrylamide gels (Bio-Rad) and transferred onto polyvinylidene difluoride (PVDF) membranes. Blots were then blocked with 5% BSA in tris-buffered saline and 0.01% tween-20 (TBS-T) for two hours at room temperature. Following blocking blots were incubated with primary antibodies in 1% BSA/TBST at 4⁰C overnight. 5mL of primary antibody diluted 1:500 in 1% BSA/TBS was used. Blots were washed with TBS-T before adding the appropriate secondary antibody. 5mL of secondary antibody diluted 1:1000 in 1% BSA/TBS was used. Antibody isotype controls were not utilized in these experiments. Supersignal west femto maximum sensitivity substrate was used to visualise

membranes by chemiluminescence utilizing the ChemiDoc MP system (Biorad). Primary antibodies utilized were anti-PAFR (Santa-Cruz Biotech) and anti-beta-actin (Abcam). Beta-actin was employed as a loading control. Anti-rabbit and anti-goat IgG HRP (R&D Systems) were the secondary antibodies utilized. The PAFR immunoblot was run under denaturing and reducing conditions. The relative abundance of the protein of interest was quantified using densitometry relative to the loading control with ImageJ software,

2.16 Reagents and buffers

The composition and vendor of all the reagents and buffers used in experiments are described in Table 2.16.

Reagent/Buffer	Composition	Source
DSS	4% DSS in H ₂ O	Affymetrix
TNBS	2/4% TNBS in acetone/olive oil solution (4:1)	TNBS – Sigma Aldrich
Acetone	(CH ₃) ₂ CO	Sigma Aldrich
Olive oil	Extra virgin olive oil	Coles
PBS	NaCl 0.138 M; KCl - 0.0027 M	Sigma Aldrich
Formalin	40% Formaldehyde in H ₂ O	Sigma Aldrich
Ethanol	C ₂ H ₆ O	Sigma Aldrich
Saline	NaCl in H ₂ O	Sigma Aldrich
Sodium citrate buffer	HOC(COONa)(CH ₂ COONa) ₂ , Tween 20, H ₂ O	Sigma Aldrich
Tween 20	Lauric acid (C ₁₂ H ₂₄ O ₂)	Sigma Aldrich
Tris-buffered saline	C ₄ H ₁₁ NO ₃ , NaCl, H ₂ O	Sigma Aldrich
Hydrogen peroxide	H ₂ O ₂	Sigma Aldrich
Bovine serum albumin	Lyophilized powder	Sigma Aldrich
Triton X-100	1% Triton X-100 in H ₂ O	Sigma Aldrich
DAB	3–diaminobenzidine	Sigma Aldrich
Red blood cell lysis buffer	Tris-buffer NH ₄ Cl	Sigma Aldrich
HEPES	4-(2-hydroxyethyl)-1-piperazineethanesulfonic acid	Sigma Aldrich
Collagenase	Collagenase type 1	Sigma Aldrich

DNase	DNase type 1	Sigma Aldrich
EDTA	Ethylenediaminetetraacetic acid	Sigma Aldrich
FCS	Foetal calf serum	Sigma Aldrich
Trizol	TRizol®	Invitrogen
iScript	MMLV-RT	Biorad
May-Grunwald	Acidic acid & methylene blue	Sigma Aldrich
Giemsa	Eosin & methylene azure	Sigma Aldrich

Table 2.16: Composition and vendor of reagents used in experiments.

2.17 Statistics

Comparisons between two groups were made using unpaired *t*-Tests. For analysis of data with two independent variables such as weight loss data a Two-way ANOVA was utilized. For analytical corrections the Grubbs test was used and a P value of < 0.05 was considered a statistical outlier. Analyses were performed using the GraphPad Prism Software (San Diego, California).

Chapter 3: The effect of intestinal inflammation on the pulmonary system in murine models of colitis

3.1 Introduction

The prevalence and phenotype of IBD-induced respiratory pathologies have been documented extensively in the clinical literature (Section 1.4). Despite these findings, our understanding of the mechanism of pathogenesis involved in these conditions is inadequate. One of the limitations to progress in this field is the lack of basic science research examining the mechanisms of gut-lung crosstalk. This seems surprising considering the numerous animal models of colitis that exhibit immunopathologies analogous to human IBD. For instance, the TNBS and DSS murine models of colitis develop systemic inflammation that is driven by bacteraemia and systemic inflammatory cytokines (Reichel, Rehberg et al. 2009, Keely, Campbell et al. 2014). Furthermore weight loss; a clinical systemic symptom of IBD is a pathological feature of both the TNBS and DSS models of colitis (Hendrickson, Gokhale et al. 2002). These studies show that the systemic aspects of IBD develop in murine models of colitis. Thus it can be postulated that murine models of colitis will also develop the common EIM of IBD that are related to systemic inflammation, such as colitis-induced pulmonary inflammation. These models may then provide a basis to study the immunological mechanisms involved in the pathogenesis of IBD-induced respiratory disease.

3.1.1 Hypothesis

In this chapter it was hypothesized that murine models of colitis will develop the common pulmonary pathologies associated with IBD and thus, provide a model to investigate the pathogenesis of colitis-induced respiratory disease.

3.1.2 Aims

To test this hypothesis, the following aims were employed;

- 1) To determine whether the physiological and immunological features of IBD-induced respiratory pathologies would present in murine models of colitis.
- 2) To phenotype the leucocytes and cytokines present in the pulmonary and circulatory system of murine models of colitis with the aim to identify pathogenic factors that can modulate inflammatory responses in the lung.

3.2 Methods

3.2.1 Characterisation of respiratory pathologies in murine models of colitis.

Experiments in this chapter utilised the DSS, TNBS and *Winnie* murine colitis models. Murine models were conducted as described in Sections 2.2 (DSS colitis model), 2.3 (TNBS colitis model) and 2.4 (*Winnie* colitis model).

Colon and lung tissues were collected for histopathological scoring according to Sections 2.5 and 2.6 respectively. Lung function was assessed according to the method described in Section 2.8. Cellular analysis of lung, blood and bone marrow was conducted as described in Sections 2.10. Airway inflammation was assessed by enumeration of leucocytes in BAL fluid as described in Section 2.9. Gene expression and cytokine analysis in colon and lung tissue was performed as described in Sections 2.12 and 2.13. Data analysis was conducted as described in Section 2.15.

3.3 Results

3.3.1 Intestinal pathology in DSS colitis

The aim of this study was to investigate the immunomodulatory factors involved in the development of colitis-induced pulmonary pathology, for this reason an acute time course of DSS colitis was used in experiments. Initial experiments aimed to establish the DSS colitis model in our laboratory and assess the severity of colitis. Severity of colitis was ascertained based on pathological features observed in both murine and human colitis. Such features included weight loss, colon shortening, histopathology and inflammatory cytokine signalling (Corfield, Wallace et al. 2011). Acute DSS colitis mice loss approximately 17% of their initial weight “normalised to control mice” over the 7-day experimental model (Figure 3.3.1A A). Normalised to control mice means that the natural weight gain of a mouse over the experimental time course was taken into account when calculating weight lost due to colitis. This calculation was performed using equation 3.3.1.

Colon shortening is a clinical symptom of colitis induced by severe intestinal inflammation (Kim, Shajib et al. 2012). Significant colon shortening was observed in acute DSS colitis mice compared to controls (Figure 3.3.1A B). Pathology in the colon was determined with a histopathological scoring system that incorporated the extent of inflammatory cell infiltrate in the mucosa/submucosa, tissue injury, colitis activity and lymphoid aggregates (Table 2.5). A significant increase in histopathological scores was observed in acute DSS mice (Figure 3.3.1B, representative images Figure 3.3.1C). Inflammatory signalling was quantified by measurement of cytokines in colon tissue. The protein levels of TNF, IFN- γ , CCL2, IL-6 and IL-1 β are significantly increased in the DSS colitis model (Figure 3.3.1D). These cytokines are up regulated in colon biopsies from IBD patients and are acknowledged to contribute to disease pathology and progression (Neurath 2014). These data demonstrates that DSS colitis

induces gross pathology and histopathological features similar to human IBD. Furthermore, weight loss is a systemic clinical symptom associated with colitis (Abraham and Sellin 2012), thus the pathology induced by DSS colitis is not limited to the GI tract but also has systemic effects.

$$\text{weight loss per day} = \frac{\text{initial weight (day 0)}}{\text{weight at experiment time point (day 0 - 6)}}$$

Average weight loss per day (control mice)

$$= \frac{\text{sum of weight change per day for each mouse}}{n}$$

weight loss per day normalised to controls

$$= \text{weight loss per day} - \text{average weight loss per day (control mice)}$$

Equation 3.3.1. Method utilized to calculate weight loss due to colitis.

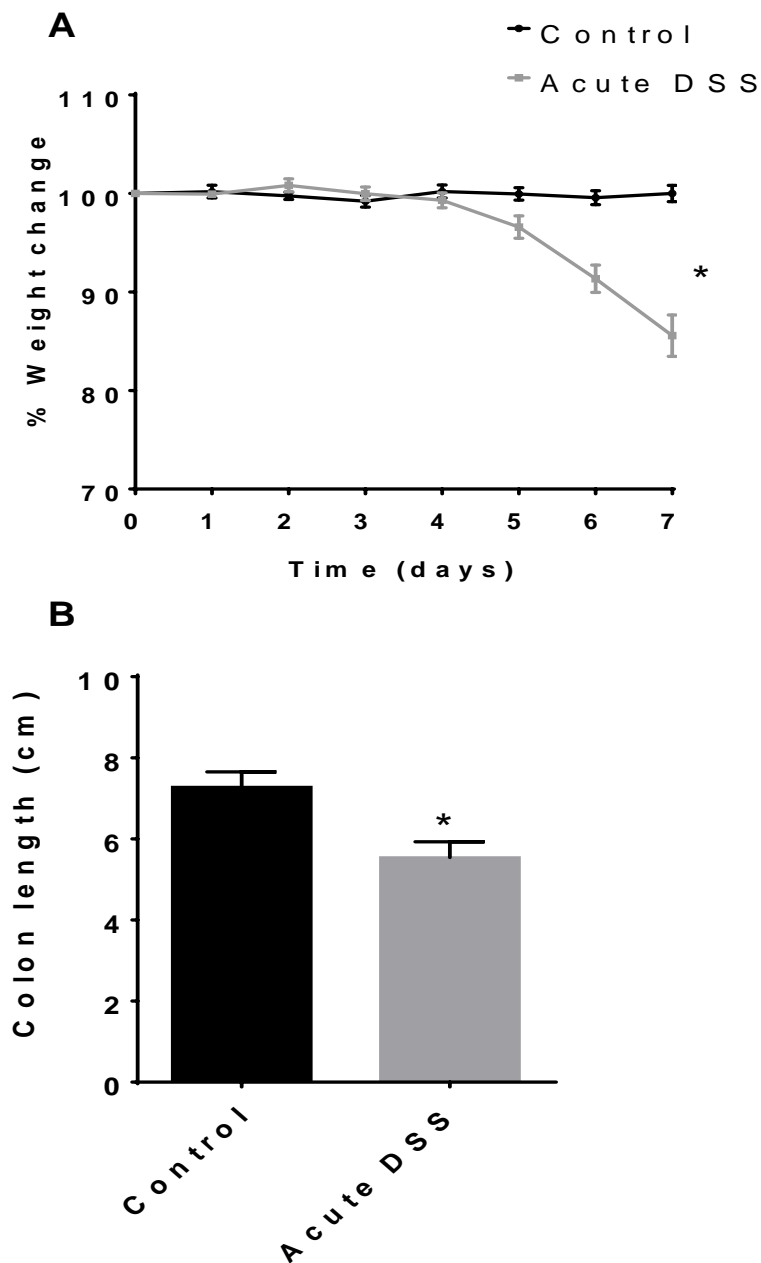


Figure 3.3.1A: Weight loss and colon shortening in acute DSS colitis. WT C57BL/6 mice were given DSS *ad libitum* for 6 days (acute DSS) and sacrificed on day 7, age matched control mice were given drinking water (control). (A) Percentage weight loss normalized to controls over the time course of colitis (n = 6). (B) Colon shortening at experimental endpoint (n = 6). All data represented as mean \pm S.E.M. *= $p < 0.05$ ****= $p < 0.0001$, (A) two-way ANOVA, (B & C) unpaired t-test.

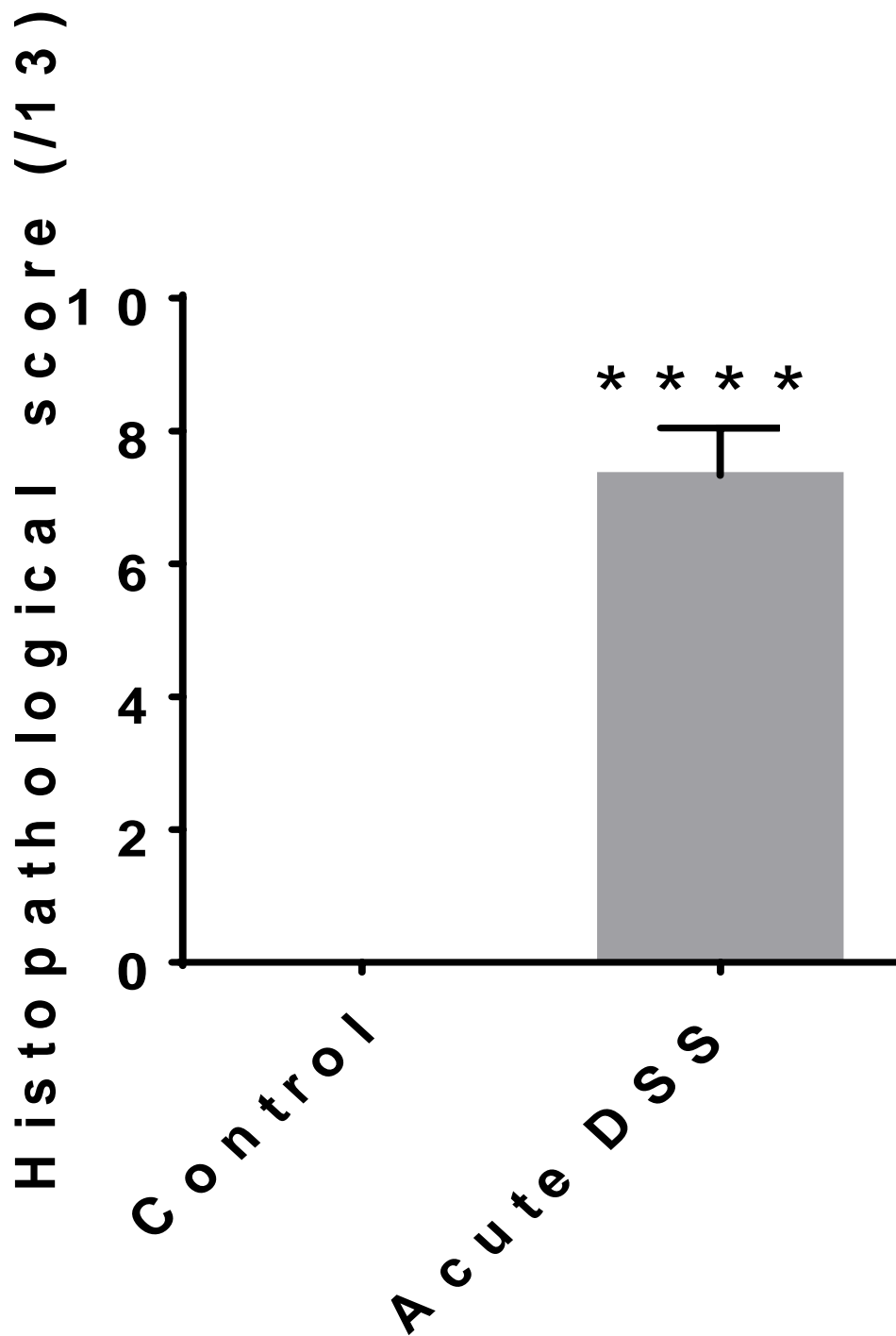
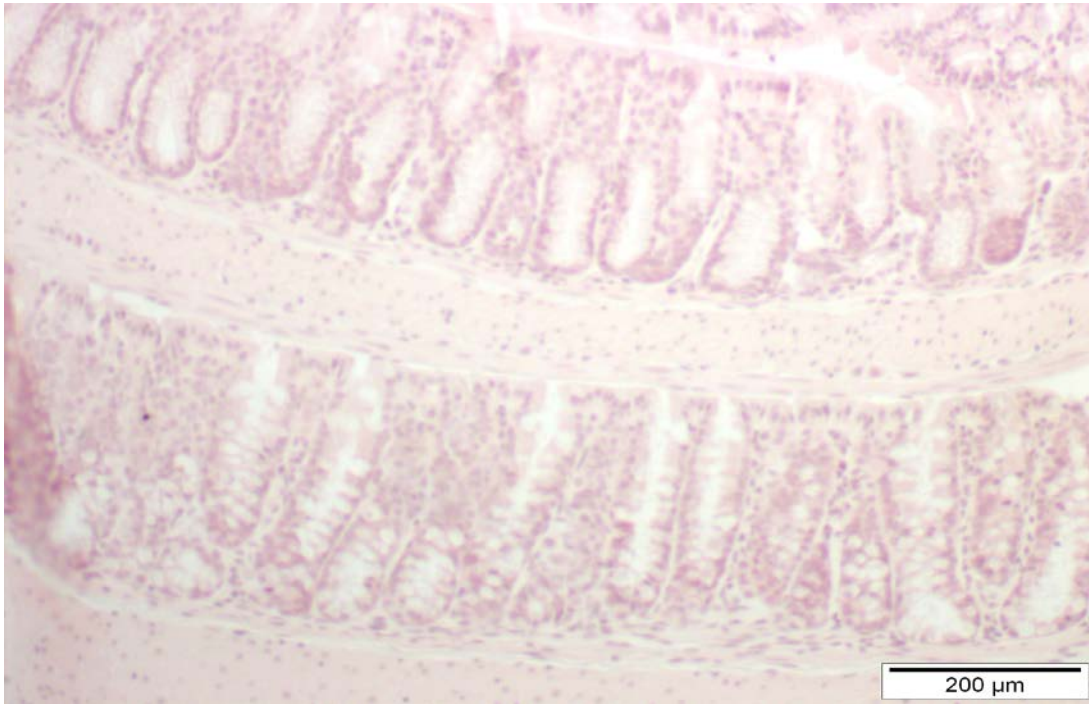
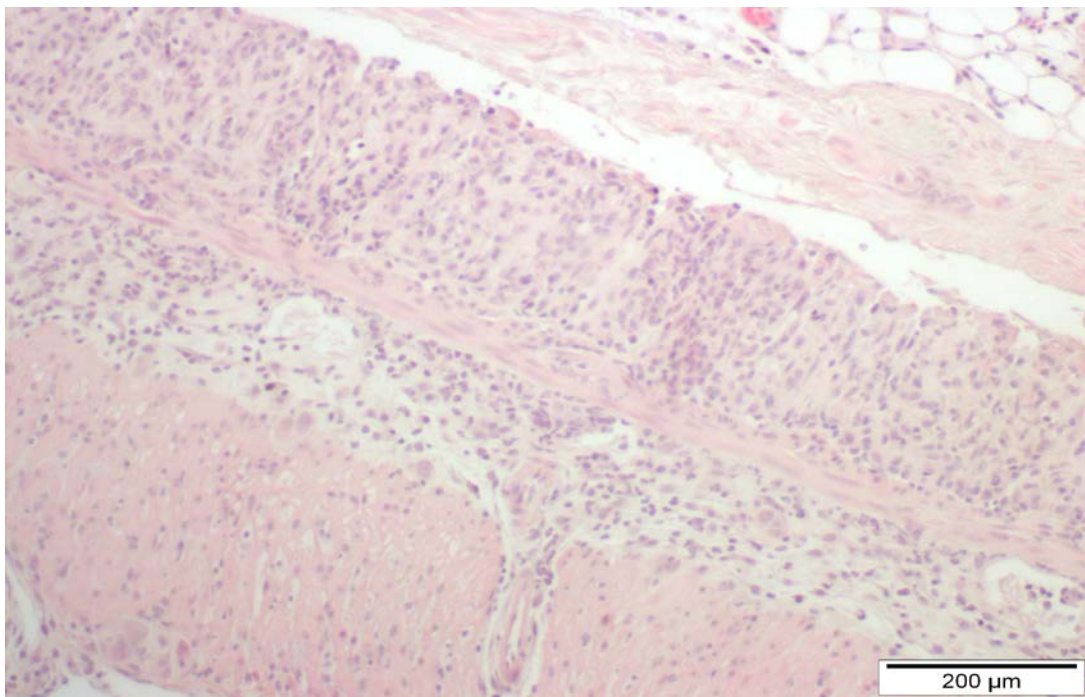


Figure 3.3.1B: Histopathological scores in colon sections from acute DSS colitis. (A) Quantitative analysis of colon histopathology as determined by scoring criteria in Table 2.5 (n = 6). (B) Representative images of pathology observed in the colon of acute DSS colitis mice (10x).



C o n t r o l



A c u t e D S S

Figure 3.3.1C: Colonic histopathology in acute DSS colitis. Representative images of pathology observed in the colon of acute DSS colitis mice (10x).

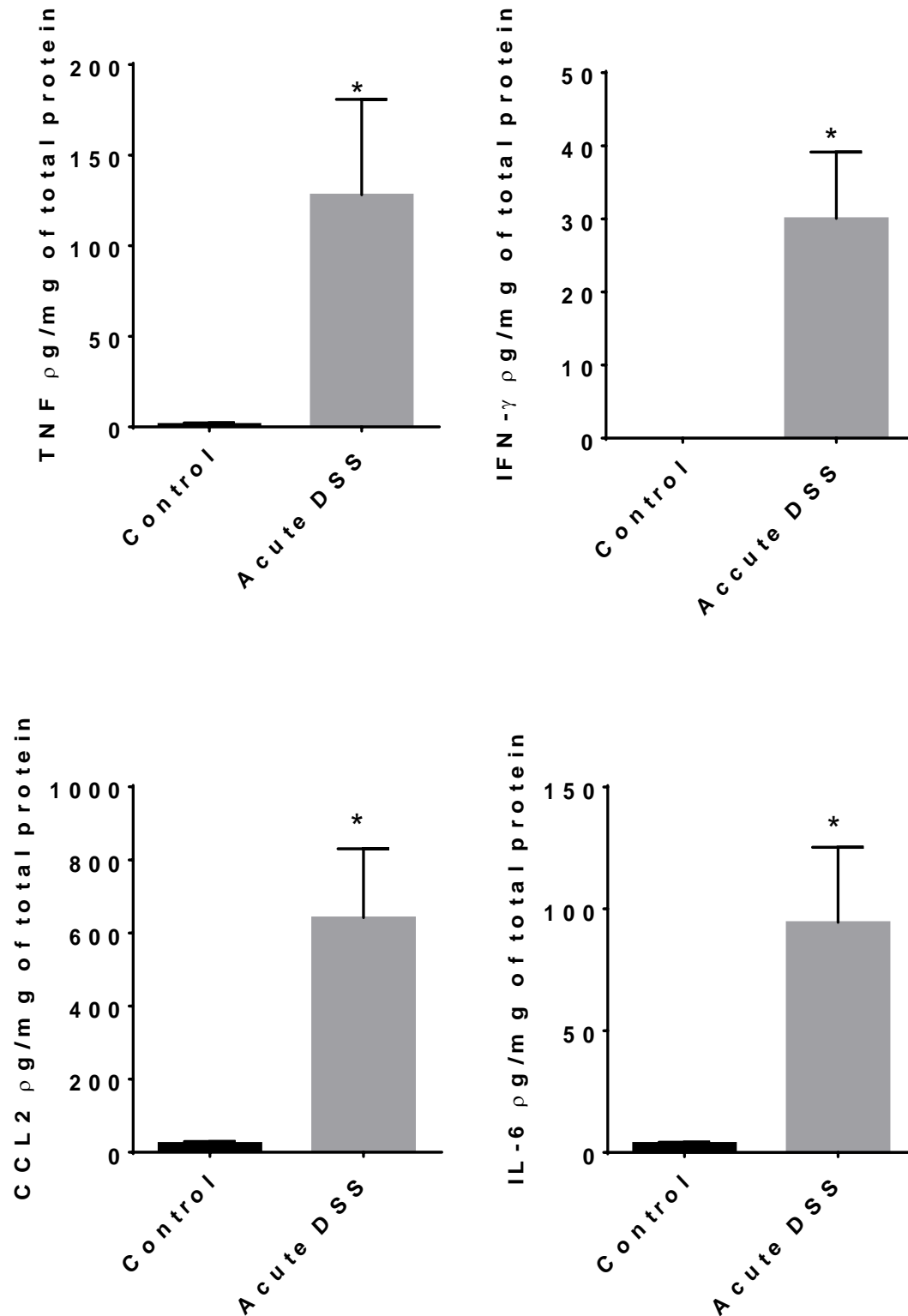
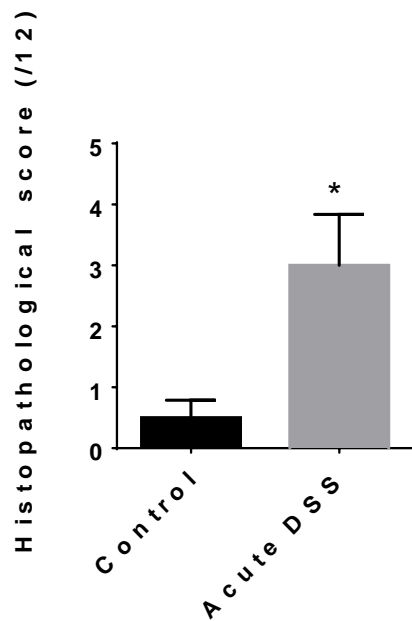


Figure 3.3.1D: Cytokine signalling in the colon of acute DSS colitis. (A) Cytokine levels in the colon of DSS colitis mice as measured by cytometric bead array ($n = 6$). All data represented as mean \pm S.E.M. $^* = p < 0.05$, unpaired t-test

3.3.2 Physiological effects of colitis on the respiratory system.

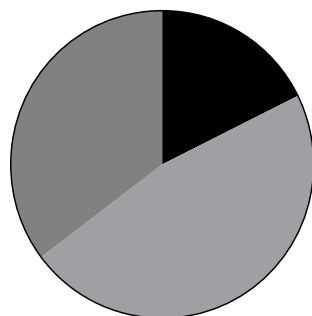
The next aim was to characterise the effect of colitis on the respiratory system. This involved analysing the physiological and immunological effects of colitis on the respiratory system. To assess the physiological effects of colitis; histopathology, lung morphology, lung function and airway mucous hypersecretion was analysed in DSS colitis mice. Histopathology was quantified based on leucocyte congregation around the airways, vasculature and parenchyma, as outlined in Table 2.6. A significant increase in histopathological scores was observed in the lungs of acute DSS colitis mice (Figure 3.3.2A, representative images Figure 3.3.2B). The magnitude of increase in histopathological scores was small, a 3 fold increase was observed. This increase represents mild inflammation, however severe inflammation was not expected as this is an acute colitis model that aims to investigate the initiating stages of disease. Separation of histopathological scores based on anatomical location revealed that the majority of inflammation occurs around the pulmonary vasculature (Figure 3.3.2A B).

A



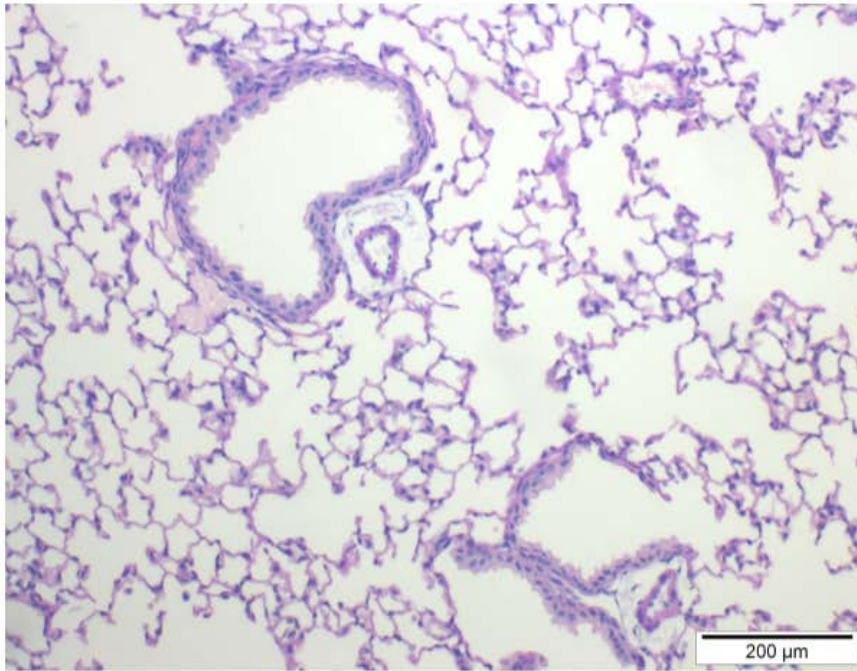
B

Breakdown of
histopathological scores
acute DSS colitis

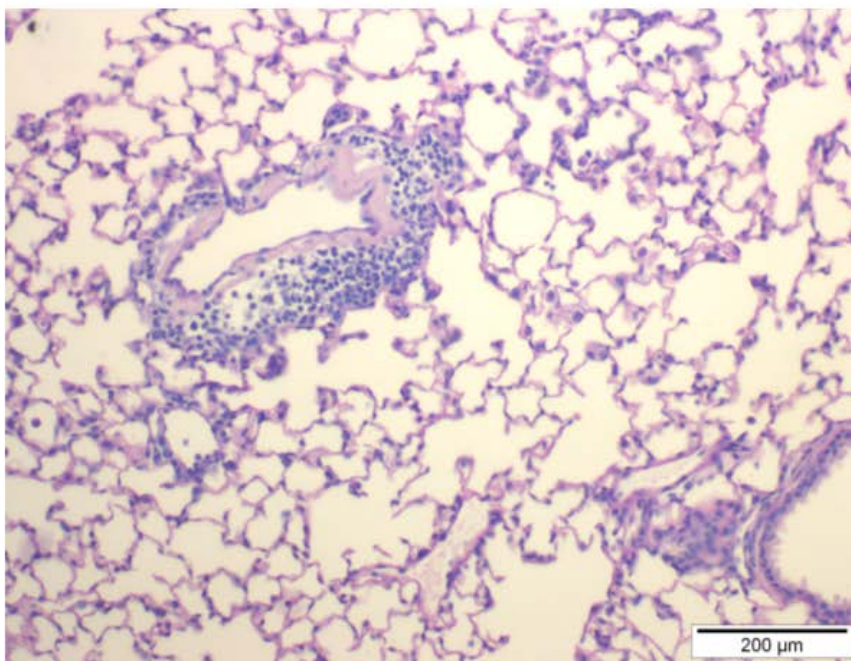


■ Airway 20 %
■ Vasculature 47 %
■ Parenchymal 33 %

Figure 3.3.2A: Histopathological scores in lung sections from acute DSS colitis. (A) Quantitative analysis of lung histopathology in acute DSS colitis as determined by scoring criteria in Table 2.6 (n = 6). (B) Breakdown of histopathological scores based upon the anatomical location of pathology in acute DSS colitis, according to the scoring criteria in Table 2.6 (n = 6). All data represented as mean \pm S.E.M. *= $p < 0.05$, unpaired t-test.



Control



Acute DSS

Figure 3.3.2B: Lung histopathology in acute DSS colitis. Representative images of the histopathology observed in the lung of acute DSS colitis mice (10x).

3.3.2 Physiological effects of colitis on the respiratory system (continued).

To determine whether colitis-induced pulmonary inflammation had any effect on lung morphology, alveoli diameter was calculated using the L_M method. There was no change in alveoli diameter between control and acute DSS colitis mice (Figure 3.3.2C A). To determine the influence of colitis on lung function, the Buxco forced manoeuvres system was utilised to measure FVC (Figure 3.3.2C B). No change in FVC was observed between DSS colitis and control mice. Airway mucus hypersecretion is a feature of chronic bronchitis, one of the more prevalent respiratory diseases associated with IBD, for this reason mucus hypersecretion in the airways of acute DSS colitis mice was analysed. Mucus hypersecretion was assessed using the PAS-AB histology stain. Qualitative analysis of lung Sections stained with PAS-AB were negative for mucous hypersecreting cells (Figure 3.3.2D). Taken together, this data demonstrates that intestinal inflammation induces pulmonary inflammation localised to the pulmonary vasculature and parenchyma, however this inflammation did not induce any changes in lung function, lung structure or airway mucous hypersecretion.

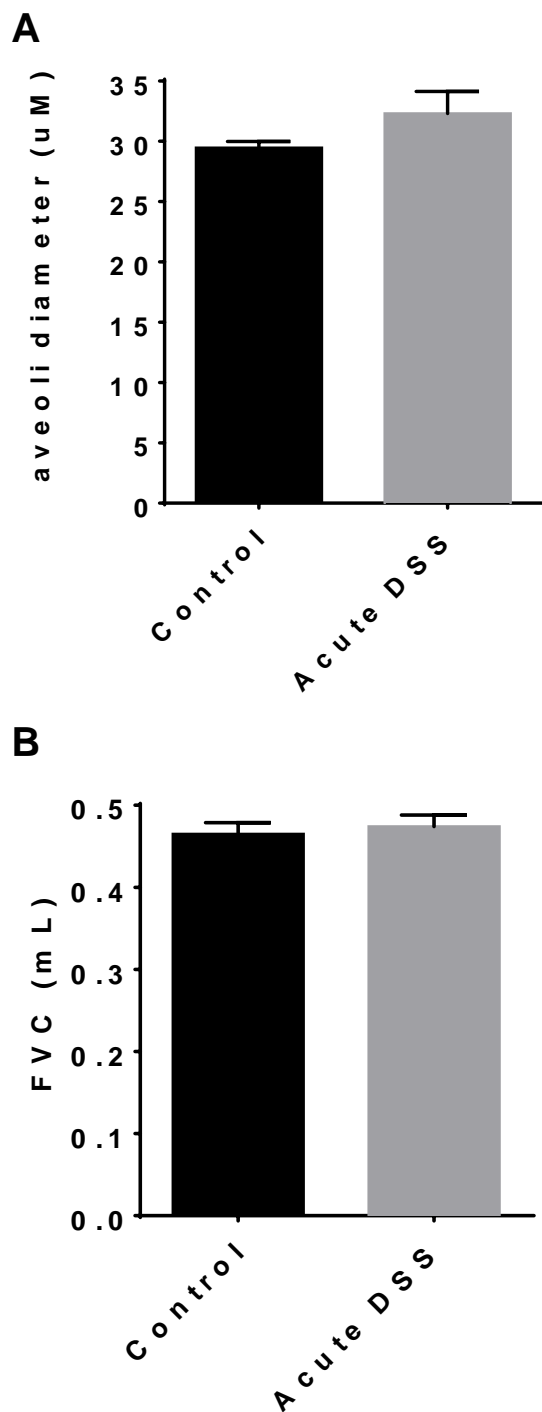
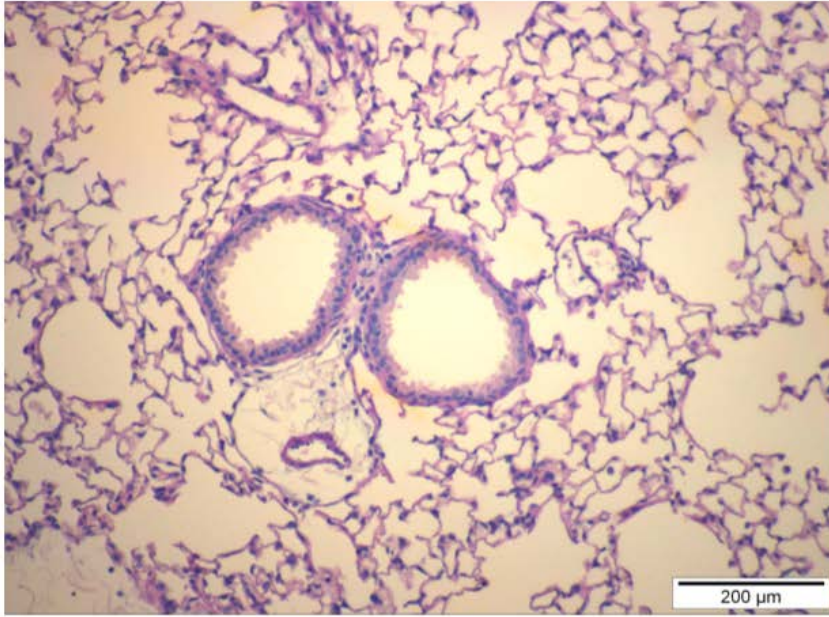
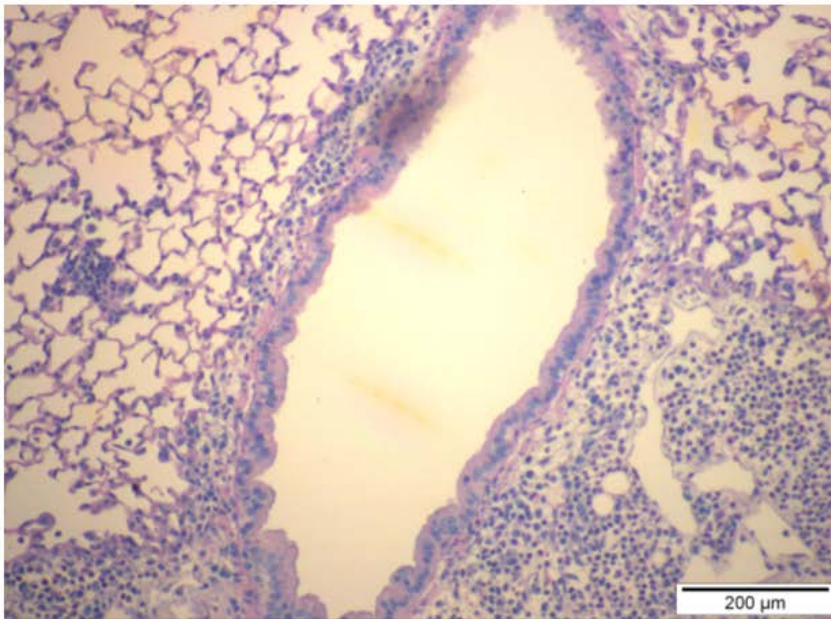


Figure 3.3.2C: Physiological effects of acute DSS colitis on the pulmonary system. (A) The diameter of alveoli in the lungs of acute DSS colitis mice, measured by the mean linear intercept method (n = 6). (B) Forced vital capacity, measured with the Buxco forced manoeuvres system.



Control



Acute DSS

Figure 3.3.2D: PAS-AB staining in lung sections from acute DSS colitis. PAS-AB stain for mucous secreting cells in the lungs of acute DSS colitis mice. Representative images from sections stained with PAS-AB from acute DSS colitis mice. Cells positive for mucous secretion appear bright violet after PAS-AB staining (n = 6).

3.3.3 Immunological effects of colitis on the pulmonary system

Based on the observation that DSS colitis induces pulmonary inflammation (Section 3.3.2), the next aim was to determine the phenotype of leucocytes that enter the lung. Flow cytometry was utilised to address this aim. Two flow cytometry staining panels were designed to resolve lymphocyte and myeloid cell populations according to the gating strategies in Table 2.10. Dot plots demonstrating the gating strategies utilised to resolve leucocyte populations in the lung are provided in the appendices (Figure 8.1.1 & Figure 8.1.2). No change in lymphocyte populations in the lung of acute DSS mice was observed (Figure 3.3.3A A). A significant increase in neutrophils and monocytes entering the lung of acute DSS colitis mice was observed (Figure 3.3.3A B). Airway inflammation was quantified by the enumeration of leucocytes in BAL fluid. No difference in leucocyte numbers in the airways was observed between acute DSS colitis and control mice (Figure 3.3.3B A). The phenotype of leucocytes in BAL fluid was determined by May Grunwald Giemsa staining. No change in the proportion of macrophage, neutrophil, eosinophil or lymphocyte population was observed between control and acute DSS colitis mice (Figure 3.3.3B B). These data corroborate the observation that pulmonary inflammation in DSS colitis mice is localised to the vasculature and parenchymal compartment of the lung. In summary, cellular analysis of the lungs of acute DSS colitis mice revealed an increase in neutrophils and monocytes entering the lung.

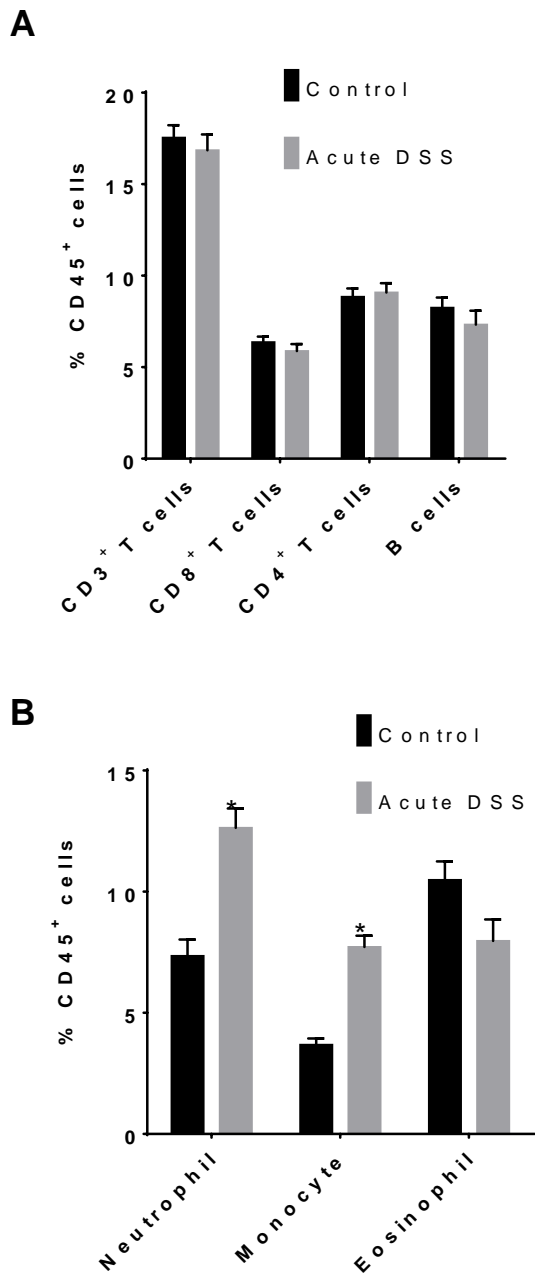


Figure 3.3.3A: Leucocyte phenotype in DSS colitis-induced pulmonary inflammation.

Cells were isolated from whole lung tissue according to the method described in section 2.10

(A) The proportion of lymphoid cells in the lungs of acute DSS colitis mice (n = 6). (B) The

proportion of myeloid cells in the lung of acute DSS colitis mice (n = 6). Cellularity was

determined by flow cytometry utilizing the gating strategy in Table 2.10 and data represented

as %CD45⁺ cells. All data represented as mean ± S.E.M. *=p<0.05, unpaired t-test.

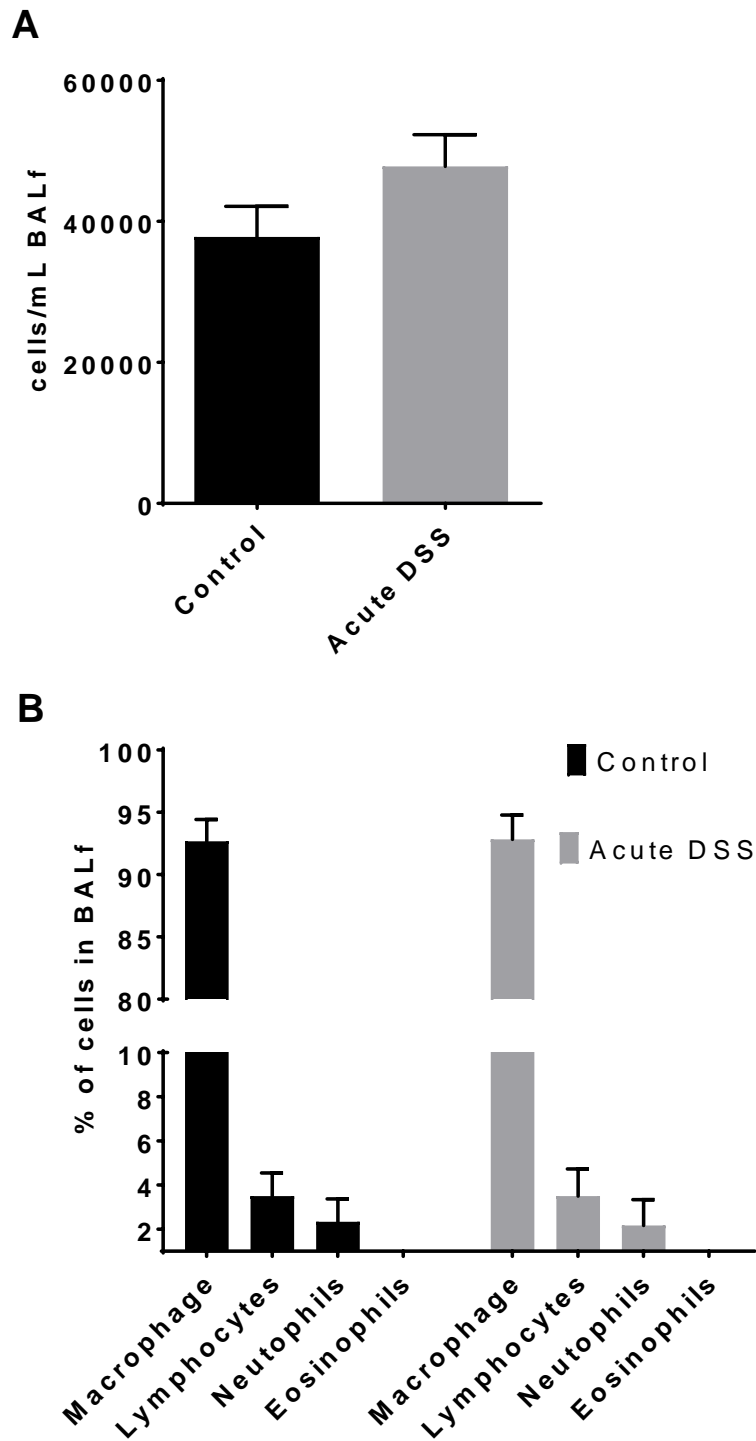


Figure 3.3.3B: Airway inflammation in acute DSS colitis. (A) Airway inflammation in DSS colitis was determined by enumeration of leucocytes in BAL fluid (n = 6). (B) Differential cell count of BAL fluid by May-Grunwald Giemsa staining, data represented as

% cells in BAL. Leucocyte phenotype was determined by morphological characteristics (n = 6).

3.3.4 Gene expression profile in the lungs of DSS colitis mice

As DSS colitis increases the proportion of myeloid cells in the lung (Section 3.3.3), the next aim was to investigate the molecular signalling pathways that initiate the extravasation of myeloid cells. In order to investigate this aim, gene expression analysis of a number of cytokines that are involved in modulating neutrophil and monocyte function was undertaken. The genes chosen for analysis were *IL-1 β* , *Ccl2*, *Ifng*, *Tnf*, *Il6*, *Ptafr*, *Tlr4* and *Tlr2*. IL-1 β facilitates innate immune responses through the expression of chemokines and adhesion molecules that recruit myeloid cells from the bloodstream (Calkins, Bensard et al. 2002). CCL2 is a chemokine that facilitates the chemoattraction of monocytes and neutrophils (Reichel, Rehberg et al. 2009). IFN- γ signalling activates the pro-inflammatory properties of macrophages, which includes the expression of adhesion molecules and chemokine receptors (Held, Weihua et al. 1999). TNF regulates the extravasation of myeloid cells through the production of an array of immunomodulatory proteins (Kim, Shajib et al. 2012). IL-6 initiates the acute phase response to local tissue injury through stimulation of cytokine and chemokine expression (Borish, Rosenbaum et al. 1989). PAFR is the GPCR for PAF. PAF/PAFR signalling can induce the chemotaxis and activation of leucocytes (Ishii, Nagase et al. 2002). *Il1b*, *Ccl2*, *Ifng*, and *Tnf* transcript levels are elevated in the lungs of acute DSS colitis mice (Figure 3.3.4A A - D). *Il6* and *Ptafr* transcript levels were also increased in the lungs of DSS colitis mice (Figure 3.3.4B A & B). Under homeostatic conditions the primary role of neutrophils and monocytes is to defend the physiological system from infection. In this role neutrophils and monocytes phagocytose pathogens and secrete inflammatory cytokines. Neutrophils and monocytes secrete cytokines to recruit leucocytes to aid in bactericidal and/or anti-viral responses. Cytokine expression in this process is regulated in part by the PRR toll-like receptor 4 (TLR4) and toll-like receptor 2 (TLR2) (Kawai and Akira 2011). For this reason, *Tlr4* and *Tlr2* gene expression was analysed in the lung of DSS colitis mice. The

expression of *Tlr4* and *Tlr2* was not changed in the lungs of DSS colitis mice (Figure 3.3.4B C & D). Studies from Oshikawa *at al.* have shown that TLR2 signalling induces *Tlr2* gene expression (Matsuguchi, Musikacharoen et al. 2000, Oshikawa and Sugiyama 2003) this mechanism of self-regulation is considered to have evolved to accelerate innate immune responses to pathogens. Thus, *Tlr2* expression can be considered a marker of TLR2 signalling. TLR4 signalling can also induce *Tlr4* gene expression in a self-regulatory pathway (Matsumura, Ito et al. 2000), however this mechanism is dependent upon the agonist. LPS has been reported to induce self-regulation of *Tlr4* expression, however the cytokines IL-1, IL-6 and TNF have not (Matsumura, Ito et al. 2000). Furthermore, TLR4 self-regulatory gene expression also varies dependent on tissue type. In the lung LPS induced TLR4 signalling induces *Tlr4* expression, therefore *Tlr4* expression can be utilized as a marker of TLR signalling (Matsumura, Ito et al. 2000). Taken together these data show that the genes of inflammatory cytokines are upregulated in the lungs of acute DSS colitis and that this phenotype is not related to TLR signalling. As neutrophil and monocyte infiltration into the lung occurs independent of *Tlr4* and *Tlr2* expression, these data imply that an alternative cytokine signalling pathway is involved. One such pathway is PAFR signalling, PAFR signalling is known to induce neutrophil chemotaxis and induce the synthesis of cytokines involved in monocyte activation (Moreno, Alves-Filho et al. 2006). PAFR signalling is therefore a possible explanation for the inconsistency in TLR expression, this possibility was investigated experimentally in chapter 5 and 6.

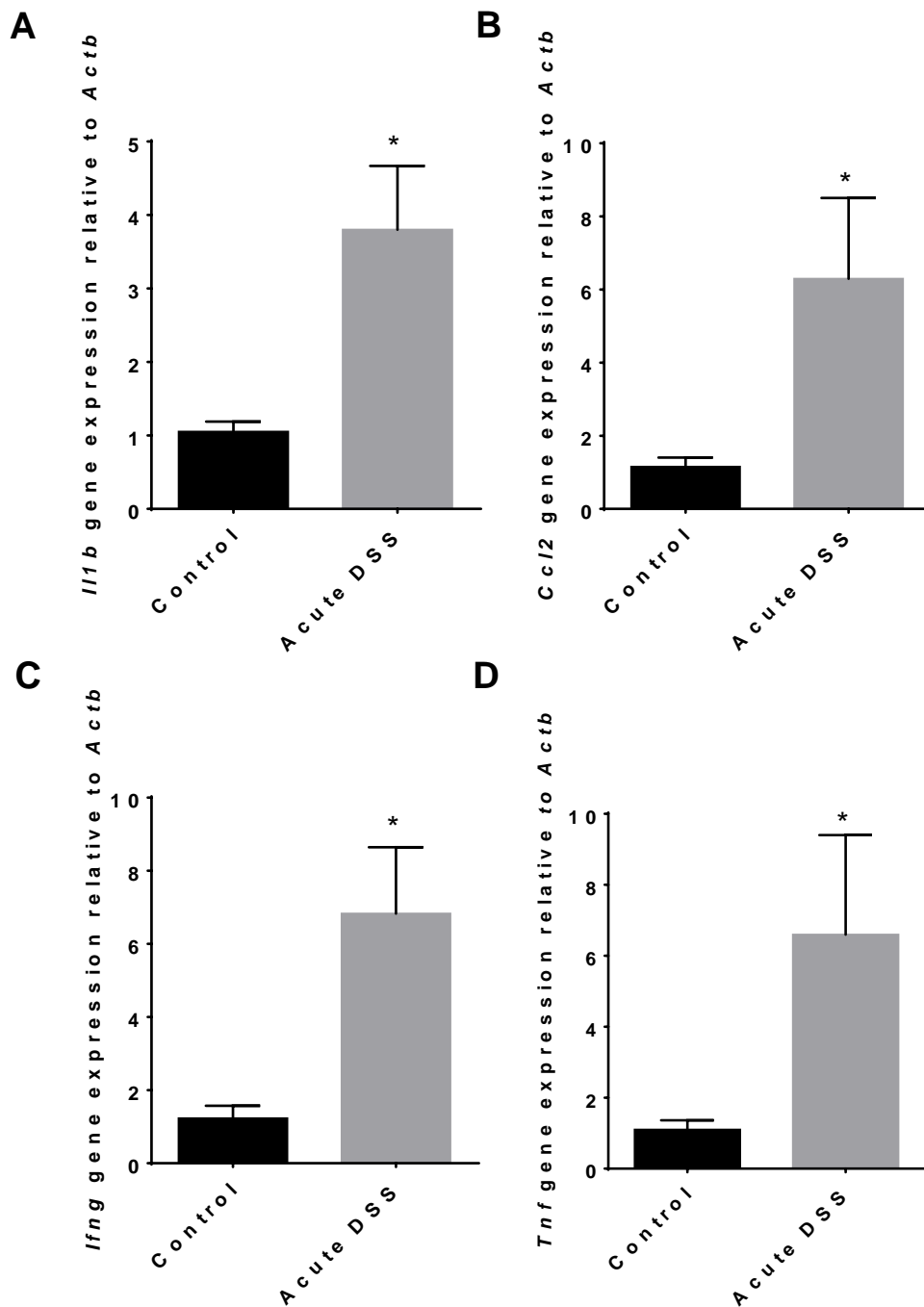


Figure 3.3.4A: Gene expression profile in the lungs of DSS colitis. Gene expression profile in the lung of DSS (A) *Il1b* (B) *Ccl2* (C) *Ifng* and (D) *Tnf* (n = 6). Gene expression was quantified by qPCR. All data represented as mean \pm S.E.M. *= $p < 0.05$ **= $p < 0.01$, unpaired t-test.

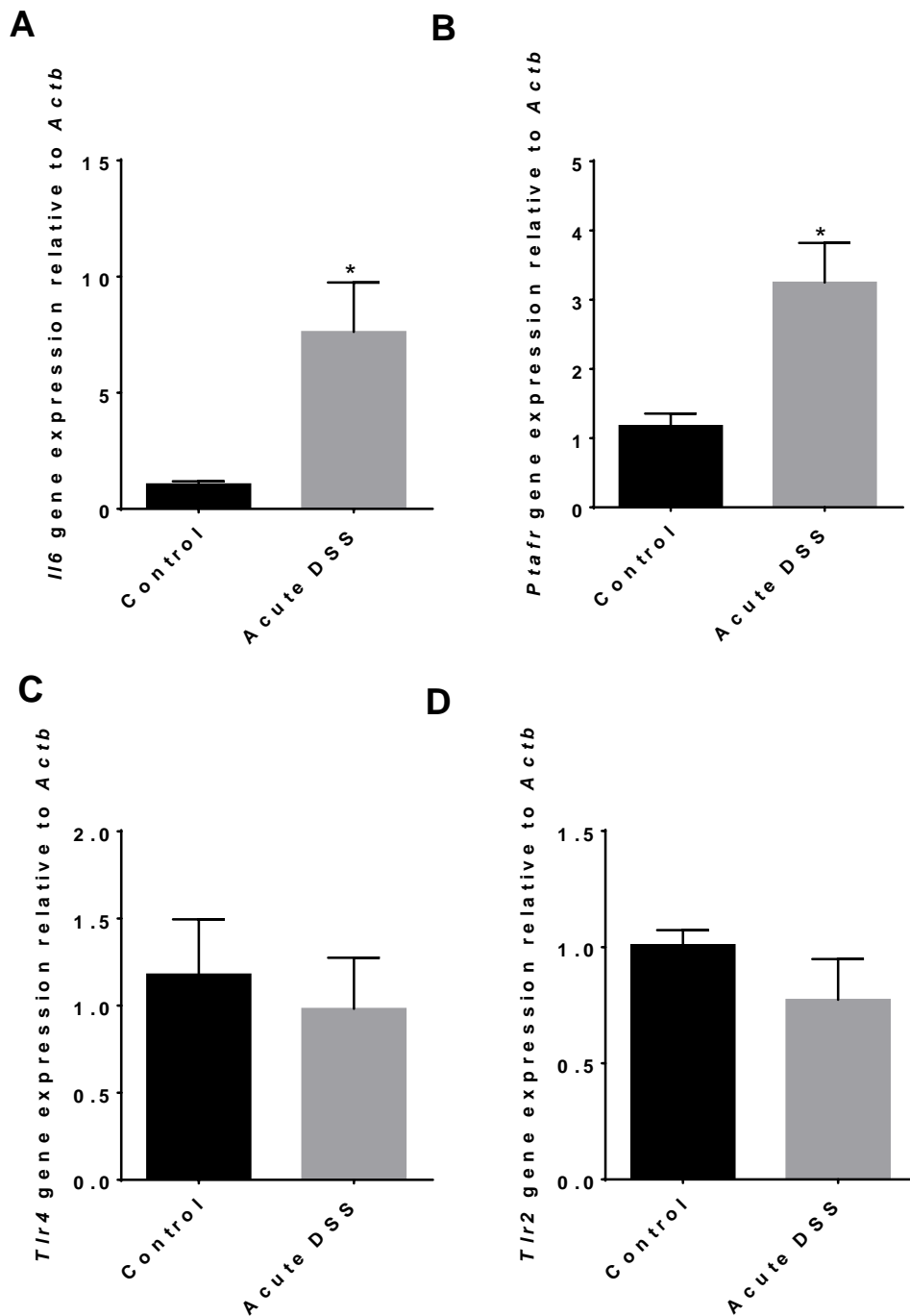


Figure 3.3.4B: Gene expression profile in the lungs of DSS colitis continued. Gene expression profile in the lungs of acute DSS colitis mice. (A) *Il6* and (B) *Ptafr* (C) *Tlr4* (D) *Tlr2* in lung tissue (n = 6). Gene expression was quantified by qPCR. All data represented as mean \pm S.E.M. *= $p < 0.05$ **= $p < 0.01$, unpaired t-test.

3.3.5 Mediators of inflammation in DSS colitis-induced pulmonary inflammation

To determine whether the gene expression observed in Figure 3.3.4 equated to protein translation, quantitative analysis of IL-1 β , CCL2, IFN- γ , TNF, IL-6 and PAFR protein levels was conducted in lungs of acute DSS colitis mice. IFN- γ , TNF and IL-6 protein levels were not increased in the lungs of acute DSS colitis mice. The active form of IL-1 β is generated from the inactive cytoplasmic precursor form pro-IL-1 β . Cleavage of pro-IL-1 β by caspase-1 results in extracellular release of active IL-1 β . As pro-IL-1 β levels are directly related to active IL-1 β secretion, pro-IL-1 β can be considered a pseudo marker of IL-1 β activation and secretion (Lopez-Castejon and Brough 2011). A significant increase in pro-IL-1 β and CCL2 protein levels was observed in the lungs of acute DSS colitis mice (Figure 3.3.5A A & B)

PAFR protein levels were measured by western blot, PAFR was detected at a molecular weight of 116kDa. As PAFR is expressed in lung tissue under physiological conditions quantitative analysis by densitometry was conducted. A statistically significant increase in PAFR protein levels was observed in the lung of acute DSS colitis mice (Figure 3.3.5B A & B), albeit the magnitude of this increase was small (2 fold increase in relative density, figure 3.3.5B A). While the protein bands may not be convincing visually this can be attributed to two factors. Firstly, acute DSS colitis induced a relatively small increase in *Ptafr* gene expression (approximately 3 fold increase in gene expression, figure 3.3.4B B), thus it is unlikely that this small increase in gene expression has the ability to induce PAFR protein expression at a level that can be measured qualitatively by visual inspection. Secondly, the blot is over resolved, this is because the PAFR protein levels present on the membrane were low and therefore a greater chemiluminescence exposure time was required. This effect was observed even when 1 μ g of protein was loaded on the gel. Further experiments where

conducted to determine whether this small increase in PAFR protein expression has a functional role in modulation pulmonary inflammation in acute DSS colitis.

Taken together these data indicating that IL-1 β , CCL2 and PAFR are involved in the modulation of colitis-induced pulmonary inflammation. These data also imply that leucocytes in the lung of DSS colitis mice are in an active state as IL-1 β and CCL2 expression is a feature of activated myeloid cells (Strober and Fuss 2011) The absence of TNF, IFN- γ and IL-6 protein levels may be due to the post-transcriptional modifications that inhibit the translation of these genes to functional protein levels, or that IL-1 β and CCL2 are upstream of these molecules in the context of this inflammatory signalling pathway.

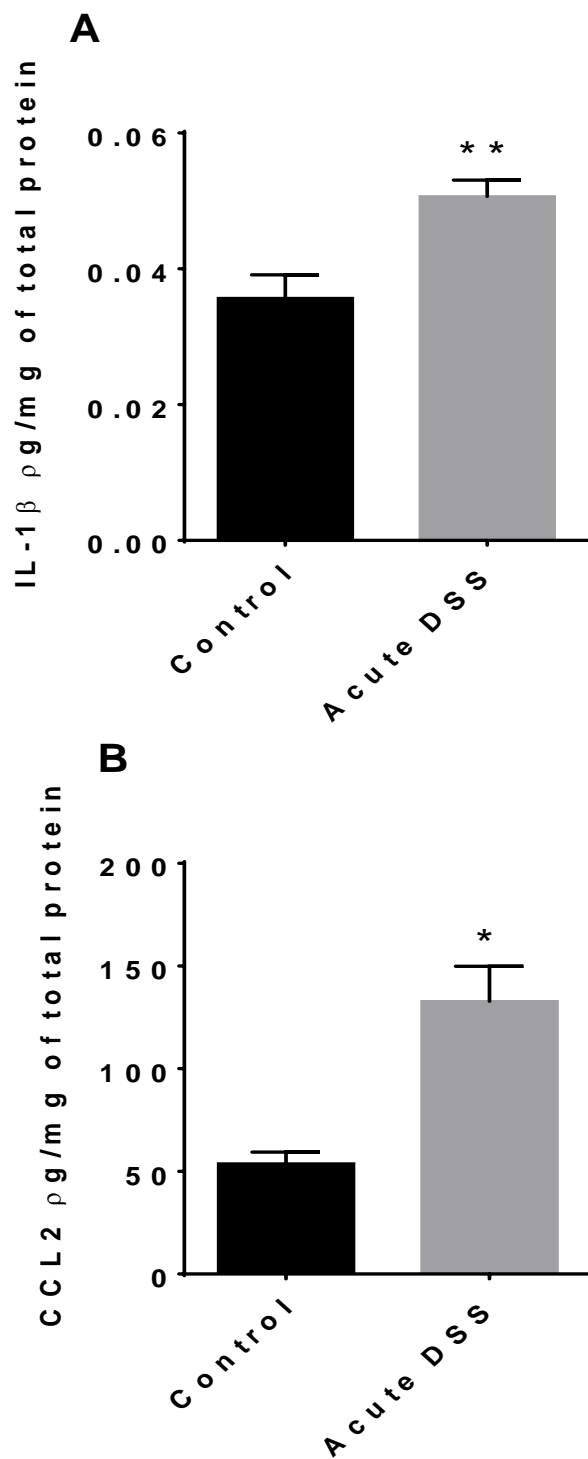
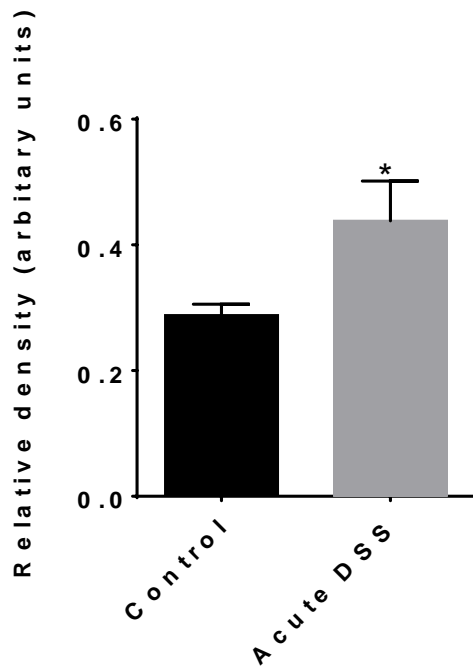


Figure 3.3.5A: IL-1 β and CCL2 protein levels in the lungs of DSS acute colitis. (A) Pro-IL-1 β and (B) CCL2 protein levels in the lungs of acute DSS colitis mice. Pro-IL-1 β was measured by ELISA and CCL2 was measured by cytometric bead array. All data represented as mean \pm S.E.M. *= p <0.05, unpaired t-test.

A



B



Figure 3.3.5B: PAFR protein level in the lungs of acute DSS colitis. The level of PAFR in the lungs of DSS colitis mice was quantified by western blot. (A) Densitometry was utilized to empirically quantify protein bands, protein bands (B) (n = 6). All data represented as mean \pm S.E.M. * = p<0.05.

3.3.6 Systemic inflammation in acute DSS colitis

Myeloid cells utilise the circulatory system to enter and exit tissues of interest; cell extravasation is mediated in part by cytokines in the circulatory system. Thus I sought to investigate the effect of colitis on systemic inflammation and determine whether there is a relationship between the systemic and pulmonary inflammation associated with colitis. Systemic inflammation was assessed by cellular analysis of blood and quantification of inflammatory cytokines in serum. An increase in the proportion of neutrophils in the circulatory system of acute DSS colitis was observed (Figure 3.3.6A A). Furthermore, there was a correlation between the percentage of neutrophils in the blood and the percentage of neutrophils in the lung, suggesting that there is a relationship between systemic inflammation and the magnitude of colitis-induced pulmonary inflammation (Figure 3.3.6B). Cellular analysis was conducted by flow cytometry, representative dot plots demonstrating the gating strategy utilised to resolve leucocyte populations is provided in the appendices (Figure 8.1.3A & B). The protein level CCL2, IFN- γ , TNF, IL-6 was quantified in the serum of acute DSS colitis mice. A significant increase in systemic IL-6 levels was observed colitis mice (Figure 3.3.6B). Together these data show that DSS colitis induces systemic inflammation that is characterised by neutrophilia and elevated systemic IL-6 levels.

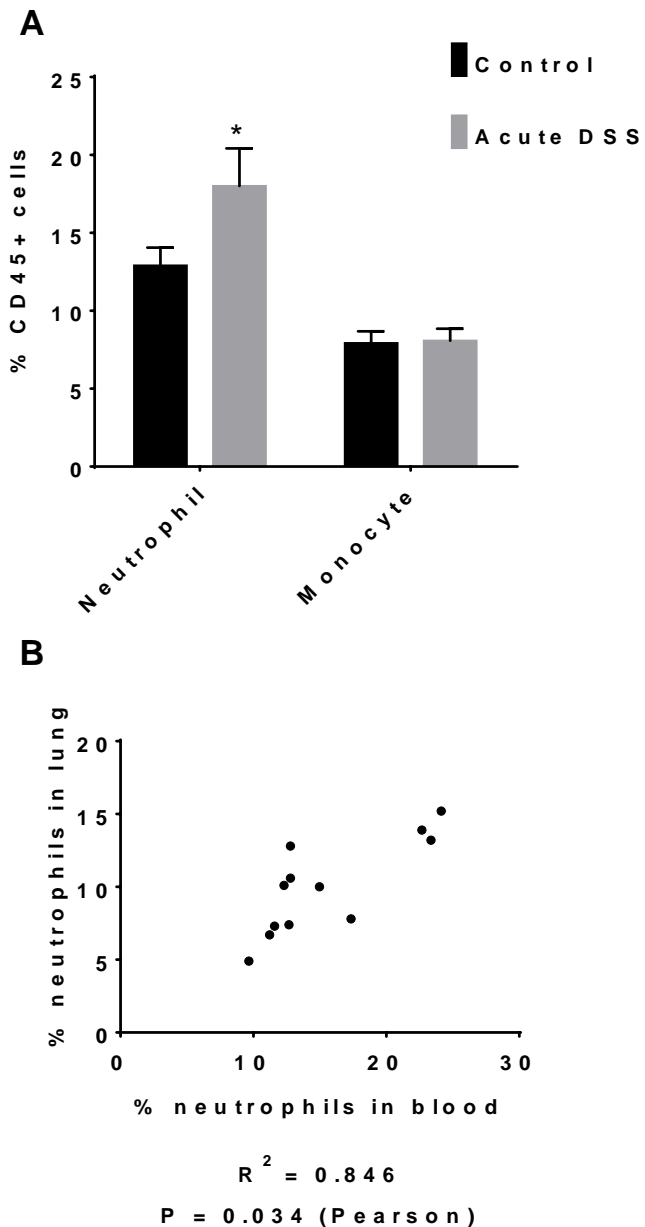


Figure 3.3.6A: Systemic inflammation in acute DSS colitis. (A) The proportion of neutrophils and monocytes in the circulatory system of acute DSS colitis mice, measured by flow cytometry according to staining panel in Table 2.10 (n = 6). (B) A correlation between the number of neutrophils in the circulatory system and the lung (n = 6) neutrophil numbers quantified by flow cytometry according to the staining panel in Table 2.10. All data represented as mean \pm S.E.M. * = $p < 0.05$, unpaired t-test.

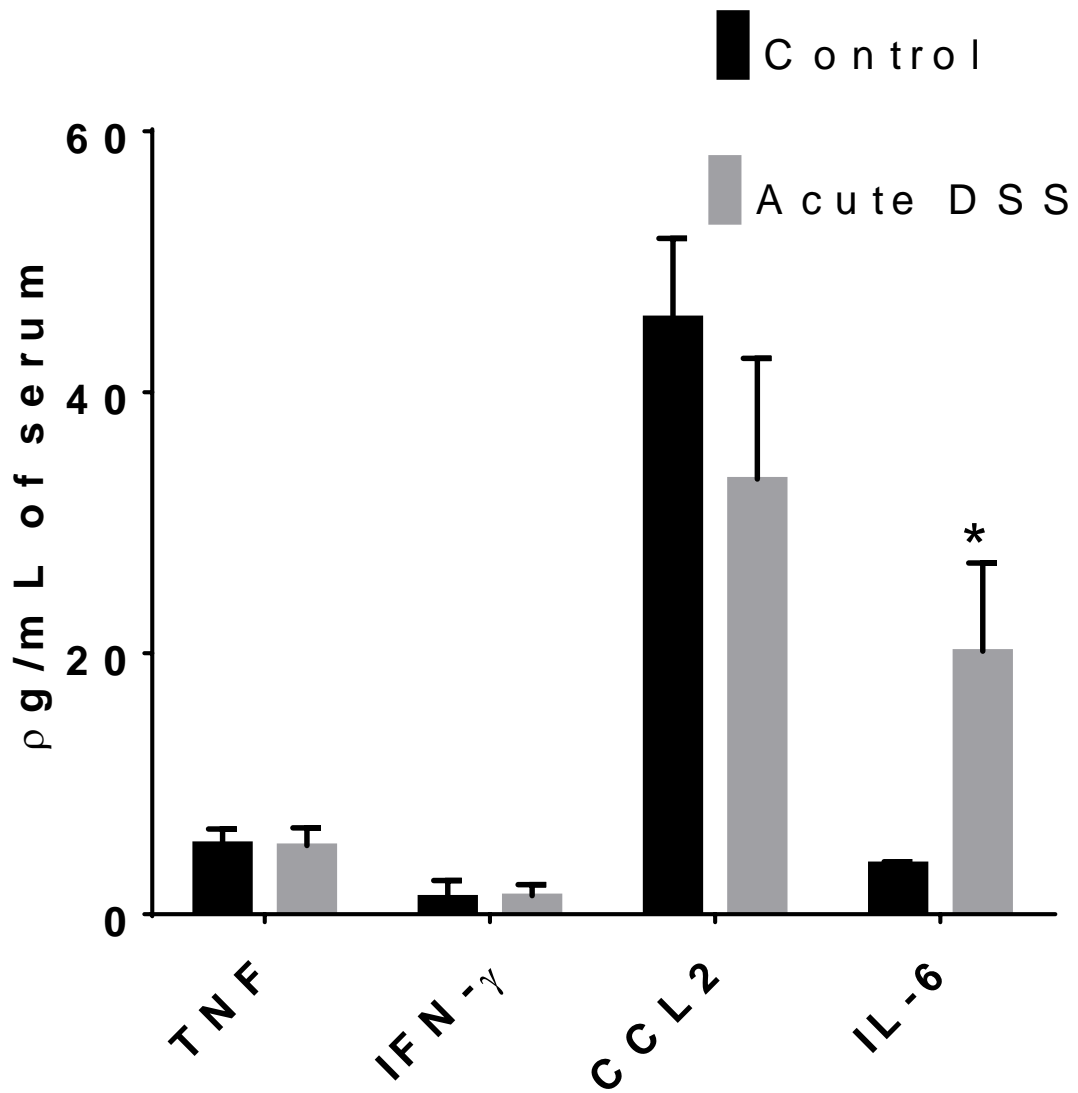


Figure 3.3.6B: Inflammatory cytokines in the circulatory system of acute DSS colitis.

Systemic cytokines in the serum of acute DSS colitis mice, measured by cytometric bead array (n = 6). All data represented as mean \pm S.E.M. * = p<0.05.

3.3.7 Myeloid cell production in DSS colitis

As myeloid cell levels are increased in both the circulatory and pulmonary system as a result of intestinal inflammation, I sought to investigate the effects of intestinal inflammation on myeloid cell development in the bone marrow. It was found that intestinal inflammation results in an increase in lineage negative cells, these cells do not express mature cell lineage markers and thus represent stem and progenitor cells (Figure 3.3.7A A). The increase in progenitor and stem cells can be attributed to an increase in multi-potent progenitor cells (MPP), not hematopoietic stem cells (HSC) (Figure 3.3.7A A). MPP cells have lost their capacity for self-renewal and are committed to the production of hematopoietic cells. A bone marrow CFU assay was utilised to functionally quantify whether these progenitor cells are committed to differentiation into the myeloid compartment of hematopoietic cells. A significant increase in granulocyte/monocyte CFU was observed (Figure 3.3.7A B), this assay demonstrates that MPP cells are committed to the production of granulocytes and monocytes. Cellular analysis of mature myeloid cells in the bone marrow revealed a significant decrease in neutrophils and an increase in monocytes (Figure 3.3.7B). The decrease in mature neutrophils in the bone marrow can be attributed to the systemic inflammation associated with colitis. This is because inflammatory cytokines in the circulatory system stimulate rapid egress of neutrophils from the bone marrow niche to the circulatory system. The increase in monocytes in the bone marrow may be due to the time point at which this analysis was undertaken. Neutrophils are the first cells to respond to acute tissue injury followed by monocytes, as this is an acute colitis model, it is hypothesized that the kinetics of monocyte production and egress from the bone marrow will not occur in parallel to neutrophils potentially accounting for the differences between these cell populations. Representative dot plots from experimental groups are provided in the appendices Figure (8.1.4 A & B)

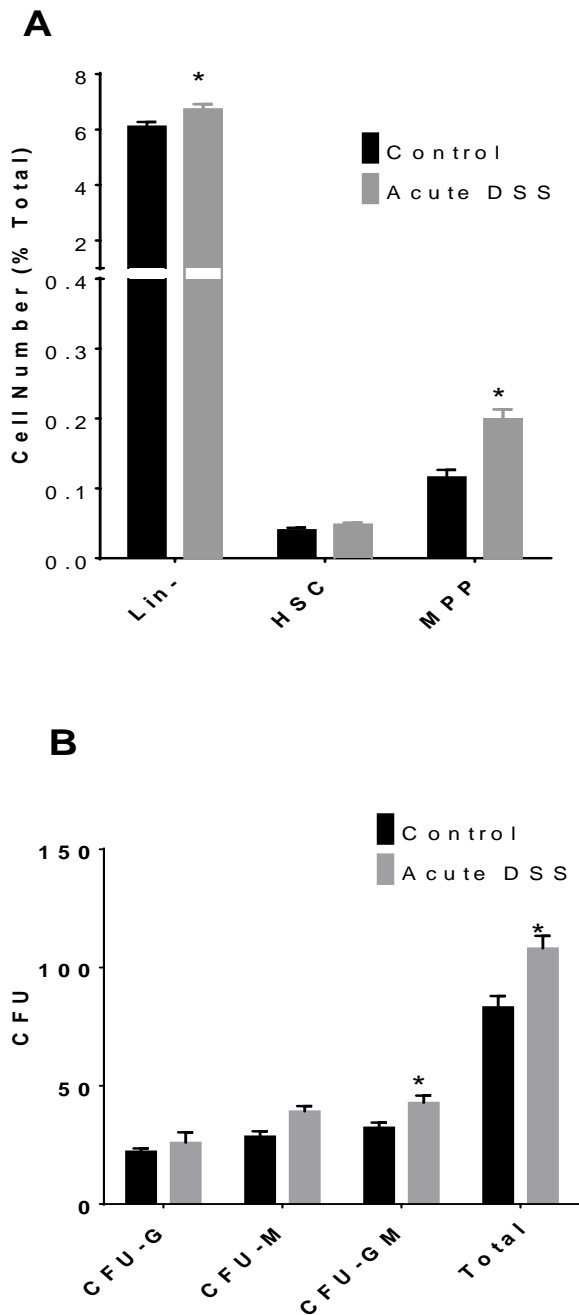


Figure 3.3.7A: Myeloid progenitor cells in the bone marrow of acute DSS colitis mice.

(A) The proportion of lineage negative cells, of hematopoietic stem cells and multipotent progenitor stem cells in the bone marrow of acute DSS colitis mice, measured by flow cytometry utilizing gating strategy in Table 2.10 (n = 6). (B) The number of granulocyte and macrophage colony forming units (CFU-GM) following culture of bone marrow cells (n = 6).

± S.E.M. * = p<0.05, unpaired t-test.

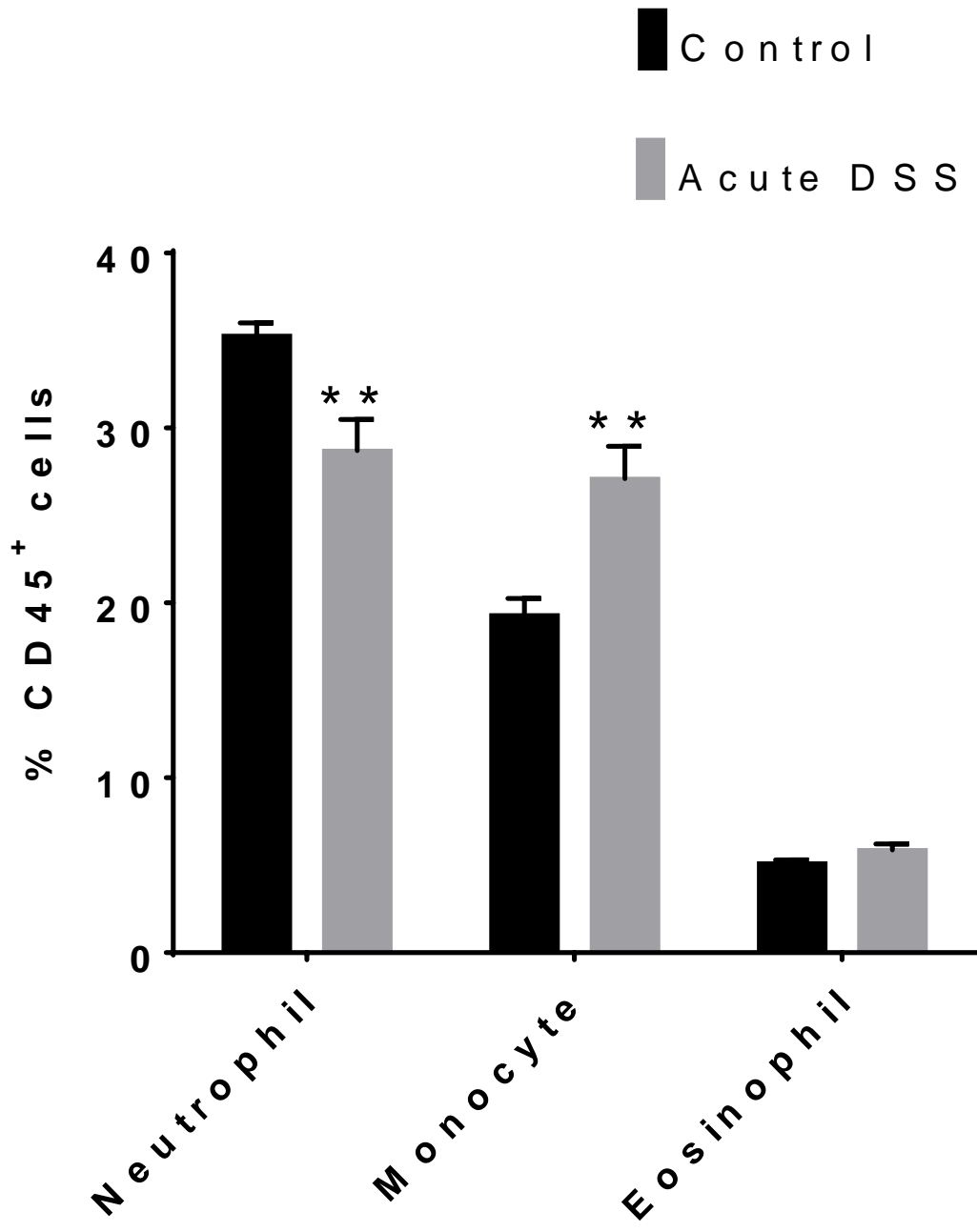
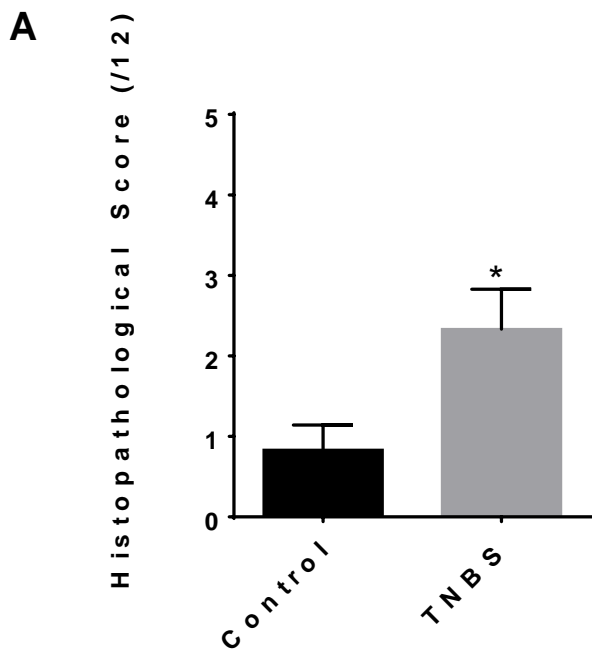


Figure 3.3.7B: Mature myeloid cell populations in the bone marrow of acute DSS colitis.

The proportion of mature neutrophils and monocytes in the bone marrow of acute DSS colitis, measured by flow cytometry according to the staining panel in Table 2.10 (n = 6). All data represented as mean ± S.E.M. * = p<0.05 ** = p<0.01, unpaired t-test.

3.3.8 Colitis-induced pulmonary pathology in the TNBS model of colitis.

Colitis-induced pulmonary inflammation was investigated in two additional murine models of colitis; the TNBS and *Winnie* colitis models. It was found that TNBS colitis mice also develop pulmonary pathologies. Pulmonary pathology in TNBS colitis was characterized as an increase in histopathological scores (Figure 3.3.8A A, representative images Figure 3.3.8B). When histopathological scores were broken-down based upon the anatomical location score it was seen that the majority of inflammation is focused around the pulmonary vasculature and parenchyma (Figure 3.3.8A B). The phenotype of leucocytes in the lung of TNBS colitis mice was analysed by flow cytometry. A significant increase in neutrophils in the lung was observed, no change in monocytes or lymphoid populations was found (Figure 3.3.8C). Taken together these data show that the TNBS colitis model has a similar of phenotype of colitis-induced pulmonary inflammation to that seen in the DSS colitis model, thus it can postulated that a similar mechanism of pathogenesis is conserved between the two models.



B Breakdown of histopathological scores prolonged TNBS colitis

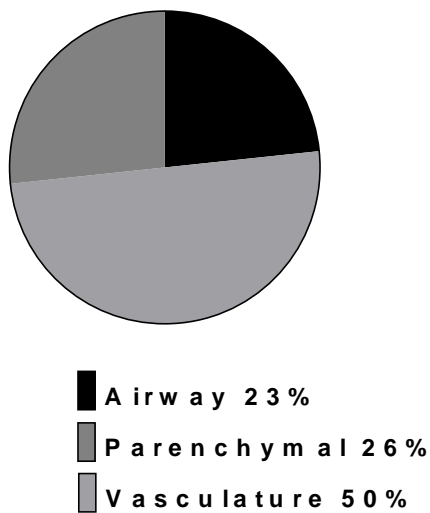
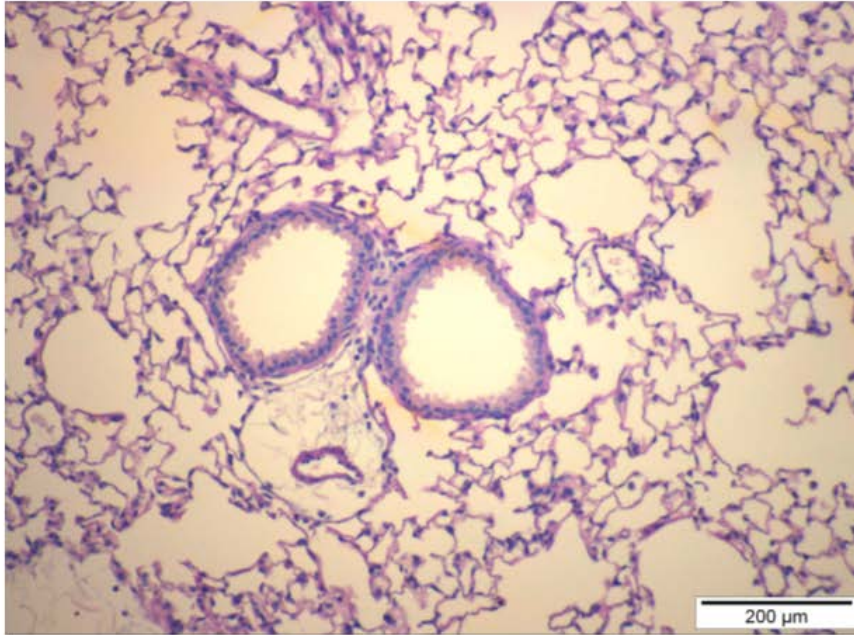
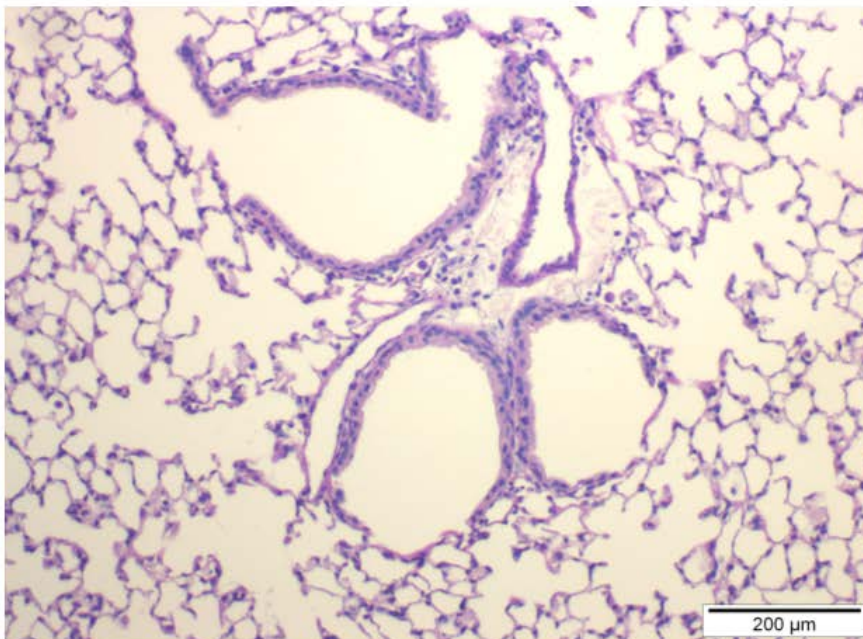


Figure 3.3.8A: Histopathological scores in lung sections from TNBS colitis. (A) Quantitative analysis of lung histopathology in TNBS colitis as determined by scoring criteria in Table 2.6, (n = 6). (B) Breakdown of histopathological scores based upon the anatomical location of pathology in TNBS colitis (n = 6). All data represented as mean \pm S.E.M. *= $p < 0.05$, unpaired t-test.



Control



TNBS

Figure 3.3.8B: Histopathology in lung sections from TNBS colitis. Representative images of the pathology observed in the lung of TNBS colitis mice (10x).

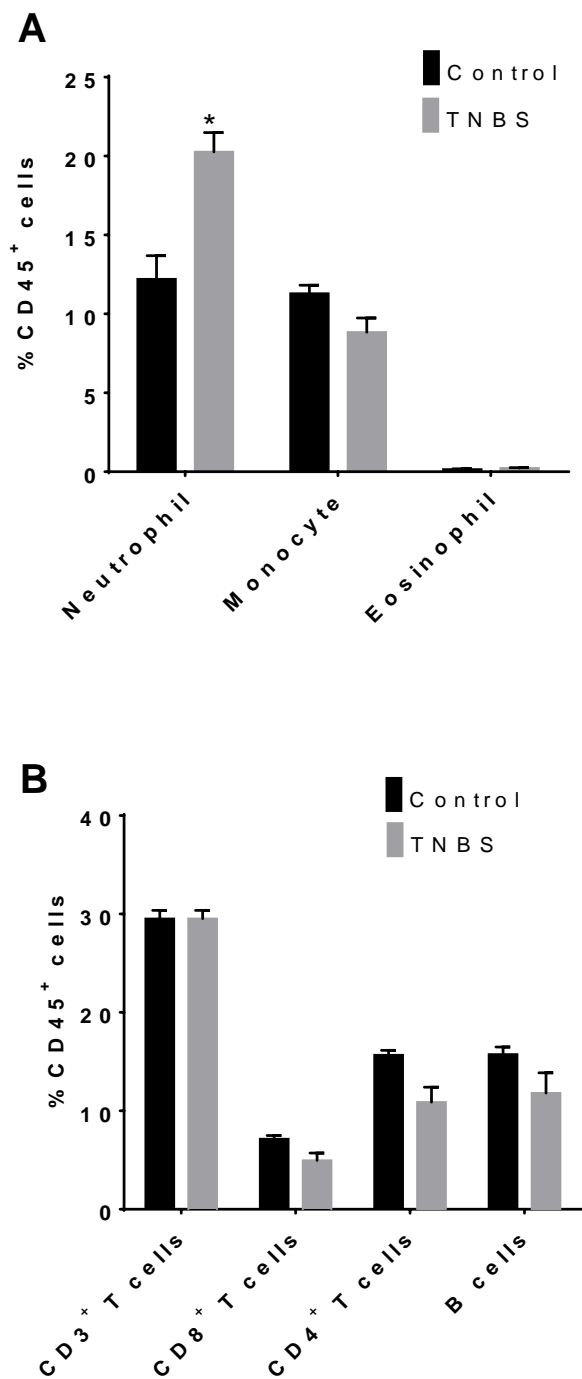


Figure 3.3.8C: Pulmonary inflammation in TNBS colitis. (A) The proportion of myeloid cells in the lung of TNBS colitis mice (n = 6). (B) The level of lymphoid cells in the lung of acute TNBS colitis mice (n = 6), cellularity measured by flow cytometry according to the gating Table 2.10. All data represented as mean \pm S.E.M. *= $p < 0.05$, unpaired t-test.

3.3.9 Colitis-induced pulmonary pathology in the *Winnie* model of colitis.

The *Winnie* colitis model, in contrast to DSS and TNBS, is not a chemically induced colitis model; rather it occurs in a transgenic mouse that carries a missense mutation in the *Muc2* mucin gene. It was found that *Winnie* mice had significantly higher lung histopathological scores than wild type mice (Figure 3.3.9A A representative images Figure 3.3.9B). Pulmonary pathology in *Winnie* can be attributed to inflammation surrounding the pulmonary vasculature and parenchyma (Figure 3.3.9A B). These results may be attributed to the lack of MUC2 in lung epithelial cells as the *Muc2* knockout is not specific to intestinal epithelial cells. MUC2 is expressed in the lung however expression is at basal levels, furthermore MUC2 and MU5AC are the prominent mucins associated with physiological and pathological function in the lung (Awaya, Takeshima et al. 2004). A caveat to these data is that the *Winnie* model is based upon a global missense mutation, thus aberrant MUC2 expression in pulmonary epithelial cells maybe be responsible for the pulmonary pathology observed in this model. To conclusively determine whether lung pathology in *Winnie* is a consequence of colitis, pulmonary pathology needs to be fully characterized on a molecular and cellular level. *Muc2* mRNA levels should be measured to determine the expression of MUC2 in the lung. A MUC2 western blot should also be conducted to analysis the presence and structural integrity of MUC2 at the protein level. Furthermore experiments by Hazelwood *et al.* have shown that the cellular location of MUC2 can be identified by immunohistochemistry and that aberrant MUC2 expression is a feature of *Winnie* in the intestine. This assay should be adapted to the lung to determine whether aberrant MUC2 expression is a feature of colitis-induced pulmonary inflammation (Heazlewood, Cook et al. 2008). These experiments are required to validate the *Winnie* model as an appropriate model to investigate the pulmonary manifestations of IBD.

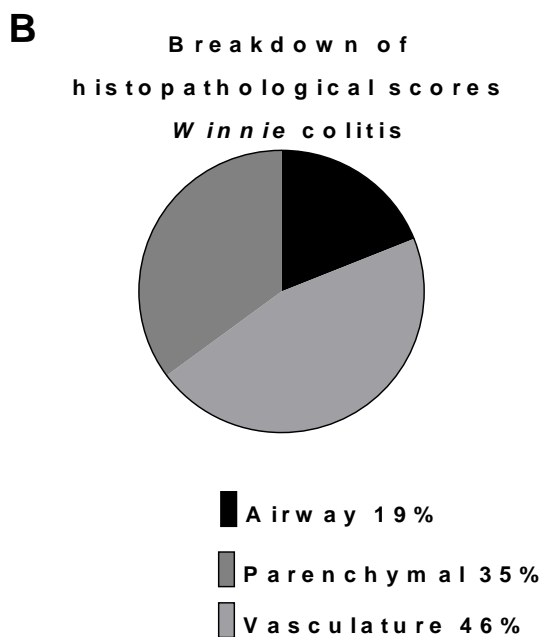
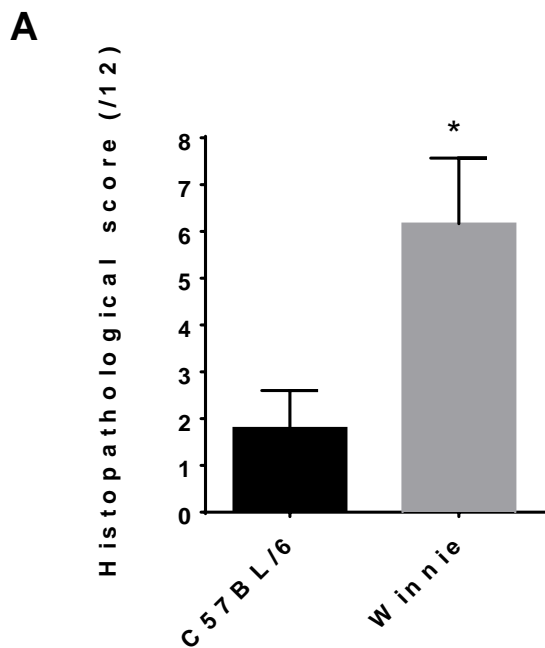
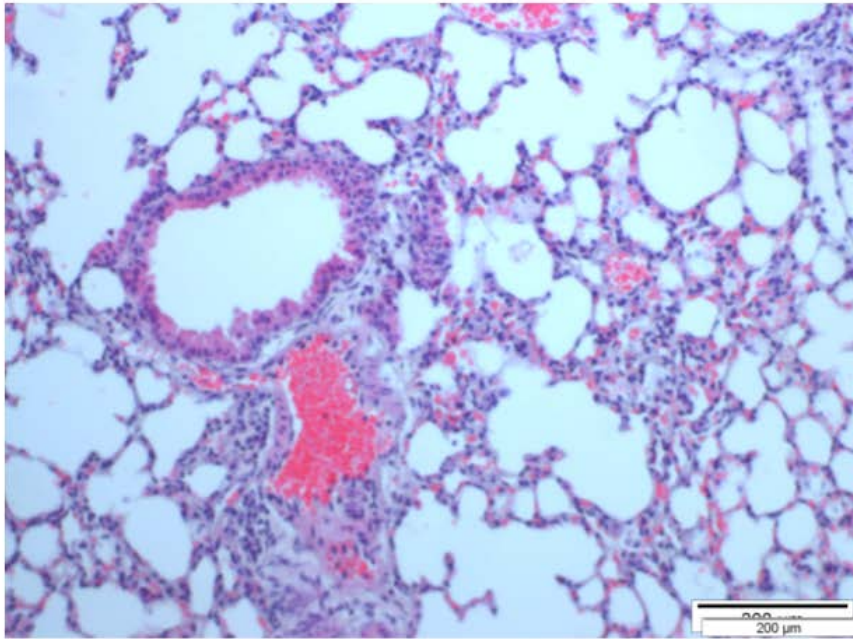
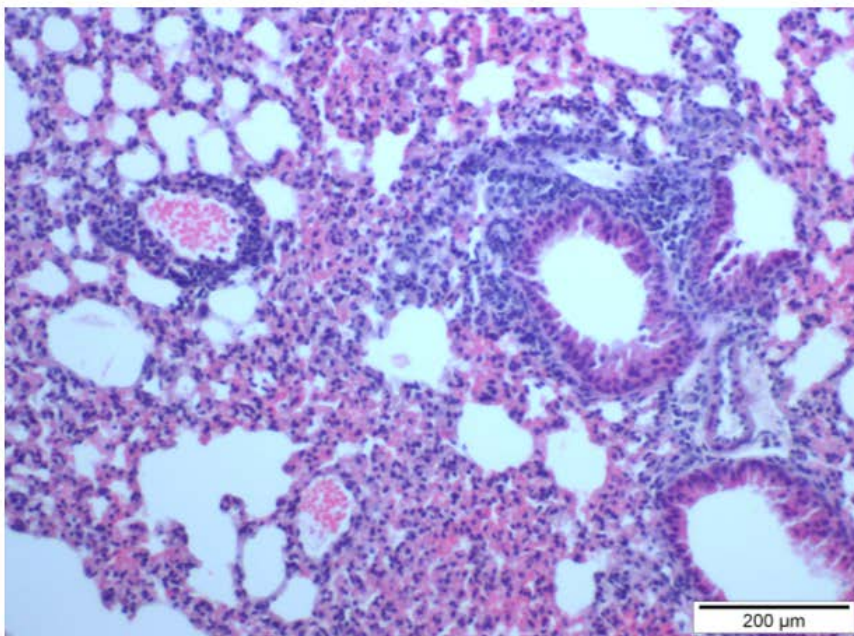


Figure 3.3.9A: Histopathological scores in lung sections from *Winnie* colitis. (A) Quantitative analysis of lung histopathology in *Winnie* colitis as determined by scoring criteria in Table 2.6, (n = 6). (B) Breakdown of histopathological scores based upon the anatomical location of pathology in *Winnie* colitis (n = 6). All data represented as mean ± S.E.M. *=p<0.05, unpaired t-test



Control



Winnie

Figure 3.3.9B Histopathology in lung sections in *Winnie* colitis continued. Representative images of the pathology observed in the lungs of *Winnie* colitis (10x).

3.4 Discussion:

The aim of experiments within this chapter was to determine whether murine models of colitis would exhibit pulmonary pathologies similar to IBD patients and secondly to utilise these models to identify potential pathogenic factors. The results from this chapter show that murine models of colitis develop pulmonary pathology and these immunopathologies can be considered comparable to that observed in IBD patients. The core work of this chapter focused on the acute DSS colitis model and significant pulmonary pathology was observed. As DSS is administered to mice *ad libitum* in drinking water it has been suggested that lung inflammation in this model is due to pulmonary aspiration of DSS. However a study on the systemic distribution of DSS demonstrates that this is not the case (Kitajima, Takuma et al. 1999). In this study by Kitajima *et al.* histochemical analysis was utilized to detect the presence of DSS in extra-intestinal tissues, this study found that DSS administered in drinking water does not disseminate to the lung (Kitajima, Takuma et al. 1999). In the experiments conducted in this study it was found that pulmonary inflammation with similar histopathological features develops in three mechanistically distinct colitis models. This observation demonstrates that pulmonary inflammation is a legitimate physiological effect of intestinal inflammation on the lung and not simply an artefact of an individual model. Furthermore, the DSS and TNBS models have contrasting mechanisms of compound delivery, TNBS is administered by intrarectal instillation and therefore it is highly unlikely that TNBS can be aspirated. The fact that pulmonary pathology develops in TNBS colitis demonstrates that it is immunological factors that initiate pulmonary pathology not the method of compound delivery. Thus, based on published research (Kitajima, Takuma et al. 1999) and experimental observations, it was concluded that pulmonary pathology in DSS colitis is induced by intestinal inflammation. Therefore, the DSS colitis model provides a tool to investigate the respiratory pathologies associated with IBD.

The features of IBD-induced pulmonary pathology include: altered spirometry, asymptomatic structural abnormalities, sub-clinical inflammation and active respiratory diseases (Camus, Piard et al. 1993). To study these features, experimental assays that are considered analogous to the clinical procedures that are performed on IBD patients were conducted. The Buxco forced manoeuvres system was used to examine the lung function of DSS colitis mice. This system is the murine equivalent to spirometry in cooperative adults (Vanoirbeek, Rinaldi et al. 2010). FVC was the measurement utilised in these experiments, FVC is the total amount of air exhaled during a forced expiration and is a measure of obstructive lung conditions. No lung function abnormalities were detected in acute DSS colitis mice. Lung structural pathologies are commonly assessed in humans with HRCT, while HRCT can be utilized for the study of murine pathology; this technique was not available for this project. Therefore, structural pathology in the parenchyma of DSS colitis mice was conducted by measurement of alveoli diameter. Alveoli enlargement in lung disease is caused by the release of proteolytic enzymes from leucocytes. These catabolic enzymes damage the architecture of structural tissue and this damage can be visualized as alveoli enlargement. Employing alveoli diameter, as a marker of structural damage induced by inflammation there was no detectable changes in the lungs of acute DSS colitis mice. While inflammation driven structural damage was not present, histopathological examination of lung sections did reveal significant pulmonary inflammation. The majority of leucocytes were localised to the pulmonary vasculature and parenchyma, suggesting that the stimulus for immune cell extravasation originates from the vasculature and not the airways. This observation is supported by BAL differential cell counts which showed no change in the composition of leucocytes in the airways. These data indicate that stimulation of the airway epithelium is not a factor that contributes to pathology in this model. Mucus hypersecretion is a characteristic of the IBD associated respiratory disease chronic bronchitis. It was found that DSS colitis-induced

pulmonary inflammation did not induce mucous hypersecretion from pulmonary epithelial cells. Sub-clinical inflammation in IBD patients has been reported as an increase in the FE_{NO} and elevated pro-inflammatory cytokines in breath condensate (Koek, Verleden et al. 2002, Krenke, Peradzynska et al. 2014). FE_{NO} is used as a surrogate marker of neutrophilic inflammation and macrophage activation in clinical studies (Munakata 2012). A similar phenotype of inflammation was observed in the lungs of acute DSS colitis mice. Pulmonary inflammation was characterised by increased numbers of neutrophils and monocytes entering the lung, along with elevated gene expression of cytokines associated with innate inflammatory responses. While studies that have investigated cytokine levels in the lung of IBD patients are limited, Krenke *et al.* reported elevated levels of IL-1 β , TNF and IL-6 in the breath condensate of a paediatric IBD population (Krenke, Peradzynska et al. 2014). These findings were mirrored in the acute DSS colitis model in respect to elevated pro-IL-1 β protein levels, however TNF and IL-6 levels were only elevated at the transcript level. Thus the key features of IBD-induced latent respiratory disease were reproduced in the acute DSS model, that being myeloid cell mediated inflammation and elevated cytokines related to innate immune responses. A limitation in drawing this conclusion is that pro-IL-1 β was measured opposed to direct measurement of the active form of IL-1 β or measurement of caspase-1 the protease that controls pro-IL-1 β catabolism. This limitation can be overcome by conducting western blots to measure these proteins in lung samples from the respective colitis models and represent a further direction for this study.

In regards to the active respiratory diseases associated with IBD, the DSS model did not reproduce the hallmark phenotypic features of bronchiectasis and chronic bronchitis. The hallmark pathologies of these conditions are airway enlargement in bronchiectasis and mucus hypersecretion in chronic bronchitis (Eller, Lapa e Silva et al. 1994, King 2009). In the DSS

model, structural pulmonary pathologies are not present and neither is mucus hypersecretion. While the DSS model does not reproduce the physiological pathologies of these conditions, the immunopathologies can be considered comparable. The immunopathologies of bronchiectasis and chronic bronchitis are associated with neutrophil and monocyte extravasation into the respiratory system; the subsequent activation of these cells induces the structural pathologies associated with these conditions (Fuschillo, De Felice et al. 2008). Extravasation of neutrophils and monocytes into the lung was also observed in acute DSS colitis. Furthermore, IL-1 β and CCL2 have been identified to mediate inflammation in bronchiectasis and chronic bronchitis, and both these cytokines are elevated in the lungs of acute DSS colitis mice.

3.5 Conclusion

In summation, the pulmonary pathology induced by DSS colitis does not reproduce the physiological features of bronchiectasis and chronic bronchitis; however, the immunopathology in respect to myeloid cell recruitment and cytokine signalling can be considered comparable. Therefore, the acute DSS colitis model can be utilised to investigate the mechanisms that underpin the recruitment of myeloid cells and cytokine expression in the lung of IBD patients. The second aim of this chapter was to identify potential pathogenic factors involved in IBD-induced pulmonary pathology. From the characterisation of pulmonary and systemic inflammation in the DSS colitis model, systemic IL-6 and pulmonary PAFR signalling were identified as potential pathogenic factors. Thus experiments investigating the role of systemic IL-6 signalling in modulating colitis-induced pulmonary inflammation is the focus of Chapter 4.

Chapter 4: The role of systemic IL-6 in the modulation of colitis-induced pulmonary inflammation.

4.1 Introduction

Clinical studies and experimental models of IBD have shown that systemic inflammation is a prominent feature of disease. Systemic inflammation in IBD is thought to develop as a result of a damaged gut mucosa and dysregulated cytokine signalling (Funderburg, Stubblefield Park et al. 2013). In this hypothesis, a loss of tolerance to luminal contents of the intestine, results in a compromised epithelial barrier. The subsequent interaction between leucocytes of the gut mucosa and microflora results in an inflammatory milieu that culminates in elevated levels of inflammatory cytokines. High concentrations of inflammatory cytokines induce vascular permeability as capillaries become dilated in order to allow the extravasation of leucocytes. This combination of inflammation and vascular permeability allows soluble cytokines to diffuse into the bloodstream. One of the cytokines that can enter the bloodstream in this manner is IL-6. IL-6 is commonly reported to be elevated in the serum of IBD patients (Funderburg, Stubblefield Park et al. 2013). IL-6 is also elevated in the serum of acute DSS colitis mice (Section 3.3.6).

IL-6 is a pleotropic cytokine with a range of immunomodulatory functions. The pleotropic effects of IL-6 are due to a unique mechanism of receptor/ligand signalling. IL-6 can signal through two mechanisms, a “classical signalling” pathway and a “trans-signalling” pathway (Neurath and Finotto 2011). The classical signalling pathway involves interaction between

IL-6; the membrane bound IL-6 receptor (IL-6R) and the signal transducer glycoprotein 130 (gp130). The IL-6R is specifically expressed on hematopoietic cells while gp130 is ubiquitously expressed, thus classical signalling can only occur on hematopoietic cells. The trans-signalling pathway, on the other hand, does not require the IL-6R. Signalling in this pathway occurs via interactions between IL-6, the soluble IL-6 receptor (sIL-6R) and gp130. As trans-signalling does not require expression of the membrane bound IL-6R, trans-signalling can induce the functions of IL-6 on a range of cells including endothelial cells, epithelial cells and hematopoietic cells (Barnes, Anderson et al. 2011).

One of the roles of IL-6 is to induce the effector functions of myeloid cells. Activation of myeloid cells via IL-6 signalling induces the expression of IL-1 β and PAF (Biffi, Moore et al. 1996, Heinrich, Behrmann et al. 1998). IL-1 β levels are elevated in the lung of acute DSS colitis mice and PAFR, the receptor for PAF, is also upregulated in the lungs of colitis mice. The increase in PAFR may be due to the increase in PAF from activated myeloid cells (Ishii and Shimizu 2000). Therefore, systemic IL-6 signalling may regulate the expression of IL-1 β and PAFR in the lungs of DSS colitis mice. Furthermore, IL-6 trans-signaling can induce the activation of endothelial cells and the subsequent expression of CCL2, facilitating the recruitment of myeloid cells (Barnes, Anderson et al. 2011). In the acute DSS colitis model, CCL2 levels are elevated in the lung in parallel with systemic IL-6 levels. Thus, systemic IL-6 signaling may induce CCL2 expression in the pulmonary endothelium and therefore facilitate myeloid cell recruitment to the lung in colitis.

4.1.1 Hypothesis

Based on the experimental observations in the DSS colitis model and the literature documenting the immunomodulatory functions of IL-6 signaling, it was hypothesized that; systemic IL-6 mediates colitis-induced pulmonary inflammation through the modulation of myeloid cell recruitment, and this occurs via the expression of IL-1 β , CCL2 and PAFR signalling.

4.1.2 Aims

To test this hypothesis, the factors that are involved in the recruitment of myeloid cells to the lung in colitis-induced pulmonary inflammation were assessed in anti-IL-6 treated acute DSS colitis mice. These factors were, the magnitude of the underlying colitis, cytokine signalling in the lung and the presence of systemic inflammation. Thus the following aims were employed;

- 1) To examine the influence of systemic IL-6 signaling on the magnitude of colitis that predisposes to the development of DSS colitis-induced lung inflammation.
- 2) To examine the influence of systemic IL-6 signaling on cytokine expression and myeloid cell recruitment to the lung of DSS colitis-induced pulmonary inflammation.
- 3) To examine the influence of IL-6 signaling on the development of the systemic inflammation associated with colitis, specifically neutrophilia, systemic cytokines levels and haematopoiesis.

4.2 Methods

4.2.1 Anti-IL-6 intervention in acute DSS colitis

Six-week-old female WT C57BL/6 mice were given 4% DSS *ad libitum* in drinking water for six days. Age matched controls received drinking water for seven days. 200 microgram (μg) of anti-IL-6 (clone MP5-20F3; BioXCell) was injected IP into DSS mice on day 3 and day 5 according to Figure 4.2.1. The isotype control, rat IgG1 (clone HRPN; BioXCell) was injected IP into control mice. These dates were chosen as it is known that DSS colitis initiates intestinal inflammation 3 days post DSS administration (Laroui, Ingersoll et al. 2012). In addition preliminary experiments in the research group showed that DSS colitis-induced pulmonary pathology develops 5 days post DSS treatment. Therefore it was concluded that colitis-induced pulmonary inflammation develops between day 3 and day 5. As the aim of these experiments was to determine the role of IL-6 in mediating the initiating stages of colitis-induced pulmonary inflammation, day 3 and day 5 were chosen as the time points for IL-6 intervention. The dosage strategy was based upon the experiments published by Sommer *et al.* (Sommer, Engelowski *et al.* 2014). On day 7 mice were sacrificed and tissues collected. Colon, blood and bone marrow were harvested for analysis as described in Section 2.2. Colon and lung tissue was collected for histopathological scoring according to Section 2.5 and 2.6 respectively. Cellular analyses of lung, blood and bone marrow was conducted as described in Section 2.10. Gene expression and cytokine analysis from lung and colon tissue was performed as described in Section 2.12, 2.13 and 2.14. As lung function abnormalities, mucous hypersecretion and airways inflammation are not present in the acute DSS model, these assays to examine these features were not conducted in this chapter.

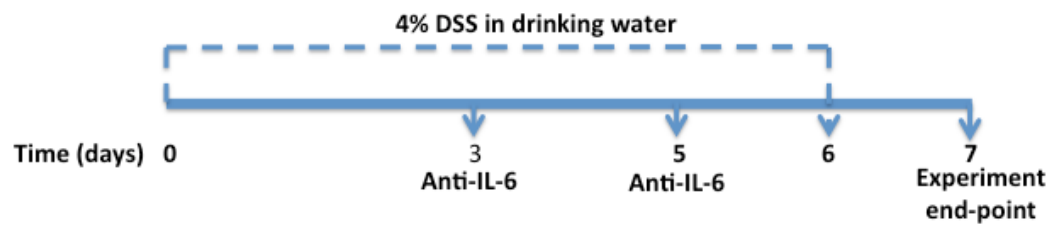


Figure 4.2.1: Time course of anti-IL-6 interventions in DSS colitis.

4.3 Results

4.3.1 Serum IL-6 levels in anti-IL-6 treated acute DSS colitis.

The aim of experiments in this chapter was to determine the effect of systemic IL-6 on the development of colitis-induced pulmonary pathology. To achieve this aim systemic IL-6 was neutralized in DSS colitis mice with a monoclonal antibody. To determine whether this treatment was capable of reducing systemic levels of IL-6, IL-6 was quantified in the serum of DSS colitis mice. It was found that systemic IL-6 levels were significantly decreased in the anti-IL-6 DSS group compared to isotype controls. These data demonstrate that the anti-IL-6 monoclonal antibody efficiently dropped the levels of systemic IL-6 (Figure 4.3.1).

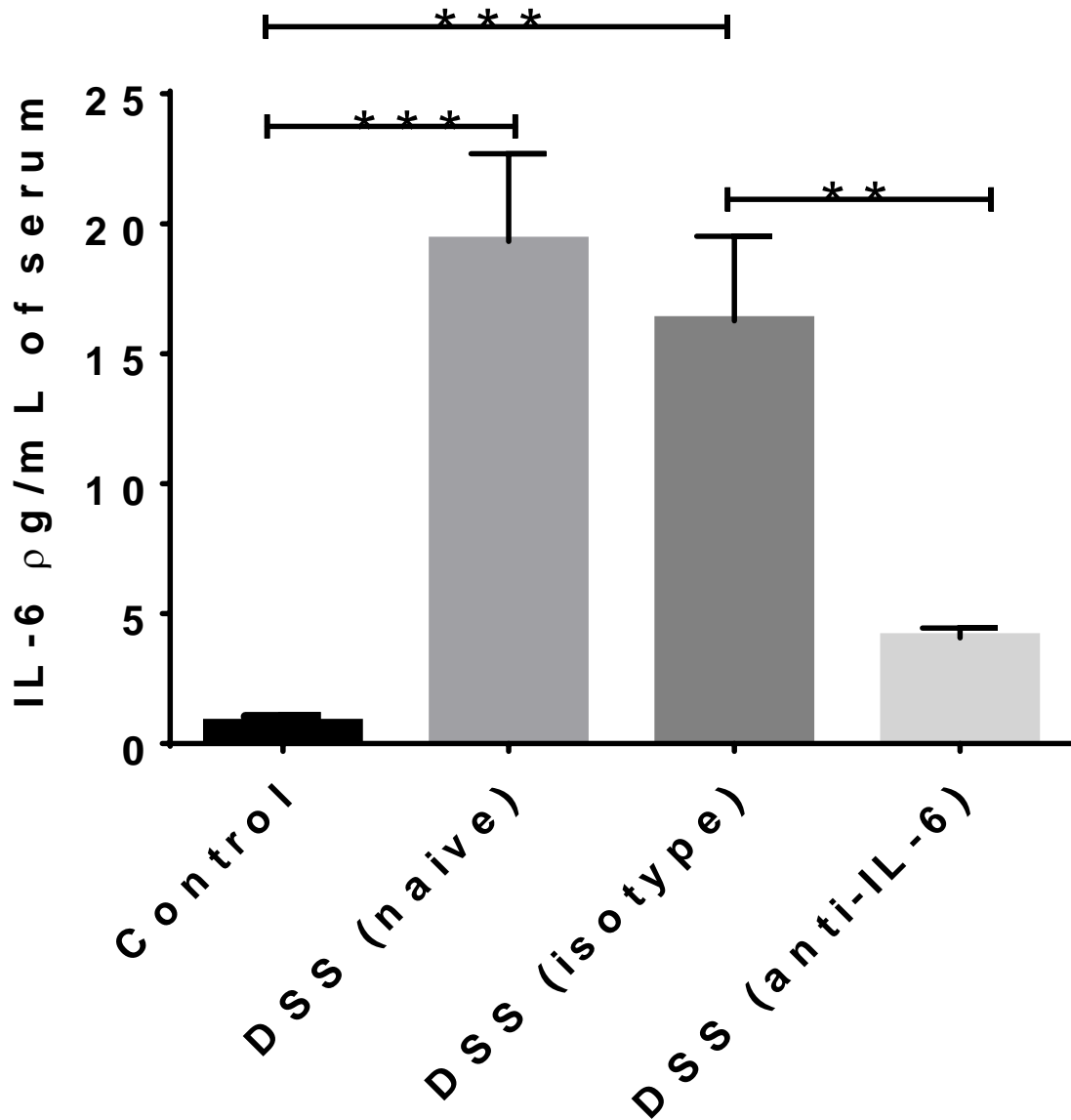


Figure 4.3.1: Systemic IL-6 levels in anti-IL-6 treated acute DSS colitis. IL-6 levels were measured in serum of anti-IL-6 treated acute DSS colitis mice by cytometric bead array. Anti-IL-6 treatment decreased the levels of systemic IL-6 compared to isotype controls (n = 6). All data represented as mean \pm S.E.M. **= $p < 0.01$, ***= $p < 0.005$, unpaired t-test.

4.3.2 Intestinal pathology in anti-IL-6 treated acute DSS colitis.

Intestinal inflammation is the principal predisposing factor in the development of colitis-induced pulmonary inflammation. Thus the initial aim of experiments in this chapter was to quantify the effect of systemic IL-6 neutralization on the magnitude of intestinal inflammation. To achieve this aim intestinal pathology was quantified based on weight loss, colon/mucosal thickening (colon weight to length ratio), histopathology and cytokine signaling in the colon of anti-IL-6 treated acute DSS colitis mice. Anti-IL-6 treated DSS mice lost significantly less weight compared to isotype treated controls (Figure 4.3.2A A). These data show that a systemic feature of DSS colitis is driven by IL-6 signaling. No change in mucosal thickening was observed between the naïve DSS, anti-IL-6 and isotype control groups (Figure 4.3.2A B). Analysis of histopathology in colon sections of anti-IL-6 treated mice revealed no significant changes between the naïve DSS, anti-IL-6 and isotype control groups (Figure 4.3.2B, representative images Figure 4.3.2C & Figure 4.3.2D). These data suggest that IL-6 is not responsible for the development of intestinal gross pathology or histopathology in the acute DSS colitis model. Cytokine signaling was quantified by the measurement of TNF, IL-6, IFN- γ , IL-1 β and CCL2 in colon tissue. The protein levels of TNF, IL-6, IFN- γ , IL-1 β and CCL2 were all significantly increased in the colon of DSS experimental groups compared to controls. There was no change in the level of these cytokines between the isotype and anti-IL-6 treated DSS colitis groups. While there is a trending increase in TNF protein levels between the DSS naïve and DSS isotype treated groups, this result is not statistically significant, therefore the null hypothesis was accepted and this observation was not investigated further. This approach was applied across the entire study to give a consistency to analysis. However the trending increase in IL-6 levels in anti-IL-6 treated mice maybe be a biological effect of the decrease in circulatory IL-6 levels. It is possible that the decrease in IL-6 levels in the circulation is due to IL-6 being sequestered at

the site of inflammation. (Figure 4.3.2E). Taken together, these data show that anti-IL-6 treatment, at this time point, did not affect mucosal inflammation. However, anti-IL-6 treatment did attenuate one of the systemic effects of colitis. Therefore, IL-6 can be considered a factor that mediates the systemic effects of colitis. Furthermore, as anti-IL-6 treatment did not influence the underlying GI pathology that induces the systemic effects of colitis, any changes that are observed in systemic pathology can be attributed to the blockade of IL-6 signaling.

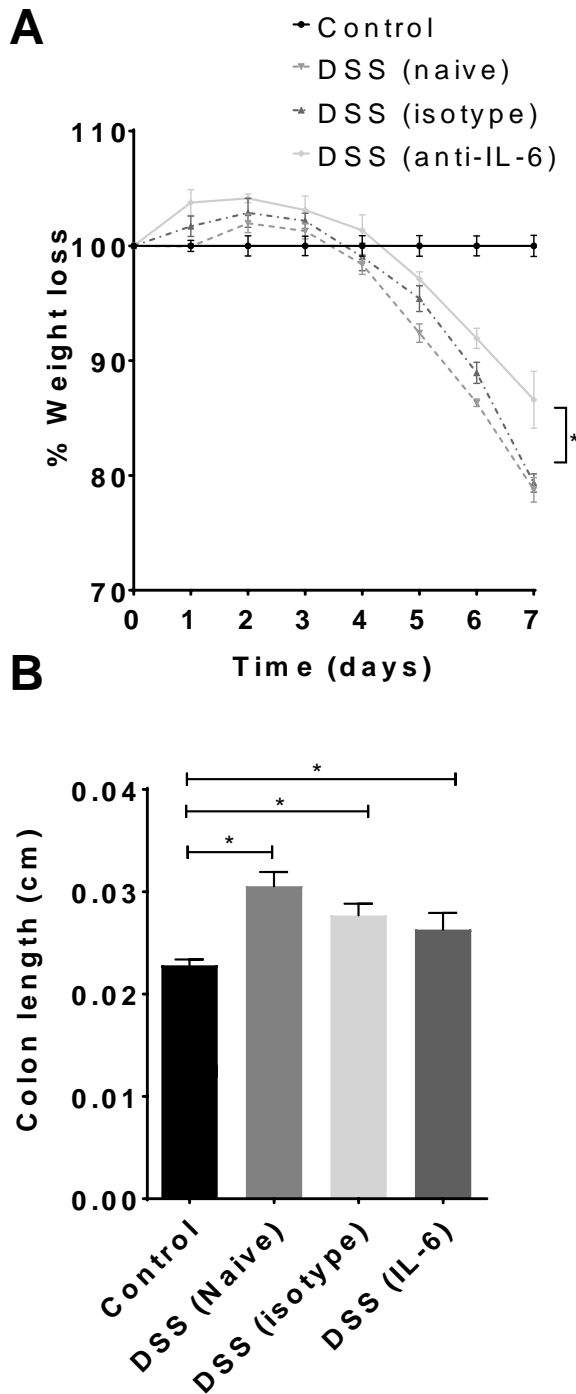


Figure 4.3.2A: Weight loss and colon/mucosal thickening in anti-IL-6 treated DSS colitis mice. (A) Percentage weight loss normalized to naïve controls (n = 8), (B) colon/mucosal thickening in anti-IL-6 treated acute DSS colitis (n = 8). Colon/mucosal thickening was calculated as colon weight to length ratio. All data represented as mean \pm S.E.M. $\ast = p < 0.05$, (A) two-way ANOVA, (B) unpaired t-test.

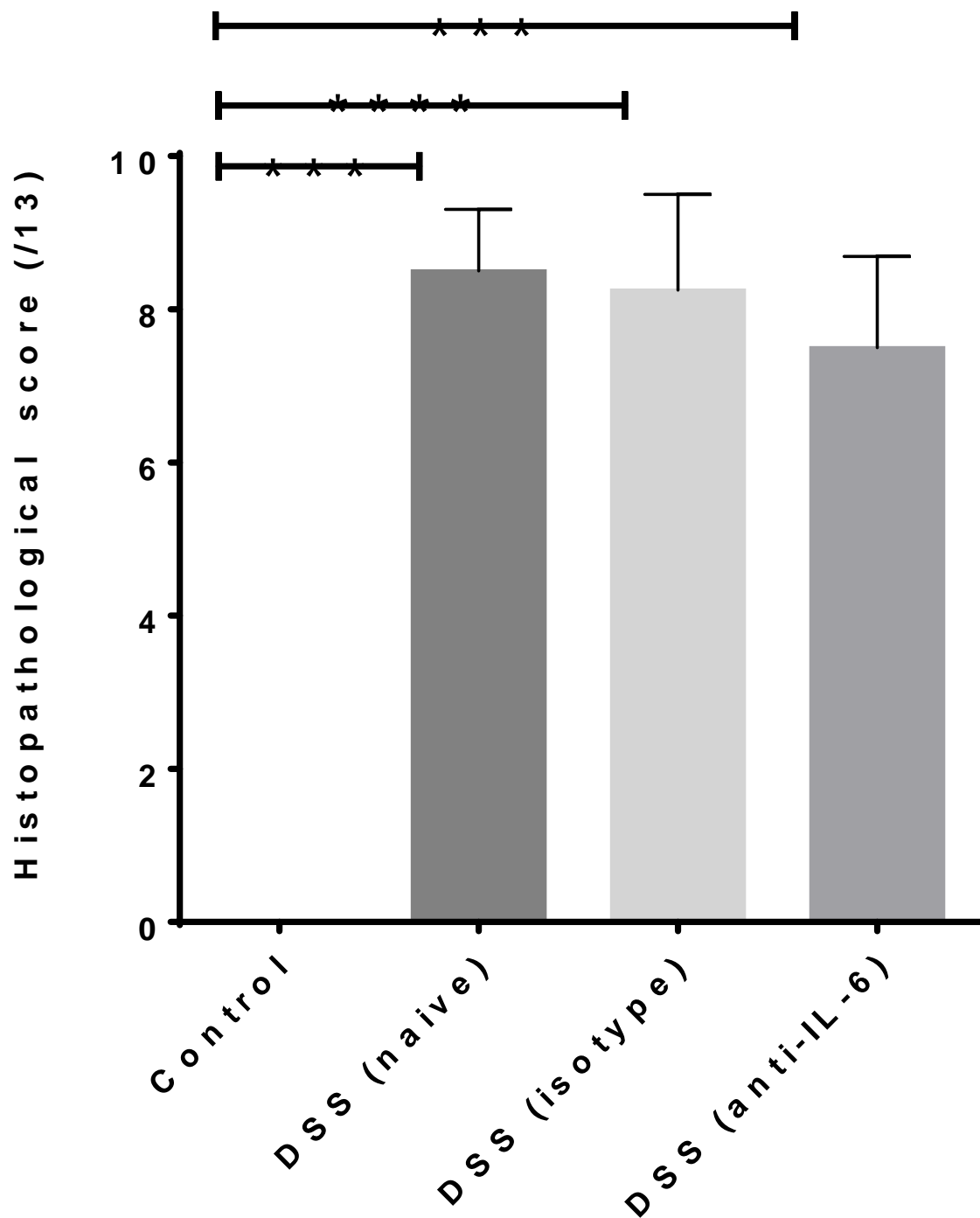
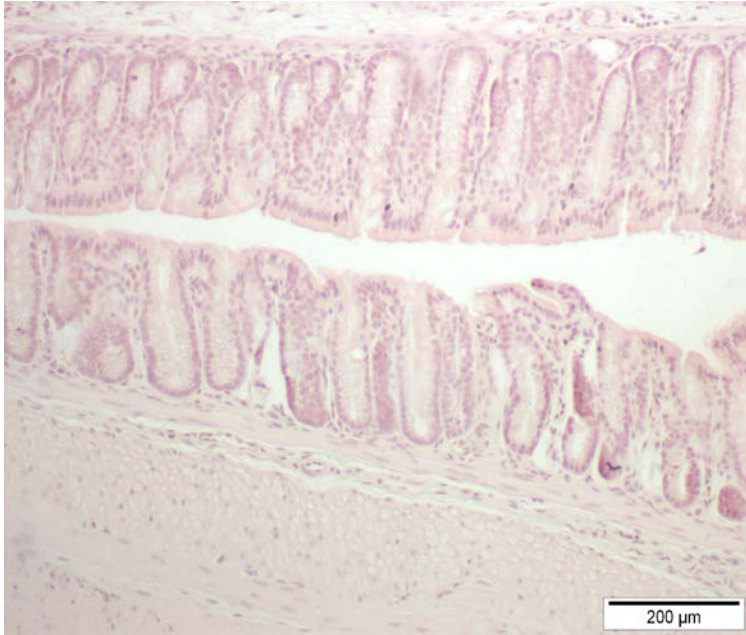
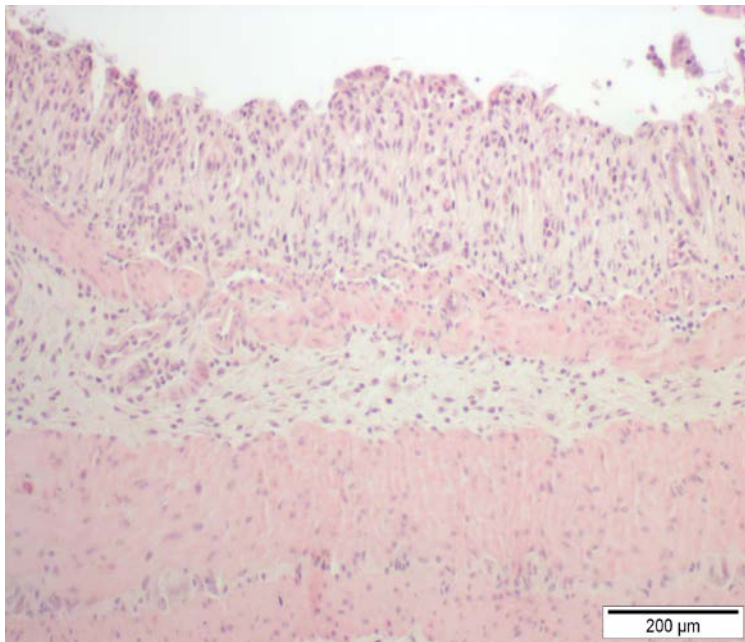


Figure 4.3.2B: Histopathological scores from colon sections in anti-IL-6 treated DSS colitis. (A) Quantitative analysis of colon histopathology in anti-IL-6 treated DSS colitis as determined by scoring criteria in Table 2.5 (n = 4). All data represented as mean \pm S.E.M, *= $p < 0.05$, *= $p < 0.01$, ***= $p < 0.001$ ****= $p < 0.0001$, unpaired t-test.



C o n t r o l



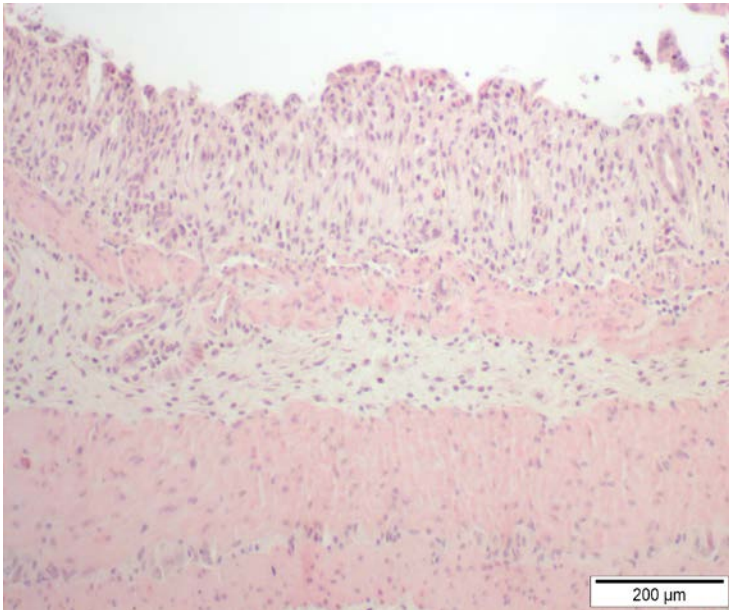
D S S (n a i v e)

Figure 4.3.2C: Histopathology in colon sections from control and naïve DSS colitis mice.

Representative images of histopathology observed in the colon of anti-IL-6 treated acute DSS colitis (10x).



D S S (i s o t y p e)



D S S (a n t i - I L - 6)

Figure 4.3.2D: Histopathology in colon sections from isotype and anti-IL-6 treated DSS colitis. Representative images of histopathology observed in the colon of anti-IL-6 treated acute DSS colitis (10x).

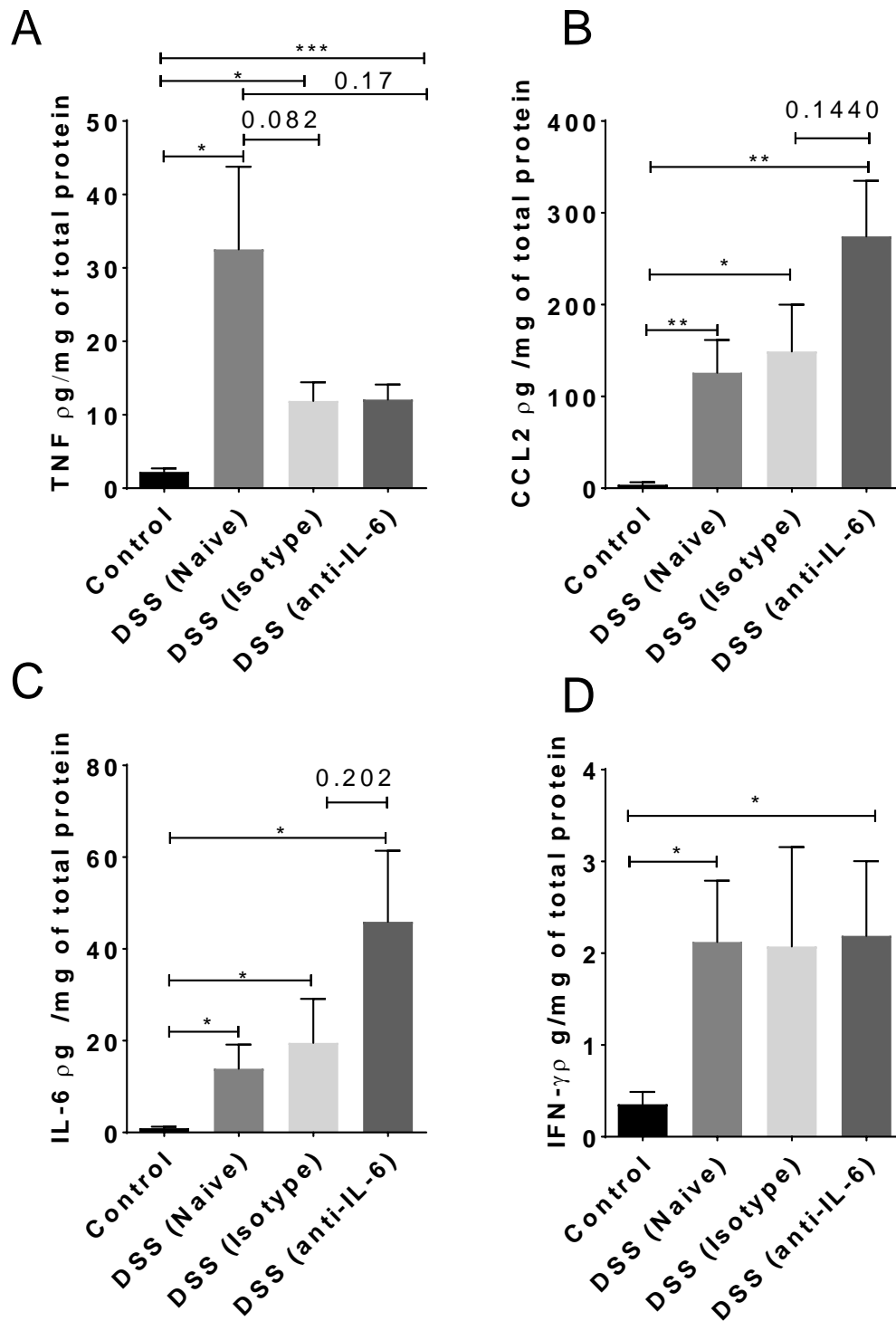


Figure 4.3.2E: Cytokine signalling in the colon of anti-IL-6 treated acute DSS colitis.

TNF, IFN- γ , CCL2 and IL-6 protein levels in the colon of anti-IL-6 treated acute DSS colitis mice, measured by cytometric bead array (n = 6). All data represented as mean \pm S.E.M,

*=p<0.05 **=p<0.01 ***=p<0.005, unpaired t-test.

4.3.3: The influence of IL-6 on colitis-induced pulmonary pathology.

IL-6 was shown to modulate the systemic effects of colitis, with respect to weight loss, thus the next aim was to determine the influence of IL-6 neutralization on another systemic effect of colitis, pulmonary pathology. The effect of systemic IL-6 on colitis-induced pulmonary pathology was determined by assessing the physiological effects of colitis on the pulmonary system in anti-IL-6 treated mice. In previous experiments, it was noted that colitis did not have any effect on lung function and pulmonary structural pathology (Section 3.3.2). For this reason, these assays to quantify these features were not undertaken in IL-6 intervention experiments. To assess the physiological changes in the lung, histopathology was quantified. No statistically significant change in histopathological scores was observed between isotype control and anti-IL-6 treated DSS colitis groups (Figure 4.3.3A, representative images Figure 4.3.3B & Figure 4.3.3C). Thus, it was concluded that systemic IL-6 neutralization did not affect the physiological pathology that is induced in the lung as a result of colitis.

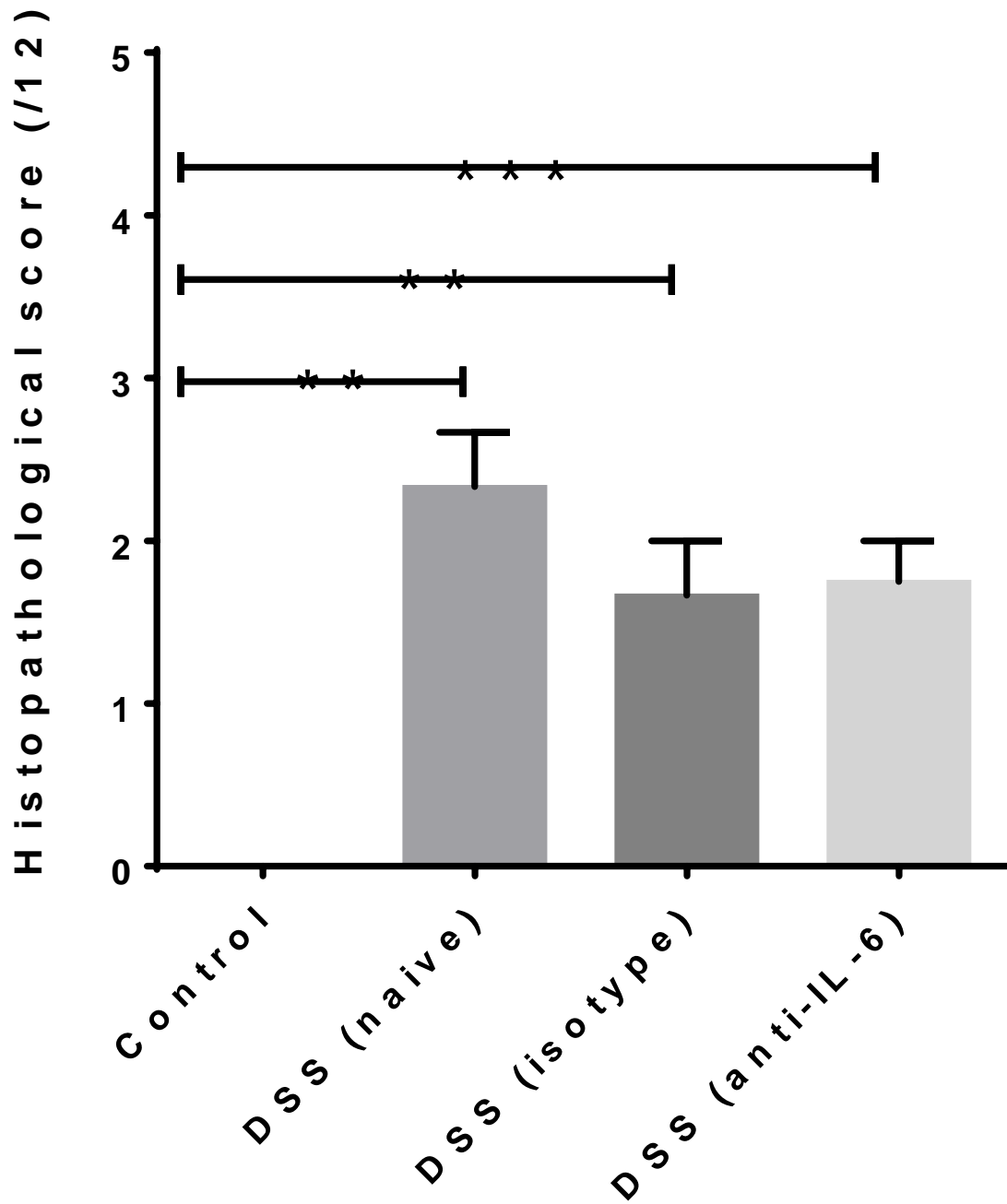
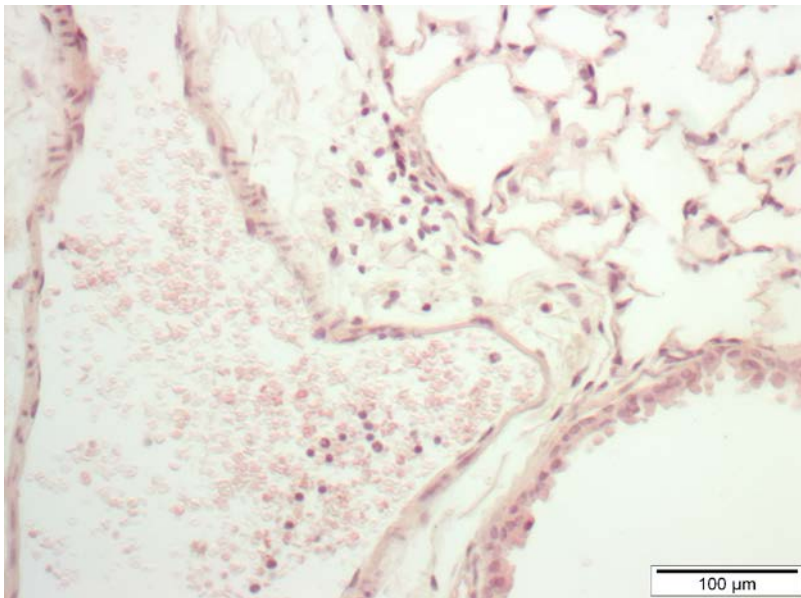


Figure 4.3.3A: Histopathological scores in lung sections from anti-IL-6 treated DSS colitis. (A) Quantitative analysis of histopathology in the lung of anti-IL-6 treated acute DSS colitis mice (n = 4). Histopathological scores generated according to the scoring criteria in Table 2.6. All data represented as mean ± S.E.M. **=p<0.01, *** = p<0.005, unpaired t-test.

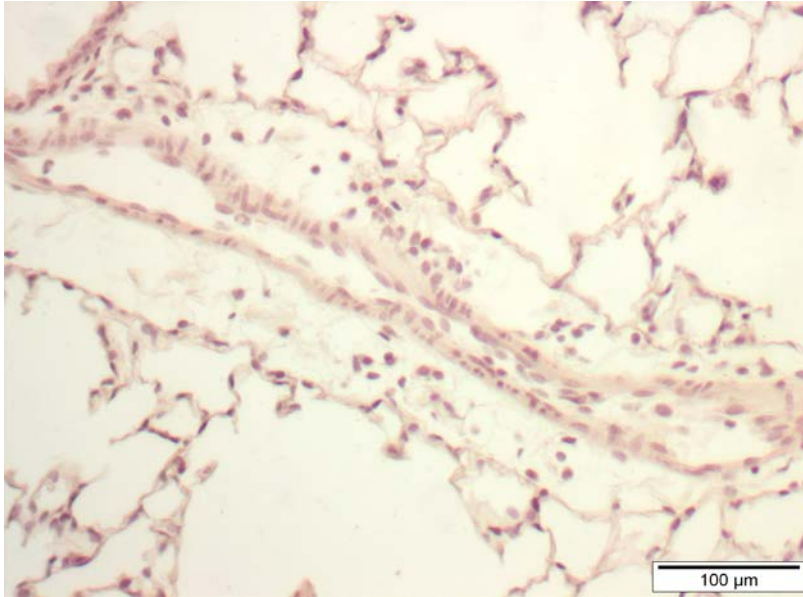


C o n t r o l

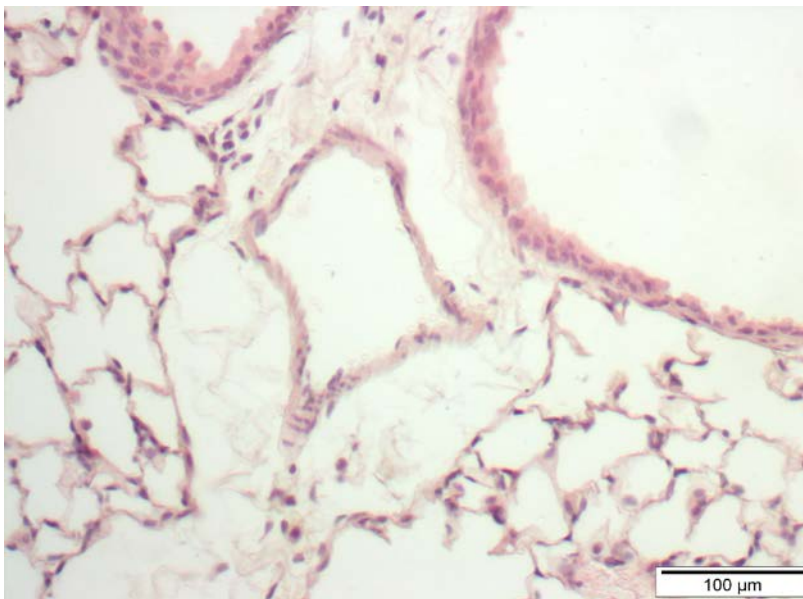


D S S (n a i v e)

Figure 4.3.3B: Histopathology in lung sections from control and naïve DSS colitis. Representative images of pathology observed in the lung of anti-IL-6 treated acute DSS colitis (10x).



D S S (i s o t y p e)



D S S (a n t i - I L - 6)

Figure 4.3.3C: Histopathology in lung sections from isotype and anti-IL-6 treated DSS colitis. Representative images of pathology observed in the colon of anti-IL-6 treated acute DSS colitis (10x).

4.3.4: The influence of IL-6 on colitis-induced pulmonary inflammation

Systemic IL-6 neutralization did not ameliorate colitis induced pulmonary pathology with respect to histopathological scores; however, IL-6 has potent immunomodulatory capabilities. For this reason, the contribution of IL-6 to colitis induced pulmonary pathology was not limited to the physiological aspects of disease but also included immunopathology. To assess the effect of IL-6 on colitis-induced pulmonary immunopathology, cellular analysis of the lungs of anti-IL-6 treated mice was undertaken. Previous experiments showed that myeloid cells are the phenotype of leucocytes that are associated with colitis-induced immunopathology (Section 3.3.3). The myeloid cell lineage is comprised of granulocytes and monocytes (Kawamoto and Minato 2004). Therefore, experiments focused on the effect of systemic IL-6 neutralization on myeloid cell recruitment to the lung. Myeloid cells were identified by flow cytometry according to the gating strategy in section 2.10. There was no statistically significant difference in the proportion of myeloid cells in the lung of anti-IL-6 treated DSS colitis mice compared to isotype treated controls (Figure 4.3.4A). Further analysis of myeloid cell populations revealed that anti-IL-6 treatment resulted in a significant decrease in neutrophils recruited to the lung of DSS colitis mice compared to isotype treated controls (Figure 4.3.4B A). IL-6 treatment had no influence on the proportion of monocytes in the lung of DSS colitis mice (Figure 4.3.4B B). Therefore, these data show that systemic IL-6 is involved in the recruitment of neutrophils to the lung in colitis-induced pulmonary inflammation. Representative dot plots illustrating the gating strategy utilized for this analysis is provided in the appendices (Figure 8.2.1 A-D).

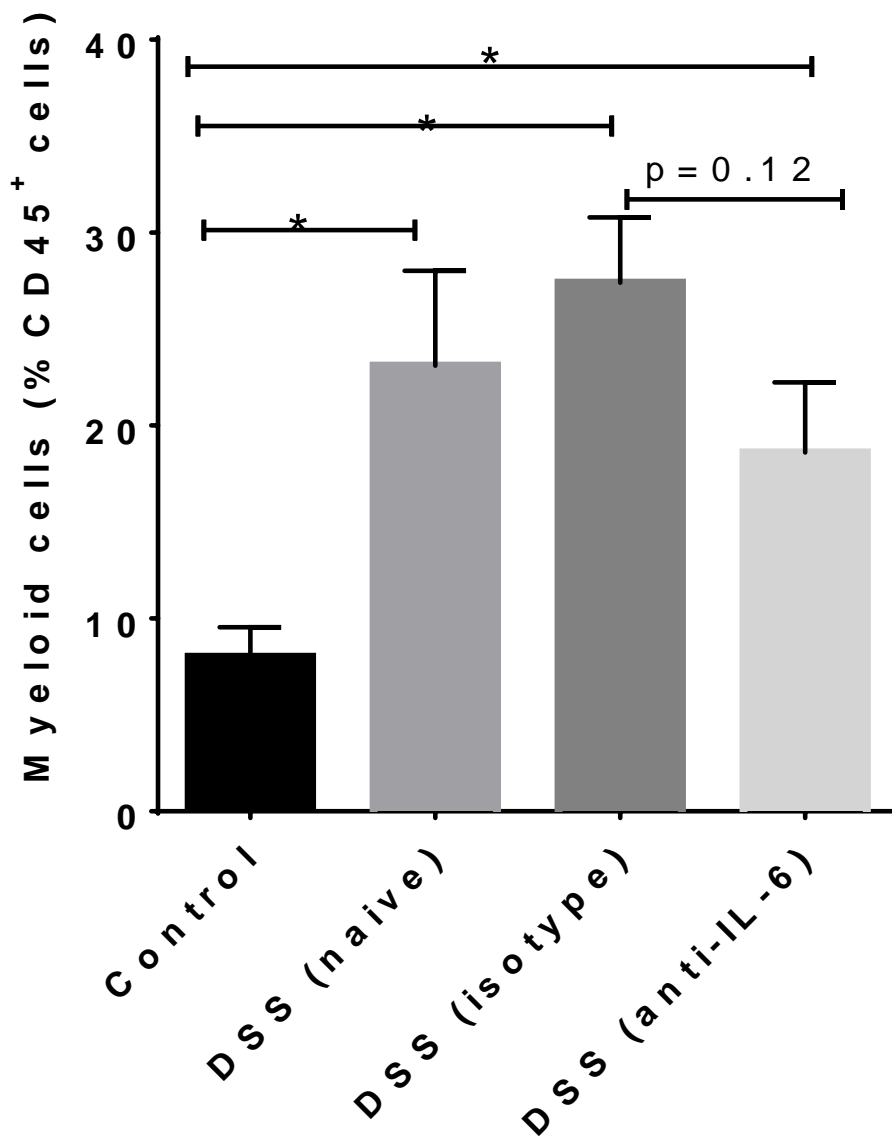


Figure 4.3.4A: Proportion of myeloid cells in the lung of anti-IL-6 treated acute DSS colitis. Cells were isolated from whole lung tissue according to the method described in section 2.10. Proportion of myeloid cells in the lung of anti-IL-6 treated acute DSS colitis mice (n = 4). Measured by flow cytometry, according to the gating strategy in Table 2.10. All data represented as mean \pm S.E.M. *=p<0.05, unpaired t-test.

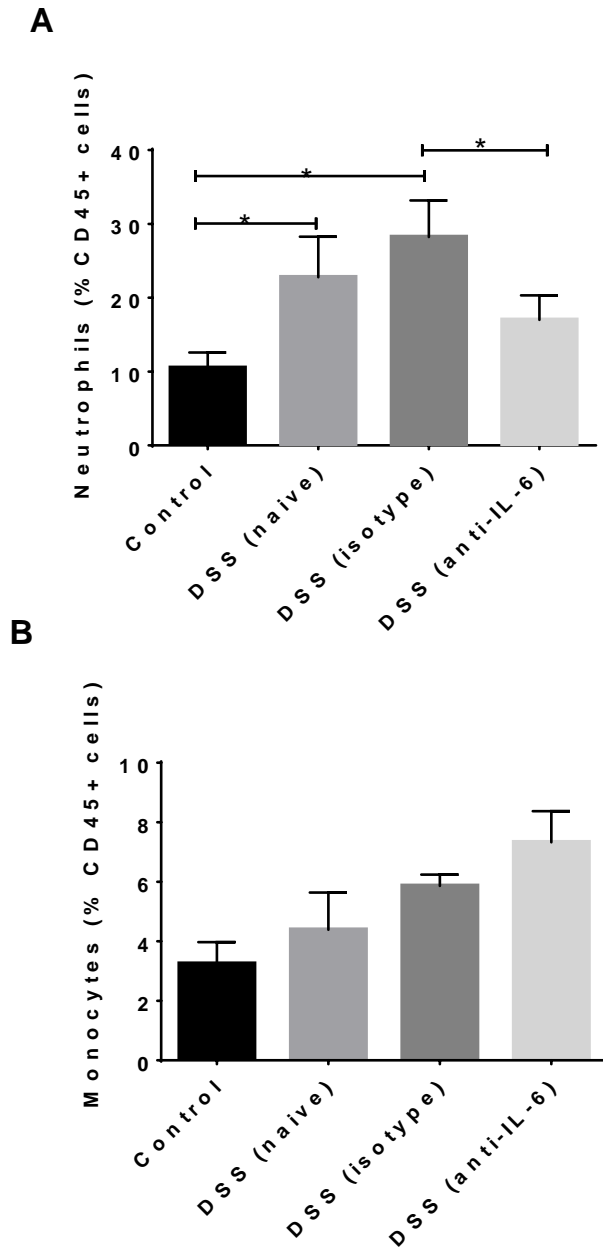


Figure 4.3.4B: Proportion of neutrophils and inflammatory monocytes in the lung of acute DSS colitis. Cells were isolated from whole lung tissue according to the method described in section 2.10. (A) Proportion of neutrophils in the lung of anti-IL-6 treated acute DSS colitis mice (n = 4). (B) Proportion of monocytes in the lung of anti-IL-6 treated acute DSS colitis mice (n = 4). Cell populations quantified by flow cytometry according to the gating strategies in Table 2.10. All data represented as mean \pm S.E.M. *= $p < 0.05$, **= $p < 0.01$, unpaired t-test.

4.3.5: Gene expression profile in the lung of anti-IL-6 treated acute DSS colitis.

In Section 4.3.4 it was shown that IL-6 signalling is involved in the recruitment of neutrophils to the lung in DSS colitis-induced pulmonary inflammation. To determine whether IL-6 signalling mediates the recruitment of neutrophils directly through the induction of inflammatory cytokines in the lung, the gene expression profile of anti-IL-6 treated colitis mice was conducted. The genes chosen for analysis were those that had been identified to be associated with colitis-induced pulmonary inflammation in previous experiments (Section 3.3.4). The transcript level of *Il1b* was decreased in anti-IL-6 treated colitis mice compared to the isotype treated controls. The transcript level of *Ifng*, *Il6*, *Tnf*, and *Ptafr* were not affected by anti-IL-6 treatment (Figure 4.3.5A and Figure 4.3.5B). These data suggest that IL-6 signaling selectively mediates IL-1 β expression in the lung. The isolated reduction in *Il1b* expression may be due to blockade of an IL-6 mediated IL-1 β specific signaling pathway that is downstream of TNF, IFN- γ and PAFR expression. This signaling pathway may be related to the decrease in neutrophils in whole lung tissue that was observed in Section 4.3.3, as neutrophils are prominent producers of IL-1 β . In this paradigm *Il1b* expressing neutrophils are not recruited to the lung due to the blockade of IL-6 signaling, resulting in a decrease in *Il1b* expression in whole lung tissue. While IL-6 neutralization did decrease *Il1b* it did not ablate cytokine expression, therefore it can be concluded that while IL-6 is a factor that contributes to colitis-induced pulmonary inflammation, it is not the initiating factor.

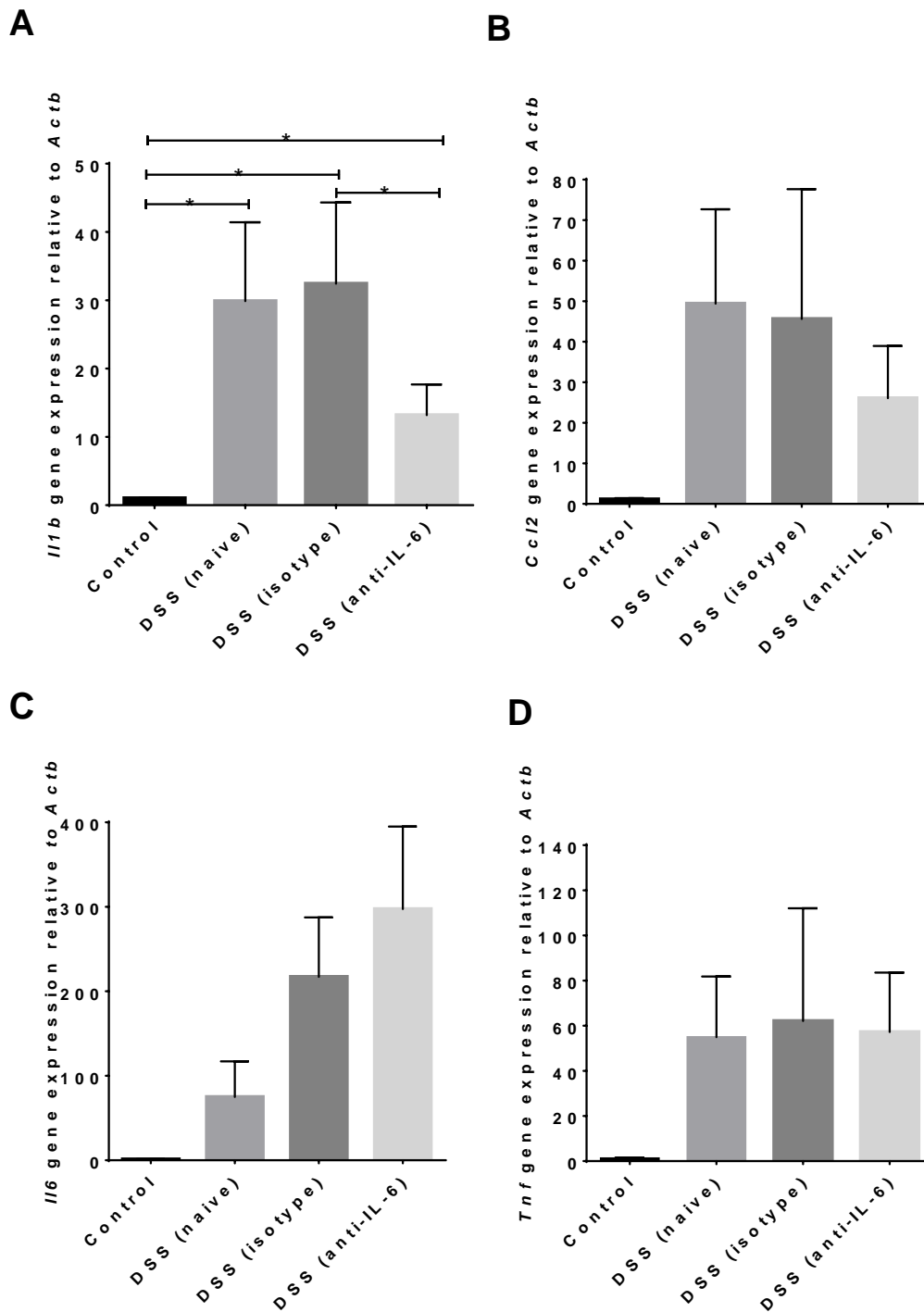


Figure 4.3.5A: Gene expression profile in the lung of anti-IL-6 treated acute DSS colitis.

Transcript level of (A) *Il1b* (B), *Ccl2* (C), *Il6* and (D) *Tnf* in the lung of anti-IL-6 treated acute DSS colitis (n = 6). Transcript level quantified by qPCR. All data represent as mean \pm S.E.M. *= $p < 0.05$, unpaired t-test.

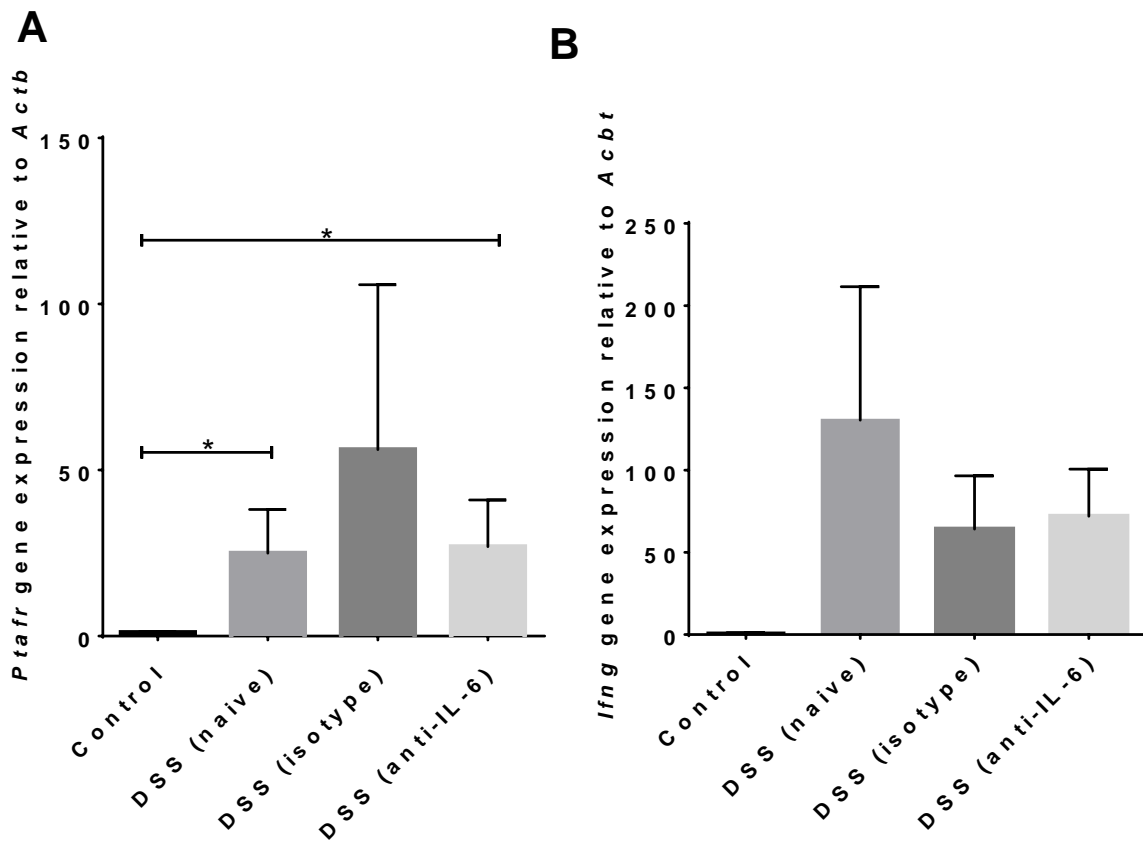


Figure 4.3.5B: Gene expression profile in the lung of anti-IL-6 treated acute DSS colitis

continued. Transcript level of (A) *Ptafr* and (B) *Ifng* in the lung of anti-IL-6 treated acute DSS colitis (n = 6) Transcript level quantified by qPCR. All data represent as mean \pm S.E.M.

*= $p < 0.05$, unpaired t-test.

4.3.6 Cytokine and PAFR protein levels in the lung of anti-IL-6 treated acute DSS colitis.

To determine the role of systemic IL-6 on cytokine expression in the lung, IFN- γ , TNF, IL-6, CCL2, IL-1 β and PAFR protein levels were quantified. These pro-inflammatory molecules have been implicated in mediating colitis-induced pulmonary inflammation in previous experiments (Section 3.3.5). There was no change in the level of IFN- γ and TNF in any of the DSS colitis groups compared to naïve controls, corroborating the observations seen in Section 3.3.5 (Figure 4.3.6A). Therefore, it can be concluded that IFN- γ and TNF are not implicated in the pathogenesis of colitis-induced pulmonary inflammation, regardless of IL-6 involvement. There was no difference in pro-IL-1 β protein levels between anti-IL-6 treated DSS colitis mice and isotype treated controls (Figure 4.3.6B A). This result is in contrast to the observation in Section 4.3.4 that shows a decrease in lung *Il1b* expression with anti-IL-6 treatment. In Section 4.3.4 it was considered that the decrease in *Il1b* expression was due to a decrease in the number of neutrophils, the potential source of *Il1b* expression in the lung. The result in figure 4.3.6A contradicts this hypothesis as lung IL-1 β protein levels are not affected with systemic IL-6 neutralisation. This discrepancy between IL-1 β protein and gene expression, may be due to IL-1 β expression by cell types other than neutrophils. Therefore the conclusion that *Il1b* gene expression is decreased due to reduced neutrophil recruitment to the lung may still be the case, however a number of cell types in the lung can express IL-1 β and these expression pathways are not related to IL-6 signaling. Therefore IL-1 β expression in the lung of DSS colitis mice is not solely regulated by systemic IL-6.

A similar result was obtained for CCL2 expression, lung CCL2 protein levels were not changed between the anti-IL-6 treated DSS colitis mice and isotype treated controls (Figure 4.3.6B B). PAFR protein levels from the lungs of DSS colitis mice treated with anti-IL-6,

were measured by western blot. There was no difference in PAFR expression between anti-IL-6 and isotype treated DSS colitis groups. Thus, it was concluded that systemic IL-6 does not induce PAFR expression in the lung of DSS colitis mice (Figure 4.3.6C A & B). These data corroborate the findings in Section 4.3.5, wherein systemic IL-6 does not directly influence CCL2 and PAFR gene expression in the lung.

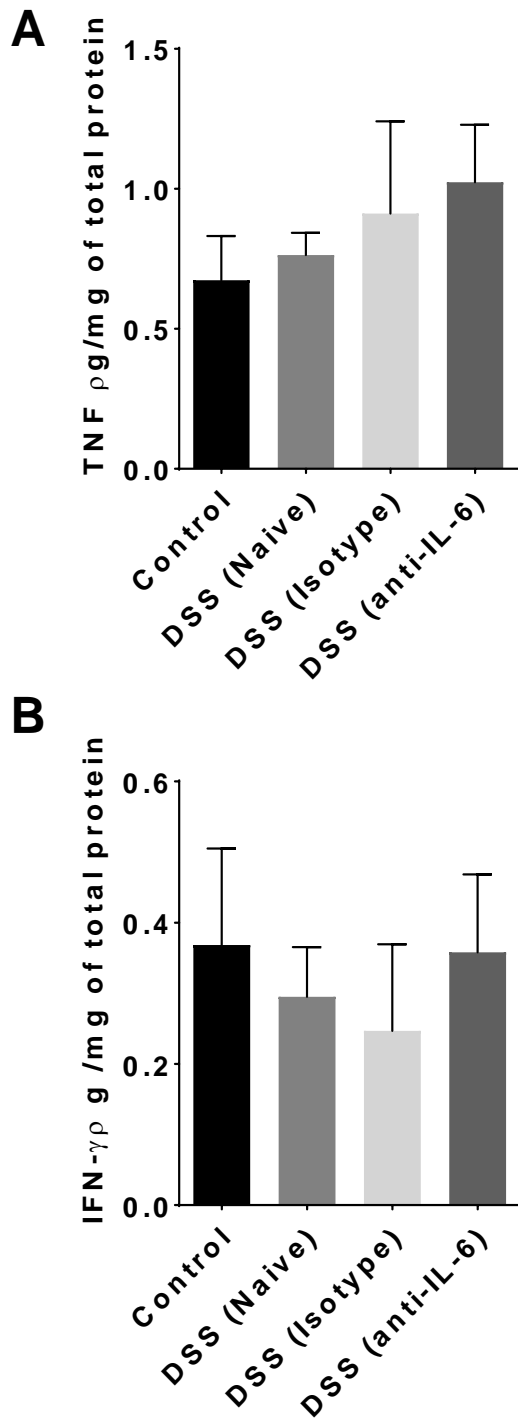


Figure 4.3.6A: TNF and IFN- γ protein levels in the lung of anti-IL-6 treated acute DSS colitis. (A) TNF and (B) IFN- γ protein levels in the lung of anti-IL-6 treated DSS colitis. TNF and IFN- γ were measured by cytometric bead array (n = 6). All data represented as mean \pm S.E.M.

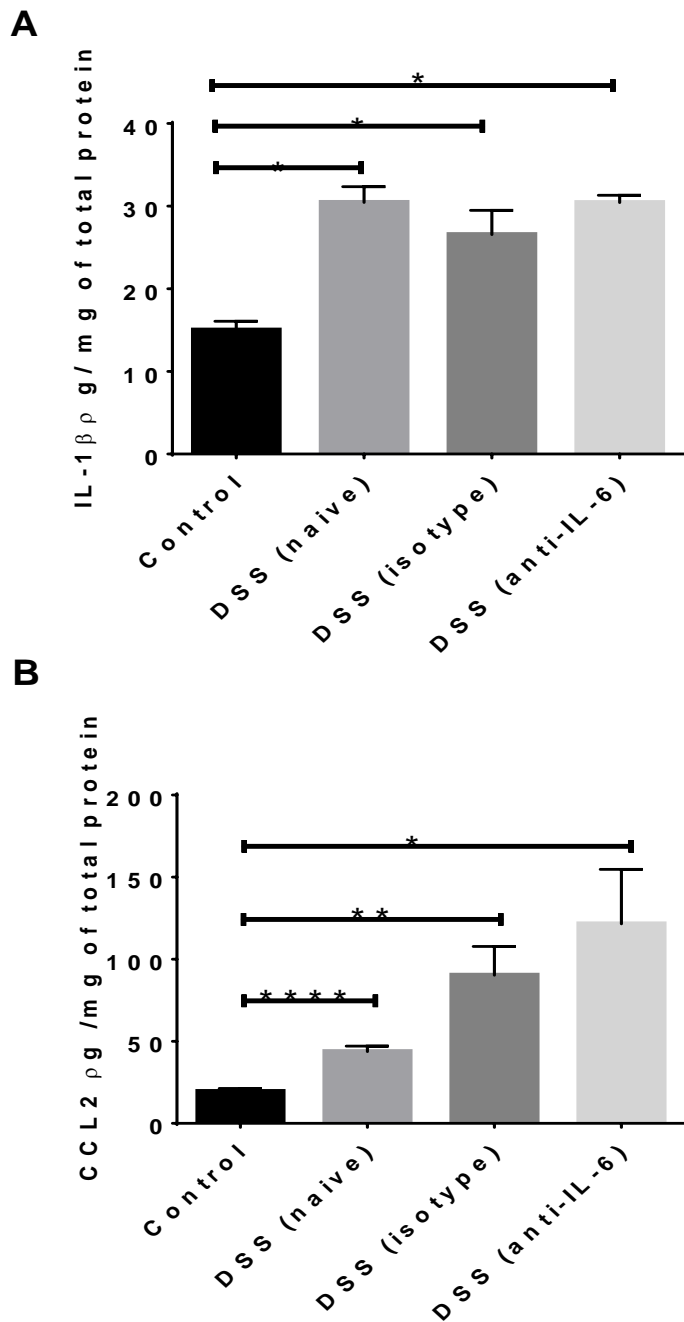


Figure 4.3.6B: CCL2 and IL-1 β protein levels in the lung of anti-IL-6 treated acute DSS colitis. (A) CCL2 protein levels in the lung of anti-IL-6 treated DSS colitis, measured by cytometric bead array (n = 6). (B) Pro-IL-1 β protein levels in the lung of anti-IL-6 treated DSS colitis, measured by ELISA (n = 6). All data represented as mean \pm S.E.M. *= p <0.05, **= p <0.01, ****= p <0.001, unpaired t-test.

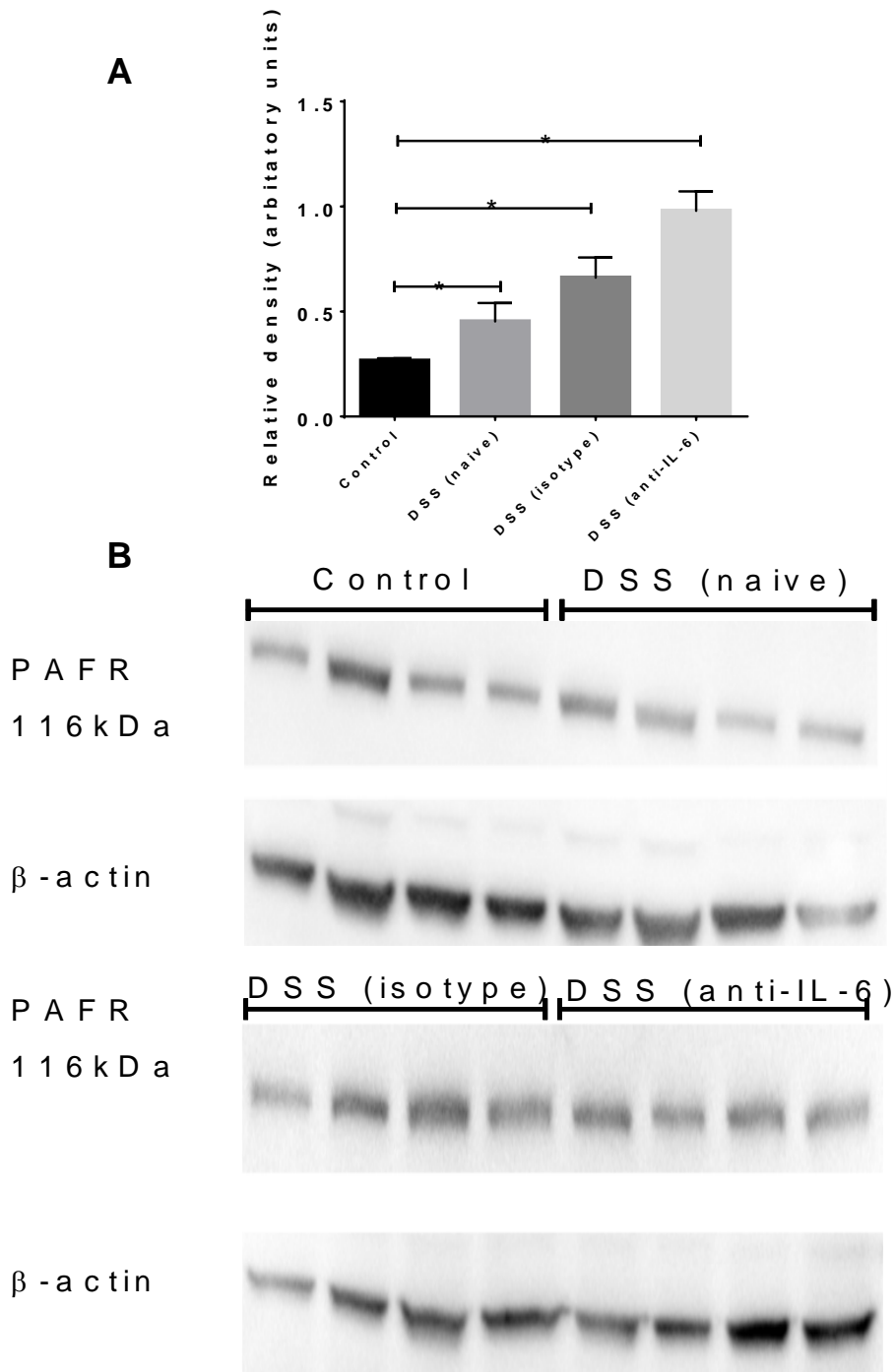


Figure 4.3.6C: PAFR protein levels in the lung of anti-IL-6 treated acute DSS colitis.

PAFR protein levels in the lung of anti-IL-6 treated acute DSS colitis mice quantified by western blot. (A) Densitometry analysis was used to empirical quantify protein bands (n = 4) (B) PAFR and β -actin protein bands (n = 4). All data represented as mean \pm S.E.M.

*= $p < 0.05$, unpaired t-test.

4.3.7 Systemic inflammation in anti-IL-6 treated acute DSS colitis.

The neutralization of systemic IL-6 did not directly affect the expression of inflammatory mediators in the lungs of colitis mice. Anti-IL-6 treatment did however reduce the proportion of neutrophils in the lung. To investigate whether IL-6 mediated systemic inflammation was accountable for the decrease in neutrophils entering the lung, the cellularity and level of inflammatory mediators in the circulatory system was quantified in anti-IL-6 treated colitis mice. The proportion of neutrophils and monocytes in the blood was quantified by flow cytometry. The proportion of neutrophils in the blood of anti-IL-6 treated DSS colitis mice was significantly decreased compared to isotype controls (Figure 4.3.7A). Therefore, it was concluded that systemic IL-6 regulates the neutrophilia associated with colitis. In regards to monocytes, anti-IL-6 treatment had no influence on the proportion of these cells in the blood (Figure 4.3.7B). Taken together, these data show that IL-6 in the circulatory system controls systemic inflammation in DSS colitis by regulating neutrophils numbers in the bloodstream. Representative dot plots illustrating the gating strategy utilized for this analysis is provided in the appendices (Figure 8.2.2 A-D).

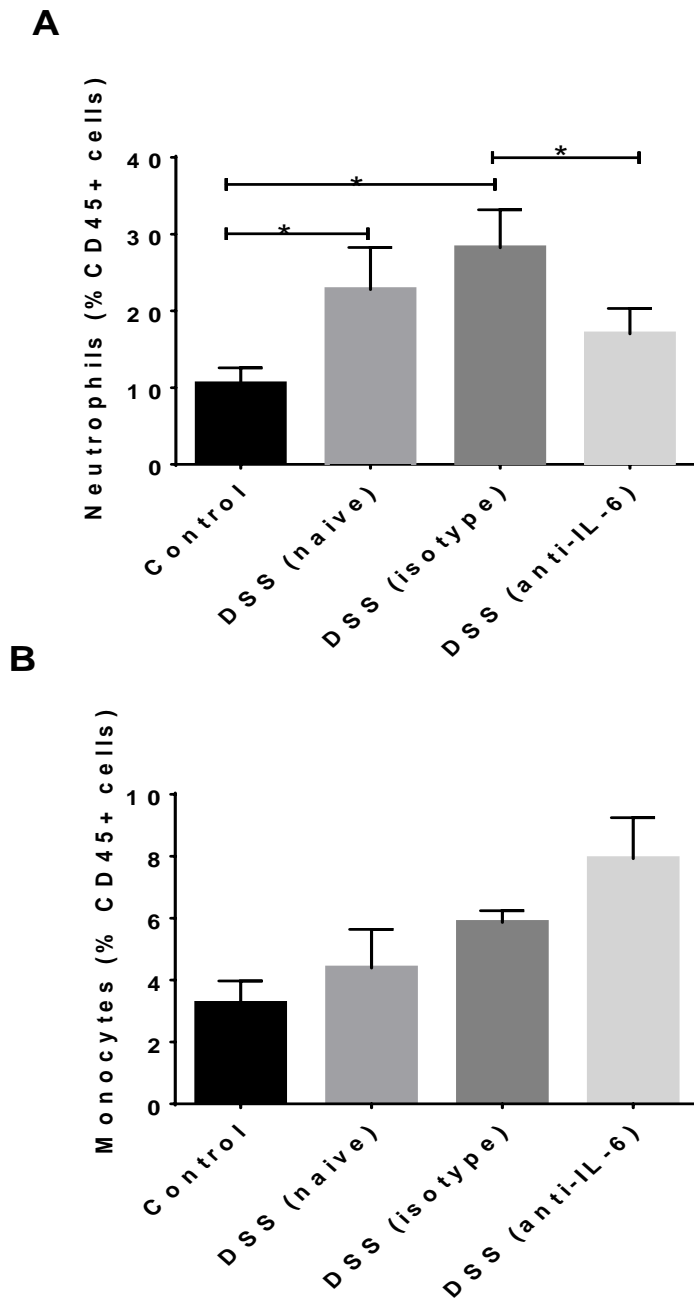


Figure 4.3.7A: Proportion of neutrophils and monocytes in the blood of anti-IL-6 treated acute DSS colitis. (A) The proportion of neutrophils in the blood of anti-IL-6 treated acute DSS colitis mice (n = 6). (B) Proportion of monocytes in the blood of anti-IL-6 treated acute DSS colitis mice (n = 6). All data represented as mean \pm S.E.M. $^* = p < 0.05$, unpaired t-test. Cellularity quantified by flow cytometry according to gating strategy in Table 2.10.

4.3.8 The effect of IL-6 on myeloid cell production in the bone marrow

Systemic IL-6 neutralization ameliorated colitis-induced neutrophilia. As it was observed in Section 3.3.7 that colitis induces the proliferation of myeloid progenitor cells in the bone marrow, it was hypothesized that the decrease in neutrophils in the circulatory system was a result of IL-6 mediated stimulation of myeloid progenitor cells. To test this hypothesis, the effect of IL-6 neutralization on neutrophil development in the bone marrow was conducted. It was found that anti-IL-6 treatment did not affect the proportion of myeloid precursor cells in the bone marrow. The proportion of MPP cells in the bone marrow was increased in all the DSS colitis groups compared to controls (Figure 4.3.8 A). The level of mature neutrophils in the bone marrow was decreased in the DSS naïve and DSS isotype groups compared to controls, while there was an increase in mature neutrophils in the anti-IL-6 treatment group in comparison to the isotype controls (Figure 4.3.8 B). These differences in the proportion of neutrophils in the anti-IL-6 treated group were attributed to blockade of IL-6 mediated egress of neutrophils from the bone marrow. Representative dot plots illustrating the gating strategy utilized for this analysis provided in the appendices (Figure 8.2.3 A-D).

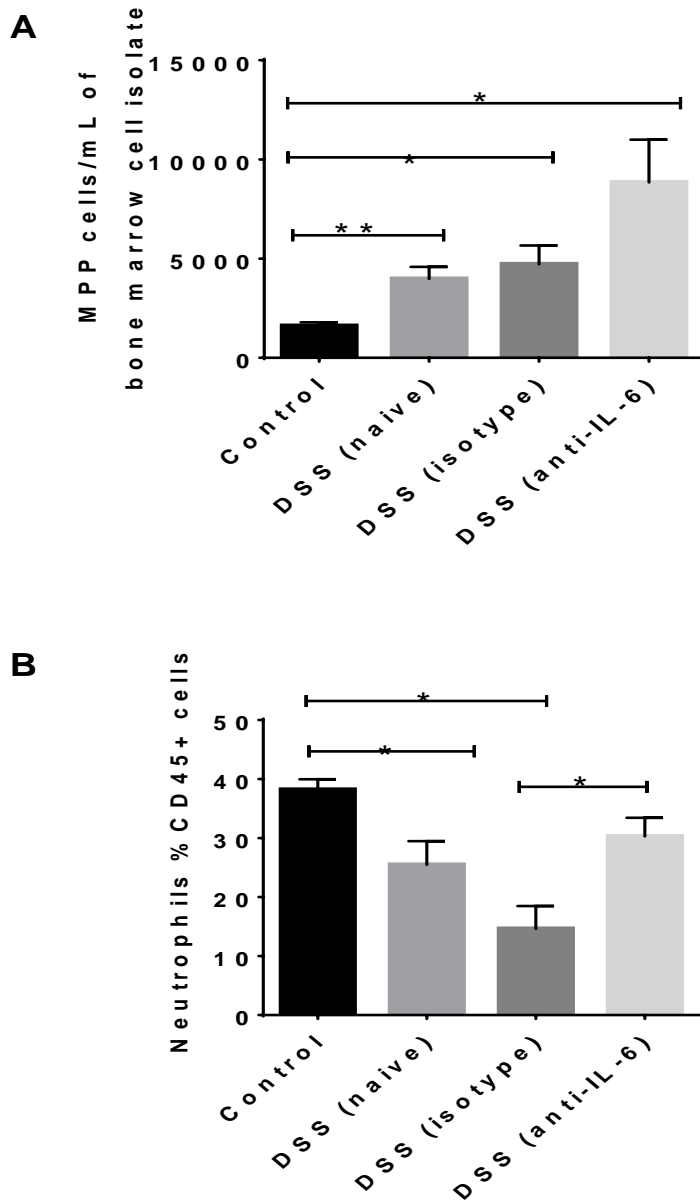


Figure: 4.3.8: The influence of IL-6 on the differentiation of myeloid progenitor cells and the proportion of mature neutrophils in the bone marrow of acute DSS colitis. (A)

The number of multi-potent progenitor (MPP) cells in the bone marrow of anti-IL-6 treated acute DSS colitis mice (n = 6). (B) The proportion of mature neutrophil levels in the bone marrow of anti-IL-6 treated acute DSS colitis. Cell populations quantified by flow cytometry, utilizing the gating strategy in Table 2.10 (n = 6). All data represented as mean \pm S.E.M.

*= $p < 0.05$, **= $p < 0.01$, unpaired t-test.

4.4 Discussion

The aim of experiments in this chapter was to investigate the role of systemic IL-6 in the recruitment of myeloid cells to the lung in colitis-induced pulmonary inflammation. To complete this, aim the effect of anti-IL-6 treatment on the factors involved in colitis-induced pulmonary inflammation was investigated. These factors include the magnitude of intestinal inflammation, cytokine expression in the lung and systemic inflammation.

The role of IL-6 in mediating intestinal inflammation has been studied extensively in the literature and the consensus is that IL-6 is a factor involved in the initiation of colitis (Naito, Takagi et al. 2004, Sander, Obermeier et al. 2008, Grivennikov, Karin et al. 2009). Grivennikov *et al.* reported that *Il6* deficient mice had reduced severity of colitis in respect to colon shortening, weight loss and histopathology (Grivennikov, Karin et al. 2009). The role of IL-6 in the development of colitis was corroborated in studies by Naito *et al.* This study reported that GI pathology in DSS colitis was reduced in *Il6* deficient mice (Naito, Takagi et al. 2004). GI pathology in experiments by Naito *et.al* was measured by histopathology, weight loss, colon shortening and cytokine gene expression (Naito, Takagi et al. 2004). Furthermore, a study by Sander *et al.*, that did not directly target IL-6 but instead targeted the IL-6 family signal transducer gp130, reported that gp130 signaling is required for the development of GI pathology in DSS colitis (Sander, Obermeier et al. 2008). Weight loss, colon shortening, cytokine levels and leucocyte infiltration into the mucosa were utilized as measurements of gastrointestinal pathology in these experiments (Sander, Obermeier et al. 2008). In the experiments conducted in this chapter, anti-IL-6 treatment had no influence on the severity of GI pathology, in respect to colon shortening, histopathology and cytokine signaling. The variation in how IL-6 interventions affect mucosal inflammation may be attributed to the nature of IL-6 interventions. In the experiments by Naito and colleagues,

acute colitis was induced in *Il6* deficient animals, thus IL-6 expression was abated. In the current study, IL-6 was blocked with an antibody after the initiation of disease, with the first treatment administered on day 3 of the colitis model. The dichotomy in results show that IL-6 is required for the initiation of mucosal inflammation but not the maintenance. This finding is supported by findings from Sander *et al.* in these studies it was reported that gp130/IL-6 signaling is required for the recruitment of leucocytes in the initiation of DSS colitis (Sander, Obermeier et al. 2008). Furthermore, Sander *et al.* found that in a myeloid cell specific deletion of gp130 that the initiation of colitis was delayed, indicating that gp130/IL-6 signaling is required for the activation of colonic resident myeloid cells in the early stage of disease (Sander, Obermeier et al. 2008). Thus, in the time course of IL-6 interventions in this model of DSS colitis, the initial stages of IL-6 signaling that propagates disease was not affected by administration of anti-IL-6 on day 3. This was the intention; as the aim of these experiments was not to study the effect of IL-6 on gastrointestinal inflammation, rather to investigate the effect of systemic inflammation secondary to colitis. Furthermore, the IL-6 antibody was administered systemically and not topically to the area of mucosal inflammation. Considering the presence of IL-6 systemically, a considerable amount of antibody would be sequestered by systemic IL-6 prior to reaching the site of mucosal inflammation. While anti-IL-6 treatment did not affect gastrointestinal inflammation, it did however reduce the effect of wasting. Naito *et al.*, Sommer *et al.* and Sander *et al.* corroborated this observation (Naito, Takagi et al. 2004, Sander, Obermeier et al. 2008, Sommer, Engelowski et al. 2014). The ability of IL-6 blockade to reduce wasting in colitis may be attributed to the pyrogenic effect elicited by IL-6 (Netea, Kullberg et al. 2000). IL-6 mediates fever through the induction of prostaglandins in the central nervous system (CNS) (Netea, Kullberg et al. 2000). Prostaglandins are hormone like lipids that can cause an increase in body temperature; and weight loss is a symptom of elevated body temperature

(Netea, Kullberg et al. 2000). Thus, it can be hypothesized that wasting in colitis is mediated by IL-6 induction of pyrogenic molecules in the CNS. In addition to controlling body temperature, prostaglandins regulate the activity of the hypothalamic-pituitary adrenal (HPA) axis (Gadek-Michalska, Tadeusz et al. 2013). Hyperactivity of the HPA axis is the fundamental biological mechanism that mediates depression. In fact, depression and anxiety are common comorbidities of IBD, thus it can be postulated that systemic IL-6 may mediate the CNS related comorbidities of colitis (Graff, Walker et al. 2009).

To assess the effect of IL-6 neutralization on pulmonary inflammation induced by colitis, the cellularity of the lung was assessed. Cytokine analysis at the transcript and protein level was conducted and histopathological scores from lung sections quantified. It was found that neutralization of IL-6 had no effect on histopathological scores or cytokine levels at both the transcript and protein levels. There was however a reduction in neutrophils entering the lung in the anti-IL-6 treated DSS colitis group. The reduction in neutrophils entering the lung may be due to the role of IL-6 in facilitating neutrophil recruitment in the initial stages of inflammation. (McLoughlin, Witowski et al. 2003).

IL-6 facilitates neutrophil requirement in acute inflammation via the expression of neutrophil tropic cytokines and phospholipids (McLoughlin, Witowski et al. 2003). Therefore reduction in neutrophils entering the lung, while not influencing IL-1 β , PAFR or CCL2 levels, was interesting as these molecules are required for the migration of myeloid cells to sites of inflammation. Sander *et.al* showed that gp130/IL-6 cytokine signaling on parenchymal cells is required for the migration of myeloid cells to mucosal sites of inflammation via the expression of cytokines that include CCL2 (Sander, Obermeier et al.

2008). The fact that IL-6 neutralization had no effect on cytokine expression in our model of colitis may be because IL-6/sIL-6R is not the ligand involved in gp130 signaling in the context of colitis-induced pulmonary inflammation. Gp130 is a heterogeneous signal transducer with affinity for the entire IL-6 family of cytokines. There are nine cytokines of the IL-6 family and these molecules include interleukin-11 (IL-11), interleukin-27 (IL-27), leukemia inhibitory factor (LIF), oncostatin M (OSM), and ciliary neurotrophic factor (CNTF) (Taga and Kishimoto 1997). The role of these molecules in modulating myeloid cell recruitment and the expression of innate cytokines has not been determined. Thus, it is possible that cytokine expression in the lungs of DSS colitis mice is mediated through gp130, via a member of the IL-6 family that is not IL-6/sIL6R. However, there is limited literature available to provide evidence for such a mechanism. Thus, it can be considered that gp130 signaling is not directly involved in this inflammatory cascade and that another mechanism is responsible for the expression of lung cytokines in colitis.

To investigate whether IL-6 mediated systemic inflammation was accountable for the decrease in neutrophils entering the lung, the cellularity and level of systemic IL-6 was quantified in the circulatory system. In addition, the proportion of mature and precursor myeloid cells was analyzed in the bone marrow. It was found that systemic neutralization of IL-6 attenuated the neutrophilia associated with colitis. Treatment with anti-IL-6 also dropped the level of IL-6 in serum to basal levels, confirming that the effect of anti-IL-6 treatment is the result of blocking the biological effect of systemic IL-6. The decrease of neutrophils in the circulatory system was associated with an increase in mature neutrophils in the bone marrow, but no change in the proportion of myeloid precursor cells. The role of IL-6 in controlling granulopoiesis and thus accumulation of neutrophils at inflammatory sites has been shown by Liu *et al.* and Chou *et al.* (Liu, Poursine-Laurent *et al.* 1997, Chou, Sworder

et al. 2012). These two studies report the role of IL-6 in regulating granulopoiesis at the early stage of cell development, however in these studies IL-6 did not directly regulate the terminal differentiation of mature neutrophils or the egress of neutrophils from the bone marrow niche, contradictory to what was observed in the DSS colitis model. Under homeostatic conditions, neutrophil egress from the bone marrow is mediated by CXCR4/SDF-1 interactions. Although in the context of inflammation, a number of chemokines have been reported to enable chemotaxis of neutrophils across the bone marrow sinusoidal endothelium. Amongst the chemokines that have been identified in this process are proteins known as complement factors. Complement proteins are components of the acute phase response which is regulated by IL-6 (Jagels, Chambers et al. 1995). Thus, while IL-6 may not directly influence neutrophil egress at the bone marrow endothelium, the proteins downstream of IL-6 are capable of sustaining a chemotactic gradient across the bone marrow sinusoidal endothelium, enabling the egress of neutrophils (Jagels and Hugli 1992, Jagels, Chambers et al. 1995). With the ablation of systemic IL-6, this chemotactic gradient does not exist, therefore the level of mature neutrophils in the bone marrow increases. As a result of this, the proportion of neutrophils present in the blood and subsequently sites of inflammation decreases in anti-IL-6 treated animals. An alternative mechanism to account for IL-6 induced neutrophilia is IL-6-induced inhibition of neutrophils apoptosis. IL-6 is known to prolong the half-life of neutrophils through inhibition of apoptosis, through this mechanism IL-6 can increase the number of neutrophils at sites of inflammation. It has also been shown that this effect can be reversed with anti-IL-6 treatment (Asensi, Valle et al. 2004). Therefore it is possible that in DSS colitis, neutrophilia is induced by inhibition of neutrophil apoptosis leading to a greater number of neutrophils in the circulation. To investigate whether this mechanism plays a role in colitis-induced lung inflammation the phenotype of neutrophils in relation to their stage in the cell cycle should be examined. This can be measured using the TUNEL assay, this assay

is designed to detect apoptotic cells that undergo extensive DNA degradation during the late stages of apoptosis.

4.5 Conclusion

In summary, the experiments in this chapter reveal that IL-6 is a factor necessary for the migration of neutrophils into the pulmonary system during intestinal inflammation. IL-6 mediates this effect by inducing neutrophilia. When systemic IL-6 is neutralized, neutrophilia is attenuated and thus the number of neutrophils in the circulation that can be attracted to the lung is decreased. However, IL-6 intervention does not abate cytokine signaling in the lung, therefore these data indicate that further factors are involved in the development of colitis-induced pulmonary inflammation. Cell signaling via PAFR is a mechanism by which inflammatory cytokine expression is known to occur (Hasegawa, Kohro et al. 2010). The ligand for PAFR, PAF is also known to be elevated in the intestine of IBD patients (Borthakur, Bhattacharyya et al. 2010). Therefore, pulmonary cytokine signaling via PAFR, as opposed to IL-6 signaling, may be the mechanism of IBD-induced pulmonary inflammation. This hypothesis was tested in Chapter 5.

Chapter 5: Platelet activating factor receptor (PAFR) signalling in the colitis-induced pulmonary inflammation.

5.1: Introduction

PAFR is a GPCR expressed in the plasma and nuclear membrane of leucocytes, platelets and structural cells (Ishii and Shimizu 2000). The primary agonist of PAFR is PAF. PAF is a phospholipid-signalling molecule that mediates leucocyte effector functions via PAFR. Experiments using PAFR knockout mice have confirmed that the effector functions of PAF are isolated to this receptor (Ishii, Kuwaki et al. 1998). The effector functions of PAF include the activation of neutrophils and macrophages. PAF-induced neutrophil activation results in chemotaxis, cytokine expression and superoxide release. PAF has a similar influence on macrophages, inducing cytokine expression and chemotaxis (Porrás-Reyes and Mustoe 1992). As PAF is a potent mediator of inflammation, PAFR signalling has been hypothesized to be involved in modulating innate inflammatory response in IBD. In support of this hypothesis several experimental models have shown that PAFR antagonism inhibits neutrophil recruitment to mucosal sites. Furthermore cultured colonic biopsies from UC patients have been shown to produce high levels of PAF (Wardle, Hall et al. 1996) and PAF has also been detected in the stool of both UC and CD patients (Hocke, Richter et al. 1999).

In addition to mediating GI pathology in IBD, PAFR signalling has been implicated in mediating a number of systemic inflammatory conditions, such as systemic lupus erythematosus and sepsis. Indeed a study by Schuster *et al.* showed that administration of a recombinant form of the endogenous PAF regulatory enzyme, PAF acetylhydrolase (PAF-AH) has the potential to prevent organ dysfunction in sepsis patients (Schuster, Metzler et al.

2003). As systemic inflammation is associated with the pulmonary pathologies of IBD, PAFR signalling may regulate IBD-induced respiratory pathologies in a similar manner.

5.1.1 Hypothesis

In Chapter 3 it was found that neutrophils are recruited to the lung of DSS colitis, a concurrent increase in PAFR expression was identified. There is a large body of literature describing the role of PAFR in mediating neutrophil recruitment to mucosal sites (Wardle, Hall et al. 1996, Uhlig, Goggel et al. 2005). Thus with these experimental observations coupled with literature describing the role of PAFR in neutrophil recruitment gave the rationale to hypothesize that PAFR signalling mediates neutrophil recruitment to the lung in colitis-induced pulmonary inflammation.

5.1.2 Aims

To test this hypothesis the influence of CV-6209 a PAFR antagonist on the factors that mediate colitis-induced pulmonary inflammation was investigated. These factors included, the magnitude of the underlying colitis, recruitment of neutrophils to the lung and cytokine signalling in lung tissue as well as the circulatory system. Another aim of these experiments was to determine whether neutrophil recruitment via PAFR signalling is predominately associated with lung resident cells or circulating leucocytes, to achieve this aim, mice were treated with CV-6209 by local administration via intra-nasal instillation (IN) or systemically via intra-venous injection (IV). To complete these aims the following specific aims were employed

- 1) To determine the influence of CV-6209 treatment by IN and IV administration on the magnitude of the underlying colitis associated with the development of pulmonary inflammation.
- 2) To determine the influence of local and systemic administration of CV-6209 on leucocyte recruitment to the lung in DSS colitis.
- 3) To determine the influence of CV-6209 treatment by IN and IV administration on cytokine signalling in the lung as well as systemic inflammation.

5.2 Methods

5.2.1 PAFR antagonist intervention in acute DSS colitis

Six-week-old female WT C57BL/6 mice were given 4% DSS *ad libitum* in drinking for six days. Age matched controls received drinking for six days. 25µg of CV-6209 (Santa Cruz Biotech) was administered to mice by IN and IV methods of administration. Mice were separated into two different treatment groups based on the method of CV-6209 administration. CV-6209 was administered on days 4, 5 and 6. Vehicle treated mice received PBS via IN and IV administration on days 4, 5 and 6 as outlined in Figure 5.2.1. IN instillation was performed by dropping 50µL of each solution on the nose of mice using a pipette. CV-6209 was diluted in PBS. Mice were anaesthetized with isoflurane. 25µg of CV-6209 was given to each mouse. To perform the IV injections mice were heated with a heat lamp, restrained and 100µL of each solution injected into the tail vein. CV-6209 was diluted in PBS. The mice were not anaesthetized. 25µg of CV-6209 was given to each mouse.

The time points utilized for the CV-6209 interventions were chosen based upon published knowledge of the DSS colitis model and the experimental aims. Intestinal inflammation in the

DSS colitis model develops 3 days post DSS treatment (Laroui, Ingersoll et al. 2012). As pulmonary inflammation develops secondary to intestinal inflammation and the aim of these experiments was to investigate the role of PAFR in the development of colitis-induced pulmonary inflammation, CV-6209 interventions were started after the initiation of colitis at day 4. Dose and time response experiments were not performed, dosage was chosen based on studies conducted by Han *et al* and McCullers *et al* (Han, Ko et al. 2002, McCullers and Rehg 2002). Animals were sacrificed on day 7. At the experiment endpoint lung, colon and blood was harvested for analysis as described in Section 2.0. Colon and lung tissue was collected for histopathological scoring according to methods described in Section 2.5 and 2.6 respectively. Cellular analysis of lung, and blood was conducted by flow cytometry as described in Section 2.10. Gene expression and cytokine analysis of lung and colon tissue was performed as described in Section 2.12, and 2.13. Data analysis was conducted as described in Section 2.15.

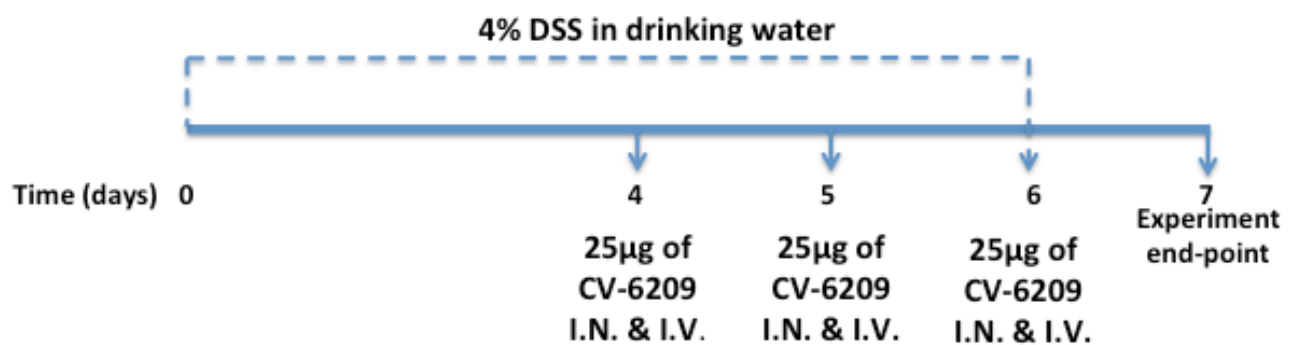


Figure 5.2.1 Time course of PAFR antagonist (CV-6209) interventions in acute DSS colitis.

5.3 Results

5.3.1 Intestinal pathology in CV-6209 treated acute DSS colitis.

The initial aim of experiments in this chapter was to quantify the influence of PAFR antagonism on the magnitude of intestinal inflammation. The magnitude of intestinal inflammation was quantified through analysis of weight loss, colon shortening, histopathology and cytokine signalling in DSS colitis mice treated with CV-6209. It was found that CV-6209 administered by IN and IV techniques had no effect on the amount of weight lost due to colitis (Figure 5.3.1A A). Thus PAFR signalling is not involved in the processes that mediate colitis-induced weight loss. There was no statistically significant change in colon length between CV-6209 treated DSS colitis mice and vehicle treated controls (Figure 5.3.1A B). Thus PAFR signalling is not the primary factor that contributes to colonic gross pathology in DSS colitis. Analysis of histopathology from colon sections of CV-6209 treated mice revealed that mice treated with IV CV-6209 had significantly lower histopathological scores than vehicle treated controls (Figure 5.3.1B A, representative images Figure 5.3.1C & Figure 5.3.1D). Histopathological scores from the colon of IN CV-6209 treated DSS colitis mice were not changed compared to vehicle treated controls (Figure 5.3.1B A, representative images Figure 5.3.1C & Figure 5.3.1D). To further analyse the role of PAFR in the development of intestinal pathology, histopathological scores were separated into four features of colitis. These features were; inflammatory scores, tissue injury, colitis activity and lymphoid aggregates. Inflammatory scores were quantified based on the magnitude of leucocyte infiltration into the mucosa; colitis activity was quantified based on the level of mononuclear cells and neutrophils in the mucosa as well as hypervascularization. Injury scores were quantified based on epithelial damage/ulceration and lymphoid aggregates was quantified based on the magnitude of lymphocyte congregation in the mucosa. This scoring system is outlined in detail in Table 2.5. IN CV-6209 treatment had no influence on

any of the pathological features analysed (Figure 5.3.1B B - E). However IV CV-6209 treatment reduced inflammatory scores and colitis activity but had no influence on tissue injury or lymphoid aggregates (Figure 5.3.1B B - E). Thus it can be concluded that IV PAFR ameliorates histopathology through a reduction in leucocyte recruitment to the mucosa, which in turn reduces colitis activity, but not tissue injury or lymphocyte aggregation. This observation may be explained by the mechanism of DSS action, DSS forms a vesicle complex with MCFA that enter colonocytes, these vesicles induce epithelial permeability and thus immune responses from epithelial cells and tissue resident macrophages irrespective of cell mediated responses from infiltrating leucocytes (Laroui, Ingersoll et al. 2012). This mechanism may account for how tissue injury is present in the colon of IV treated DSS mice, while inflammatory scores are decreased. Alternatively, tissue injury that persists in IV treated DSS colitis mice, may be due to the absence of recruited neutrophils. While neutrophils are largely considered to pathogenic in inflammatory situations, in DSS colitis, it has been shown that infiltrating neutrophils produce interleukin-22 (IL-22) which aids in the restitution of epithelial cells (Zindl, Lai et al. 2013). Therefore as IV CV-6209 treatment reduced leucocyte infiltration it may also have blocked the recruitment of a neutrophil phenotype that aids in epithelial repair, in this case epithelial permeability and tissue injury would persist even with the abrogation of leucocyte recruitment. To determine the influence of PAFR antagonism on cytokine signalling TNF, IFN- γ , CCL2 and IL-6 protein levels were measured in colon tissue of CV-6209 treated DSS colitis mice. It was found that CV-6209 treatment by IN and IV methods of administration did not influence TNF, IFN- γ , CCL2 and IL-6 levels in the colon (Figure 5.3.1E). These data suggest that PAFR signalling is not required for the development of tissue injury or TNF, IFN- γ , CCL2 and IL-6 expression in the colon, however PAFR is required for the recruitment of leucocytes. Thus, it was

concluded that PAFR antagonism does not directly regulate local inflammatory signalling in the colon.

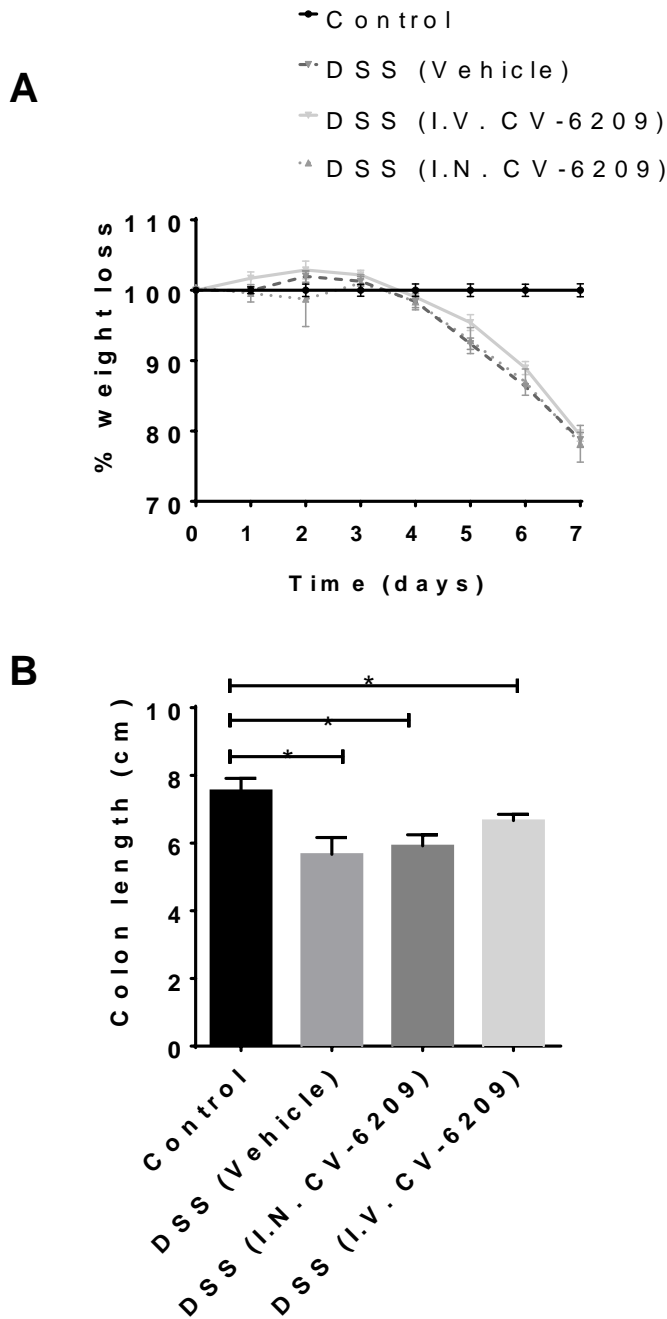


Figure 5.3.1A: Weight loss and colon shortening in CV-6209 treated DSS colitis. Acute DSS mice were treated with CV-6209 by two separate methods of administration, intranasal administration (I.N. CV-6209) and intravenously injection (I.V. CV-6209). (A) Percentage

weight loss normalized to naïve to controls (n =6). (B) Colon shortening in CV-6209 treated acute DSS colitis (n = 6). All data represented as mean ± S.E.M. *= $p < 0.05$, unpaired t-test.

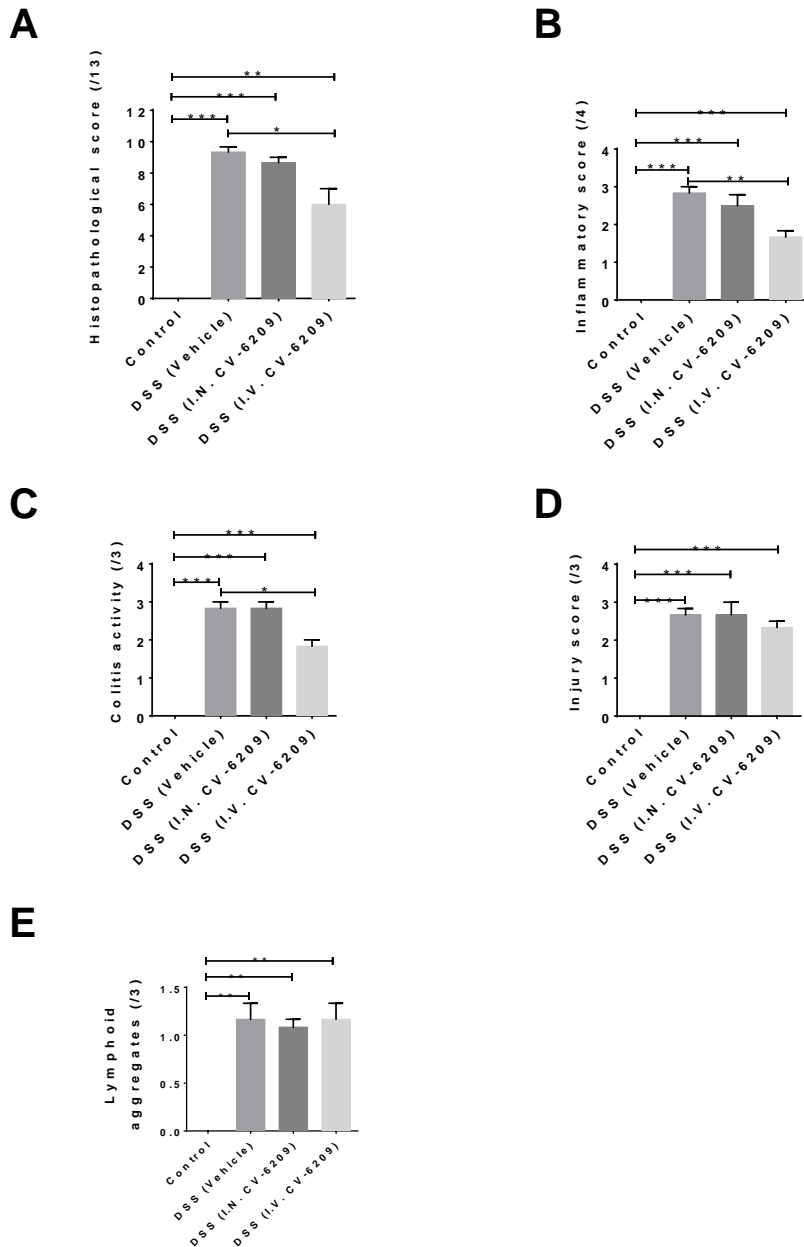
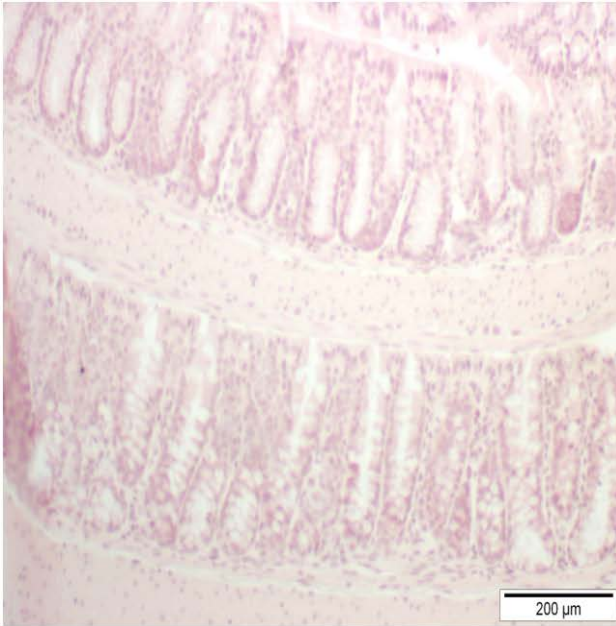
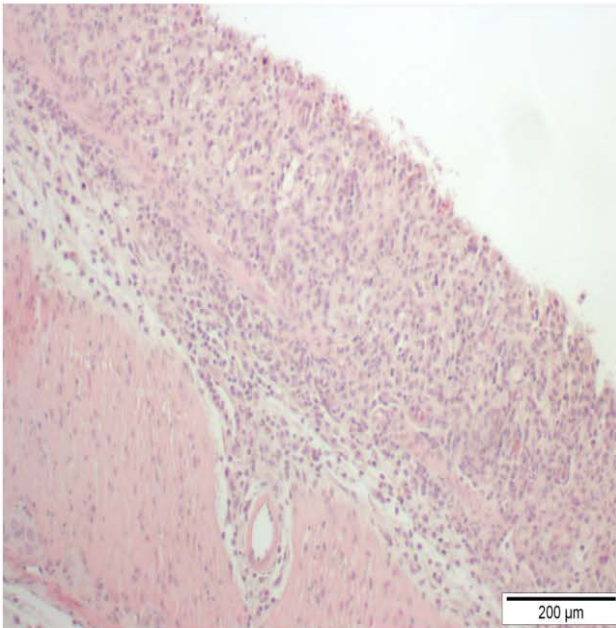


Figure 5.3.1B: Histopathological scores from colon sections in CV-209 treated DSS colitis. (A) Quantitative analysis of colon histopathology in CV-6209 treated DSS colitis as determined by scoring criteria in Table 2.5 (n = 4). Histopathology scores were separated into the pathological features quantified in the scoring system (Table 2.5). (B) Inflammatory

score, (C) Colitis activity, (D) injury score, (E) lymphoid aggregates. All data represented as mean \pm S.E.M, **= $p < 0.01$, ***= $p < 0.001$ 0001, (A) two-way ANOVA, (B & C) unpaired t-test.

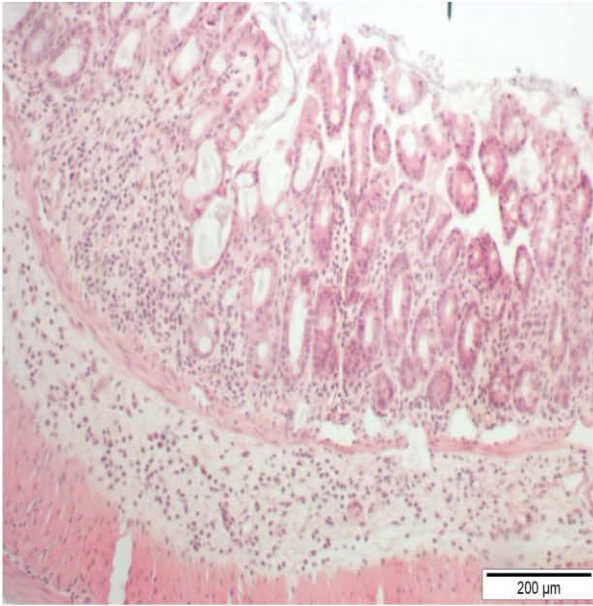


Control

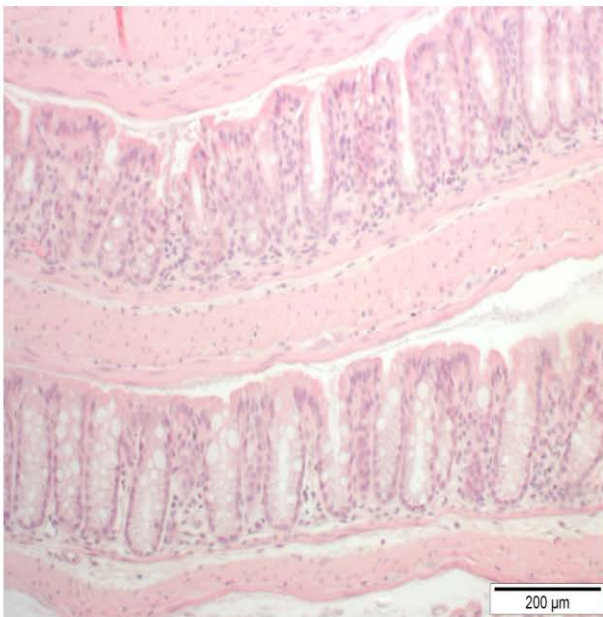


DSS (Vehicle)

Figure 5.3.1C: Histopathology in colon sections from control and vehicle treated DSS colitis. Representative images of histopathology observed in colon sections (10x).



DSS (I.N. CV-6209)



DSS (I.V. CV-6209)

Figure 5.3.1D: Histopathology in colon sections from I.N. and I.V. CV-6209 treated DSS colitis. Representative images of histopathology observed in colon sections (10x).

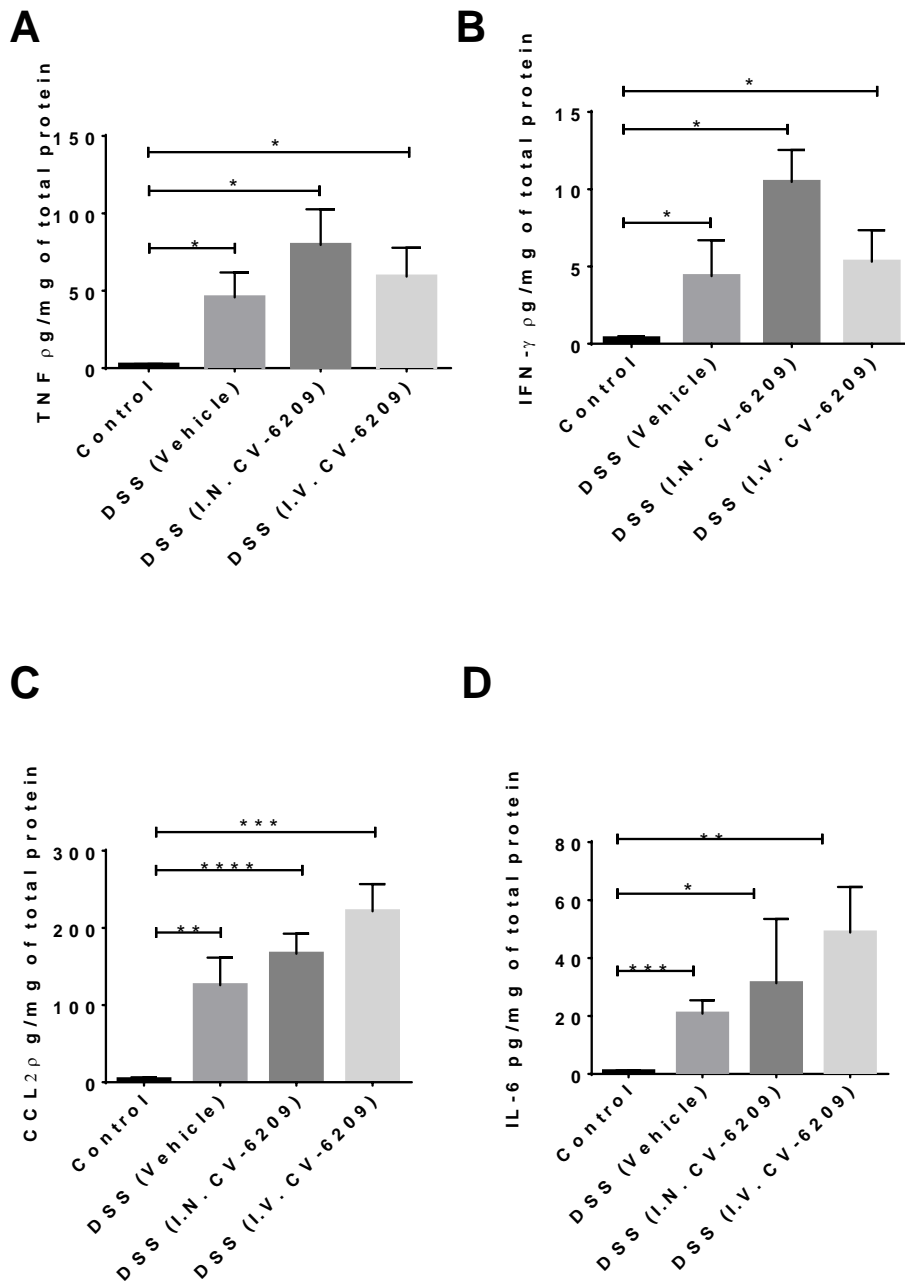


Figure 5.3.1E: Cytokine signalling in the colon of CV-6209 treated DSS colitis. The cytokines TNF, IFN- γ , CCL2 and IL-6 were measured in the colon of acute DSS colitis mice treated with CV-6209 by I.N. and I.V. methods of administration (n = 6). Cytokines measured by cytometric bead array. All data represented as mean \pm S.E.M. * = p<0.05, ** = p<0.01, *** = p<0.005, ****=p<0.0001 unpaired t-test.

5.3.2: The influence of PAFR antagonism on colitis-induced pulmonary pathology.

The next aim of experiments was to determine whether PAFR signalling is responsible for the pulmonary histopathology that is induced by colitis. To address this aim lung histopathological scores were quantified in CV-6209 treated DSS colitis mice. Histopathology was quantified based on inflammation around the airways, vasculature and parenchyma according to Table 2.6. No statistically significant change in histopathological scores was observed in the lungs of DSS colitis mice treated with CV-6209 by IN and IV administration compared to vehicle treated controls (Figure 5.3.2A, representative images Figure 5.3.2B & Figure 5.3.2C). While not statistically significant a trending decrease in histopathology was observed, however the low level of pathology and small group size makes a definitive conclusion on the influence of PAFR antagonism on colitis-induced pulmonary difficult. The low grade of pulmonary pathology is a limitation of the DSS colitis model, to overcome this limitation more sensitive assays to quantify the recruitment of leucocytes and cytokine signalling in the lung of CV-6209 treated DSS colitis mice were conducted.

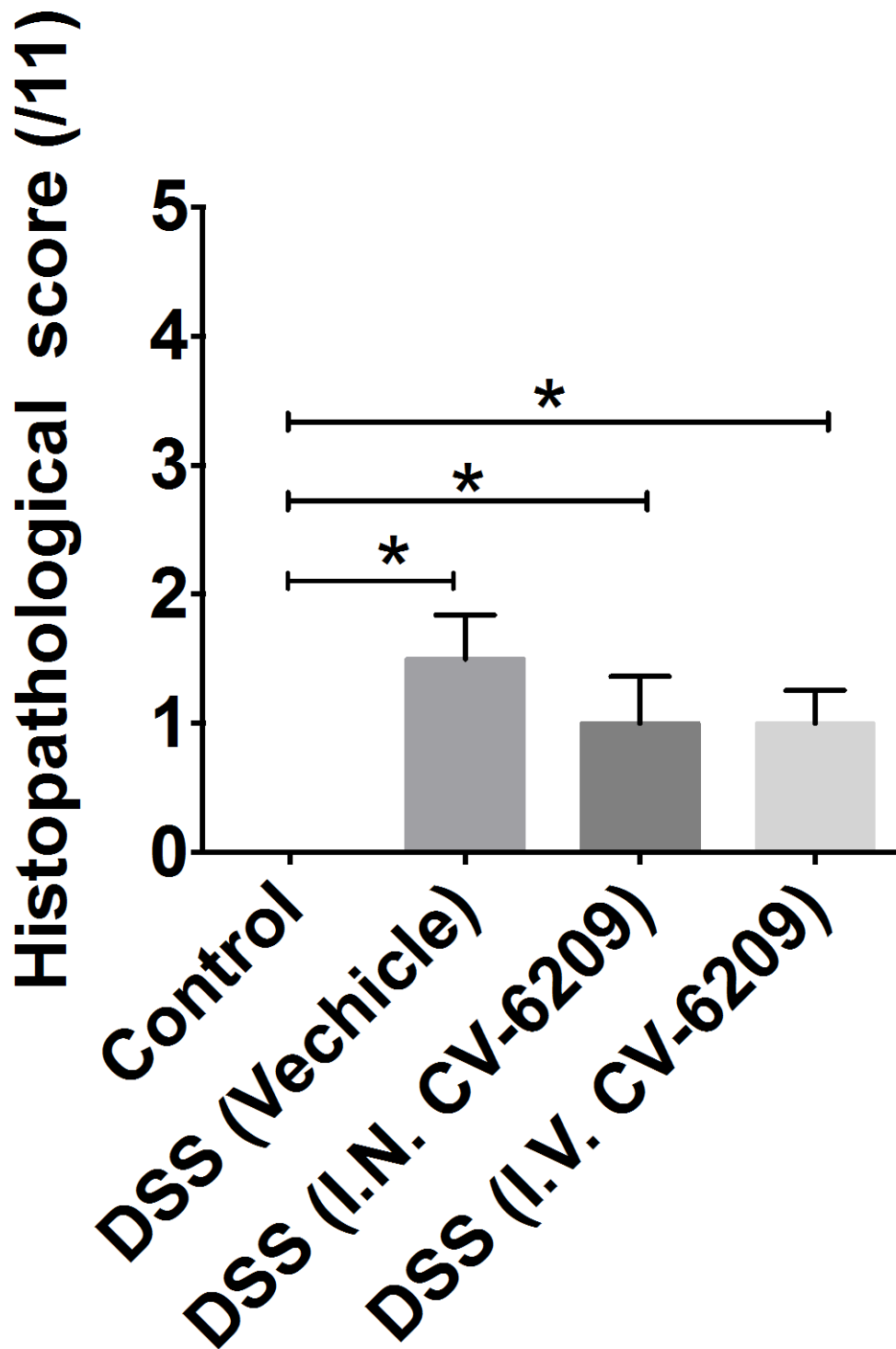
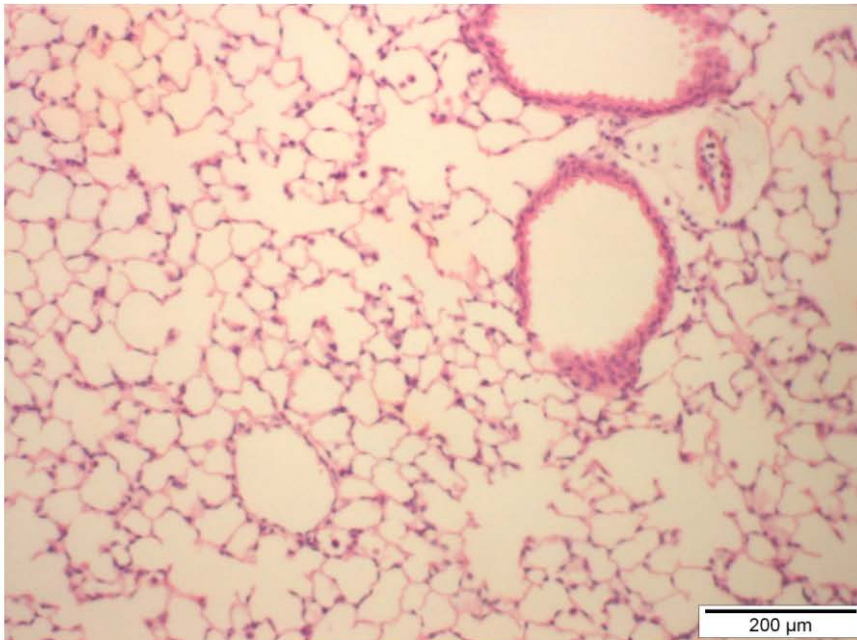


Figure 5.3.2A: Histopathological scores from lung sections in CV-6209 treated DSS colitis. (A) Quantitative analysis of histopathology in the lung of I.N and I.V. CV-6209 treated acute DSS colitis (n = 6), histopathological scores generated according to the scoring

criteria in Table 2.6. All data represented as \pm S.E.M. $*=p<0.05$, $*** = p<0.005$, unpaired t-test.



Control

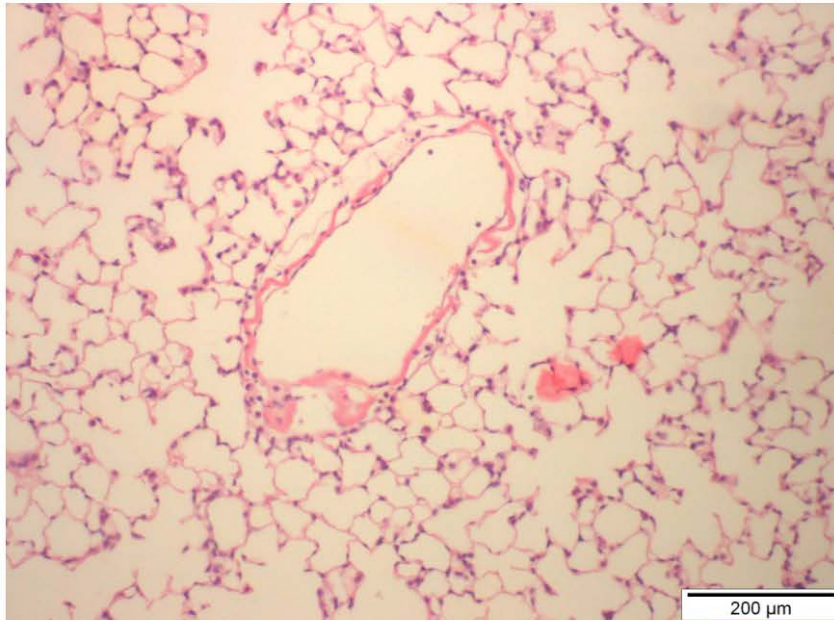


DSS (Vehicle)

Figure 5.3.2B: Histopathology in lung sections from control and vehicle treated DSS colitis. Representative images of histopathology observed in lung sections (10x).



DSS (I.N. CV-6209)



DSS (I.V. CV-6209)

Figure 5.3.2C: Histopathology in lung sections from I.N. and I.V CV-6209 treated DSS colitis. Representative images of histopathology observed in lung sections (10x).

5.3.3: The role of PAFR signalling in colitis-induced pulmonary inflammation.

PAFR signalling plays a prominent role in the activation and chemotaxis of myeloid cells, thus while PAFR antagonism did not influence pulmonary histopathology, it was hypothesized that PAFR antagonism would inhibit the recruitment of myeloid cells to the lung. Thus the effect of CV-6209 treatment on the recruitment of neutrophils and monocytes to the lungs of colitis mice was examined. IN administration of CV-6209 significantly reduced the recruitment of myeloid cells to the lungs of DSS colitis mice compared to vehicle treated controls (Figure 5.3.3A). CV-6209 treatment via the IV method administration did not achieve statistical significance, however a trending decrease in myeloid cells recruited to the lung was observed. Further analysis revealed that this decrease in myeloid cells can be attributed to a reduction in neutrophils recruited to the lung. Neutrophil numbers in the lung of IN CV-6209 treated DSS mice were significantly reduced compared to vehicle treated controls (Figure 5.3.3B A). A similar effect was observed in DSS colitis mice treated with IV CV-6209, however this result did not achieve statistical significance. CV-6209 treatment had no influence on the proportion of monocytes in the lungs of DSS colitis mice (Figure 5.3.3B B). Taken together these data show that PAFR signalling is a pivotal mediator of colitis-induced pulmonary inflammation through the recruitment of neutrophils. While the two methods of administration showed a similar trend in reducing neutrophil recruitment, localised IN administration led to a statistically significant reduction in neutrophil numbers. However a small sample size was used for this analysis. Therefore with the trend towards statistical significance in the IV treated group it can be concluded that the mechanism of action is similar and that the dichotomy in the level of neutrophil recruitment inhibition is due to higher levels of CV-6209 localized in the pulmonary system with IN treatment. Whereas IV delivery of CV-6209 will have disseminated the antagonist systemically, reducing

bioavailability of the molecule in the lung. Representative dot plots illustrating the gating strategy utilized for this analysis is provided in the appendices (Figure 8.3.1 A-D).

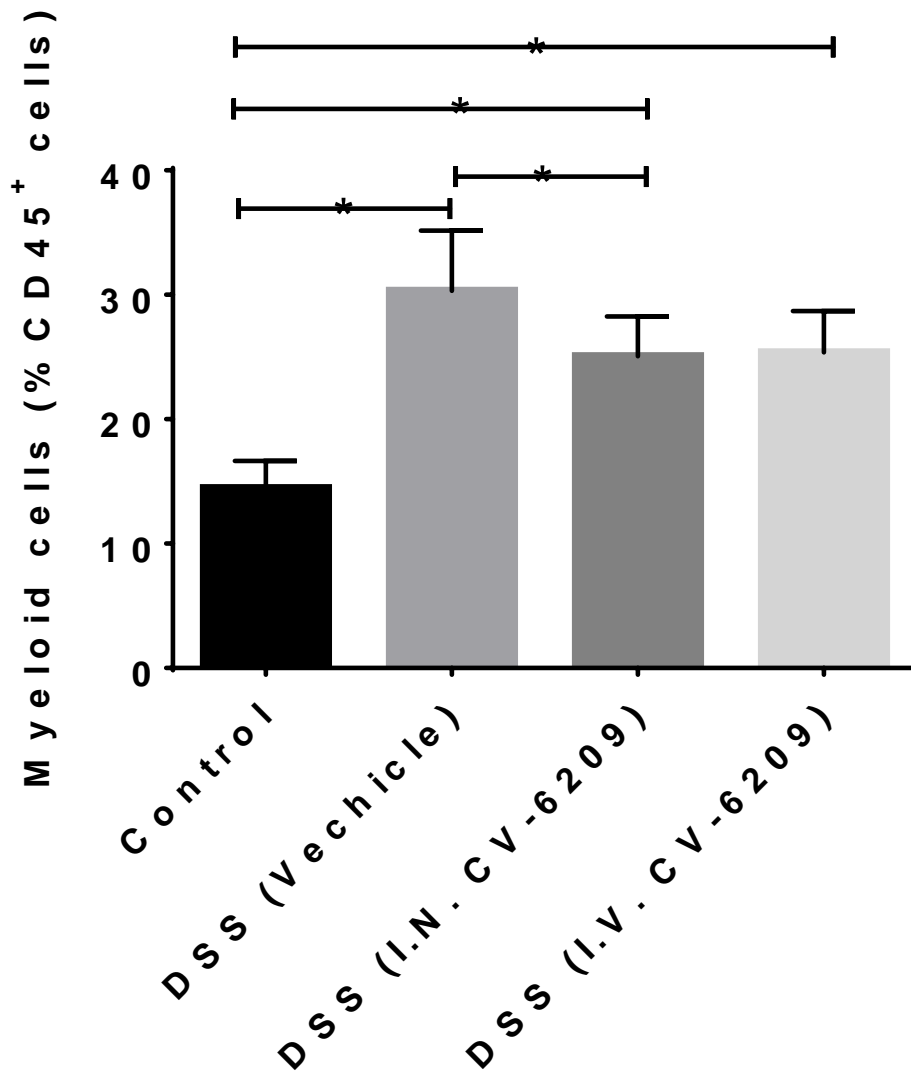


Figure 5.3.3A: Proportion of myeloid cells in the lung of DSS colitis. Cells were isolated from whole lung tissue according to the method described in section 2.10. The proportion of myeloid cells in the lung of acute DSS colitis mice treated with I.N. and I.V. CV-6209 (n = 6), quantified by flow cytometry according to Table 2.10. All data represented as \pm S.E.M. *= $p < 0.05$, unpaired t-test.

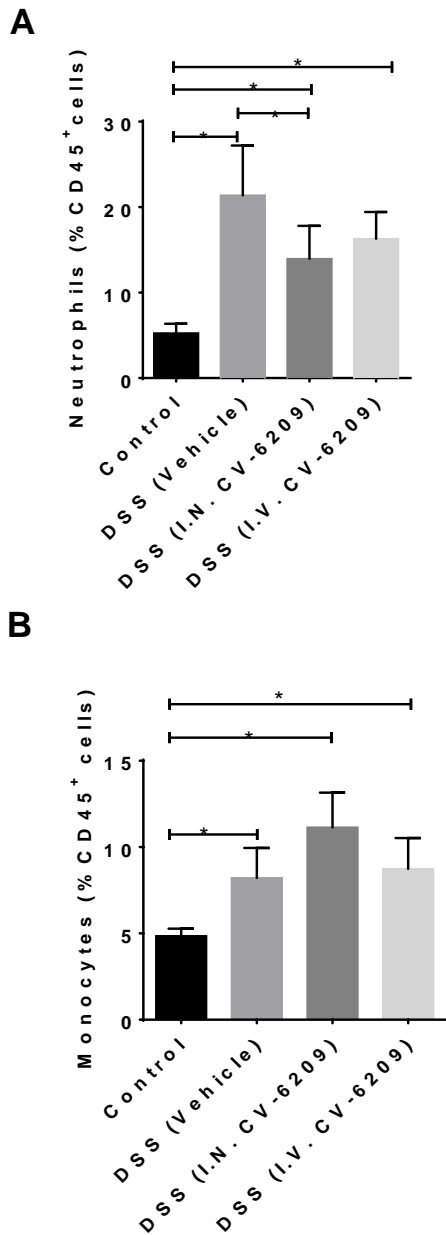


Figure 5.3.3B: Proportion of neutrophils and monocytes in the lung of DSS colitis. Cells were isolated from whole lung tissue according to the method described in section 2.10. (A) The proportion of neutrophils in the lung of acute DSS colitis mice treated with I.N. and I.V. CV-6209 (n = 6). Cellularity of the lung was quantified by flow cytometry according to the gating strategy in Table 2.10. All data represented as \pm S.E.M. $\ast = p < 0.05$, unpaired t-test.

5.3.4: Gene expression profile in the lung of CV-6209 treated acute DSS colitis.

In Section 5.3.3 it was shown that PAFR mediates the recruitment of neutrophils to the lung in DSS colitis-induced pulmonary inflammation. To determine whether PAFR signalling mediates the recruitment of neutrophils through the induction of inflammatory cytokines in the lung, the gene expression profile of CV-6209 treated colitis mice was conducted. The genes chosen for analysis were those that had been identified to be associated with colitis-induced pulmonary inflammation in previous experiments (Figure 3.3.4). It was found that CV-6209 treatment administered by both IN and IV methods reduced *Il1b* transcript to basal levels in the lungs of DSS colitis mice (Figure 5.3.4 A). CV-6209 treatment had no effect on the expression of *Ifng*, *Il6*, *Ccl2* or *Tnf* in the lungs of DSS colitis mice compared to vehicle treated controls (Figure 5.3.4 B, C, D, E). Thus PAFR signalling is required for *Il1b* specific gene expression in the lungs of colitis mice. IN treatment with CV-6209 reduced the level of *Ptafr* transcript albeit; this was not a statistically significant reduction ($p = 0.0856$, unpaired t-test, $n = 6$). Taken together these data show that PAFR signalling is required for *Il1b* gene expression in the lungs of colitis mice. Therefore, PAFR induced *Il1b* gene expression may be a mechanism by which neutrophils are recruited to the lungs of colitis mice. However the concurrent drop in neutrophil recruitment and *Il1b* expression implies that neutrophil influx drives *Il1b* expression. Furthermore, the specific reduction in *Il1b* expression and not the other genes associated with colitis-induced pulmonary inflammation would further suggest that neutrophils are the cellular source of *Il1b* expression.

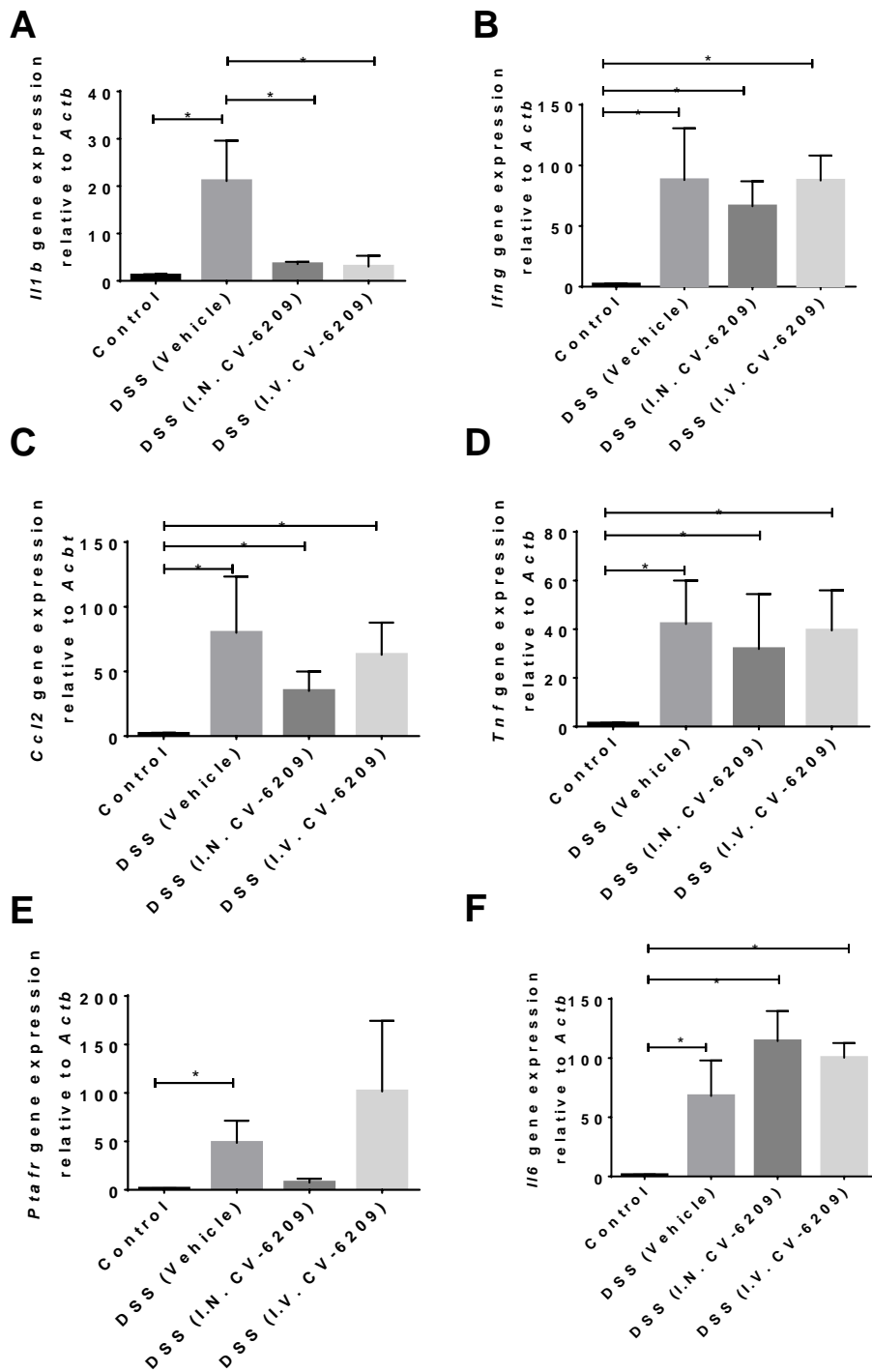


Figure 5.3.4 Gene expression profile in the lung of CV-6209 treated DSS colitis.

Transcript levels of (A) *Il1b* (B), *Ifng* (C), *Ccl2* (D), *Tnf* (E), *Ptafr* (F) and *Il6* in the lung of DSS colitis mice treated CV-6209 by I.N. and I.V methods of administration (n = 6). All data represented as mean \pm S.E.M. *= $p < 0.05$, unpaired t-test.

5.3.5: IL-1 β and CCL2 levels in the lung of CV-6209 treated acute DSS colitis.

To determine whether the decrease in *Illb* transcript induced by CV-6209 resulted in an equivalent reduction in IL-1 β cytokines levels, the protein level of IL1 β in the lungs of CV-6209 treated DSS colitis mice was measured. CV-6209 treatment by IN and IV methods of administration significantly decreased IL1 β protein levels in the lungs of DSS colitis mice compared to vehicle treated controls (Figure 5.3.5 A). Thus PAFR signalling is responsible for IL1 β production in the lungs of colitis mice. To determine whether PAFR regulated IL1 β expression was responsible for the induction of CCL2, a cytokine that has been identified to be involved in colitis-induced pulmonary inflammation in Section 3.3.5, CCL2 levels were measured in the lungs of CV-6209 treated colitis mice. CV-6209 treatment did not result in any reduction in CCL2 levels in the lungs of colitis mice compared to vehicle treated controls (Figure 5.3.5 B). These data complement the gene expression results in Figure 5.3.4 wherein CV-6209 treatment reduced the transcript expression of *Illb* and but not *Ccl2*. Thus these data show that PAFR is required for IL-1 β expression in the lungs of colitis mice. These data also show that PAFR induced IL-1 β expression is not involved in the expression of CCL2, therefore CCL2 expression is either upstream of IL-1 β in this signalling pathway or that CCL2 expression is regulated by a pathway that is not related to PAFR.

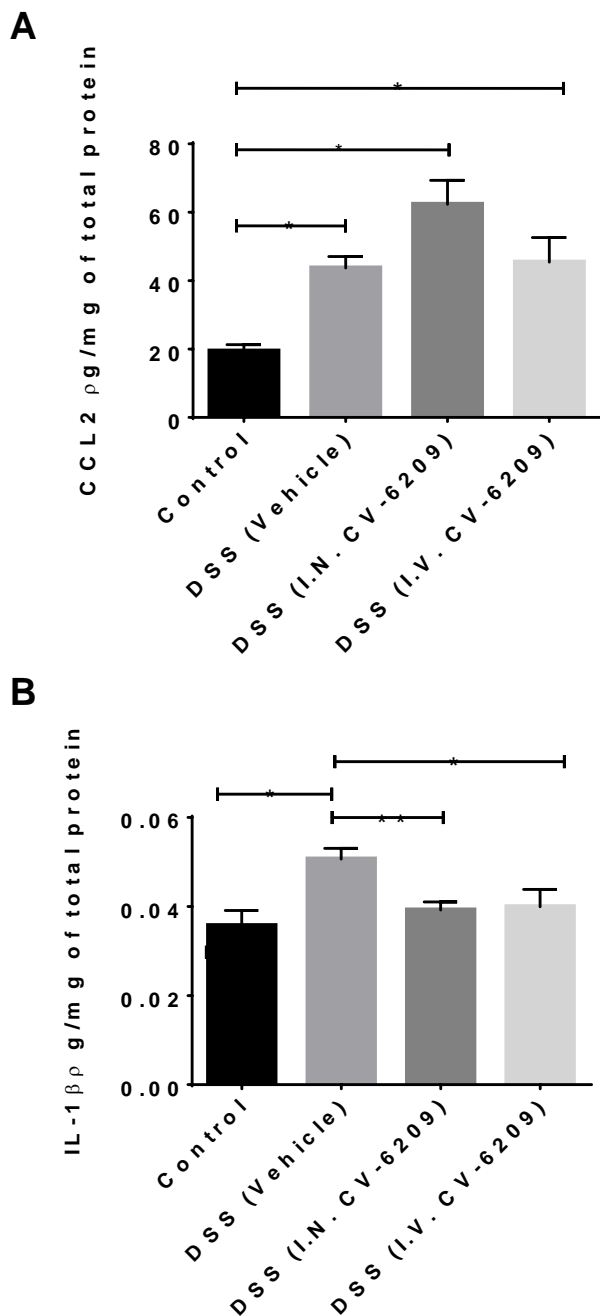


Figure 5.3.5: CCL2 and IL1β levels in the lung of CV-6209 treated DSS colitis. Protein levels of CCL2 and IL-1β in the lungs of DSS colitis mice treated with CV-6209 by I.N. and I.V. methods of administration. CCL2 levels measured by cytometric bead array (n = 6) and IL-1β measured by ELISA (n = 6). All data represented as mean ± S.E.M. *=p<0.05, **=p<0.01 unpaired t-test.

5.3.6: Systemic inflammation in CV-6209 treated acute DSS colitis.

To determine whether the effect of PAFR antagonism on colitis-induced pulmonary inflammation was related to systemic inflammation. The proportion of leucocytes and the level of inflammatory cytokines in the circulatory system of CV-6209 treated DSS colitis mice were quantified. It was found that neither IN or IV CV-6209 treatment resulted in a statistically significant decrease in neutrophils in the circulatory system. There was however a trending decrease in blood neutrophils in IN and IV CV-6209 treated DSS colitis mice. Both IN and IV CV-6209 treatment had no influence on the proportion of monocytes in the circulatory system of DSS colitis mice, compared to vehicle treated controls (Figure 5.3.6A A & B). Representative dot plots illustrating the gating strategy utilized for this analysis is provided in the appendices (Figure 8.3.2 A-D). CV-6209 treatment by IN and IV methods of administration decreased the level of IL-6 in the serum of DSS colitis mice compared to vehicle treated controls. A statistically significant decrease was observed in the IN treated group whereas a trending decrease was observed in the IV treated group. These data imply that PAFR signalling mediates expression of systemic IL-6. This may be due to direct inhibition of IL-6 production from circulating leucocytes and/or containment of intestinal mucosa produced IL-6 due to a reduction GI pathology. Taken together data show that PAFR signalling mediates colitis-induced systemic inflammation in respect to circulatory levels of IL-6, however the magnitude of this decrease is not sufficient to induce a statistically significant reduction in circulatory neutrophils.

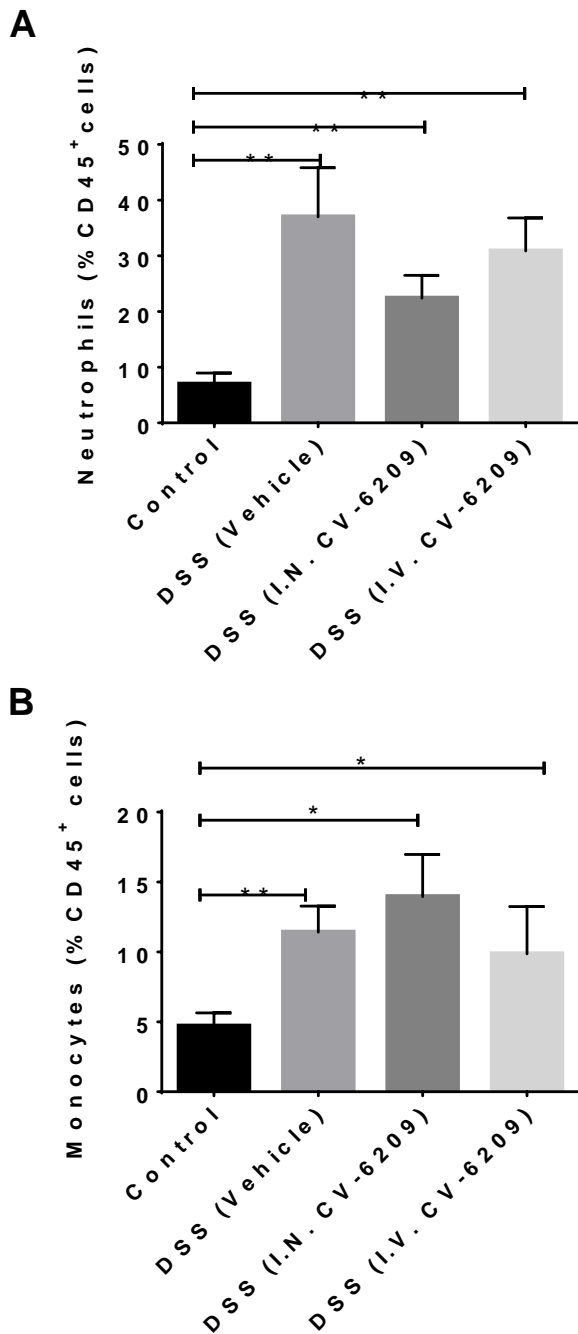


Figure 5.3.6A: Proportion of neutrophils and monocytes in the blood of CV-6209 treated DSS colitis. The proportion of neutrophils (A) and monocytes (B) in the circulatory system of DSS colitis mice treated with CV-6209 by I.N. and I.V. methods of administration. Cellularity of blood was quantified by flow cytometry according to the gating strategy in

Table 2.10 (n = 6). All data represented as mean \pm S.E.M. *= $p < 0.05$, **= $p < 0.01$, unpaired t-test.

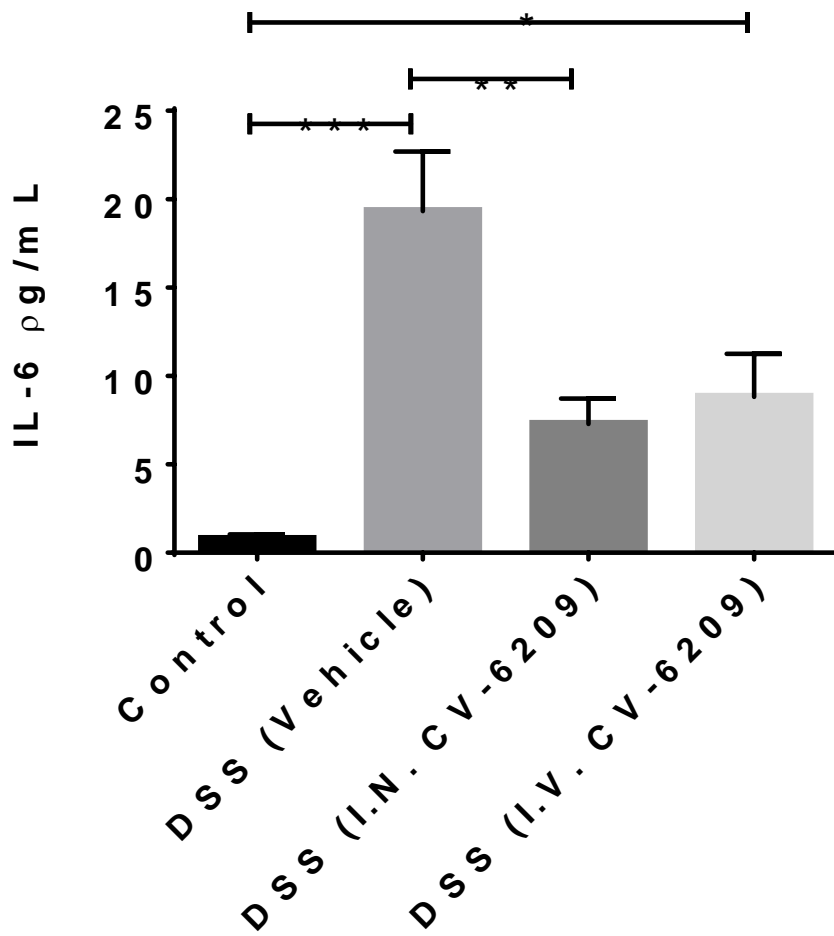


Figure 5.3.6B: Systemic IL-6 levels in CV-6209 treated DSS colitis. Systemic IL-6 levels were measured by cytometric bead array in the serum of I.V. and I.N. CV-6209 treated acute DSS colitis mice. All data represented as mean \pm S.E.M. *=p<0.05, **=p<0.01, ***=p<0.005 unpaired t-test.

5.4 Discussion

PAFR signalling has been shown to mediate neutrophil recruitment to mucosal tissues in a number of experimental systems (Uhlir, Goggel et al. 2005). PAF the agonist of PAFR has also been implicated in modulating gastrointestinal pathology in IBD patients (Wardle, Hall et al. 1996). This knowledge in combination with the experimental observations that colitis-induced pulmonary pathology involves neutrophil recruitment and PAFR expression in the lung, gave the rationale to hypothesise that PAFR signalling mediates colitis-induced pulmonary inflammation. Thus the aim of experiments in this chapter was to investigate the effect of CV-6209, a PAFR antagonist on the factors that induce colitis-induced pulmonary inflammation.

The first aim of experiments was determine the influence of PAFR signalling on the magnitude of colitis. It was found that PAFR antagonism reduced the magnitude of colitis in respect to colon histopathology but had no influence on the magnitude of mucosal inflammation in respect to cytokine signalling. Studies that have examined the effect of PAFR signalling on the severity of colitis report a decreases in colitis severity with PAFR antagonism, validating the observations in this study (Wallace 1988, Meenan, Grool et al. 1996, Hirayama, Yokoi et al. 2003). A reduction in gross pathology and myeloperoxidase levels (MPO) in the colon of a rabbit model of colitis treated with a PAFR antagonist was reported by Meenan *et al.* (Meenan, Grool et al. 1996). In addition Hirayama *et al.* found that PAFR antagonism in a rat model of DSS colitis ameliorated intestinal inflammation in respect to neutrophil and macrophage infiltration into the colon but had no effect on TNF expression (Hirayama, Yokoi et al. 2003). The experiments in this chapter corroborate these findings of Hirayama *et al.*; colitis severity was decreased in respect to histopathological scores however colon cytokine levels (CCL2, TNF, IFN- γ , and IL-6) were not altered. It is

intriguing that while PAFR antagonism decreased histopathology it had no influence on the level of inflammatory cytokines. This observation may be due to the position of PAFR in the inflammatory signalling cascade involved in the pathogenesis of DSS colitis. It is known that the pathogenic effect of PAFR is largely mediated through the recruitment of neutrophils and neutrophils are the end stage effector cells involved in the inflammatory damage at mucosal sites (Garcia, Russo et al. 2010). In this paradigm PAFR signalling and neutrophilic damage are amongst the final events in the inflammatory signalling cascade. Therefore, CCL2, TNF, IFN- γ , and IL-6 would be upstream of PAFR signalling. In this context PAFR antagonism would not influence the level of CCL2, TNF, IFN- γ , and IL-6. Furthermore, while neutrophils are capable of expressing CCL2, TNF, IFN- γ , and IL-6, tissue resident macrophages and structural cells can also produce abundant amounts of these cytokines, therefore inhibition of neutrophil migration and activation may not influence the level of these cytokines in the mucosa. Thus in the context of DSS colitis it can be concluded that mucosal inflammation is mediated, in part, by CCL2, TNF- α , IL-6 and IFN- γ expression from tissue resident macrophages and structural cells initiated by damage to the intestinal epithelial barrier by DSS. These factors propagate inflammation, however chemotaxis and activation of neutrophils is mediated by PAFR signalling. There have not been in-depth mechanistic studies undertaken to investigate the protective effect of PAFR antagonism on colitis pathogenesis, thus this hypothesis would have to be tested by cellular analysis of DSS colitis mice treated with CV-6209.

The systemic inflammation induced by colitis is directly related to the pulmonary inflammation associated with this condition. This relationship is mediated through IL-6 induced neutrophilia as demonstrated in Chapter 3. As systemic inflammation is a feature that contributes to colitis-induced pulmonary inflammation the effect of PAFR antagonism on

neutrophilia and circulatory IL-6 levels was analysed. It was found that CV-6209 treatment by both IN and IV methods of administration resulted in a statistically significant decrease in systemic IL-6 levels and a trending decrease in neutrophils in the circulatory system. The drop in neutrophils albeit, not statistically significant can be considered to be a result of the decrease in systemic IL-6 levels. While the decrease in neutrophils was not significant this could be due to the fact that PAFR antagonism did not drop IL-6 levels to the same extent as anti-IL-6 treatment. The mechanism by which PAFR augments systemic IL-6 levels is not known. The observation that both IN and IV CV-6209 treatments had the same effect on circulatory IL-6 levels demonstrate that the reduction in IL-6 is not due to the decrease in colonic pathology. Therefore PAFR antagonism must directly regulate systemic IL-6 levels, this concept is supported by animal models of sepsis that have shown that PAFR antagonism reduces systemic levels of TNF and IL-6, however the molecular mechanism of this phenotype was not elucidated (Moreno, Alves-Filho et al. 2006). A recent study that examined the contribution of PAFR to the pathogenesis of non-small cell lung cancer, reported that in a human bronchial epithelial cell line PAFR signalling has the potential to induce IL-6 expression (Chen, Lan et al. 2015). While this study was conducted in a cancer cell line and a human alveolar cell line it does illustrate the capability of PAFR to induce IL-6 expression in structural cells, which may include endothelial cells (Ishii and Shimizu 2000). Therefore, it can be postulated that systemic IL-6 levels in colitis may be driven by PAFR induced IL-6 expression in vascular endothelial cells.

It was found that PAFR antagonism did not influence pulmonary histopathology. The observation that IV CV-6209 treatment reduced colonic histopathology but did not abate pulmonary histopathology provides a basis to postulate about the mechanisms of disease progression that initiate extra-intestinal inflammation. Analysis of gut pathology revealed that

IV CV-6209 ameliorated intestinal pathology with respect to the magnitude of leucocyte infiltration, however mucosal immune responses in regard to cytokine signalling was not altered. These data imply that local immune response in the gut provide the stimulus for colitis-induced pulmonary inflammation, independent of infiltrating leucocytes and the severity of gut pathology. Intestinal epithelial cells might provide this stimulus through cytokine expression that is independent of PAFR signalling. The fact that IV CV-6209 treatment did not abate neutrophilia shows that immunomodulatory factors originating from the gut are still present in the circulatory system even when gut pathology is decreased. Therefore, immunomodulatory factors produced by intestinal epithelial cells and resident leucocytes may enter the circulatory system and induce systemic immune response irrespective of the magnitude of colitis activity. These immunomodulatory factors may include TNF, IL-6, IFN- γ or CCL2. However, it was shown in Chapter 2 that TNF, IFN- γ and CCL2 levels are not increased in the circulatory system. Therefore, it is unlikely that these cytokines initiate colitis-induced pulmonary inflammation.

In response to inflammatory conditions intestinal epithelial cells are known to express PAF the agonist of PAFR, thus PAF produced by intestinal epithelial cells might enter the circulatory system and induce pulmonary inflammation via PAFR signalling (Egea, Gimenez et al. 2008). An alternative mechanism is that damage to the intestinal epithelial barrier results in translocation of enteric bacteria into the circulatory system, which provide a stimulus for inflammation in the lung. This process may be mediated by local IFN- γ signalling, IFN- γ aids translocation of commensal enteric bacteria across gut epithelial cells through the induction of paracellular permeability (Clark, Hoare et al. 2005). Through this mechanism enteric microbial components may enter the bloodstream, disseminate to lung and induce inflammation through PAFR signalling on resident leucocytes. In fact

lipopolysaccharide (LPS) a component of enteric bacteria is known to induce the production of PAF from alveolar macrophages (Bulger, Arbabi et al. 2002, Wang, Rui et al. 2008). Therefore, it is fair to hypothesize that systemic bacterial components released from the gut may induce pulmonary inflammation via PAFR signalling. This mechanism would be independent of gut PAFR signalling, as both epithelial damage and IFN- γ signalling persist with IV CV-6209 treatment (Clark, Hoare et al. 2005).

In chapter 3 it was shown that IL-6 regulated neutrophil recruitment to the lung this effect was hypothesized to be due to IL-6 mediated neutrophilia as opposed to inflammatory signalling in the lung. Thus an additional signalling pathway was thought to be involved as anti-IL-6 had no effect on cytokine or PAFR levels in the lung. The experiments in this chapter suggest that PAFR signalling maybe that pathway. PAFR antagonism inhibited IL-1 β production but had not influence on CCL2 production or TNF, IL-6 or IFN- γ gene expression. The mechanism of PAFR induced IL-1 β production is unknown. The current paradigm of IL-1 β production involves a molecular pathway that includes extracellular receptors, inflammasomes and caspases. In this mechanism inflammasome formation is triggered by extracellular receptors that include GPCR and PRR in response to a range of agonists that include cytokines, lipids, bacterial/viral components and metabolic products (Latz, Xiao et al. 2013). Inflammasome formation in this manner results in caspase activation and cleavage of the biologically inactive pro-IL-1 β to mature IL-1 β . As PAFR is a GPCR it is possible that PAFR signalling can induce inflammasome formation and subsequent IL-1 β production. Rossol *et al.* reported that two G protein coupled calcium sensing receptors can induce the formation of the NACHT, LRR, and PYD domains-containing protein 3 (NALP3) inflammasome and subsequent IL-1 β production, in response to extracellular calcium levels (Rossol, Pierer et al. 2012). Extracellular calcium levels are increased at sites of inflammation

as calcium is released from activated leucocytes. Furthermore Rossel *et al.* demonstrated that inflammation associated extracellular calcium inflammasome formation can be inhibited by GPCR antagonism (Rossol, Pierer et al. 2012). Thus while PAFR has not been shown to regulate inflammasome formation it is a GPCR and colitis-induced pulmonary inflammation is associated with the activation of leucocytes, consequently local extracellular calcium level will be elevated. Therefore, inflammasome formation induced by PAFR signalling in response to extracellular calcium may be a potential mechanism that regulates IL-1 β production in colitis-induced pulmonary inflammation.

Alternatively, PAFR-induced IL-1 β expression may be mediated by direct interaction of PAFR with the phospholipid agonist PAF. Hasegawa *et al.* reported that PAFR antagonism inhibited the expression of IL-1 β in a model of injury-induced inflammation in the CNS. In this study Hasegawa *et al.* also found that a similar inflammatory phenotype could be reproduced by administration of PAF (Hasegawa, Kohro et al. 2010). This study shows that PAF/PAFR signalling can induce IL-1 β expression, however the capability of PAF/PAFR signalling to induce inflammasome formation was not assessed. PAF can be synthesised at sites of inflammation through a mechanism that is mediated by CCL2 (Reichel, Rehberg et al. 2009). CCL2 is highly expressed in the lungs of DSS colitis mice, thus the phenotype of inflammation induced by colitis creates conditions favourable for PAF synthesis. Furthermore Reichel *et al.* showed that PAF synthesised in response to CCL2 has the ability to recruit neutrophils from the bloodstream. Therefore, it can be hypothesized that CCL2 mediated PAF/PAFR signalling can induce neutrophil migration into the lung and subsequent IL-1 β expression. This hypothesis is supported by the experimental observations that PAFR antagonism had no effect on the expression of CCL2, suggesting that PAFR is downstream of CCL2 signalling.

5.5 Conclusions

In summary experiments in this chapter found that PAFR antagonism mediates colitis-induced pulmonary inflammation in regards to neutrophil recruitment and IL-1 β expression. Local administration of a PAFR antagonist was sufficient to prevent neutrophil recruitment and IL-1 β expression. These observations indicate that PAFR antagonism works through the inhibition of inflammatory signalling in lung tissue. It was found that PAFR antagonism ameliorated histopathology in the colon of DSS mice, however PAFR antagonism had no influence on colon mucosal immune responses in respect to cytokine signalling. Pulmonary pathology still developed in colitis mice that were protected from colonic histopathology. Thus it may be concluded that immunomodulatory factors derived from local colonic mucosal immune responses regulate pulmonary inflammation associated with colitis via PAFR signalling in the lung. Mucosal immune responses in the gut result in a comprised epithelial barrier; enteric bacteria can exploit this feature to disseminate through the circulatory system. Thus bacterial components in the blood stream may initiate immune responses via PAFR signalling and thus initiate colitis-induced pulmonary inflammation.

Chapter 6: The role of PAFR signalling in the modulation of myeloid cells in colitis-induced pulmonary inflammation.

6.1 Introduction

In Chapter 5 it was identified that PAFR signalling is involved in mediating colitis-induced pulmonary inflammation. It was observed that local administration of a PAFR antagonist ameliorated neutrophil recruitment and IL-1 β expression in the lung of DSS colitis mice. This observation implies that the beneficial effect of PAFR antagonism is derived from modulating inflammatory signalling directly in lung tissue. Alveolar macrophages are a population of sentinel pulmonary leucocytes that can express PAFR (Chen, Ziboh et al. 1997). The biological function of alveolar macrophages is to protect the lung from pathogenic microbes and toxic particles, to fulfil this role alveolar macrophages have potent inflammatory capabilities. The inflammatory properties of alveolar macrophages include the recruitment of neutrophils through the secretion of cytokines such as PAF and CCL2 (Wang, Rui et al. 2008, Balamayooran, Batra et al. 2011). Alveolar macrophages produce PAF in response to microbial antigens and cytokine signalling (Wang, Rui et al. 2008, Balamayooran, Batra et al. 2011) (Bulger, Arbabi et al. 2002).

As bacteria and systemic cytokines are present in the circulatory system of IBD patients it is possible that these immunomodulatory factors can activate alveolar macrophages. In this hypothesis a damaged intestinal mucosa in combination with the vasodilation caused by acute inflammation, results in the translocation/diffusion of bacteria and/or cytokines into the visceral bloodstream. Bacterial products and/or cytokines that are not removed by the

filtering effect of the liver can then enter the systemic circulation and encounter alveolar macrophages as they enter the alveoli in the oxygenation process. As these immunomodulatory factors encounter alveolar macrophages they induce PAF production and thus stimulate PAFR signalling in an autocrine manner. This hypothesis is supported by studies from Wang *et al.* that showed that the inflammatory response in the lungs of septic mice involves PAF production from alveolar macrophages. Jarrar *et al.* also showed that the inflammatory properties of alveolar macrophages can be induced by bacterial products in the circulatory system. Thus one may postulate that the immunomodulatory factors released from the GI tract as a result of colitis can induce the inflammatory properties of macrophages via PAFR signalling, culminating in the recruitment of neutrophils.

6.1.1 Hypothesis:

The following hypotheses were developed to account for PAFR mediated colitis-induced pulmonary inflammation.

- 1) Immunomodulatory factors present in the circulatory system can disseminate into the lung and activate alveolar macrophages via PAFR signalling.
- 2) CCL2 is an immunomodulatory factor can activate alveolar macrophages and induce the recruitment of neutrophils through PAFR signalling.

6.1.2 Aims

To test these hypotheses, the following aims were employed;

- 1) To identify the cellular source of PAFR expression in acute DSS colitis mice.

- 2) To utilize a monocyte cell line, to model alveolar macrophage and determine whether immunomodulatory factors in the serum of DSS colitis mice can activate the inflammatory properties of these cells via PAFR signalling.
- 3) To utilize reductionist in-vitro experiments to investigate the immunomodulatory factors that can utilize PAFR to activate alveolar macrophages.

6.2 Methods

Analysis of cytokine signalling in this chapter was performed as described in Section 2.13. Gene expression analysis was conducted as described in Section 2.12 and immunohistochemistry staining and analysis was performed as described in Section 2.7.

6.2.1 Cell culture

The murine macrophage cell line RAW 264.7 was cultured in high glucose Dulbecco's modified eagle medium (DMEM) containing 10% fetal calf serum, 5mM L-glutamine, 1% penicillin-streptomycin and 1% non-essential amino acids. Cells were cultured at 37°C and 5% CO². All reagents were supplied by Sigma Aldrich.

6.2.2 DSS serum induced macrophage activation via PAFR signalling

RAW 264.7 macrophages were seeded into 6 well flat bottom cell culture plates and grown until confluent. At confluence, CV-6209 positive cells were incubated in 3mL of 1µM CV-6209 in DMEM for 1 hour. CV-6209 negative cells were incubated in DMEM. Following incubation CV-6209 positive and negative cells were incubated with 300µL of serum harvested from acute DSS colitis or control mice for 20 hours. The acute DSS colitis model was conducted as described in Section 2.2. Following incubation supernatants cells were

collected for cytokine and gene expression analysis as described in section 2.13 and 2.12 respectively.

6.2.3 CCL2 and LPS macrophage activation via PAFR signalling

RAW 264.7 macrophages were seeded into 6 well flat bottom cell culture plates and grown until confluent. At confluence, CV-6209 positive cells were incubated in 3mL of 1 μ M CV-6209 in DMEM for 1 hour. CV-6209 negative cells were incubated in DMEM. Following incubation cells were incubated with 30ng/mL of recombinant CCL2 (Biolegend) or 1ng/mL of LPS (Sigma-Aldrich) for 20 hours. Vehicle treated controls received PBS. Following incubation supernatants were collected for cytokine analysis as described in section 2.13 and cells collected for gene expression analysis 2.12. Supernatant samples were also collected for PAF analysis described in Section 6.2.4.

6.2.4 PAF analysis

The concentration of PAF was measured in cell culture supernatants with the QTRAP 5500 liquid chromatography–mass spectrometry system (SCIEX), QTRAP was operated according to manufacturer's instructions.

6.2.5 Bone Marrow neutrophil isolation

The femur and tibia was dissected from naïve female C57BL/6 mice. The apices of the femur and tibia were removed and the bones flushed with Hanks buffered salt solution (HBSS) containing 15mM EDTA and 1% BSA until clear. Cell suspensions were passed through a cell strained and centrifuged at 400g, 10min, 4⁰C. Cells were resuspended in 1mL of HBSS containing 15mM EDTA and 1% BSA and placed on a three-layer percoll gradient of 78%,

69% & 52% percoll diluted in HBSS. Percoll gradient was centrifuged at 1500g for 30min at RT (without braking). Following centrifugation, neutrophils were collected from the 69 and 52% interface. Collected cells were centrifuged at 400g, 10min, 4⁰C and resuspended in HBSS for subsequent experiments.

6.2.6 Assessment of Neutrophil activation via PAFR signalling from products of CCL2 and LPS activated macrophages.

Bone marrow derived neutrophils were isolated from naïve male C57BL/6 mice as described in Section in 6.2.5. Neutrophils were seeded in 6 well flat bottom polystyrene cell culture plates at 500,000 cells per well. Cells were incubated in DMEM containing 1 μ M CV-6209 for CV-6209 positive group or DMEM for CV-6209 negative group for 1 hour. Following incubation cells were incubated with 500 μ L of supernatants obtained from CCL2, LPS and vehicle treated RAW 264.7 macrophages as described in Section 6.2.3. Neutrophils were incubated with macrophage supernatants for 4 hours. The rationale for exposing neutrophils to supernatants for 4 hours is due to the short half-life of these cells, estimates vary between 6 – 12 hours (Summers, Rankin et al. 2010). 4 hours were chosen to allow for the transcription of the factors necessary to induce neutrophil activation while avoiding neutrophils entering a quiescent state as they approach their half-life. Following incubation cells were centrifuged at 400g, 10min, 4⁰C and resuspend in 200 μ L PBS. Cells were stained with flow cytometry antibodies APC conjugated anti-GR1, FITC conjugated anti-Ly6G and PerCP-Cy5.5 conjugated CD11b for 45min at 4⁰C. Following staining cells were centrifuged at 400g, 10min, 4⁰C resuspended in PBS and incubated in 10 μ M dihydroethidium (DHE) for 30min at 37⁰C. DHE is a cell permeable redox indicator, DHE is oxidized by superoxide to form ethidium which intercalates with DNA to stain the cell nucleus red. The ethidium/DNA fluorescent product can be analysed by flow cytometry at 605nm. The amount of superoxide

in a cell can then be calculated as fluorescent intensity at 605nm is proportional to superoxide levels.

After incubation with DHE cells were washed in PBS and analysed on the BD FACS Canto II. Neutrophils were identified as Gr1⁺ Ly6G⁺ double positive population. Neutrophil activation was determined by CD11b expression and superoxide production. CD11b expression was quantified as the geometric mean fluorescent intensity of CD11b staining on neutrophils. Superoxide production was quantified as the geometric mean fluorescent intensity of DHE staining in neutrophils.

6.2.7 Fluorescent *in situ* hybridisation analysis by flow cytometry (FISH-Flow)

Lungs tissue harvested from acute DSS colitis mice and stored in PBS at -80°C until analysis. Lung tissue was homogenized in PBS and centrifuged at centrifuged (8000g, 3 minutes, 4°C). The samples were then incubated with 0.1M Tris-EDTA solution containing 1µg of lysozyme for 10 minutes. Lysozyme is an enzyme that can hydrolyse the cell membrane of bacteria which improves the recovery of nucleic acids. The samples were then centrifuged (8000g, 3 minutes, 4°C) and resuspended hybridisation buffer (0.72M sodium chloride, 0.016M Tris-HCl, 0.016% sodium dodecyl sulfate and 24% formamide in deionised water) for 2 hours at 37°C in the dark. The probes used were a 16S rRNA-targeted oligonucleotide probe (5' GCTGCCTCCCGTAGGAGT 3') termed (EUB) used by Aman *et al.*, (1990) on the PE channel and a negative control probe (5' ACATCCTACGGGAGGC 3') termed (NON) used by Waller *et al.*, (1993) on the APC channel. The cells were then centrifuged, the supernatant containing excess probe discarded and the cells washed with PBS. The bacterial cells were then analysed on the BD FACSCanto™II. To identify bacterial cells, a gate was drawn around a high forward scatter and medium forward scatter group of cells. Cells within this

group expressing signals for the negative control probe (APC) were excluded as non-bacterial autofluorescence. The PE population represented the EUB⁺ 16sRNA⁺ bacterial population. The mean fluorescent intensity of this population was considered proportional to bacterial load in the lung.

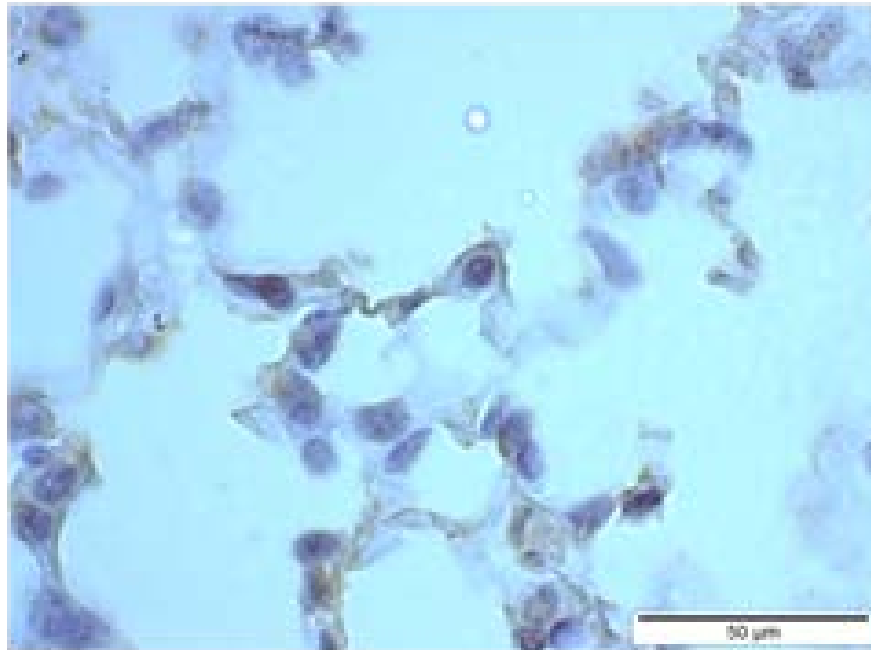
6.2.8 Endotoxin assay

BAL fluid was collected from acute DSS colitis as described in Section 2.9. The level of endotoxin in BAL fluid was quantified by a chromogenic limulus amoebocyte lysate (LAL) assay (Genescript). Samples were incubated in LAL for 40min at 37⁰C. Following incubation 100μL of chromogenic stabilisation buffer was added to samples for 5min followed by 100μL of stop solution. Absorbance was read at 545nm in a spectrophotometer and endotoxin levels calculated from known standards.

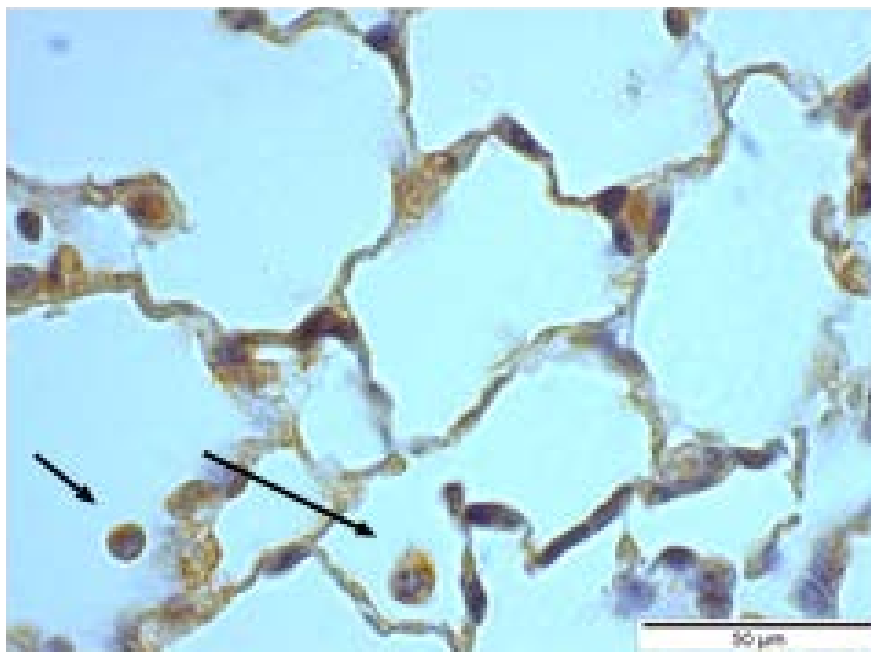
6.3 Results

6.3.1 PAFR expression in the lung of acute DSS colitis mice.

In Chapter 5, PAFR signalling was shown to regulate neutrophil migration and IL-1 β expression in the lung of DSS colitis mice, furthermore in Chapter 3 an increase in PAFR protein levels was found in the lung of DSS colitis mice. While experiments in these chapters identified a role for PAFR in modulating colitis-induced pulmonary inflammation, the cellular location of PAFR was not identified. To examine the mechanism of PAFR signalling in greater detail the cellular location of PAFR expression was identified by immunohistochemistry in lung sections from acute DSS colitis mice. It was found that PAFR expression is localised to leucocytes in the lung (Figure 6.3.1A). Qualitative morphological analysis of PAFR⁺ cells by light microscopy revealed that macrophages and neutrophils are the phenotype of PAFR⁺ leucocytes (Figure 6.3.1A). PAFR was also expressed on parenchymal cells, PAFR is known to be expressed by pulmonary epithelial cells under inflammatory conditions. Therefore it is possible that PAFR is also expressed by pulmonary epithelial cells in DSS colitis (Garcia, Russo et al. 2010). From qualitative analysis it could be seen that the majority of PAFR expression was localised to leucocytes, for this reason quantitative analysis was undertaken to enumerate the number of PAFR⁺ leucocytes in the lung of acute DSS colitis. Quantitative analysis revealed a significant increase in PAFR⁺ leucocytes in the lung of acute DSS colitis mice compared to controls (Figure 6.3.1B). These data indicate that the majority of PAFR expression is localised to alveolar macrophages and infiltrating neutrophils in the lung of DSS colitis mice. Therefore it can be considered that the beneficial effect of PAFR antagonism observed in Chapter 5 occurs through the amelioration of inflammatory signalling in these cells.



Control



Acute DSS

Figure 6.3.1A: PAFR expression in the lungs of acute DSS colitis. Representative images of PAFR immunohistochemistry in lung sections of acute DSS colitis mice. Arrows denote PAFR⁺ leucocytes.

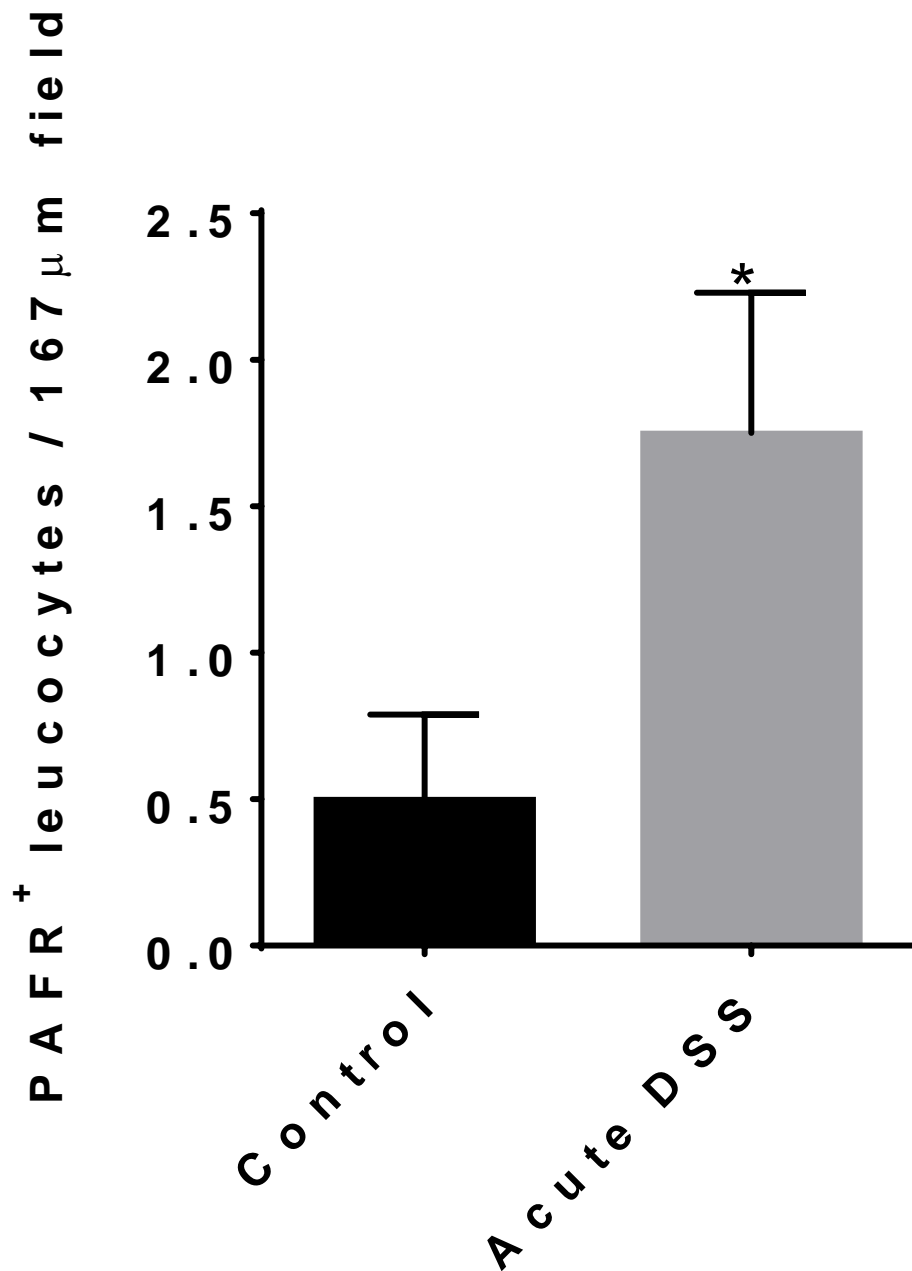


Figure 6.3.1B: Quantification of PAFR⁺ leucocytes in the lung of acute DSS colitis mice.

PAFR positive cells were identified by immunohistochemistry in lung sections, PAFR positive leucocytes were enumerated by counting the number of PAFR positive cells in a 10mm² grid at 60x (n = 5). All data represented as mean. ± S.E.M. * = p<0.05, unpaired t-test.

6.3.2 Immunomodulatory factors in the serum of acute DSS colitis mice initiate inflammatory gene expression in macrophages via PAFR signalling.

Alveolar macrophages are a population of sentinel macrophages present in the pulmonary alveolus that can initiate innate immune responses. Upon activation by immunomodulatory factors alveolar macrophages synthesise an array of cytokines that recruit neutrophils from the bloodstream. PAFR is acknowledged to be a receptor that can activate the inflammatory properties of alveolar macrophage (Schaberg, Haller et al. 1991). Thus it was hypothesized that immunomodulatory factors present in the serum of acute DSS colitis mice can activate the inflammatory properties of macrophages via PAFR. To test this hypothesis RAW 264.7 macrophages were incubated with serum harvested from DSS colitis and control mice in the presence and absence of CV-6209. Following incubation, the gene expression and secretion of IL-1 β was analysed. The genes *Ccl2*, *Il1b* and *Ptafr* were chosen for analysis as they have been implicated in mediating colitis-induced pulmonary inflammation in Section 3.3.4. It was found that immunomodulatory factors present in the serum of DSS colitis mice induced a significant increase in *Ccl2* expression in RAW 264.7 macrophages compared to serum from control mice (Figure 6.3.2A A). Treatment of RAW 264.7 macrophages with CV-6209 prior to incubation with serum from DSS colitis mice resulted in a significant decrease in *Ccl2* gene expression compared to RAW264.7 macrophages treated with the vehicle (Figure 6.3.2A A). *Ptafr* gene expression in RAW 264.7 macrophages was increased in cells incubated with serum from DSS colitis mice compared to serum from control mice (Figure 6.3.2A B) and it was found CV-6209 treatment induced a trending decrease in *Ptafr* gene expression (Figure 6.3.1A B). These data show that systemic factors in DSS colitis can activate proinflammatory gene expression in macrophage via PAFR signalling. *Il1b* gene expression was unable to be quantified from RAW264.7 macrophages; a Ct reading was not

present within the 40 PCR cycles that was utilized for qPCR. From this observation it was concluded that transcriptional activation of *Iilb* was not present at this time point, as IL-1 β expression is an early phase response in was considered that the transcriptional IL-1 β response was missed at the 20-hour time point. For this reason, IL-1 β secreted protein levels were quantified in supernatants from RAW 264.7 macrophages incubated with serum from DSS colitis mice in the presence and absence of CV-6209. It was found that IL-1 β protein levels were elevated in supernatants from macrophages incubated with serum from DSS colitis mice compared to controls (Figure 6.3.2B). CV-6209 treatment prior to incubation with serum for DSS colitis mice led to a significant decrease in secreted IL-1 β protein levels (Figure 6.3.2B). Taken together these data show that immunomodulatory factors present in the serum of colitis mice utilize PAFR to induce inflammatory signalling in macrophage.

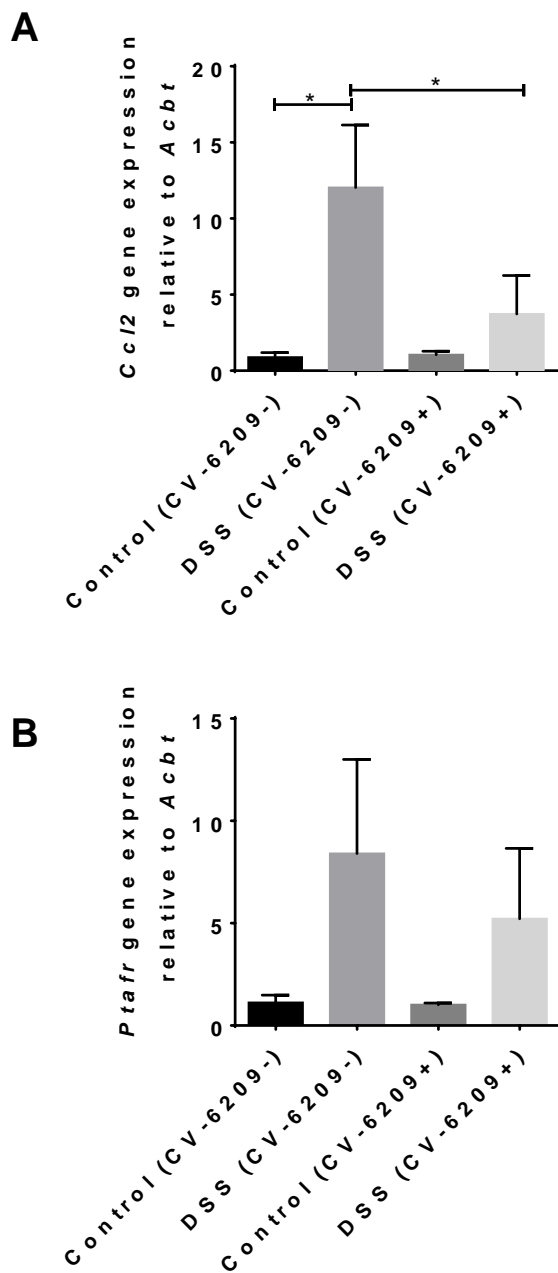


Figure 6.3.2A: Gene expression in RAW 264.7 macrophages exposed to serum from DSS colitis mice and treated with CV-6209. (A) *Ccl2* gene expression in RAW 264.7 macrophages incubated with serum from acute DSS colitis mice and control mice in the presence and absence of CV-6209 (n = 3). (B) *Ptafr* gene expression in RAW 264.7 macrophages incubated with serum from acute DSS colitis and control mice in the presence

and absence of CV-6209 (n = 3). All data represented as mean. \pm S.E.M. * = $p < 0.05$, unpaired t-test.

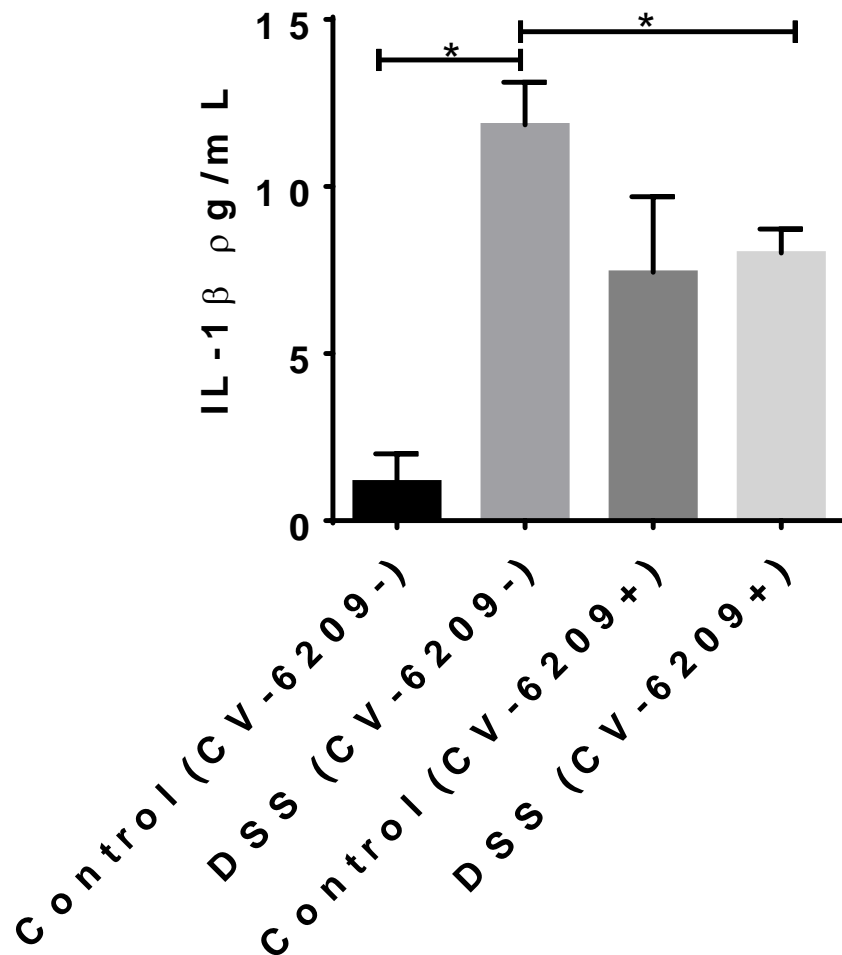


Figure 6.3.2B: IL-1 β secreted by RAW 264.7 macrophages exposed to serum from DSS colitis mice treated with CV-6209. Secreted IL-1 β levels were measured in the supernatants from RAW 264.7 macrophages incubated with serum from DSS and control mice (n = 3). All data represented as mean \pm S.E.M., *= $p < 0.05$, unpaired t-test. IL-1 β levels measured by ELISA.

6.3.3 Bacterial load is increased in the lungs of acute DSS colitis mice

The next aim of experiments was to identify the immunomodulatory factors in the serum of DSS colitis mice that utilize PAFR to activate macrophages. It was hypothesized that the bacteraemia associated with colitis can result in bacteria entering the lung and inducing pulmonary inflammation via PAFR signalling. The first step in testing this hypothesis was to determine whether the bacterial load is increased in acute DSS colitis mice. Bacterial load was determined through the quantification of 16S rRNA levels in lung homogenates by fluorescent in-situ hybridization flow cytometry. It was found that DSS colitis increased the level of 16s rRNA in lung tissue compared to controls (Figure 6.3.3 A). The cytometry gating strategy utilized to quantify 16sRNA and dot plots from experimental group is shown Figure 8.4. To further examine bacterial load in the lung and to specifically assess the presence of Gram-negative bacteria, LPS levels were measured in the BAL fluid from acute DSS colitis mice. A significant increase in LPS levels was found in the BAL fluid from DSS colitis mice. While LPS does not signal directly through PAFR, LPS can initiate PAFR signalling through an autocrine mechanism involving PAF (Han, Ko et al. 2002) (Bulger, Arbabi et al. 2002). Together these data suggest that colitis-associated bacteraemia results in dissemination of bacteria into the lung and these bacteria are of the Gram-negative species (figure 6.3.3 A). However it cannot be definitively concluded that bacteria disseminate to the lung via the circulation unless bacteria have been identified in blood from these experiments. This is a limitation of this study as it is also possible that the shift in immunological conditions in the lung could have resulted in the observed changes in bacterial composition. Dysbiosis of this nature is acknowledged to occur in a conditions where the immunological status of the gut and lung shift towards a proinflammatory milieu and therefore may also be a possibility in

this model (Kim, Udayanga et al. 2014, Budden, Gellatly et al. 2017). Therefore changes in bacterial load and composition initiated by bacterial dissemination and/or lung dysbiosis may provide the stimulus required to initiate colitis-induced pulmonary inflammation.

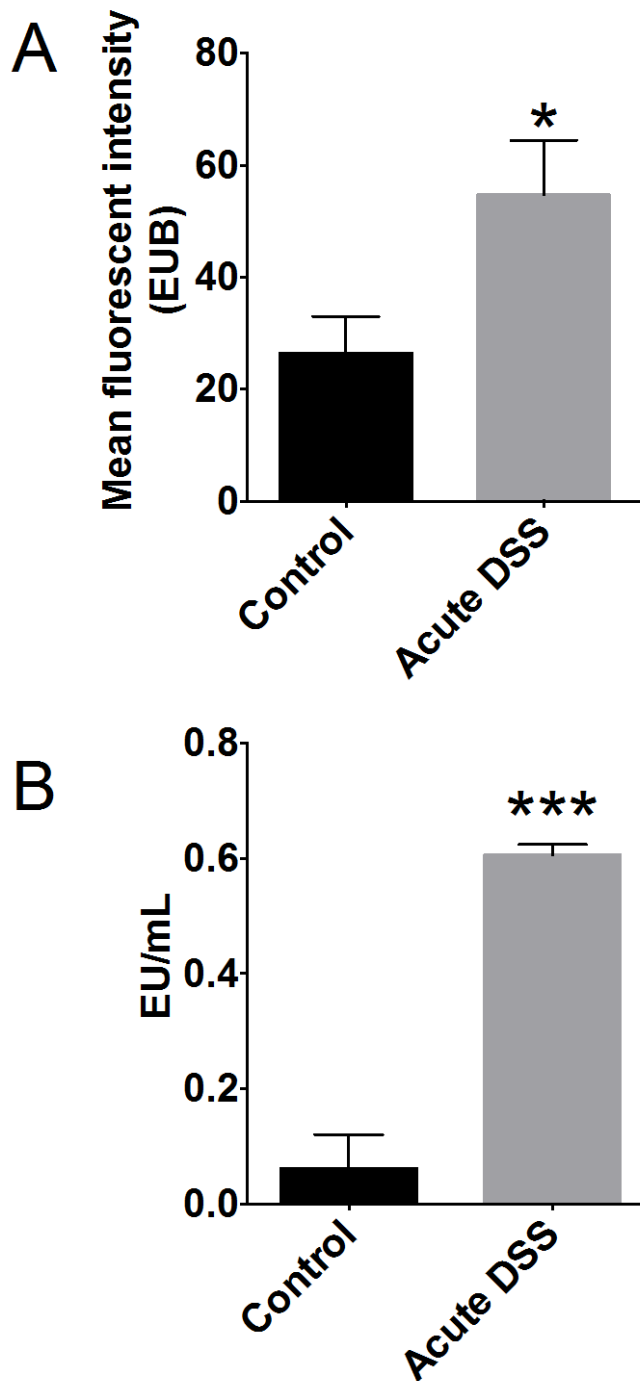


Figure 6.3.3A: Bacterial load in the lungs of acute DSS colitis mice. (A) Bacterial load in the lungs of acute DSS mice was quantified by fluorescent in-situ hybridization flow cytometry (n = 5). (B) Endotoxin levels in BAL fluid from acute DSS colitis mice was observed in the lung of acute DSS colitis mice (n = 5). Endotoxin was measured in the BAL

fluid with an LAL endotoxin kit. All data represented as mean \pm S.E.M., *=p<0.05
***=p<0.005, unpaired t-test.

6.3.4 LPS-induced macrophage activation via PAFR signalling.

LPS levels are elevated in the lung of DSS colitis mice (Section 6.3.3) and LPS-induced PAF production is acknowledged as a mechanism that can utilize PAFR to activate macrophages (Bulger, Arbabi et al. 2002). While LPS does not signal directly through PAFR, LPS can initiate PAFR signalling through an autocrine mechanism involving PAF (Han, Ko et al. 2002). Furthermore, immunomodulatory factors in the serum of DSS colitis mice also utilize PAFR signalling to induce inflammatory signalling in macrophages (Section 6.3.2). Based on these observations I hypothesized that LPS can induce CCL2 and IL-1 β expression in macrophages via PAFR signalling. To test this hypothesis CCL2 and PAFR gene expression was analysed in RAW 264.7 macrophage treated with LPS in the presence and absence of CV-6209. It was found that *Ccl2* gene expression was significantly increased in RAW264.7 macrophages treated with LPS. However, CV-6209 treatment had no influence of LPS-induced *Ccl2* expression (Figure 6.3.4A A). *Ptafr* gene expression was increased in LPS treated RAW264.7 macrophages, however this effect was not inhibited by CV-6209 treatment (Figure 6.3.4A B).

LPS is known to induce PAFR expression, this response is thought to enable autocrine PAF signalling during infection and inflammation (Ishii, Matsuda et al. 1996). Therefore while CV-6209 will inhibit the function of PAFR signalling it is unlikely that CV-6209 will have any effect on LPS-induced *Ptafr* RNA expression as this effect is upstream of CV-6209/PAFR antagonism.

Secreted IL-1 β levels were measured in supernatants from LPS treated RAW264.7 macrophages in the presence and absence of CV-6209. It was found that secreted IL-1 β protein levels are increased in response to LPS stimulation, however IL-1 β expression is not regulated by PAFR signalling (Figure 6.3.4B). However with n = 3 this cannot be conclusively determined. Therefore these data suggest that LPS induces the activation of macrophages in respect to *Ccl2* and *Ptafr* gene expression as well as IL-1 β production however this process does not occur via PAFR signalling. Based on these findings it was concluded that LPS in the lung of DSS colitis mice is not the mechanism by which PAFR signalling activates macrophages.

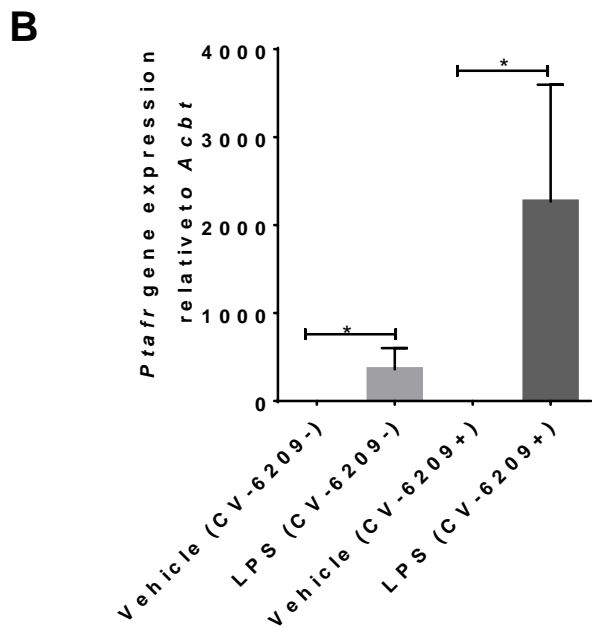
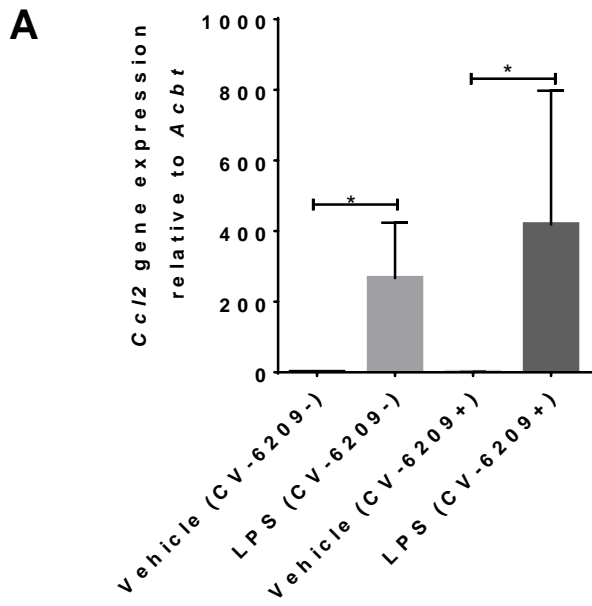


Figure 6.3.4A Gene expression in RAW 264.7 macrophage treated with LPS and CV-6209. (A) *Ccl2* gene expression in RAW 264.7 macrophages treated with LPS in the presence and absence of CV-6209 (n = 3). (B) *Ptafr* gene expression in RAW 264.7 macrophages treated with LPS in the presence and absence of CV-6209 (n = 3). All data represented as mean \pm S.E.M., $*=p<0.05$, unpaired t-test. Gene expression quantified by qPCR.

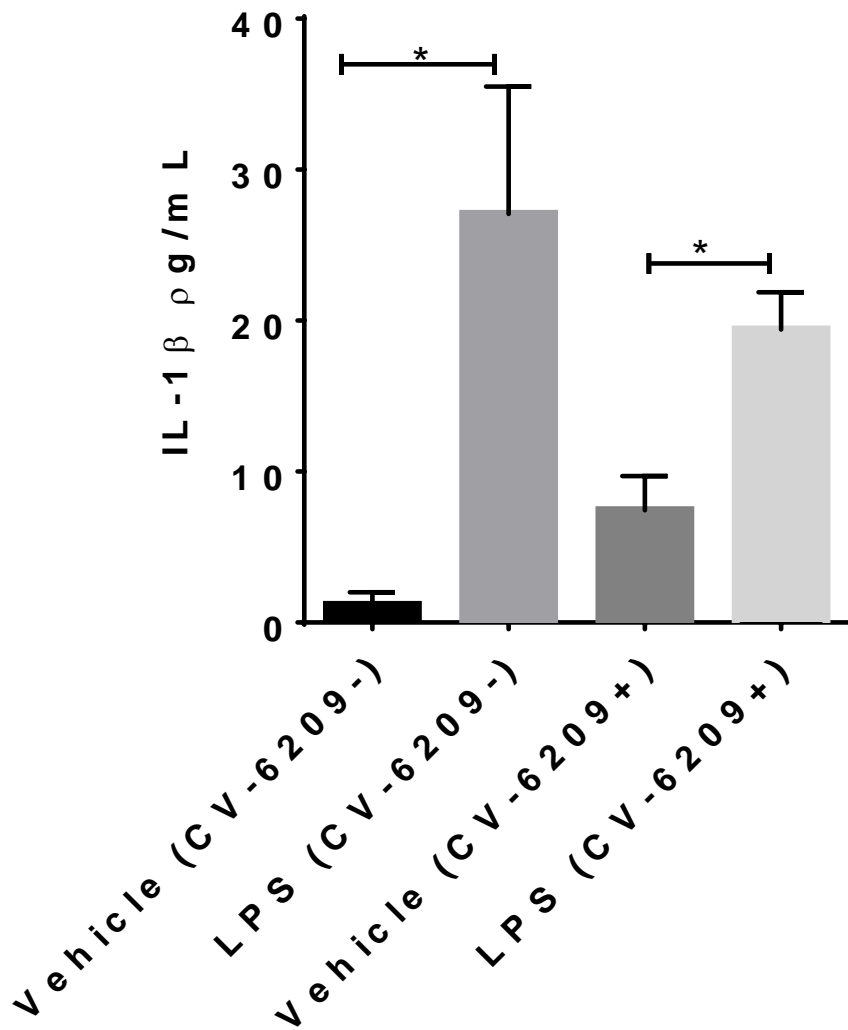


Figure 6.3.4B: IL-1 β secreted by RAW 264.7 macrophages treated with LPS and CV-6209. Secreted IL-1 β levels were measured in the supernatants from LPS treated RAW 264.7 macrophage in the presence and absence of CV-6209 (n = 3). All data represented as mean \pm S.E.M., *=p<0.05, unpaired t-test.

6.3.5 CCL2-induced macrophage activation via PAFR signalling.

In Section 6.3.4 it was determined that LPS is not an immunomodulatory factor that utilizes PAFR to induce inflammatory signalling in macrophages. Another mechanism by which PAFR signalling can occur is via cytokine induced PAF production (Chang 1994). CCL2 is a cytokine that can induce PAF synthesis and thus initiate PAFR signalling (Reichel, Rehberg et al. 2009). Furthermore, CCL2 expression is highly elevated in the colon and lung as a result of DSS colitis. Based upon these observations it was hypothesised that CCL2 can induce the inflammatory properties of macrophage via PAFR signalling. To test this hypothesis RAW264.7 macrophages were treated with recombinant CCL2 in the presence and absence of CV-6209. *Ccl2* and *Ptafr* gene expression as well as secreted IL-1 β protein levels was analysed in these cells. It was found that *Ccl2* gene expression was increased in macrophage treated with recombinant CCL2 compared to vehicle treated controls (Figure 6.3.5A A). CCL2-induced *Ccl2* gene expression was ameliorated with CV-6209 treatment (Figure 6.3.5A A). *Ptafr* gene expression was also increased in macrophages treated with CCL2 and CV-6209 treatment prior to CCL2 stimulation ameliorated *Ptafr* gene expression compared to vehicle treated controls (Figure 6.3.5A B). Secreted IL-1 β protein levels were elevated following CCL2 stimulation of macrophages; treatment of macrophages with CV-6209 prior to CCL2 stimulation did not reduce the level of secreted IL-1 β compared to vehicle treated controls (Figure 6.3.5B). Together these data show that two different cell signalling pathways are involved in CCL2 induced macrophage activation. The induction of CCL2 gene expression by CCL2 stimulation requires a PAFR signalling dependent pathway, however IL-1 β production from CCL2 activated macrophages involves a PAFR independent pathway.

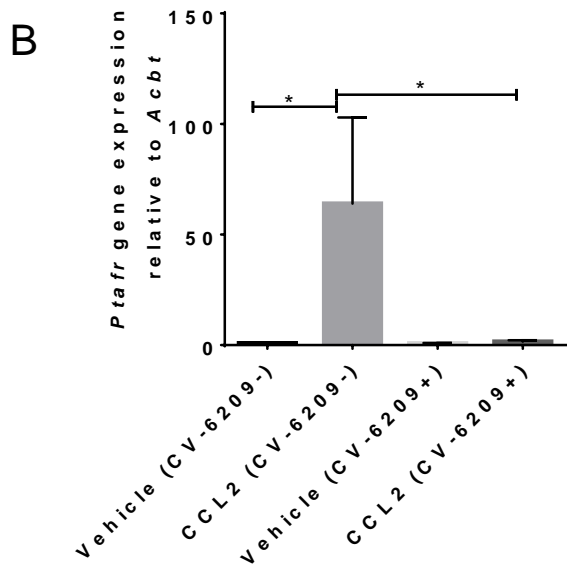
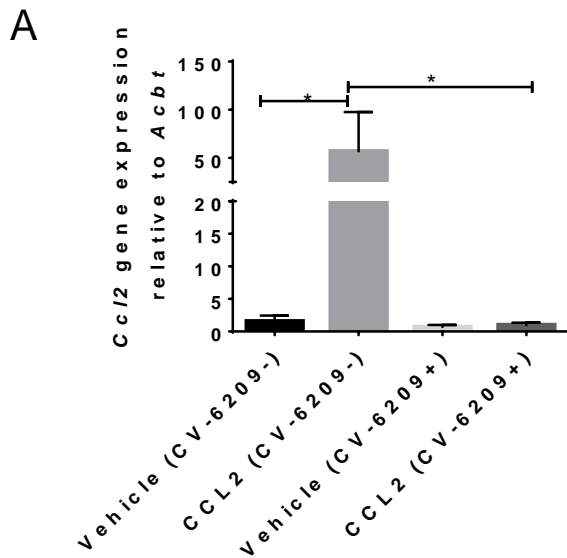


Figure 6.3.5A Gene expression in RAW 264.7 macrophage treated with CCL2 and CV-6209. (A) *Ccl2* gene expression in RAW 264.7 macrophages treated with CCL2 in the presence and absence of CV-6209 (n = 3). (B) *Ptafr* gene expression in RAW 264.7 macrophages treated with CCL2 in the presence and absence of CV-6209 (n = 3). All data represented as mean \pm S.E.M., *= $p < 0.05$, unpaired t-test. Gene expression quantified by qPCR.

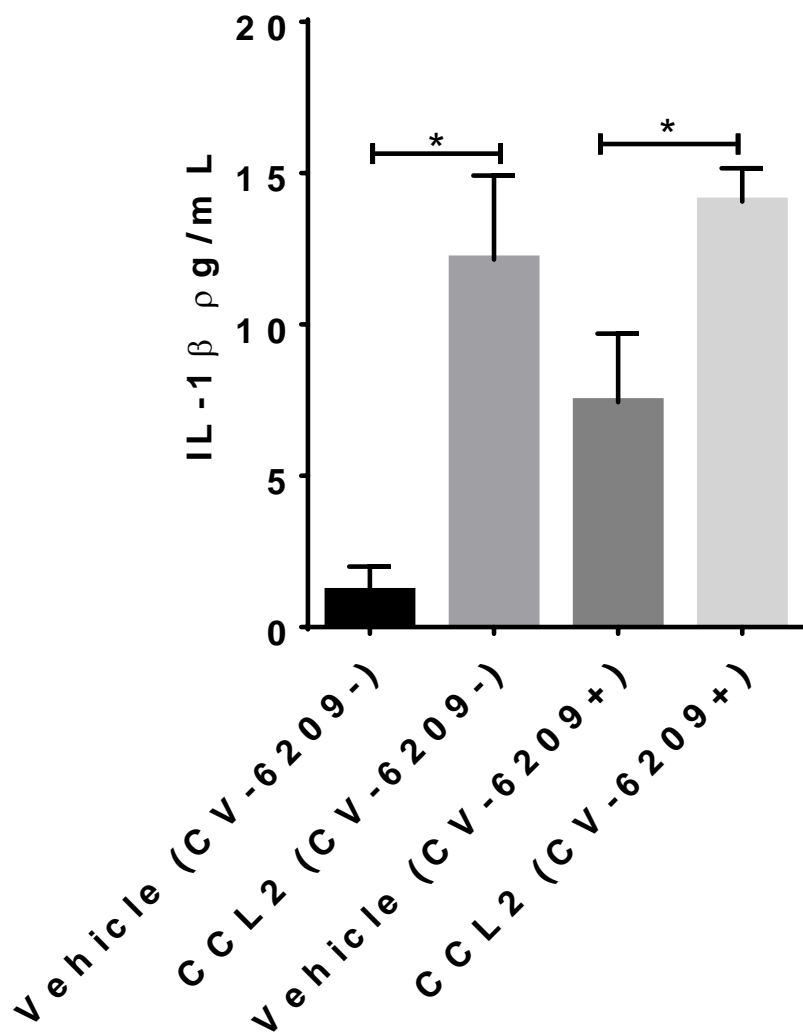


Figure 6.3.5B: IL-1 β secreted by RAW 264.7 macrophages treated with CCL2 and CV-6209. Secreted IL-1 β levels were measured in the supernatants from CCL2 treated RAW 264.7 in the presence and absence of CV-6209 (n = 3). All data represented as mean \pm S.E.M., *=p<0.05, unpaired t-test. IL-1 β levels measured by ELISA.

6.3.6 PAF secretion from CCL2 treated macrophage.

CCL2 and LPS treatment induced the expression of CCL2 and PAFR gene expression in macrophages. In CCL2 stimulated macrophages, CCL2 gene expression was shown to be the result of PAFR signalling (Section 6.3.5). To determine whether PAFR signalling is the result of *de novo* PAF synthesis by CCL2 stimulated macrophages, the level of secreted PAF from CCL2 treated RAW 264.7 macrophages in the presence and absence of CV-6209 was quantified. There were no detectable changes in the level of secreted PAF between experimental groups in this assay (figure 6.3.6A). These data suggest that PAF synthesis does not occur in this experimental system.

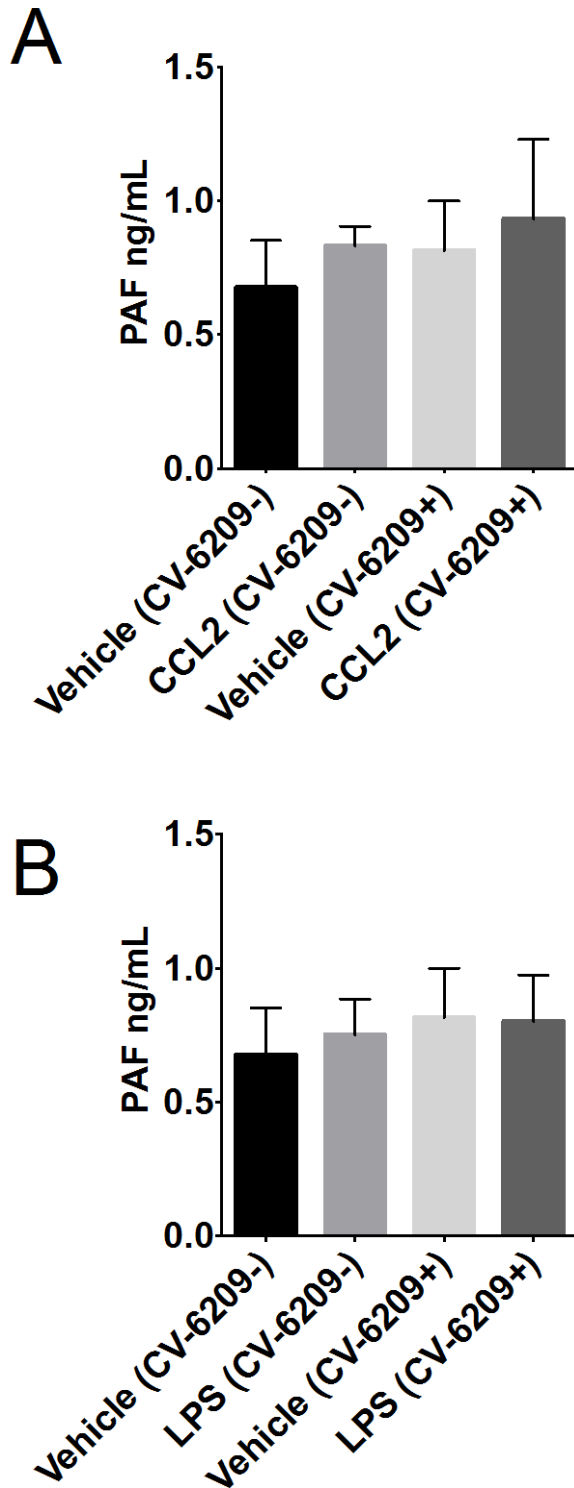


Figure 6.3.6: PAF secreted by RAW 264.7 macrophages treated with CCL2 and LPS in the presence of CV-6209. (A) Secreted PAF from RAW 264.7 macrophages was not increased with CCL2 treatment (n = 3). (B) Secreted PAF from RAW 264.7 macrophages was not increased with LPS treatment (n = 3). PAF was measured by mass spectrometry.

6.3.7 The ability of CCL2 activated macrophages to induce the activation of neutrophils via PAFR signalling.

In Chapter 5 it was reported that PAFR antagonism inhibits neutrophil recruitment to the lung in colitis-induced pulmonary inflammation. PAFR antagonism had no influence on CCL2 expression or the proportion of monocytes in the lung. Furthermore, it was shown in Section 6.3.5 that CCL2 could induce inflammatory cytokine gene expression in macrophages. Based on these observations it was considered that PAFR mediated neutrophil activation is downstream of CCL2 induced macrophage activation. Thus it was hypothesised that the secretory products of CCL2 activated macrophages can recruit neutrophils via PAFR. To test this hypothesis neutrophils were isolated from the bone marrow of naïve mice and incubated with the supernatants from CCL2 treated macrophages in the presence and absence of CV-6209. CD11b expression and superoxide production were utilized as markers of neutrophil activation. CD11b is the adhesion molecule that is responsible for neutrophil adhesion to the endothelium and superoxide production is increased as a function of activated neutrophils (Siddiqi, Garcia et al. 2001). Thus, increases in these markers are indicative of neutrophil migration and activation. Furthermore both CD11b expression and superoxide production in neutrophils is known to be mediated by PAFR signalling (Barden, Graham et al. 1997). CD11b expression was quantified on neutrophils by the mean fluorescent intensity of anti-CD11b flow cytometry staining. Superoxide production was quantified as the mean fluorescent intensity of DHE staining; the gating strategy for quantification of superoxide production is displayed in appendices section 8.5. The results obtained from these experiments show that incubation of bone marrow derived neutrophils with the supernatants from CCL2 and vehicle control treated macrophages in the absence of CV-6209 did not alter the activation status of neutrophils. (Figure 6.3.7 A & B). In addition, there was not change in the activation status of neutrophils incubated with the supernatants from CCL2 stimulated

macrophages in the presence of CV-6209. Taken together these data show that CCL2 signalling in macrophage is not sufficient to induce the activation of neutrophils. Therefore, a secondary signal in combination with CCL2 is required to induce neutrophil activation *in vivo*. The cytometry gating strategy utilized in this experiment and the representative dot plots from experimental groups are shown in Figure 8.5A-E

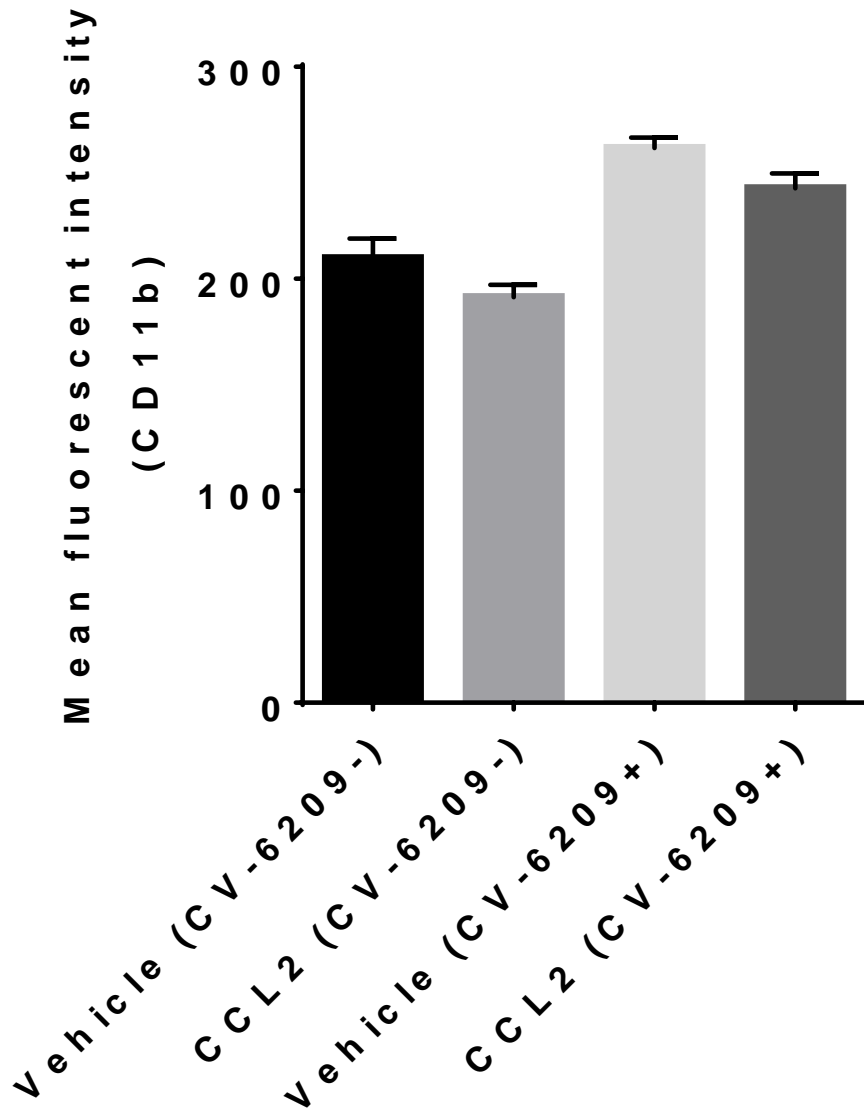


Figure 6.3.7A: The ability of secretory factors from CCL2 stimulated RAW 267.4 macrophage to induce CD11b expression on neutrophils via PAFR signalling. Supernatants from CCL2 treated vehicle treated RAW267.4 macrophage were incubated with bone marrow derived neutrophils in the presence and absence of CV-6209.

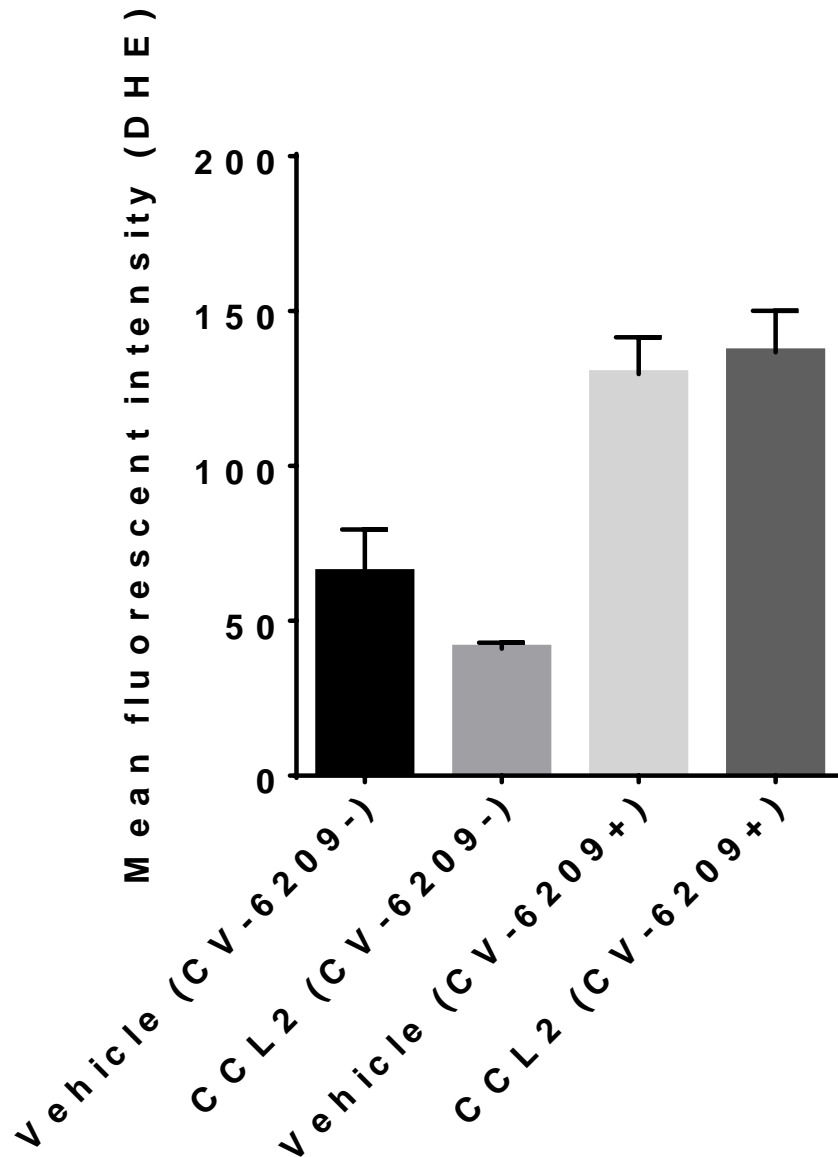


Figure 6.3.7B: The ability of secretory factors from CCL2 stimulated RAW 267.4 macrophage to induce superoxide production from neutrophils via PAFR signalling. Supernatants from CCL2 treated and vehicle treated RAW267.4 macrophage were incubated with bone marrow derived neutrophils in the presence and absence of CV-6209. Superoxide production was utilized as a marker of neutrophil activation and was quantified by the intensity of DHE staining by flow cytometry.

6.4 Discussion:

In chapter 5 it was identified that PAFR antagonism decreased the level of neutrophils recruited to the lungs of DSS colitis mice, it was also shown that PAFR antagonism decreased the level of IL-1 β expression in the lungs of DSS mice. PAFR antagonism did not influence the number of monocytes recruited to the lung or the expression of CCL2 in lung tissue. Based upon these observations a number of hypothesis were developed to account for PAFR mediated colitis associated pulmonary inflammation. Firstly, it was hypothesized that leucocytes in the lung express PAFR. Secondly, it was hypothesized that immunomodulatory factors present in the circulatory system can activate alveolar macrophages via PAFR signalling. The final hypothesis was based on the observation that PAFR antagonism had no influence on CCL2 expression in the lung, thus it was considered that PAFR mediated neutrophil recruitment is downstream of CCL2 expression. In this hypothesis CCL2 activates alveolar macrophages and induces the recruitment of neutrophils via PAFR. Thus the overall goal of this chapter was to investigate the aforementioned hypotheses with the aim of understanding the mechanism of PAFR mediated colitis associated pulmonary inflammation in greater detail. The first hypothesis tested was that PAFR expression is localised to leucocytes in the lung of acute DSS colitis mice. It was found that the majority of PAFR expression in the lungs of DSS colitis mice is localised to alveolar macrophages and neutrophils. PAFR expression was also identified on pulmonary parenchymal cells. However a significant increase in leucocytes expressing PAFR was observed. Based on this observation it was concluded that the leucocytes that are recruited to the lung express PAFR. A number of studies corroborate this observation that activated leucocytes express PAFR. In particular, a study by Chen *et al.* reported that PAFR is functionally upregulated on alveolar macrophage in a hamster model of pulmonary fibrosis (Chen, Ziboh et al. 1997). In a guinea pig model of extrinsic allergic alveolitis Perez-Arellano *et al.* found that PAFR expression on

alveolar macrophage mediated lung injury (Perez-Arellano, Martin et al. 1998). Furthermore Schaberg *et al.* identified PAFR expression on human alveolar macrophages and demonstrated the role of PAFR in modulating the inflammatory properties of these cells (Schaberg, Haller et al. 1991). The expression of PAFR on recruited neutrophils is not surprising as the role of PAFR in modulating neutrophil activation and migration is well documented (Mitchell, Lin et al. 2014). Therefore it was concluded that the beneficial effect of PAFR antagonism observed in Chapter 5 occurs through the amelioration of inflammatory signalling in alveolar macrophages and neutrophils.

It is recognised that the immunomodulatory factors that mediate intestinal inflammation can enter the circulatory system (Neurath 2014), thus it was hypothesised that the immunomodulatory factors that activate alveolar macrophages originate from the bloodstream. Experiments designed to test this hypothesis found that immunomodulatory factors present in the serum of DSS colitis mice induce the expression of IL-1 β and CCL2 in macrophages. Furthermore, it was found that expression of these cytokines is dependent upon PAFR signalling. These data demonstrate that the systemic inflammation associated with colitis can induce the inflammatory properties of macrophage via PAFR signalling. This finding is important as it represents a mechanism by which colitis can initiate inflammation at extra-intestinal sites (Loftus , Harewood et al. 2005). This finding is particularly important for organs that are highly vascularized and contain resident macrophage populations, such as the lung but also the liver. The liver is directly connected to the gastrointestinal system via the portal vein and the liver contains a population of sentinel macrophages called Kupffer cells (Broome and Bergquist 2006), thus it can be postulated that Kupffer cell activation via PAFR may play a role in the development of hepatobiliary disease associated with colitis.

CCL2 has been shown to induce activation of myeloid cells through the synthesis of PAF and subsequent PAFR signalling (Reichel, Rehberg et al. 2009). As CCL2 levels are highly elevated in the lung and colon of DSS colitis mice it was hypothesized that CCL2 can activate macrophage and induce neutrophil recruitment via PAFR signalling. To test this hypothesis two separate aims were employed, firstly *in-vitro* experiments were conducted to determine whether CCL2 could activate macrophage via PAFR and secondly to determine whether CCL2 activated macrophage could activate neutrophils via PAFR signalling. It was found that CCL2 induced macrophage activation in respect to IL-1 β production, as well as CCL2 and PAFR gene expression. CCL2-induced IL-1 β production involved a PAFR independent mechanism, whereas CCL2 and PAFR gene expression were directly regulated by PAFR signalling.

To determine whether CCL2 activation of macrophage and subsequent PAFR dependent CCL2 gene expression, was the result of *de novo* PAF synthesis and autocrine signalling. The ability of CCL2 stimulated macrophage to produce PAF was assessed. There was no change in the level of PAF in supernatants from CCL2 stimulated macrophage, this data suggests that PAF is not involved in this experimental system. However this finding is contradictory to the results obtained in Section 6.3.5, where it was shown that PAFR antagonism inhibited CCL2-induced inflammatory gene expression. CCL2 has no reported affinity for PAFR; therefore, PAFR antagonism would have no influence on the biological activity of CCL2. As PAF is the primary agonist of PAFR, the biological effect of PAFR antagonism must be due to the blockade of PAF/PAFR signalling (Ishii, Nagase et al. 2002). While lipoteichoic acid (LTA), a component of Gram-positive bacteria is also an agonist of PAFR (Han, Kim et al. 2006),

these experiments were conducted in a sterile system, thus the contribution of LTA to PAFR signalling can be considered negligible. Therefore, PAFR signalling must be due to autocrine PAF signalling induced by CCL2, however PAF was not detectable in this assay. The discrepancies in these data may be due to the methodology utilized to measure PAF. PAF is a difficult molecule to quantify; the difficulty in measuring PAF comes from the potency of the phospholipid as well as the complex process of PAF synthesis. As PAF is a highly potent agonist, the concentration of PAF in biological samples is very low. In addition a network of ubiquitously expressed PAF acetylhydrolases rapidly degrade PAF resulting in a very short half-life, these features of PAF make quantifying meaningful concentrations hard to obtain (Stephens, Graham et al. 1993). In addition, there is a very limited range of commercially available PAF antibodies. These factors make the quantification of PAF technically challenging. Many studies overcome these problems through indirect measurements utilizing the platelet aggregation properties of PAF or by using the biological effect of PAFR antagonism as evidence of PAF production (Hasegawa, Kohro et al. 2010). Studies that have achieved direct quantification of PAF have utilized thin-layer chromatography and scintillation proximity radioimmunoassays and perhaps these techniques would be better suited for the quantification of PAF (Ou, Kawasaki et al. 1991).

The ability of PAFR antagonism to inhibit CCL2 expression but not IL-1 β production may be due to the different intracellular mechanisms that synthesize these cytokines. CCL2 production occurs via a p38 mitogen-activated protein kinases pathway (p38 MAPK) (Deshmane, Kremlev et al. 2009, Lee, Lee et al. 2011) and PAFR antagonism has been reported to inhibit cytokine synthesis via disruption of the p38 MAPK pathway in experiments by Jung-Hwa *et al* (Choi, Choi et al. 2007). Therefore it can be concluded that

the expression of *Ccl2* from macrophages stimulated with CCL2 is a PAFR dependent mechanism possibly involving the p38 MAPK pathway.

In regards to IL-1 β production from CCL2 stimulated macrophage, it was found that PAFR signalling was not involved. PAFR dependent IL-1 β production is a feature of macrophage treated with the serum from DSS colitis mice. These observations imply that CCL2 is not the immunomodulatory factor present in the serum of colitis mice that activates alveolar macrophages. Therefore, another agonist must be involved, this agonist may be LTA. LTA is a component of the outer wall of Gram-positive bacteria (Broome and Bergquist 2006). As the bacterial load is increased in the lung of colitis mice it is fair to postulate that LTA is the immunomodulatory factor that initiates activation of alveolar macrophages. This hypothesis is supported by experiments that were conducted to determine if the products secreted by CCL2 activated macrophage could induce neutrophil activation. In these experiments it was found that the secreted factors from CCL2 stimulated macrophages did not induce neutrophil activation. Therefore CCL2 in isolation does not have the ability to initiate colitis-induced pulmonary inflammation, thus additional immunostimulatory factors are required. This immunostimulatory factor may be LTA, however this hypothesis was not tested experimentally.

6.5 Conclusions

Taken together, these experiments provide further detail into the role of PAFR signalling in modulating colitis-induced pulmonary inflammation. These experiments show that alveolar macrophage and neutrophils are among the cells in the lung that express PAFR in colitis-induced pulmonary inflammation. Thus it is fair to conclude that the beneficial effect of PAFR antagonism is mediated via inhibition of inflammatory signalling within these cells.

These experiments also show that it is the immunomodulatory factors present in the circulatory system of DSS colitis mice that initiate PAFR signalling in alveolar macrophages. While experiments in this chapter did not identify the agonist that initiates PAFR signalling in alveolar macrophages, these experiments did rule out LPS and CCL2 as factors that utilize PAFR to initiate inflammation. Taken together the results in this chapter show, PAFR signalling can initiate immune response in the lung through the inflammatory properties of alveolar macrophages mediated by immunomodulatory mediators of gut origin.

Chapter 7: Final discussions

7.1 Study findings

7.1.1 Respiratory pathologies in murine models of colitis

There have not been any conclusive studies that have investigated pulmonary pathologies in multiple murine models of colitis. This study is the first of its kind to report respiratory pathologies in the DSS and *Winnie* murine models of colitis. A study by Liu *et al.* did investigate IBD-induced respiratory inflammation in the TNBS model (Liu, Wang *et al.* 2013). In this study it was found that TNBS-induced pulmonary inflammation in respect to endothelial activation and expression of vascular endothelial growth factor (VEGF), however a mechanism was for this association was not found (Liu, Wang *et al.* 2013). In the present study respiratory pathologies in the DSS, TNBS and *Winnie* models of colitis was observed. Respiratory pathologies developed as immune cell infiltrate surrounding the pulmonary vasculature. The fact that this observation was conserved in all three models of colitis implies that this phenotype is due to the influence of intestinal inflammation on the physiological system. Therefore these murine models can be utilized to investigate the mechanisms of organ-cross talk that are responsible for the development of IBD-induced respiratory disease.

In-depth characterisation of the effect of colitis on the respiratory system was undertaken in the DSS model. These studies involved analysis of lung function, lung morphology, mucous hyper-secretion and inflammatory phenotyping. These studies found that while physiological pathologies i.e. lung function and morphological abnormalities were absent, there was immunopathology in the lung. Immunopathologies were identified as an increase in

neutrophils and monocytes in the lung as well as the expression of inflammatory cytokines. While the magnitude of these immunopathologies was subtle, they were measurable and developed consistently across three different colitis models.

Neutrophils and monocytes have been implicated in the latent and active respiratory diseases associated with IBD. Subclinical inflammation has been reported as an increase in the fraction of exhaled nitric oxide in the lung (Malerba, Ragnoli et al. 2011), a product of active myeloid cells. In addition the cytokines associated with the recruitment of these cells have been identified in the breath condensate of paediatric IBD patients with subclinical respiratory inflammation. In regards to the active respiratory diseases associated with IBD, neutrophils mediate the structural pathologies associated with bronchiectasis and chronic bronchitis (Hoidal 1994). Therefore, the DSS model exhibits similar immunological features to IBD-induced respiratory pathologies.

While DSS colitis did not fully recapitulate the pathological features of IBD-induced respiratory diseases, it is unlikely that an acute mouse model can completely reflect a heterogeneous chronic disease. In the case of bronchiectasis, diagnosis is based on the identification of permanent enlargement of the airways (King 2009), such a severe structural pathology is unlikely to develop in an acute model of DSS colitis. However the leucocytes and the cytokines that are responsible for pathology in bronchiectasis are present. Therefore, in a chronic setting these “mild” immunopathologies may progress into structural and functional respiratory pathologies. In fact subclinical immunopathologies have been reported in a paediatric IBD population by Krenke *et al.*, the mean age of this cohort was 13.8 ± 3.3 years (Krenke, Peradzynska et al. 2014). This study indicates that respiratory inflammation is

present even at the early development of gut disease. If this respiratory inflammation is to persist over the entire life span of disease, it may culminate in inflammation-induced functional respiratory pathologies. Mild respiratory inflammation may also determine how the pulmonary mucosal immune system responds to commensal bacteria and environmental pathogens. The lung in addition to the gut has a diverse microflora, thus the presence of activated myeloid cells may initiate inappropriate immune responses to these species. Furthermore, the lung is continuously exposed to exogenous antigens in inhaled air, thus the presence of primed myeloid cells with high cytotoxic potential may result in exaggerated immune responses to pathogenic microorganism. In fact, chronic exaggerated inflammatory responses to bacterial infection is a mechanism that induces the pathological features of bronchiectasis. Therefore, the factors that mediate the recruitment of these cells into the lung may act as a stimulus for the idiopathic respiratory diseases associated with IBD. For this reason the mechanisms by which colitis can induce respiratory inflammation is worthy of investigation and this study demonstrates that the DSS colitis model can be utilized for this task.

7.1.2 IL-6 mediates systemic inflammation associated with colitis.

In this study it was found that IL-6 signalling mediates the systemic inflammation associated with colitis potential through the modulation of neutrophil egress from the bone marrow. This observation is important as neutrophilic inflammation correlates with the severity of respiratory disease (Dente, Bilotta et al. 2015), therefore anti-IL-6 treatments may be an efficacious therapeutic approach for reducing the magnitude of IBD-induced respiratory diseases. In fact clinical trials with a human anti-IL-6 receptor antibody have shown efficacy for the treatment of gut pathology in CD patients (Ito, Takazoe et al. 2004). In the DSS model of colitis it was shown that the efficacy of anti-IL-6 treatment was not due to a reduction in

local gut cytokine levels but the modulation of systemic neutrophilia. This finding is important as it identifies IL-6 as a potential therapeutic strategy for the treatment of the systemic effects of colitis. Therefore anti-IL-6 treatment may be applicable for the treatment of a number of the extra-intestinal manifestations of IBD that involve neutrophilic inflammation, such as primary sclerosing cholangitis and erythema (Thurber and Kohler 2006).

This view is supported by the observation of the protective effect of anti-IL-6 treatment on another systemic effect of colitis, weight loss. The general opinion on DSS-induced weight loss is that intestinal inflammation induces pyrogenic responses induced by IL-1 β , IL-6 and TNF (Keely, Campbell et al. 2014). Pyrogens mediate weight loss by regulating factors that control body temperature in the CNS (Netea, Kullberg et al. 2000). Thus it can be speculated that IL-6 has a pyrogenic effect in DSS colitis. Therefore, in colitis, IL-6 not only modulates the immune system but also has the capability to induce pathogenic responses in the CNS. This is an important finding as IBD is associated with a number of neurological pathologies that include pain sensitization and depression (Graff, Walker et al. 2009, Farrell, Callister et al. 2014). Therefore, it is possible to hypothesize that IL-6 signalling may also be involved in initiating these conditions.

7.1.3 Cytokine signalling in colitis-induced pulmonary inflammation.

The recruitment of myeloid cells to the lung is orchestrated by cytokine and chemokine signalling (Hogg and Doerschuk 1995). For this reason, the cytokine profile in the lungs of DSS colitis mice was analysed. It was found that IL-1 β and CCL2 were elevated at the protein level and TNF, IFN- γ , and IL-6 were elevated at the transcript level. Due to the

absence of detectable protein levels of TNF, IFN- γ , and IL-6 it was considered that these cytokines are downstream of IL-1 β , CCL2 in the context of this inflammatory signalling cascade. The identification of IL-1 β as pathogenic factor involved in the development of colitis-induced pulmonary inflammation is corroborated by a clinical study by Krenke *et al.* CCL2 expression in the lung of IBD patients has never been identified. However in this study CCL2 was identified as a pathogenic factor involved in development of DSS colitis-induced pulmonary inflammation. CCL2 was found to be expressed by alveolar macrophages in response to PAFR signalling from immunomodulatory factors derived from intestinal inflammation in an *in-vitro* setting. This study implies that PAFR signalling initiates colitis-induced pulmonary inflammation, however in an *in-vivo* setting PAFR antagonism does not inhibit CCL2 expression, suggesting that *in-vivo* PAFR independent signalling also contributes to the development of pulmonary inflammation. In fact, it was shown that CCL2 induces CCL2 gene expression and IL-1 β production *in-vitro* through a PAFR independent mechanism. Thus in an *in-vivo* setting both PAFR dependent and independent mechanisms may modulate inflammatory signalling in the lung. In this paradigm CCL2 signalling would work in combination with PAFR signalling to initiate and/or sustain colitis-induced pulmonary inflammation. CCL2 intervention studies are required to test this hypothesis and should be a future direction for this study. Furthermore in this study CCL2 was examined in the context of innate immunity, however CCL2 also plays a prominent role in lymphocyte migration (Berencsi, Rani et al. 2011) As IBD is a chronic lymphocyte mediated disease and the respiratory diseases associated with IBD also involve lymphocyte-mediated pathologies (King 2009), pulmonary CCL2 expression may take a secondary role in a chronic setting, potential facilitating the migration of lymphocytes into the lung.

7.1.4 The role of PAFR signalling in the initiation of colitis-induced pulmonary inflammation.

In this study it was found that PAFR is expressed on alveolar macrophages and neutrophils in the lung in response to colitis-induced pulmonary inflammation. Furthermore, it was found that PAFR antagonism ameliorated IL-1 β expression and neutrophil recruitment in DSS colitis-induced pulmonary inflammation. *In-vitro* experiments showed PAFR signalling can induce the activation of macrophages through systemic immunomodulatory factors derived from intestinal inflammation. From these observations it is fair to conclude that PAFR signalling on alveolar macrophages via immunomodulatory factors released from the gut during intestinal inflammation modulates DSS colitis-induced pulmonary inflammation. There are two major limitation of this paradigm, firstly that the agonist of PAFR is unknown and secondly it was observed that PAFR is also expressed on pulmonary parenchymal cells. PAFR expression by pulmonary epithelial cells has been shown to be involved in inflammatory responses (Shukla, Sohal et al. 2014), therefore the parenchymal PAFR expression in this model may have a functional role. As there was no change in the composition of leucocytes in BAL fluid it was concluded that airway epithelial stimulation was not a factor that contributes to colitis-induced pulmonary pathology, thus making the functional of PAFR on airway epithelial cells unlikely. However since the immunopathology's in this model are subtle, this conclusion cannot be definitively made until in-depth molecular analysis of cytokine expression by pulmonary epithelial cells is conducted.

Experiments in this study did not identify the agonist of PAFR, however two potential mechanism for PAFR signalling were investigated. It was hypothesised that PAFR signalling occurs through an in-direct mechanism involving the induction of *de-novo* PAF synthesize in

alveolar macrophages. CCL2 was hypothesized as a cytokine that can induce this response. To test this hypothesis, the ability of CCL2 to activate the inflammatory properties of macrophage via PAFR signalling was examined *in vitro*. These experiments found that CCL2 could not recapitulate the immunological responses induced by PAFR signalling akin to the factors present in the circulatory system of DSS colitis mice. Thus it was concluded that indirect PAFR activation by CCL2 is not a mechanism by which alveolar macrophages are activated in DSS colitis-induced pulmonary inflammation. Therefore, an alternative hypothesis was developed, this hypothesis was that LPS from enteric bacteria enter the circulatory system and initiate PAFR signalling on alveolar macrophages as they pass through the microvasculature of the lung. To test this hypothesis, the bacterial load in the lung of DSS colitis mice was quantified and the ability of LPS to activate macrophage via PAFR signalling *in-vitro* was examined. The results from these experiments found that the bacterial load in the lung of DSS colitis mice is elevated and this increase in bacteria is associated with LPS. However, *in-vitro* experiments showed that LPS does not induce the inflammatory properties of macrophage via PAFR signalling. Thus it was concluded that LPS is not the systemic agonist that activates alveolar macrophages in colitis-induced pulmonary inflammation. While these experiments did not elucidate the agonist of PAFR signalling they did yield an important finding. The observation of increased bacterial load has many implications for mucosal immune responses in the lung. For instance, LTA is a component of Gram-positive bacteria and an agonist of PAFR. Therefore, bacteraemia associated with colitis may result in the dissemination of LTA into the lung and initiate immune responses in alveolar macrophages via PAFR. This hypothesis provides a promising further direction for this project.

7.2 Future directions:

The observations in this study have shown that respiratory pathologies are associated with murine models of colitis. This finding can provide the basis for further basic science research in this field. In this study it was identified that CCL2 can act as a pathogenic factor associated with colitis-induced pulmonary inflammation. Intervention based CCL2 experiments should be conducted to delineate the role of CCL2 in the modulation of colitis-induced pulmonary inflammation. This study also identified that PAFR signalling is involved in the development of colitis-induced pulmonary inflammation. The ability of bacteraemia associated with colitis to induced PAFR signalling via LTA provides a promising target as an agonist of PAFR. In addition, this study found that DSS colitis can alter the bacterial composition of the lung, this finding is important as research in recent years has demonstrated that alterations in microbial communities at mucosal sites can have many implications for host immune responses. Therefore, the effect of colitis on host immune responses to respiratory pathogens might be altered due to dysbiosis of the respiratory microflora. This would provide be an interesting area of research, especially since the pathogenesis of bronchiectasis is associated with chronic infections.

7.3 Study limitations

This study focused on understanding the immunological initiating factors involved in the pathogenesis of colitis-induced pulmonary inflammation. For this purpose, the acute DSS colitis model is an appropriate tool. In general, DSS colitis is a robust reproducible model with pathology well documented in the literature. The limitation of the acute DSS colitis model in this study arises from the basal levels of pulmonary histopathology observed in lung sections. While pulmonary pathology does present in lung sections, the magnitude of leucocyte infiltration is quite low, therefore it can be difficult to quantify. This becomes a

limitation in intervention-based studies as subtle changes between experimental groups can be overlooked. To overcome this limitation, a range of techniques were utilized to characterize pathology based on a number of features. These techniques included flow cytometry, qPCR and ELISA. Another limitation of this study is the difficulty in quantifying the PAF analyte. As PAF has not been the topic of a lot of research in the last decade there is a limited amount of modern published methodologies. Furthermore, there are very few commercially available assays that can be used to quantify PAF. To overcome this limitation mass spectrometry was utilized to measure PAF. While mass spectrometry is a highly sensitive technique, PAF was unable to be detected in LPS treated macrophage. LPS has been documented to induce PAF mediated process, therefore the inability to measure PAF in this experimental group raises questions over the sensitivity of this assay. To overcome the challenges of PAF quantification a number of studies utilize PAF-acetylhydrolase interventions in addition to PAFR antagonism to deduce the biological function of PAF. PAF acetylhydrolase is an enzyme that metabolises PAF, thus experiments designed with this intervention are able to functionally assess PAF/PAFR signalling without the need for the quantification of the PAF analyte. The incorporation of PAF-AH intervention into future experimental design may represent a method to overcome the problems quantifying PAF.

Another analytical limitation in this study was in the experiments that aimed to measure IL-1 β . The ELISA used for these assays measures pro-IL-1 β , Pro-IL-1 β is not the active form of IL-1 β . Therefore while this assay can give an indication of the translation level of IL-1 β in a system it cannot be conclusively determine whether translation results in secretion of the active form of IL-1 β . To measure the active form of IL-1 β a western blot to measure the proteolytically cleaved peptide should be conducted. The active form is quite small but can

measured by western blot at 17.5kDa. Alternatively a western blot to measure the proteases (caspase-1) that cleaves pro- IL-1 β should be conducted.

In the *in-vitro* experiments RAW macrophages were used to model alveolar macrophages, however RAW macrophages are not alveolar macrophages and therefore can exhibit different immunological responses. For future experiments on this topic it would be beneficial to sort alveolar macrophage by flow cytometry and culture these cells to reduce the risk of differential immune responses from RAW macrophage.

A number assays in these experiments had a sample size of $n = 4$, some would consider this sample size too low to draw definitive conclusions. Therefore going forward future experiments on this topic should increase the sample size to make assays more robust. A further critique of the experimental plans in this thesis is the limited number of cytokines that were investigated, neutrophil migration is strongly controlled by CXCL cytokines, specifically CXCL1 which is known to be a potent neutrophil chemoattractant and therefore may play a role in this model.

7.4 Concluding remarks

IBD pathology is not limited to the GI tract and can manifest in the lung. Our understanding of these conditions is limited and more basic science research is required to elucidate the mechanism by which these lung pathologies occur. In this study it is shown that murine models of colitis can be utilized to serve this purpose. This study identifies a number of pathogenic factors involved in DSS colitis-induced respiratory pathologies. These factors include PAFR signalling, systemic IL-6 and pulmonary expression of CCL2. Based on these finding I propose a mechanism to account for colitis-induced pulmonary inflammation;

intestinal inflammation induces IL-6 expression in the intestinal mucosa, vasodilation of the intestinal microvasculature allows IL-6 to disseminate systemically. Systemic IL-6 mediates neutrophil egress from the bone marrow into the circulatory system providing the cells required to perpetuate inflammation at extra-intestinal sites. In parallel immunomodulatory factors from the gut enter the bloodstream in a similar manner to IL-6. Due to the close connections of the circulatory and pulmonary systems, these immunomodulatory factors enter the lung. Sentinel alveolar macrophages interact with these immunomodulatory factors, initiating inflammatory responses via PAFR signalling. PAFR signalling induces the expression of CCL2 and IL-1 β from alveolar macrophages, which recruit neutrophils from the bloodstream.

8.0 Appendices

8.1 Cellular analysis of the lung blood and bone marrow of acute DSS colitis mice.

8.1.1 Flow cytometry gating strategies for the analysis of lymphoid populations in the lung of acute DSS colitis mice.

Flow cytometry was utilized to quantify and phenotype lymphoid cells in the lung of acute DSS colitis mice. The staining panel used in these experiments is described in Section 2.10. The gating strategies utilized in these experiments as well as representative dot plots from experimental group is shown in Figures 8.1.1A & B.

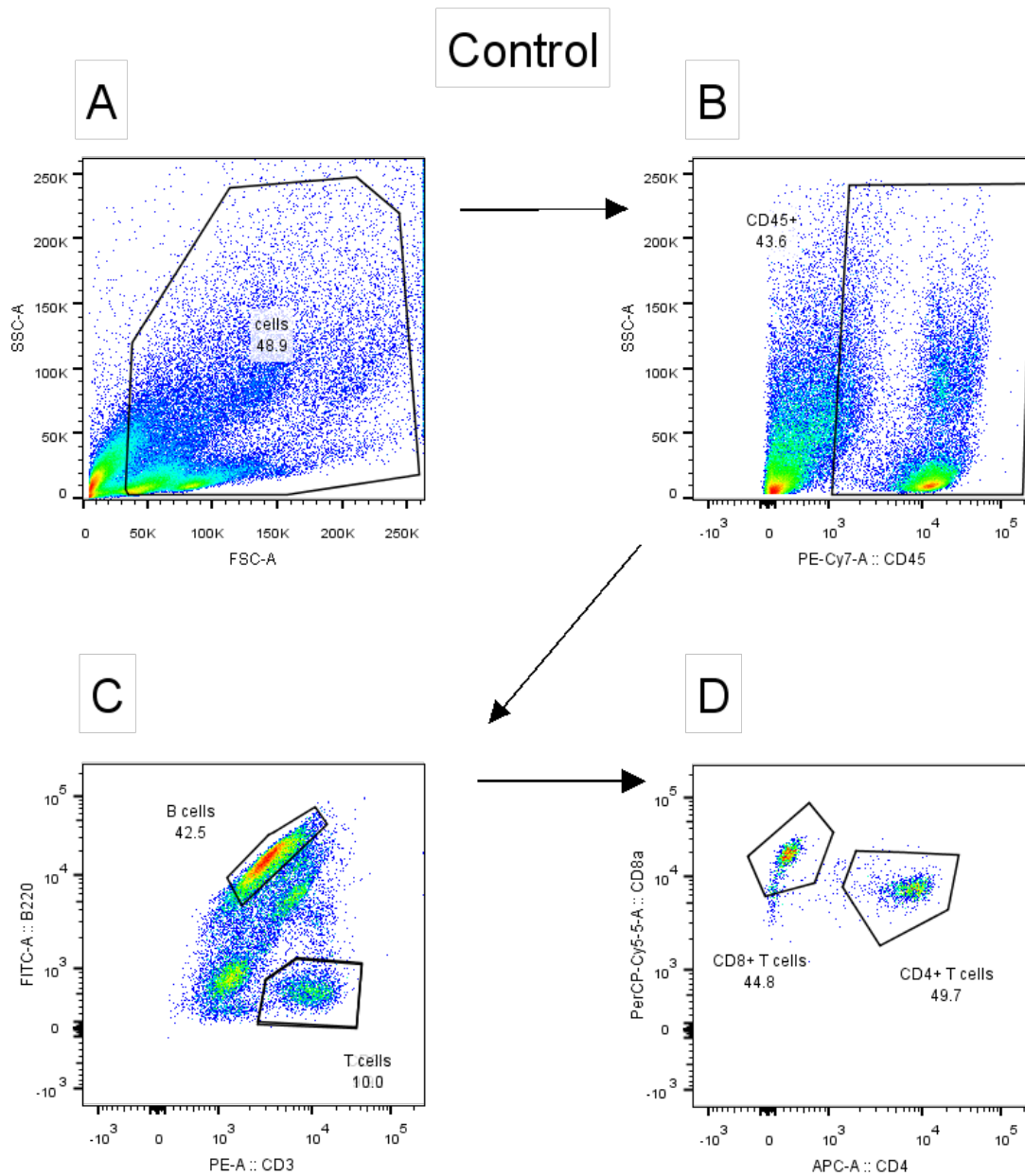


Figure 8.1.1A: Lymphoid populations in the lungs of control mice. Representative dot plots from the lungs of control mice. Cells isolated from whole lung tissue according to section 2.10. (A) Cells were identified with a gate that excluded very low side and forward scatter events. (B) Hematopoietic cells were identified as $CD45^+$ cells. (C) B cells were identified as $B220^+$ cell population, T cells were identified as $CD3^+ B220^-$ population. (D) $CD8^+$ T cells were identified as $CD8^+ CD4^-$ T cell population, $CD4^+$ T cells were identified as a $CD4^+$ T cell population.

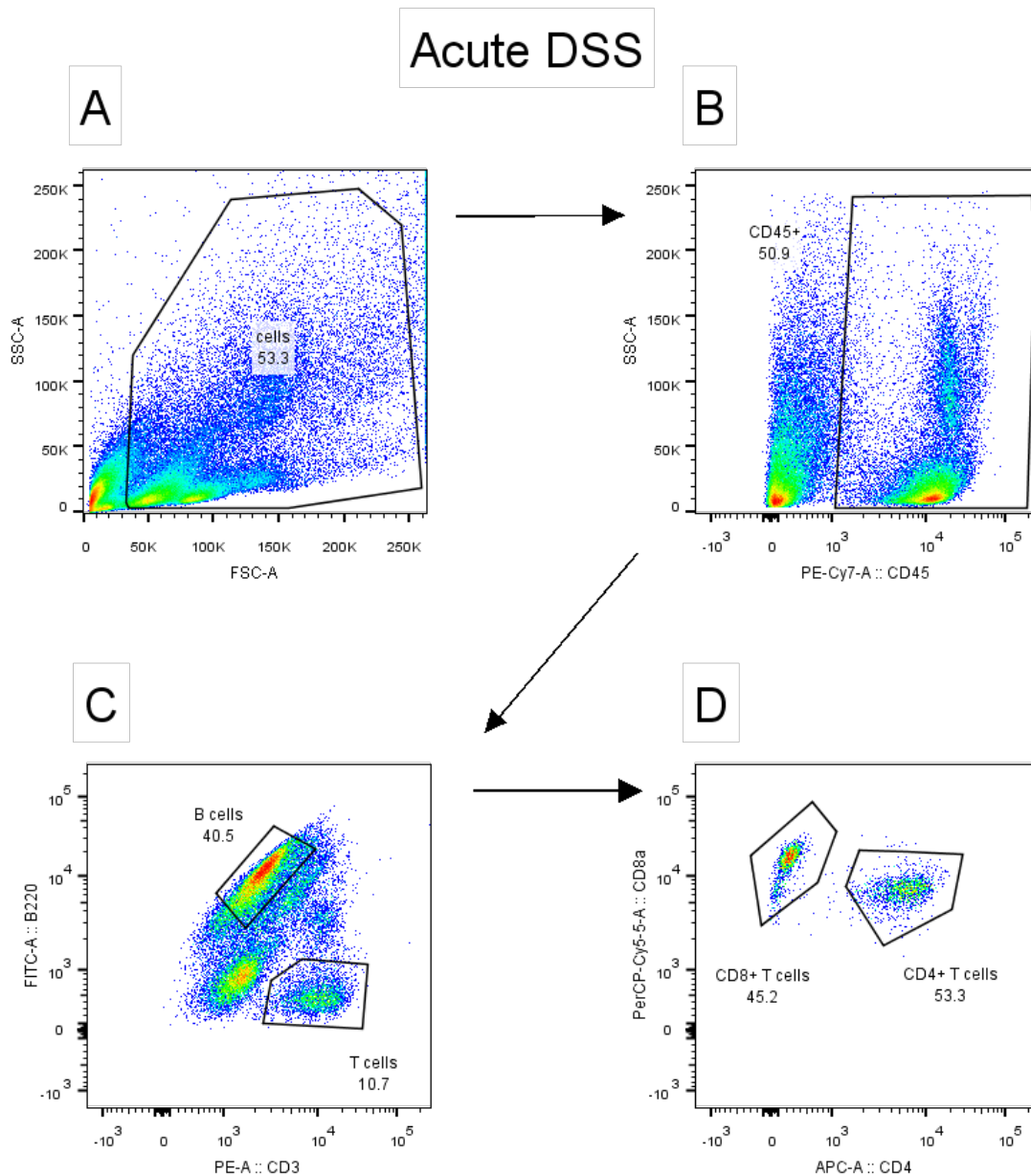


Figure 8.1.1B: Lymphoid populations in the lungs of acute DSS colitis mice. Representative dot plots from the lungs of acute DSS colitis mice. Cells isolated from whole lung tissue according to section 2.10. (A) Cells were identified with a gate that excluded very low side and forward scatter events. (B) Hematopoietic cells were identified as CD45⁺ cells. (C) B cells were identified as B220⁺ cell population, T cells were identified as CD3⁺ B220⁻ population. (D) CD8⁺ T cells were identified as CD8⁺ CD4⁻ T cell population, CD4⁺ T cells were identified as a CD4⁺ T cell population.

8.1.2 Flow cytometry gating strategies for the quantification of myeloid cell populations in the lung of acute DSS colitis mice.

Flow cytometry was utilized to quantify myeloid cell populations in the lung of acute DSS colitis mice. The staining panel used in these experiments is described in Section 2.10 and the gating strategies utilized as well as representative dot plots from experimental groups are shown in Figures 8.1.2A & B

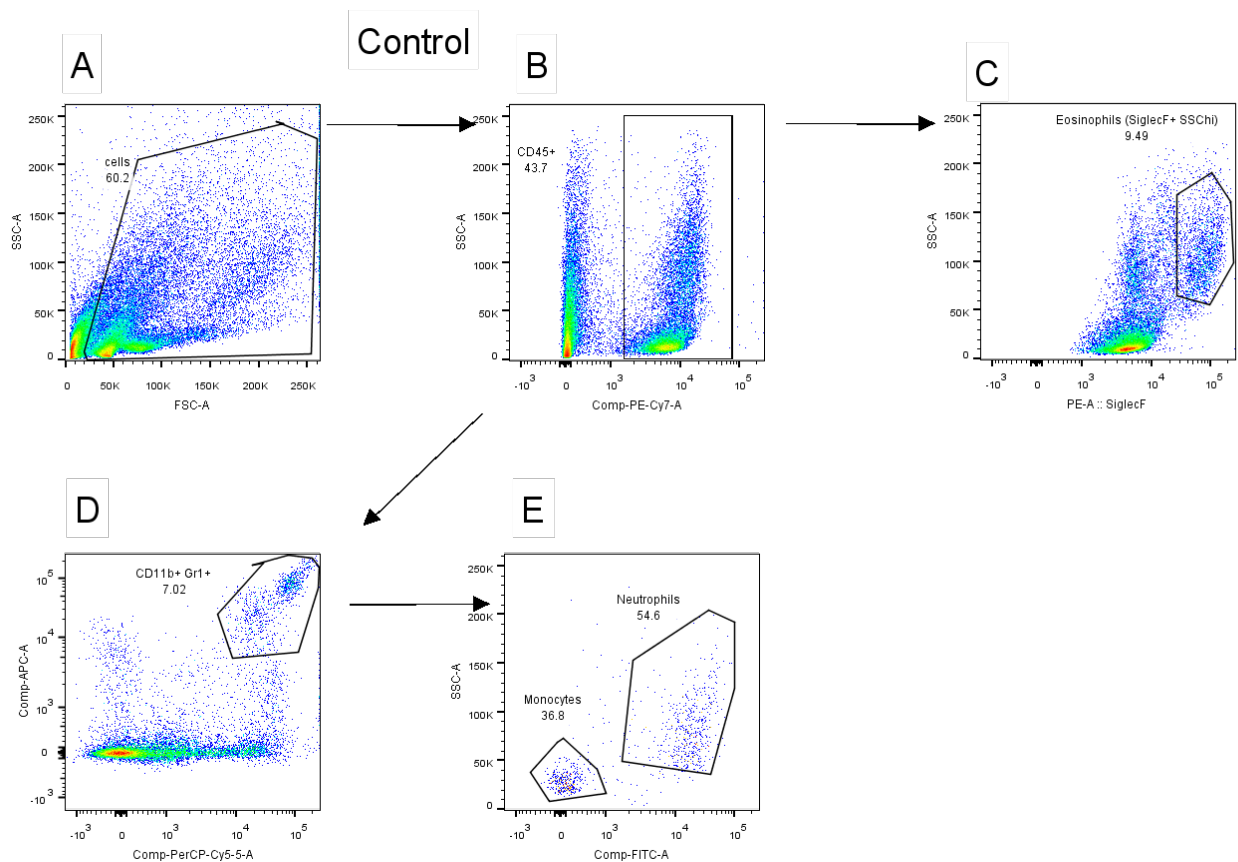


Figure 8.1.2A: Myeloid cell populations in the lungs of control mice. Representative dot plots from the lungs of control mice. (A) Cells were identified with a gate that excluded very low side and forward scatter events. (B) Hematopoietic cells were identified as CD45⁺ cells. (C) Eosinophils were identified as a CD45⁺ SiglecF⁺ cell population. (D) Myeloid cell were gated as CD11b⁺ Gr1⁺ population. (E) Neutrophils were identified as Ly6G⁺ (FITC) SSChi cell population and monocytes were identified as Ly6G⁻ (FITC) SSClo cell population.

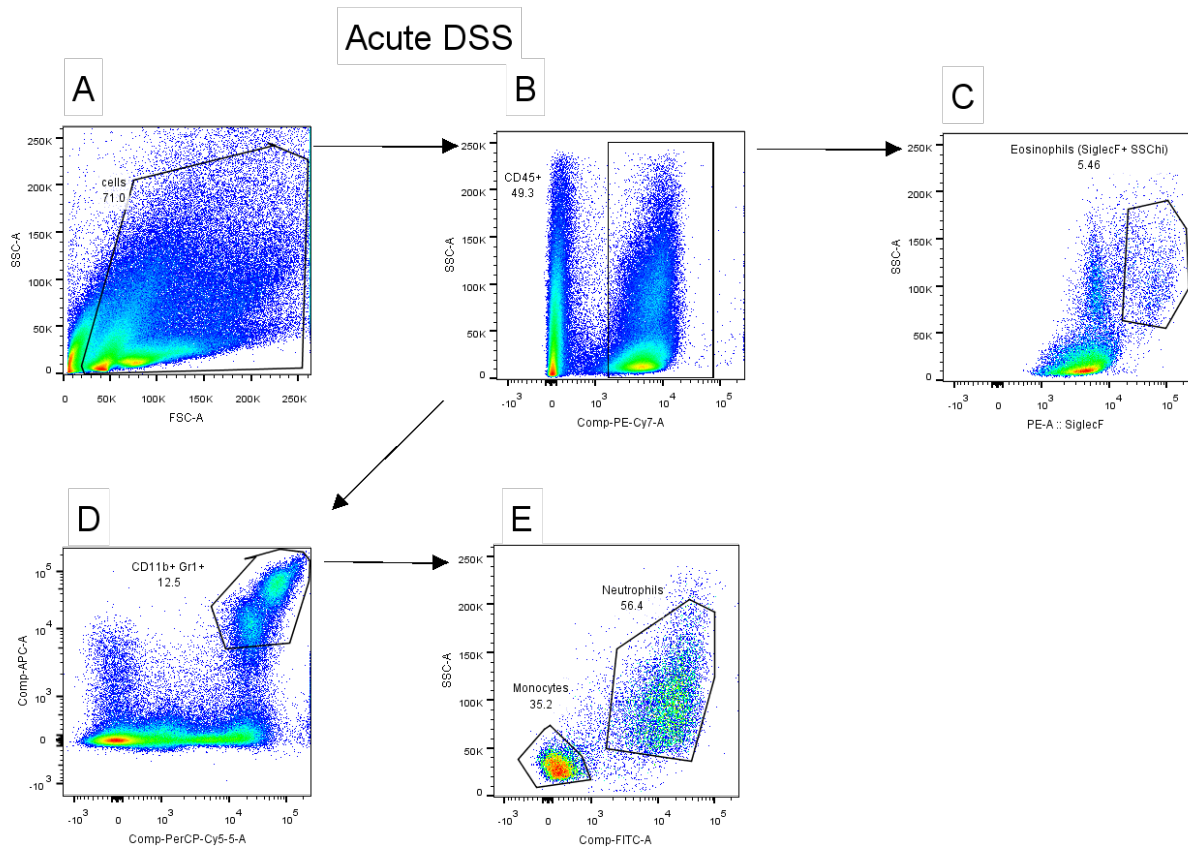


Figure 8.1.2B: Myeloid cell populations in the lungs of acute DSS colitis mice. Representative dot plots from the lungs of acute DSS colitis mice. (A) Cells were identified with a gate that excluded very low side and forward scatter events. (B) Hematopoietic cells were identified as CD45⁺ cells. (C) Eosinophils were identified as a CD45⁺ SiglecF⁺ cell population. (D) Myeloid cell were gated as CD11b⁺ Gr1⁺ population. (E) Neutrophils were identified as Ly6G⁺ (FITC) SSChi cell population and monocytes were identified as Ly6G⁻ (FITC) SSClo cell population.

8.1.3 Flow cytometry gating strategies for the quantification of myeloid cell populations in the circulatory system of acute DSS colitis mice.

Flow cytometry was utilized to quantify myeloid cell populations in the blood of acute DSS colitis mice. The staining panel used in these experiments is described in Section 2.10 and the gating strategies utilized as well as representative dot plots from experimental groups are shown in Figures 8.1.3A & B.

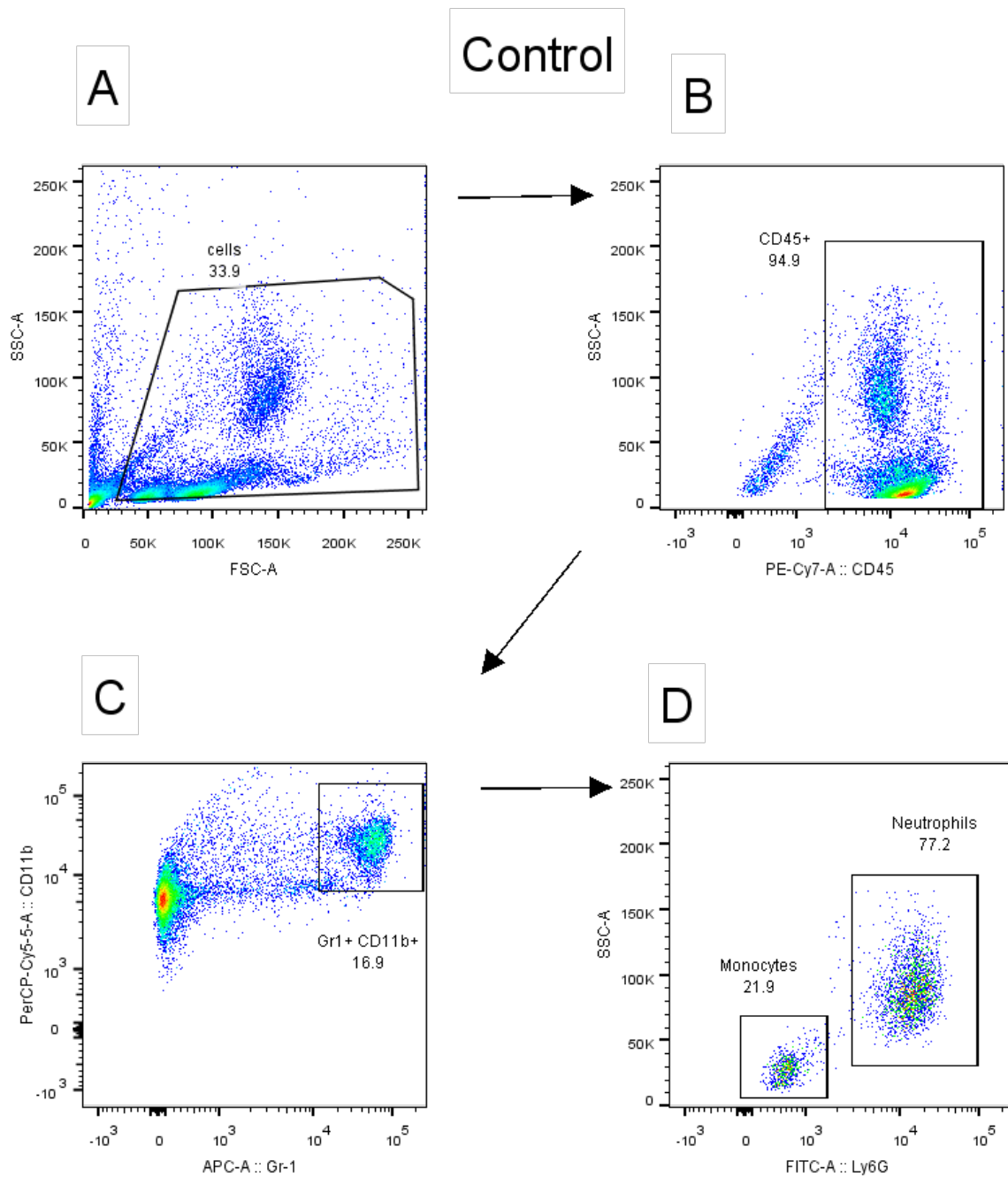


Figure 8.1.3A: Myeloid cell populations in the blood of control mice. Representative dot plots from the blood of control mice. (A) Cells were identified with a gate that excluded very low side and forward scatter events. (B) Hematopoietic cells were identified as CD45⁺ cells. (C) Myeloid cells were identified as CD11b⁺ Gr1⁺ population. (E) Neutrophils were identified as Ly6G⁺ SSChi population and monocytes were identified as Ly6G⁻ SSClo population.

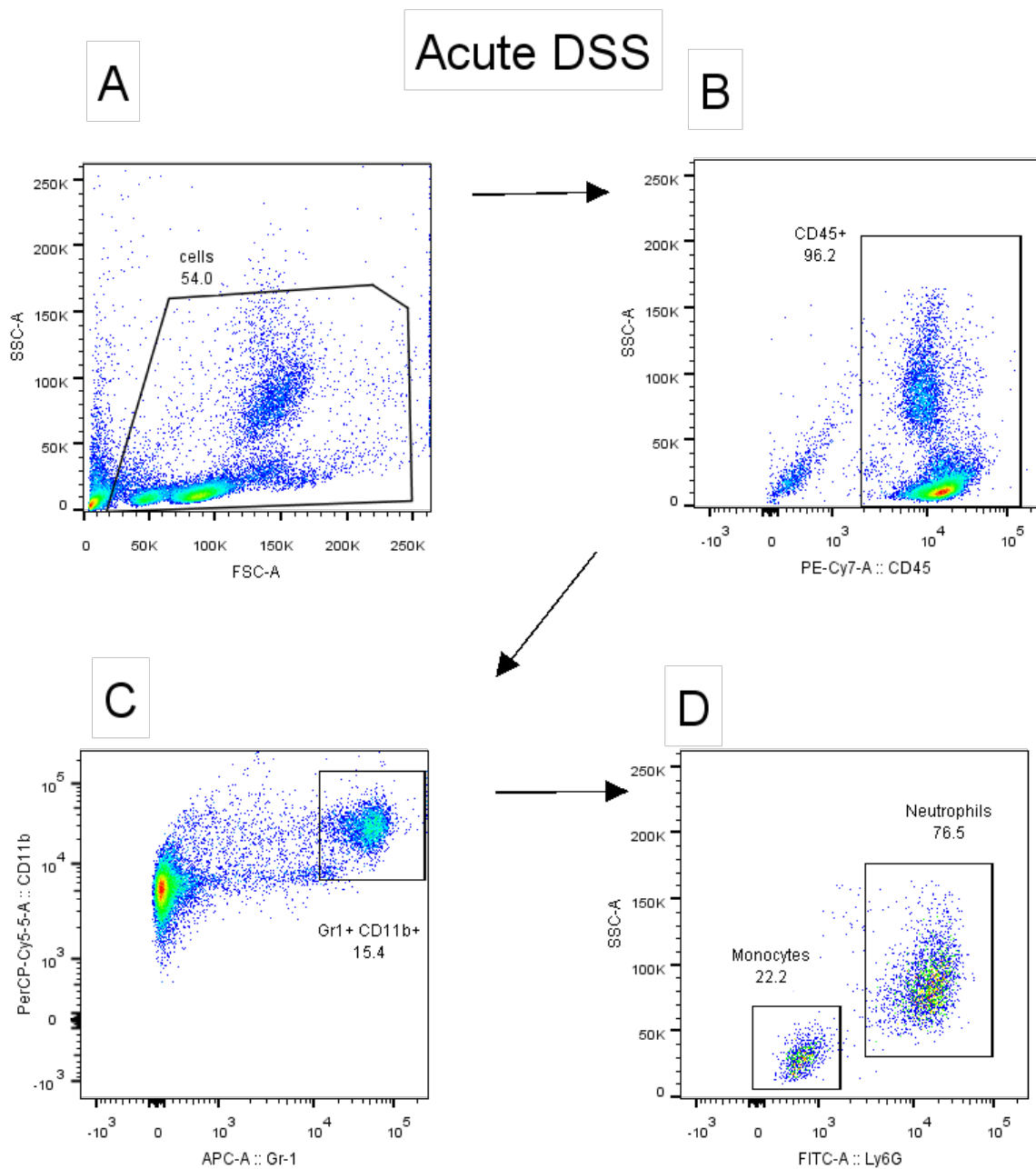


Figure 8.1.3B: Myeloid cell populations in the blood of acute DSS colitis mice. Representative dot plots from the blood of acute DSS colitis mice. (A) Cells were identified with a gate that excluded very low side and forward scatter events. (B) Hematopoietic cells were identified as CD45⁺ cells. (C) Myeloid cells were identified as CD11b⁺ Gr1⁺ population. (E) Neutrophils were identified as Ly6G⁺ SSC^{hi} population and monocytes were identified as Ly6G⁻ SSC^{lo} population.

8.1.4 Flow cytometry gating strategies for the quantification hematopoietic stem cell and progenitor cells in the bone marrow of acute DSS colitis mice.

Flow cytometry was utilized to quantify hematopoietic stem cells and progenitor cells in the bone marrow of acute DSS colitis mice. The staining panel used in these experiments is described in Section 2.10 and the gating strategies utilized as well as representative dot plot from control mice is shown in Figures 8.1.4.

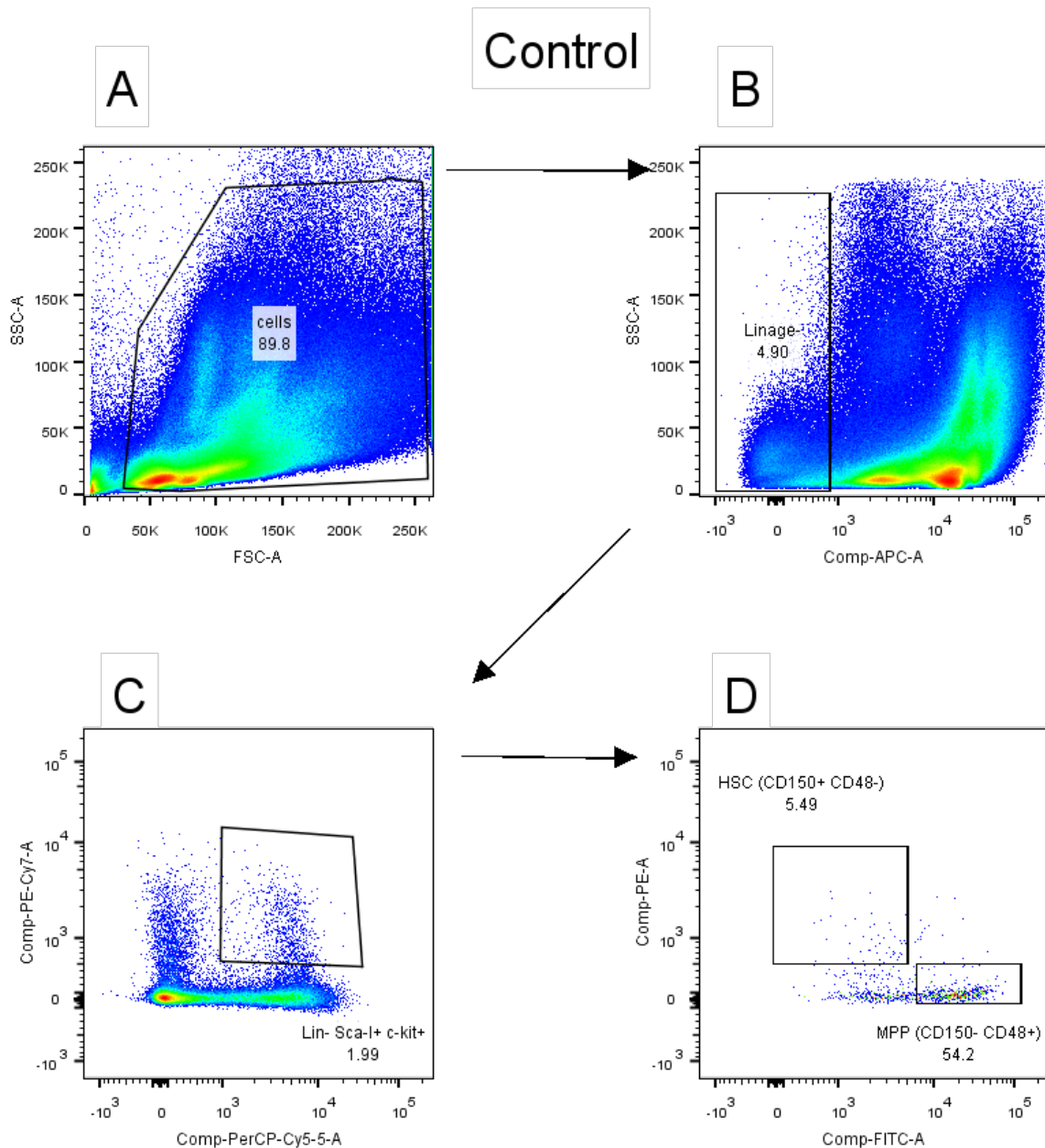


Figure 8.1.4A: Hematopoietic stem and progenitor cells in the bone marrow of control mice. Representative dot plots from the bone marrow of control mice. (A) Cells were identified with a gate that excluded very low side and forward scatter events. (B & C) Stem cells were identified as a lineage⁻ Sca-I⁺ c-kit⁺ population. (D) Hematopoietic stem cells were identified as a CD150⁺ and CD48⁻ population, multipotent progenitor cells were identified as a CD150⁻ CD48⁺ population.

8.1.5 Flow cytometry gating strategies for the quantification mature myeloid cells in the bone marrow DSS colitis mice.

Flow cytometry was utilized to quantify mature myeloid cells in the bone marrow of acute DSS colitis mice. The staining panel used in these experiments is described in Section 2.10 and the gating strategies utilized as well as representative dot plots from experimental groups are shown in Figures 8.1.5A & B.

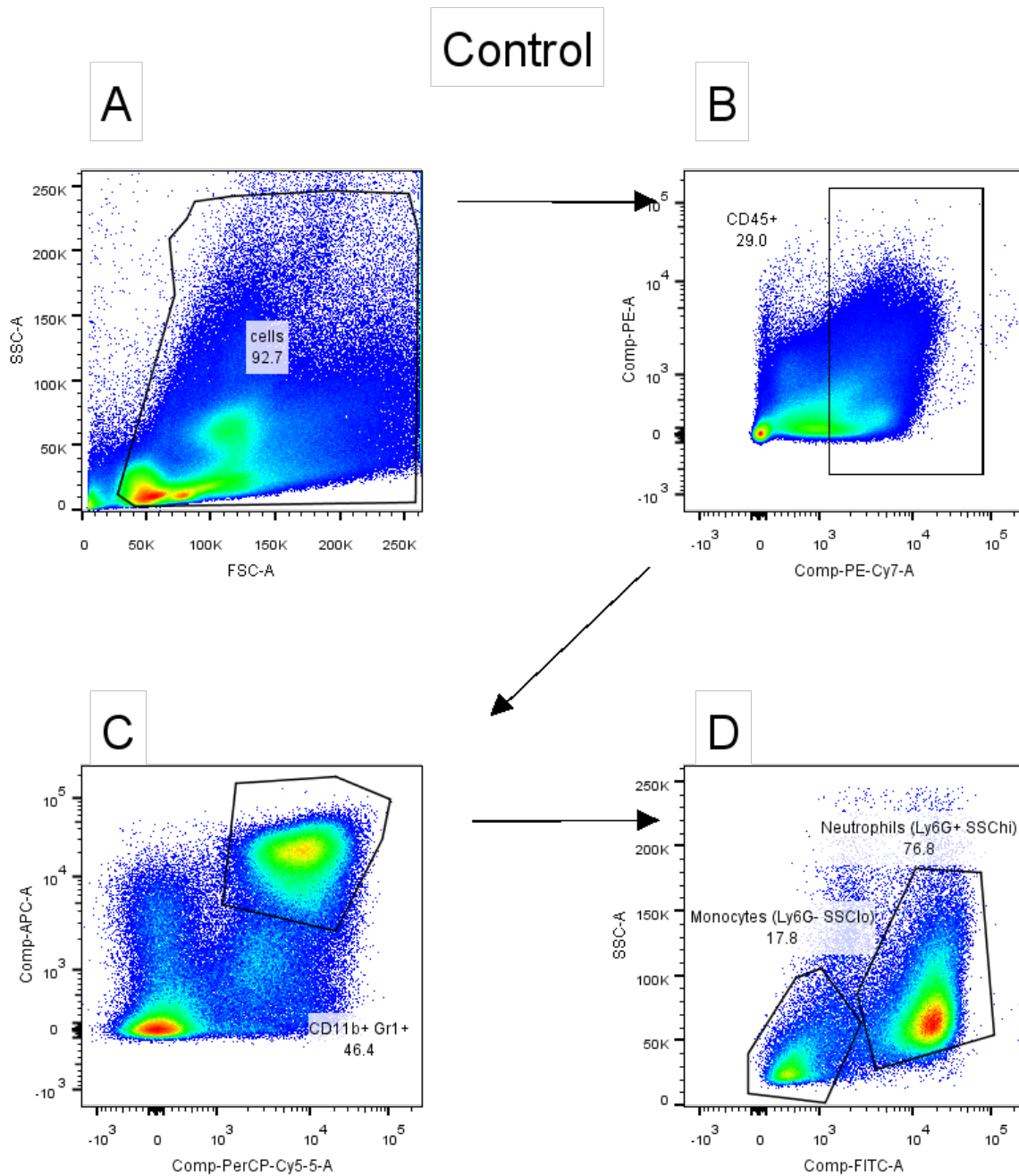


Figure 8.1.5A: Mature myeloid populations in the bone marrow of control mice. Representative dot plots from the bone marrow of control mice. (A) Cells were identified with a gate that excluded very low side and forward scatter events. (B) Hematopoietic cells were identified as CD45⁺ cells. (C) Myeloid cells were identified as CD11b⁺ Gr1⁺ population. (E) Neutrophils were identified as Ly6G⁺ SSChi population and monocytes were identified as Ly6G⁻ SSClo population.

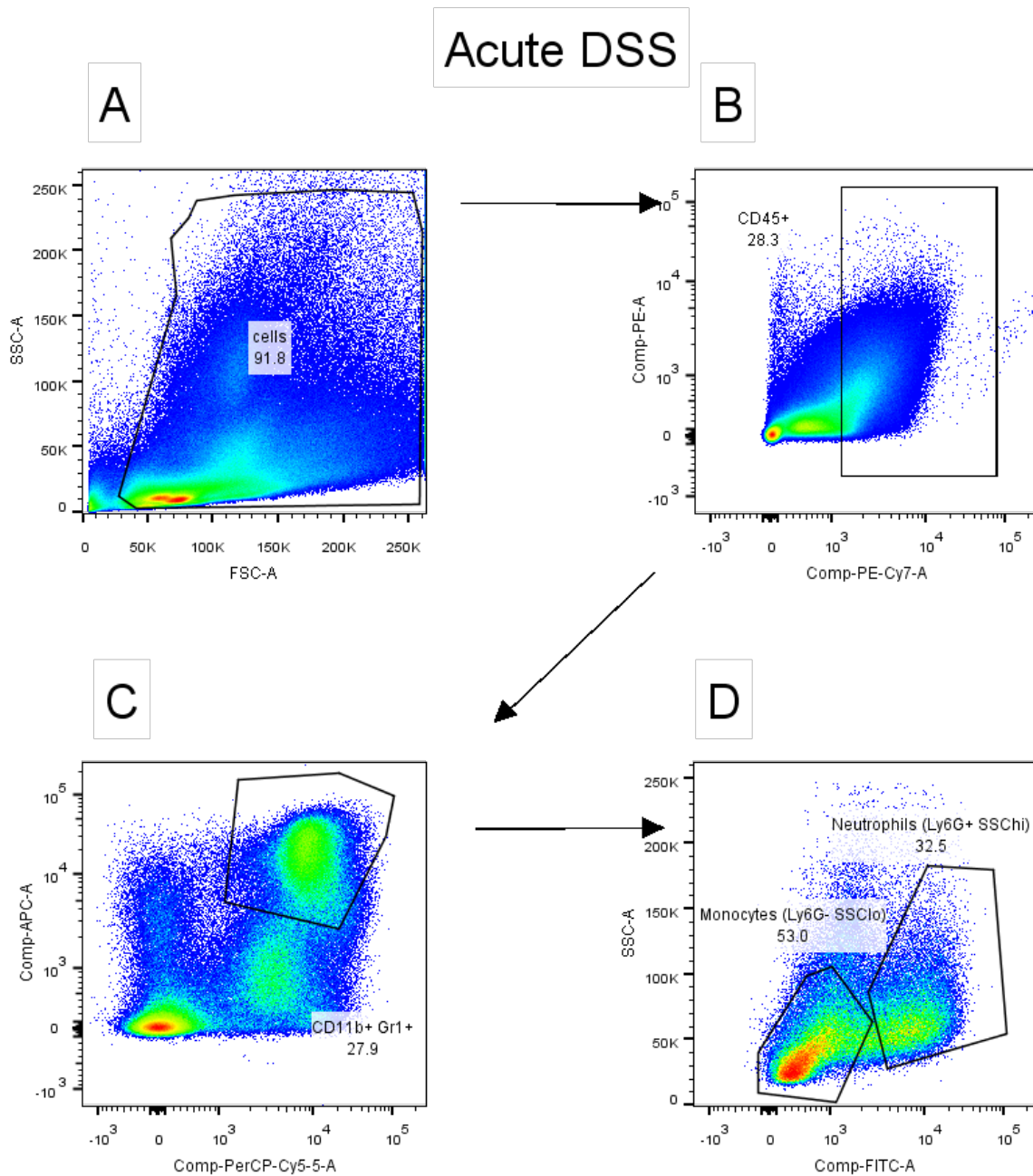


Figure 8.1.5B: Mature myeloid populations in the bone marrow of DSS colitis mice. Representative dot plots from the bone marrow of control mice. (A) Cells were identified with a gate that excluded very low side and forward scatter events. (B) Hematopoietic cells were identified as CD45⁺ cells. (C) Myeloid cells were identified as CD11b⁺ Gr1⁺ population. (E) Neutrophils were identified as Ly6G⁺ SSChi population and monocytes were identified as Ly6G⁻ SSClo population.

8.2 Cellular analysis of the lung, blood and bone marrow from anti-IL-6 treated DSS colitis mice.

8.2.1 Flow cytometry gating strategies for the quantification of myeloid cell populations in the lung of anti-IL-6 treated DSS colitis mice.

Flow cytometry was utilized to quantify myeloid cell populations in the lung of anti-IL-6 treated DSS colitis mice. The staining panel used in these experiments is described in Section 2.10 and the gating strategies utilized as well as representative dot plots from experimental groups are shown in Figures 8.2.1A – D.

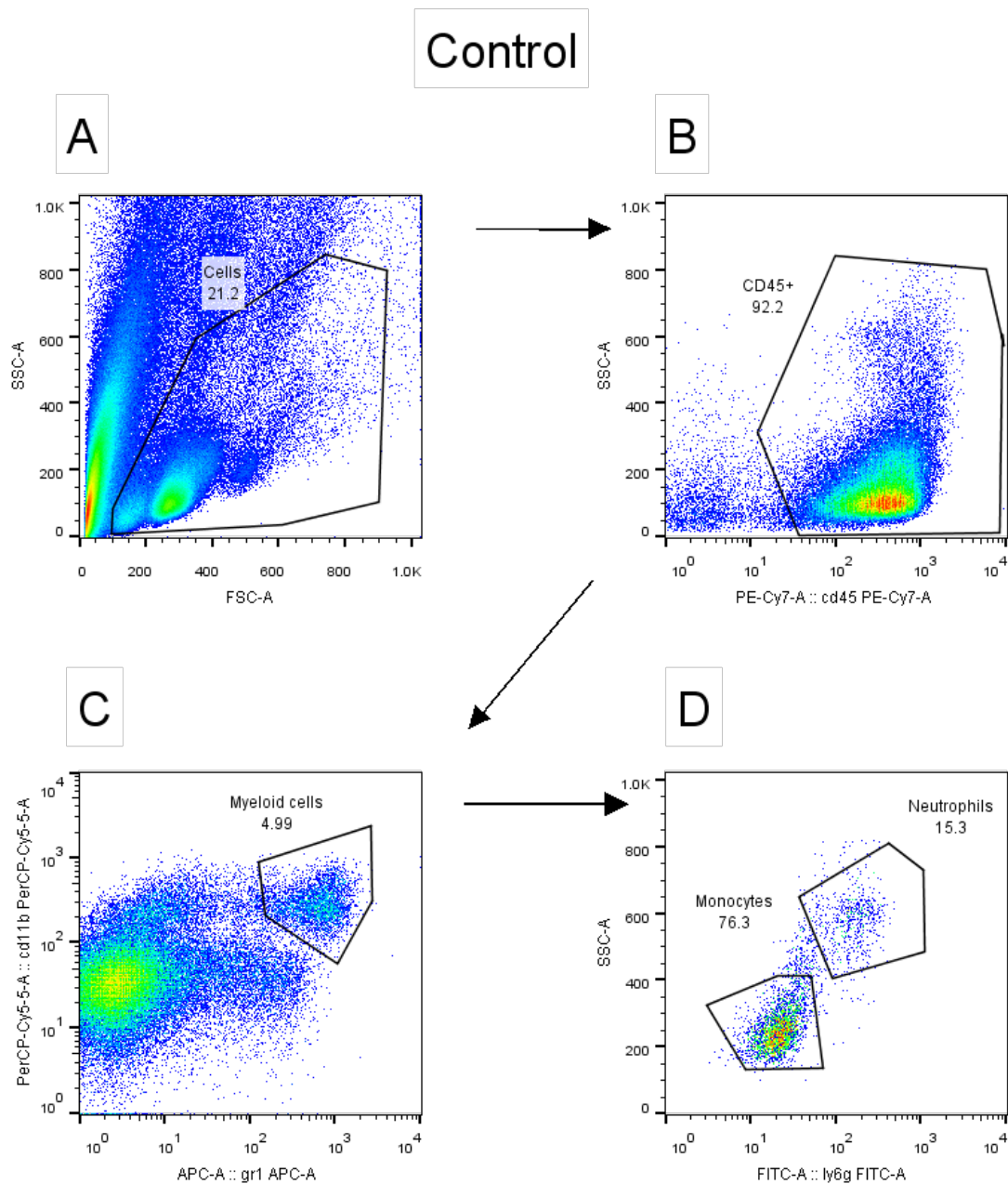


Figure 8.2.1A: Myeloid cell populations in the lungs control mice. Representative dot plots from the lungs of control mice. (A) Cells were identified with a gate that excluded very low side and forward scatter events. (B) Hematopoietic cells were identified as CD45⁺ cells. (C) Myeloid cells were identified as Gr1⁺ and CD11b⁺ cells. (D) Neutrophils were identified as Ly6G⁺ side scatter high cells and monocytes were identified as Ly6G⁻ side scatter low cells. Myeloid, neutrophil and monocyte levels were calculated as the frequency of CD45⁺ cells.

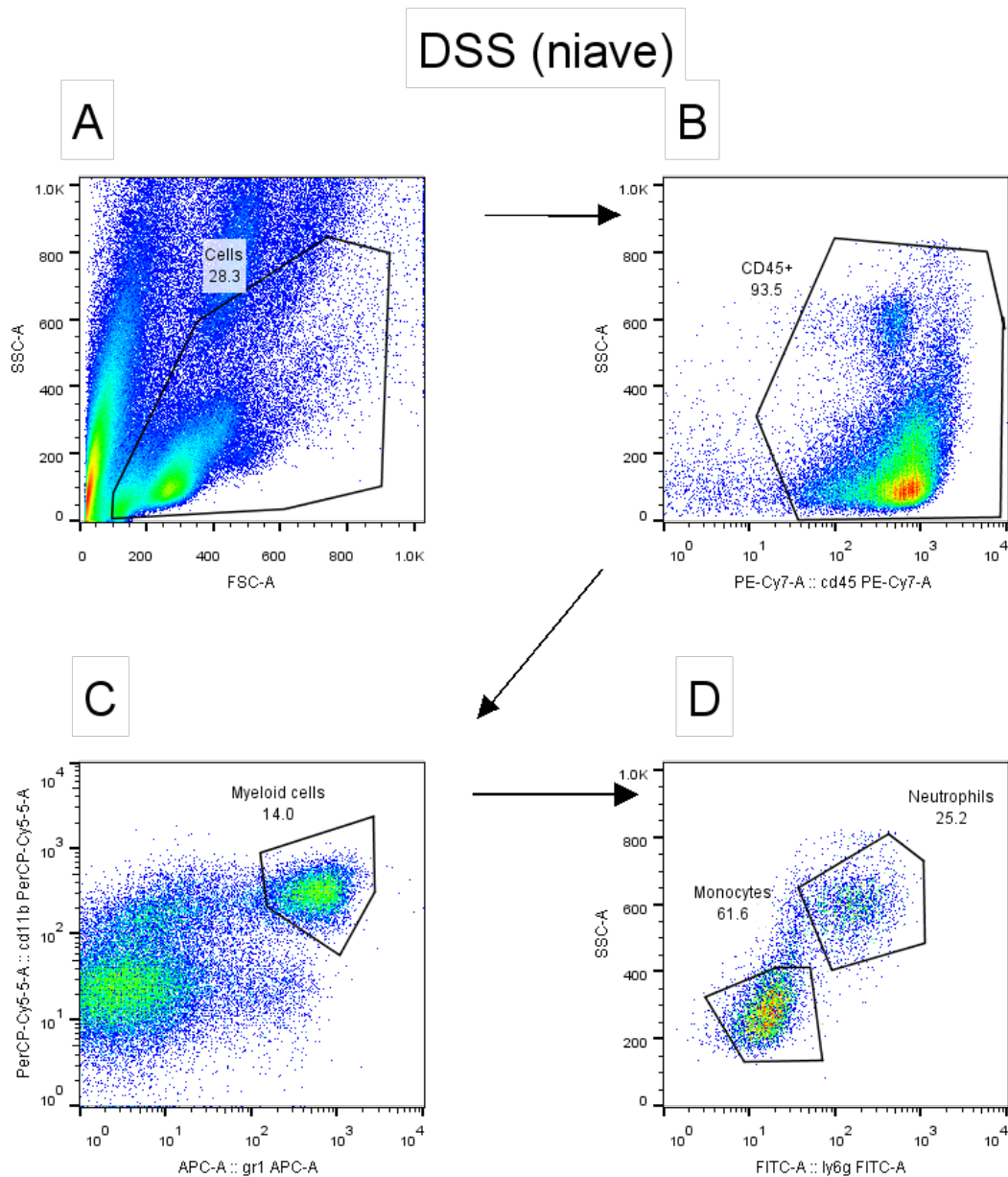


Figure 8.2.1B: Myeloid cell populations in the lungs of naïve DSS colitis mice.

Representative dot plots from the lungs of naïve DSS mice. (A) Cells were identified with a gate that excluded very low side and forward scatter events. (B) Hematopoietic cells were identified as CD45⁺ cells. (C) Myeloid cells were identified as Gr1⁺ and CD11b⁺ cells. (D) Neutrophils were identified as Ly6G⁺ side scatter high cells and monocytes were identified as Ly6G⁻ side scatter low cells. Myeloid, neutrophil and monocyte levels were calculated as the frequency of CD45⁺ cells.

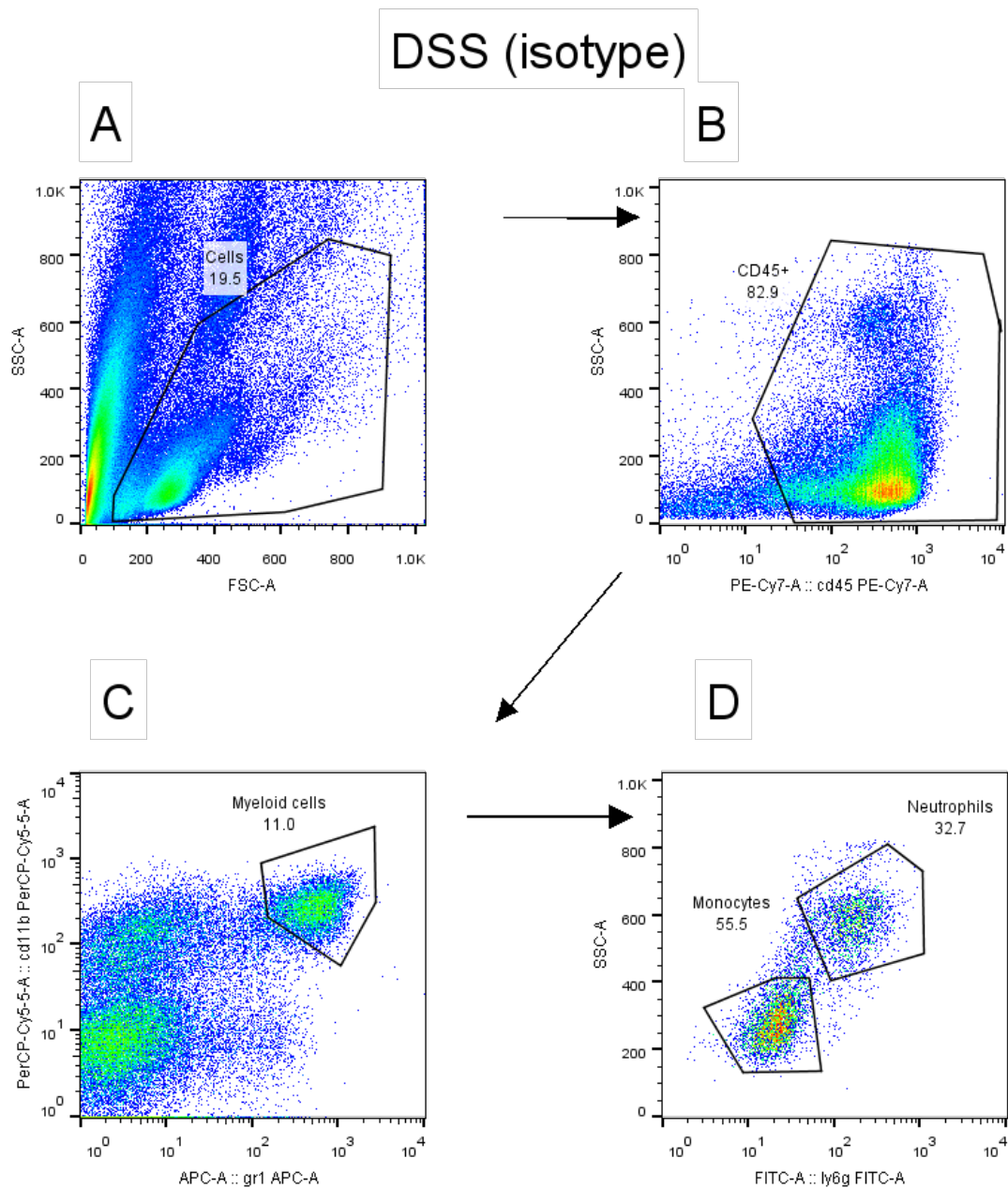


Figure 8.2.1C: Myeloid cell populations in the lungs of isotype treated DSS colitis mice.

Representative dot plots from the lungs of isotype treated DSS mice. (A) Cells were identified with a gate that excluded very low side and forward scatter events. (B) Hematopoietic cells were identified as CD45⁺ cells. (C) Myeloid cells were identified as Gr1⁺ and CD11b⁺ cells. (D) Neutrophils were identified as Ly6G⁺ side scatter high cells and monocytes were identified as Ly6G⁻ side scatter low cells. Myeloid, neutrophil and monocyte levels were calculated as the frequency of CD45⁺ cells.

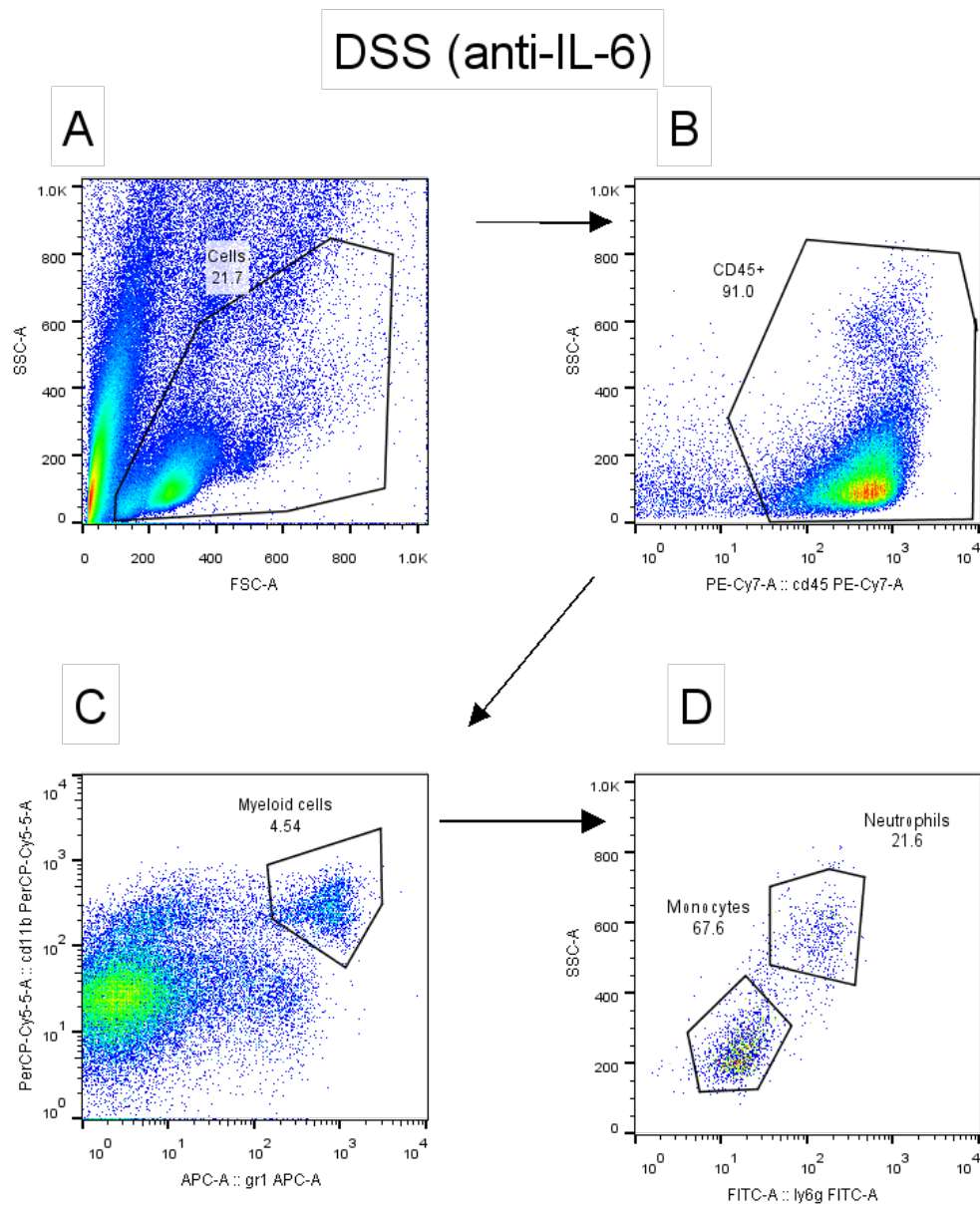


Figure 8.2.1D: Myeloid cell populations in the lungs of anti-IL-6 treated DSS colitis mice. Representative dot plots from the lungs of anti-IL-6 treated DSS mice. (A) Cells were identified with a gate that excluded very low side and forward scatter events. (B) Hematopoietic cells were identified as CD45⁺ cells. (C) Myeloid cells were identified as Gr1⁺ and CD11b⁺ cells. (D) Neutrophils were identified as Ly6G⁺ side scatter high cells and monocytes were identified as Ly6G⁻ side scatter low cells. Myeloid, neutrophil and monocyte levels were calculated as the frequency of CD45⁺ cells.

8.2.2 Flow cytometry gating strategies for the quantification of myeloid cell populations in the circulatory system of anti-IL-6 treated DSS colitis mice.

Flow cytometry was utilized to quantify myeloid cell populations in the blood of anti-IL-6 treated DSS colitis mice. The staining panel used in these experiments is described in Section 2.10 and the gating strategies utilized as well as representative dot plots from experimental groups are shown in Figures 8.2.1A – D.

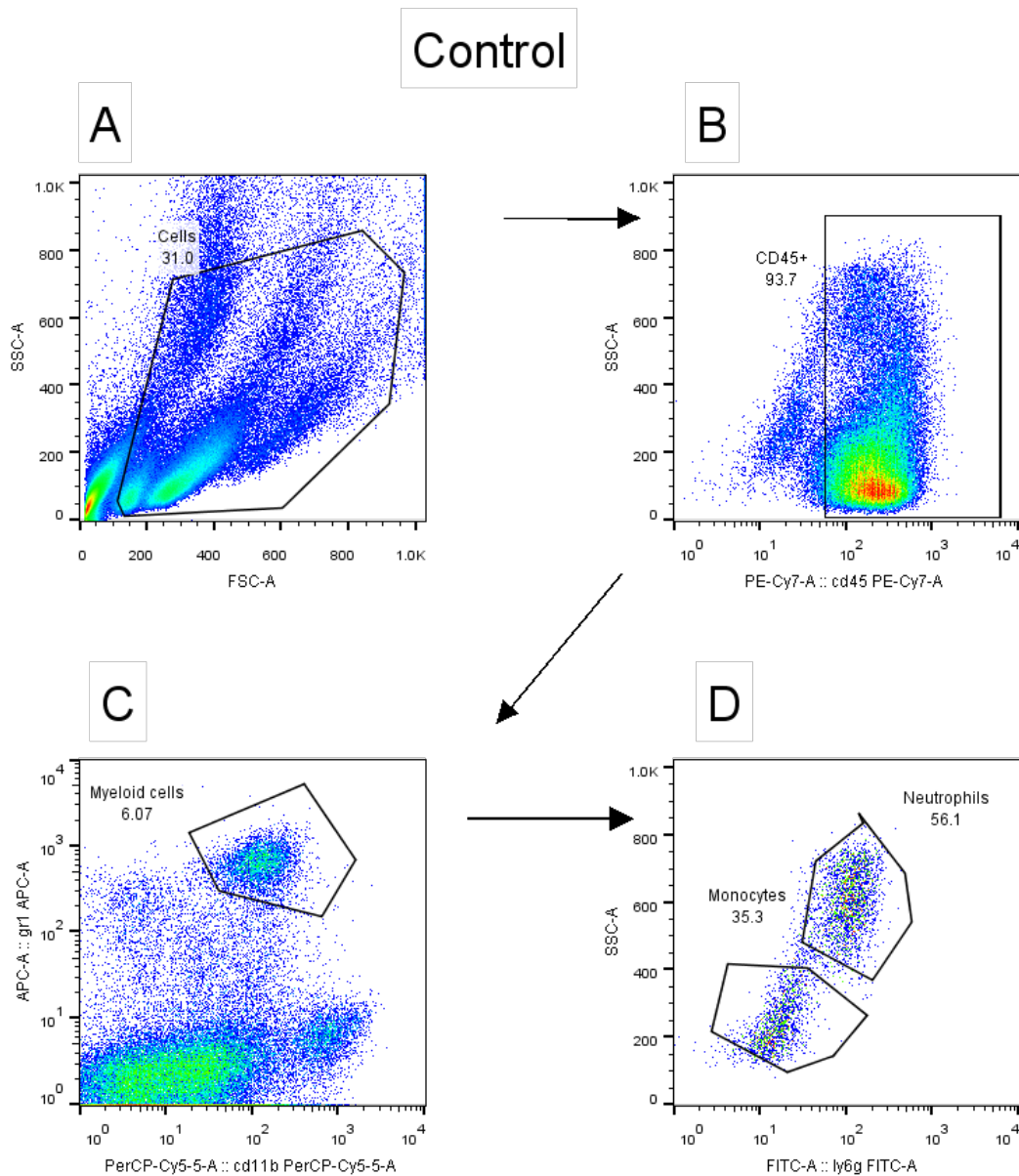


Figure 8.2.2A: Myeloid cell populations in the blood of control mice. Representative dot plots from blood of control mice. (A) Cells were identified with a gate that excluded very low side and forward scatter events. (B) Hematopoietic cells were identified as CD45⁺ cells. (C) Myeloid cells were identified as Gr1⁺ and CD11b⁺ cells. (D) Neutrophils were identified as Ly6G⁺ side scatter high cells and monocytes were identified as Ly6G⁻ side scatter low cells. Myeloid, neutrophil and monocyte levels were calculated as the frequency of CD45⁺ cells.

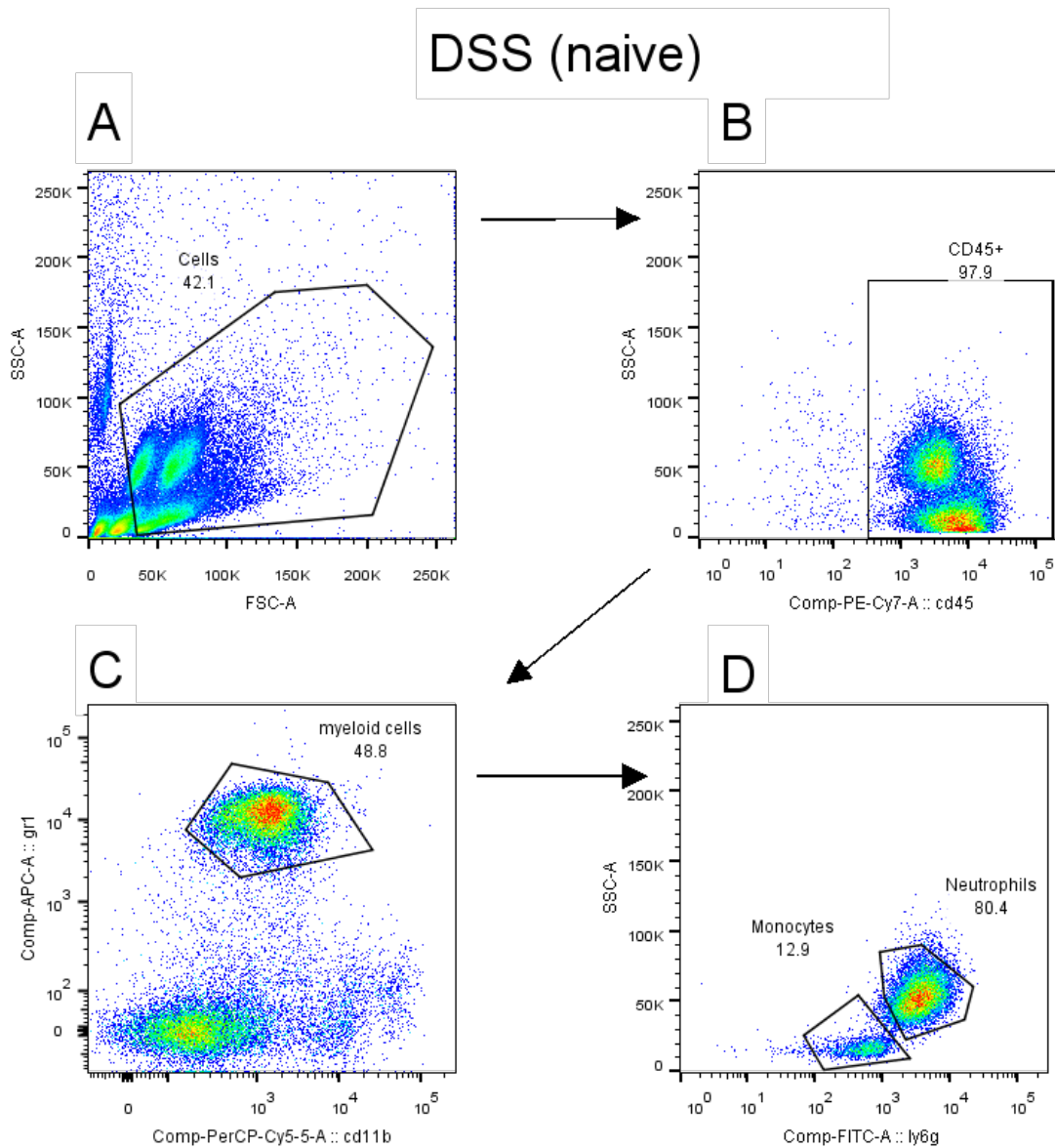


Figure 8.2.2B: Myeloid cell populations in the blood of naïve DSS colitis mice. Representative dot plots from blood of naïve DSS mice. (A) Cells were identified with a gate that excluded very low side and forward scatter events. (B) Hematopoietic cells were identified as CD45⁺ cells. (C) Myeloid cells were identified as Gr1⁺ and CD11b⁺ cells. (D) Neutrophils were identified as Ly6G⁺ side scatter high cells and monocytes were identified as Ly6G⁻ side scatter low cells. Myeloid, neutrophil and monocyte levels were calculated as the frequency of CD45⁺ cells

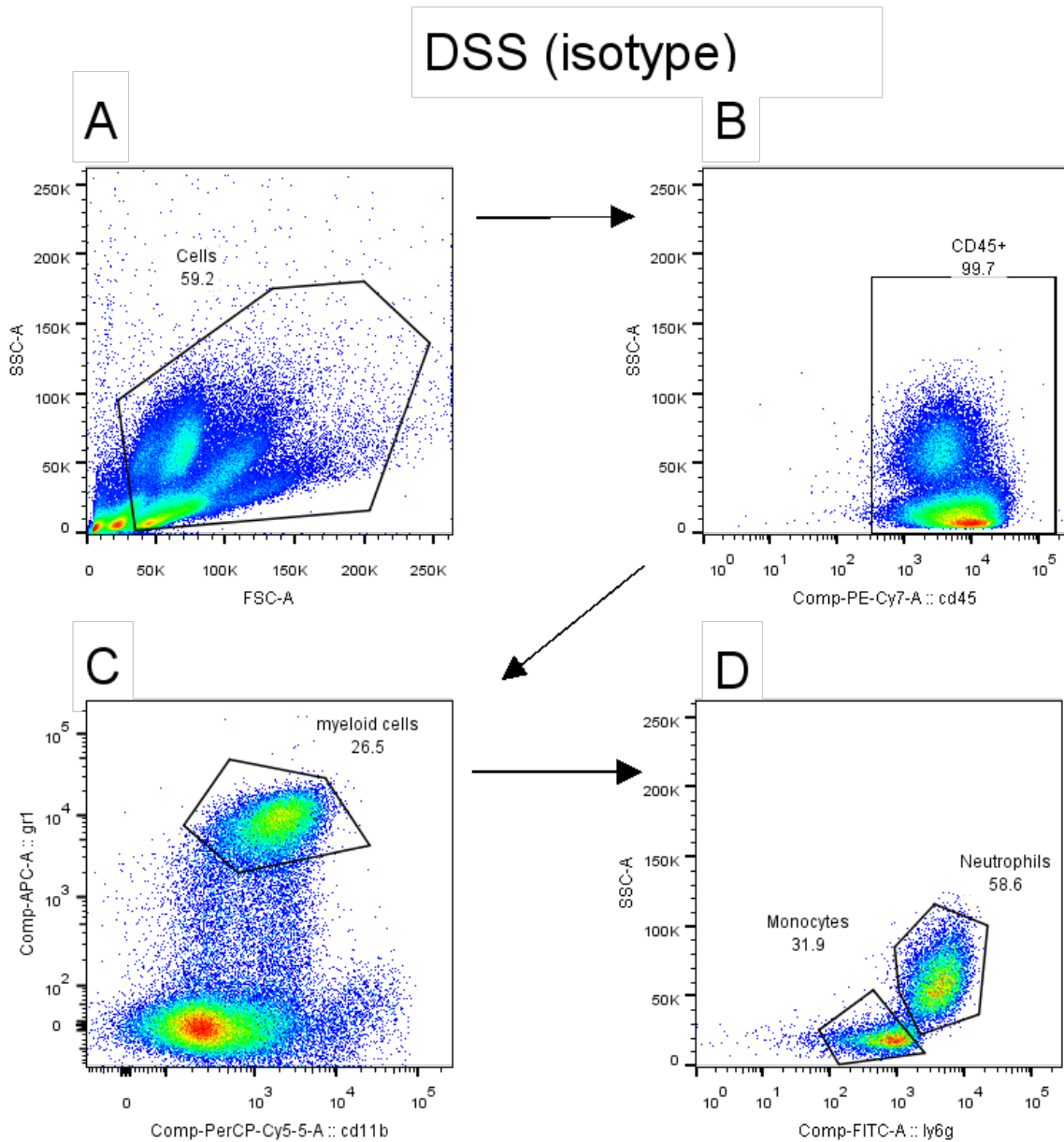


Figure 8.2.2C: Myeloid cell populations in the blood of isotype treated DSS colitis mice.

Representative dot plots from the lungs of control mice. (A) Cells were identified with a gate that excluded very low side and forward scatter events. (B) Hematopoietic cells were identified as CD45⁺ cells. (C) Myeloid cells were identified as Gr1⁺ and CD11b⁺ cells. (D) Neutrophils were identified as Ly6G⁺ side scatter high cells and monocytes were identified as Ly6G⁻ side scatter low cells. Myeloid, neutrophil and monocyte levels were calculated as the frequency of CD45⁺ cells.

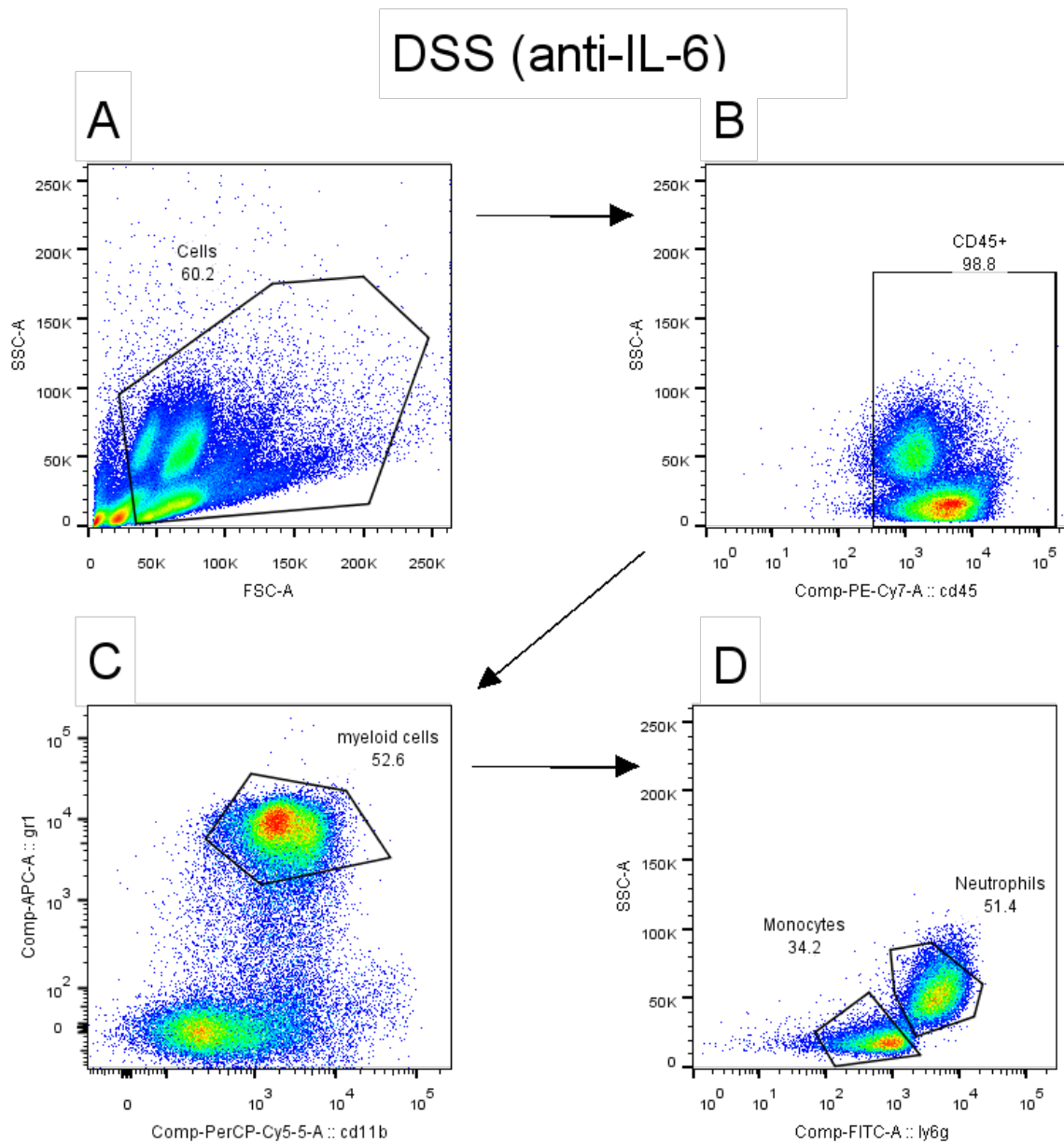


Figure 8.2.2D: Myeloid cell populations in the blood of anti-IL-6 treated DSS colitis mice. Representative dot plots from the lungs of control mice. (A) Cells were identified with a gate that excluded very low side and forward scatter events. (B) Hematopoietic cells were identified as CD45⁺ cells. (C) Myeloid cells were identified as Gr1⁺ and CD11b⁺ cells. (D) Neutrophils were identified as Ly6G⁺ side scatter high cells and monocytes were identified as Ly6G⁻ side scatter low cells. Myeloid, neutrophil and monocyte levels were calculated as the frequency of CD45⁺ cells.

8.2.3 Flow cytometry gating strategies for the quantification of hematopoietic stem and progenitor cells in the bone marrow of anti-IL-6 treated DSS colitis mice.

Flow cytometry was utilized to quantify hematopoietic stem and progenitor cells in the bone marrow of anti-IL-6 treated acute DSS colitis mice. The staining panel used in these experiments is described in Section 2.10 and the gating strategies utilized as well as representative dot plots from experimental groups are shown in Figures 8.2.3 A - D.

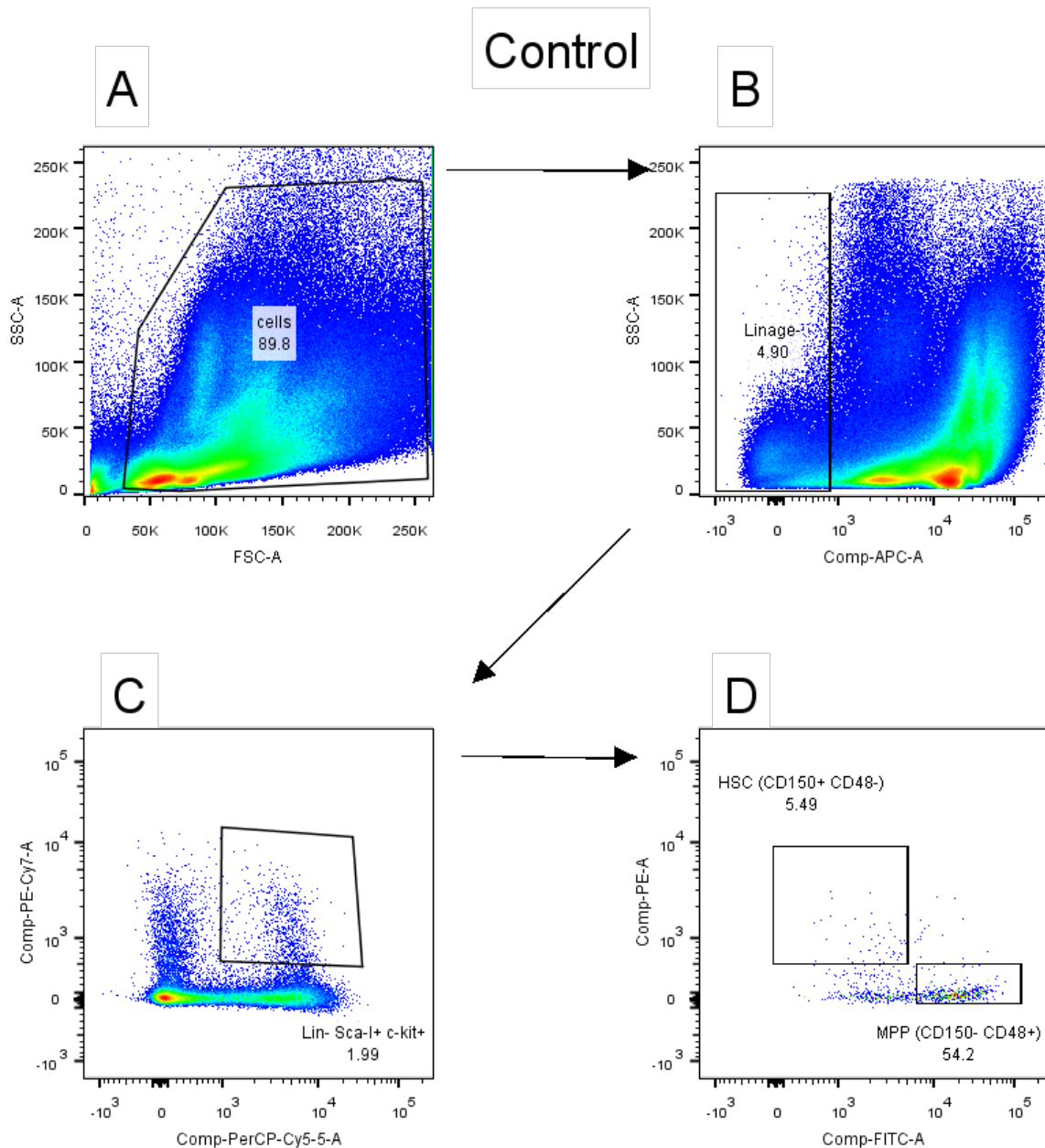


Figure 8.2.3A: Hematopoietic stem and progenitor cells in the bone marrow of control mice. Representative dot plots from the bone marrow of control mice. (A) Cells were identified with a gate that excluded very low side and forward scatter events. (B & C) Stem cells were identified as a lineage⁻ Sca-I⁺ c-kit⁺ population. (D) Hematopoietic stem cells were identified as a CD150⁺ and CD48⁻ population, multipotent progenitor cells were identified as a CD150⁻ CD48⁺ population.

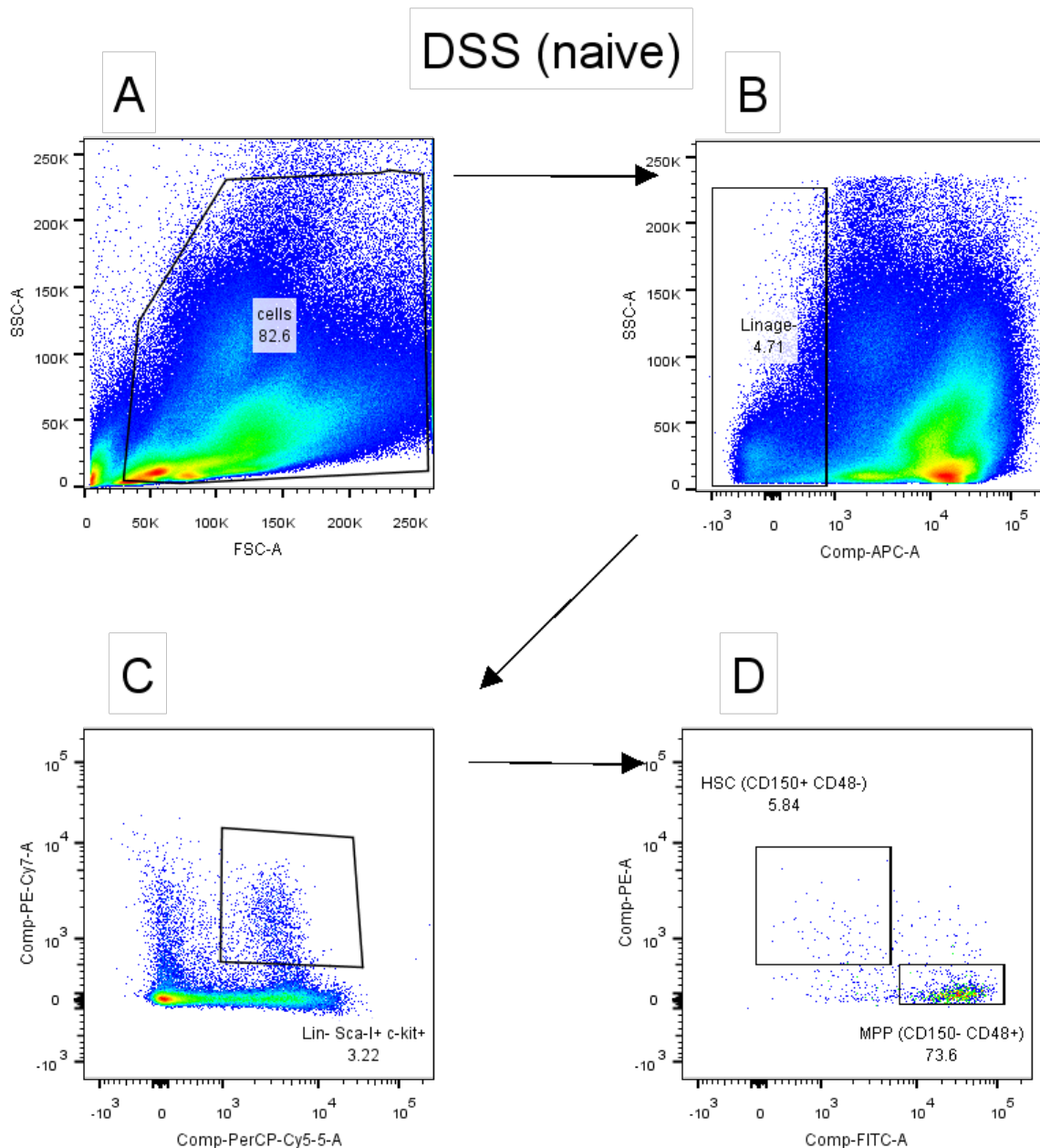


Figure 8.2.3B: Hematopoietic stem and progenitor cells in the bone marrow of naïve DSS colitis mice. Representative dot plots from the bone marrow of naïve DSS colitis mice control (A) Cells were identified with a gate that excluded very low side and forward scatter events. (B & C) Stem cells were identified as a lineage⁻ Sca-I⁺ c-kit⁺ population. (D) Hematopoietic stem cells were identified as a CD150⁺ and CD48⁻ population, multipotent progenitor cells were identified as a CD150⁻ CD48⁺ population.

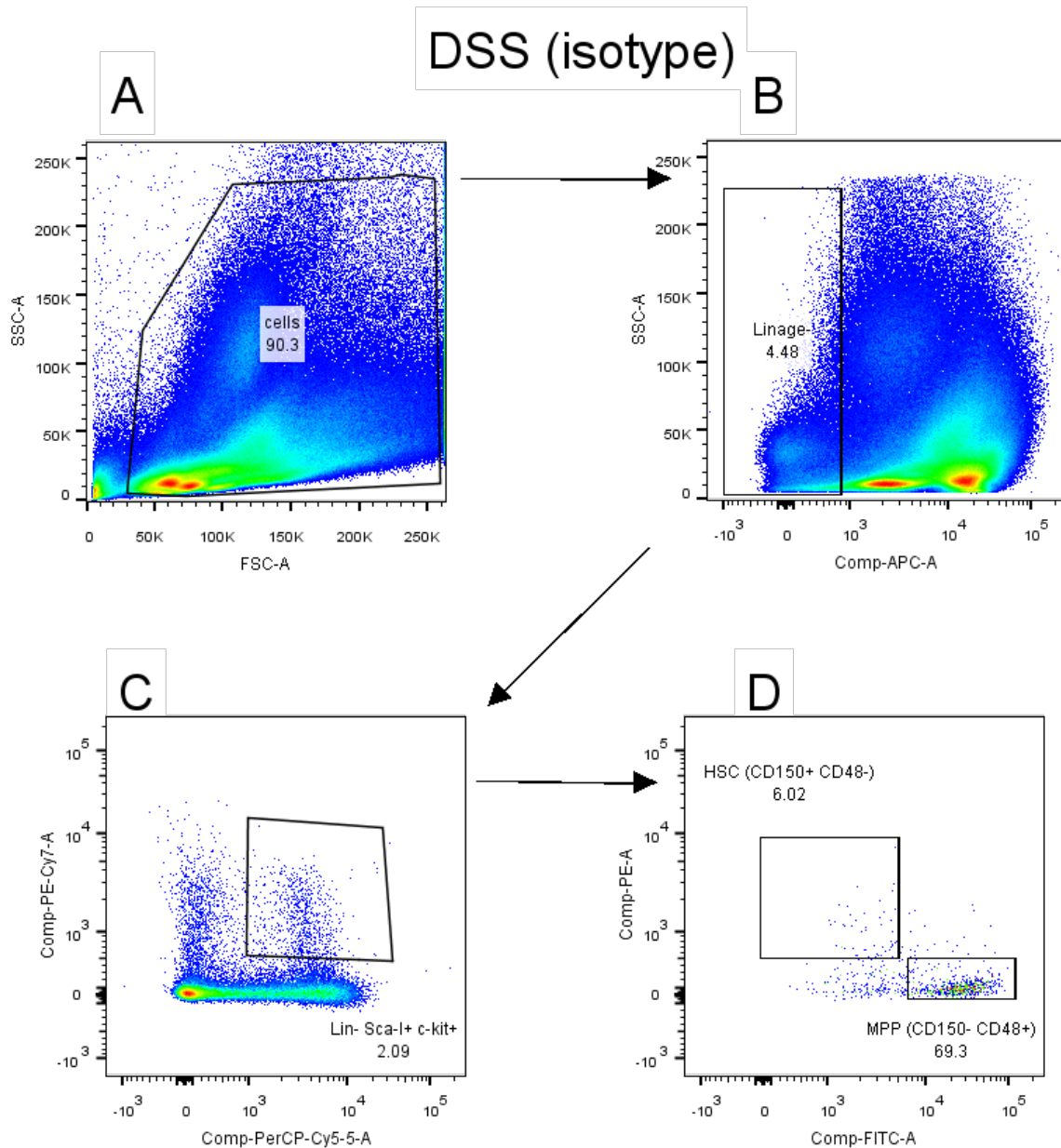


Figure 8.2.3C: Hematopoietic stem and progenitor cells in the bone marrow of isotype treated DSS colitis. Representative dot plots from the bone marrow of isotype treated DSS colitis mice control (A) Cells were identified with a gate that excluded very low side and forward scatter events. (B & C) Stem cells were identified as a lineage⁻ Sca-I⁺ c-kit⁺ population. (D) Hematopoietic stem cells were identified as a CD150⁺ and CD48⁻ population, multipotent progenitor cells were identified as a CD150⁻ CD48⁺ population.

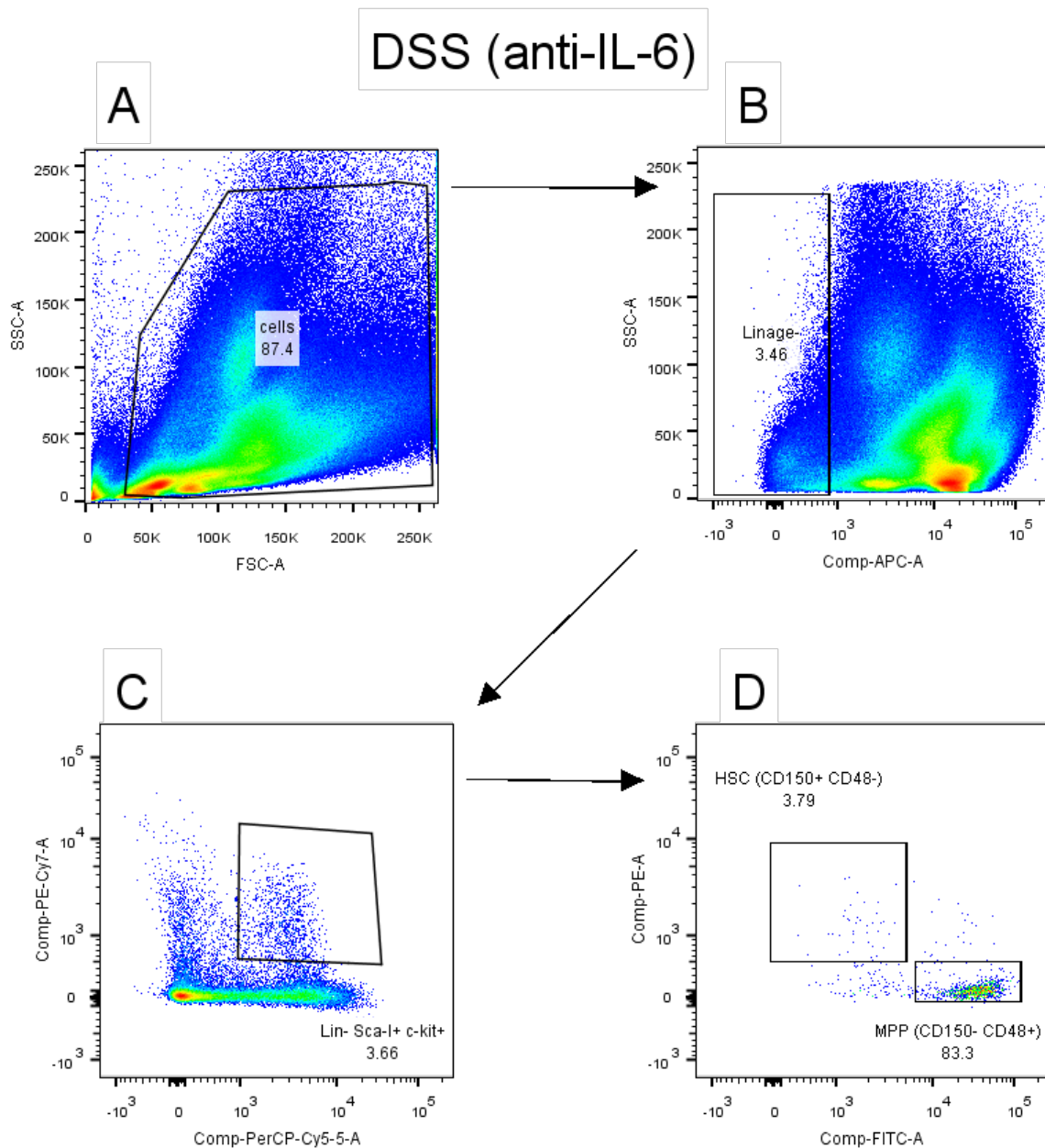


Figure 8.2.3D: Hematopoietic stem and progenitor cells in the bone marrow of anti-IL-6 treated DSS colitis mice. Representative dot plots from the bone marrow of anti-IL-6 treated DSS colitis mice control (A) Cells were identified with a gate that excluded very low side and forward scatter events. (B & C) Stem cells were identified as a lineage⁻ Sca-I⁺ c-kit⁺ population. (D) Hematopoietic stem cells were identified as a CD150⁺ and CD48⁻ population, multipotent progenitor cells were identified as a CD150⁻ CD48⁺ population.

8.3 Quantification of myeloid cell populations in CV-6209 treated DSS colitis mice.

8.3.1 Flow cytometry gating strategies for the quantification of myeloid cell populations in the lung of CV-6209 treated DSS colitis mice.

Flow cytometry was utilized to quantify myeloid cell populations in the lung of CV-6209 treated DSS colitis mice. The staining panel used in these experiments is described in Section 2.10 and the gating strategies utilized as well as representative dot plots from experimental groups are shown in Figures 8.2.1A – D.

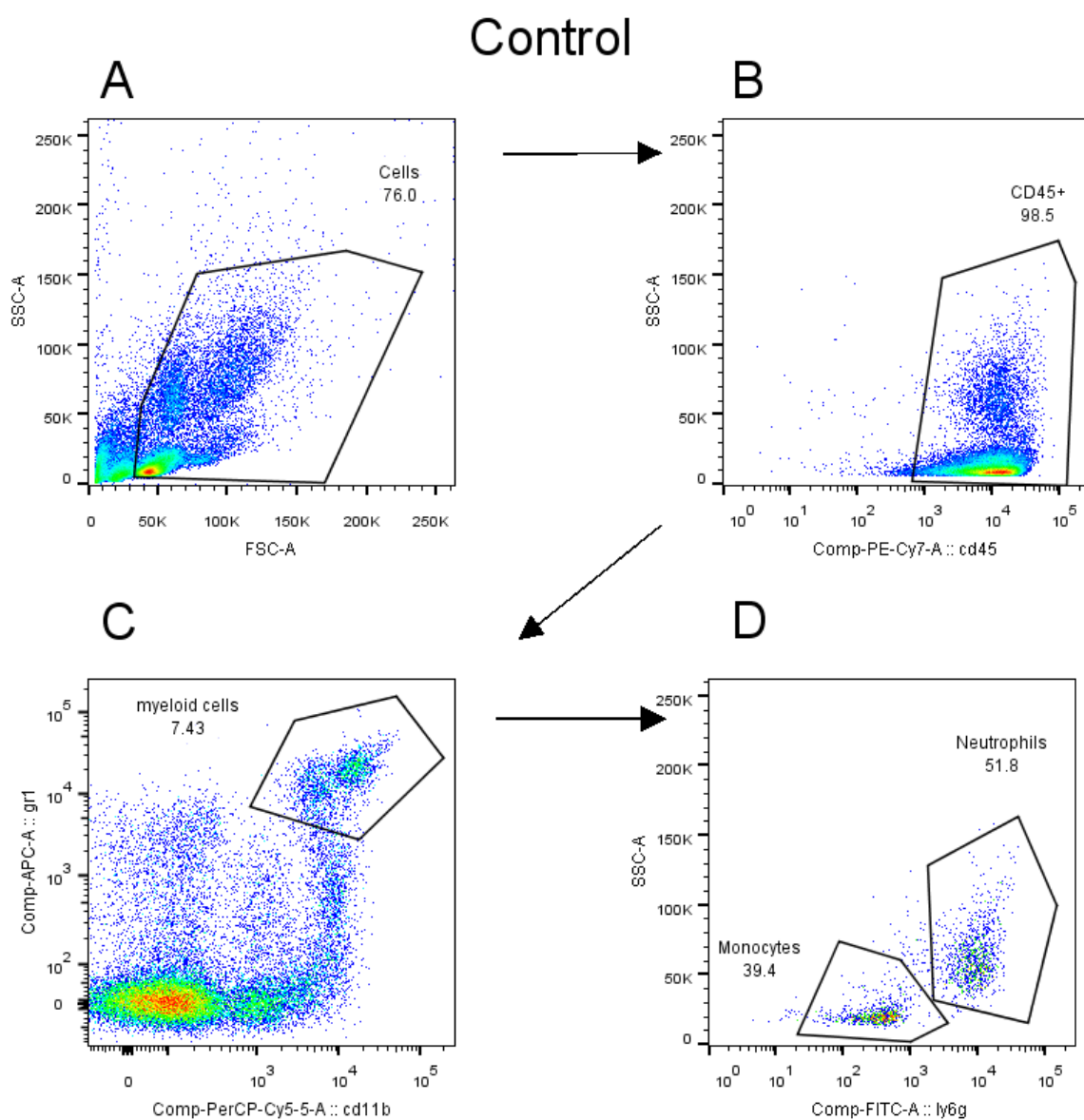


Figure 8.3.1A: Myeloid cell populations in the lungs of control mice. Representative dot plots from the lungs of control mice (A) Cells were identified with a gate that excluded very low side and forward scatter events. (B) Hematopoietic cells were identified as CD45⁺ cells. (C) Myeloid cells were identified as Gr1⁺ and CD11b⁺ cells. (D) Neutrophils were identified as Ly6G⁺ side scatter high cells and monocytes were identified as Ly6G⁻ side scatter low cells. Myeloid, neutrophil and monocyte levels were calculated as the frequency of CD45⁺ cells.

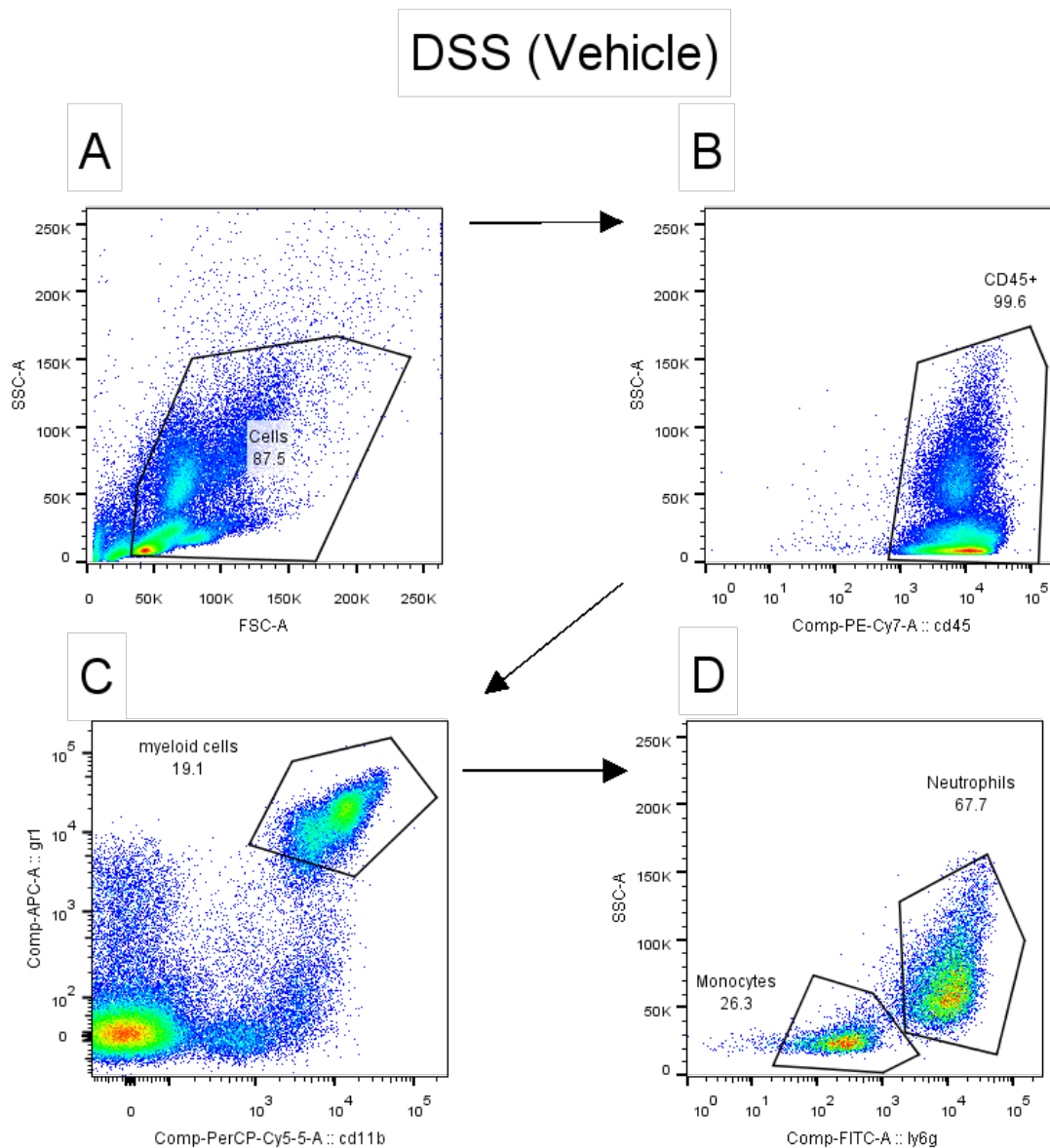


Figure 8.3.1B: Myeloid cell populations in the lungs of vehicle treated DSS colitis mice.

Representative dot plots from the lungs of vehicle treated DSS colitis mice. (A) Cells were identified with a gate that excluded very low side and forward scatter events. (B) Hematopoietic cells were identified as CD45⁺ cells. (C) Myeloid cells were identified as Gr1⁺ and CD11b⁺ cells. (D) Neutrophils were identified as Ly6G⁺ side scatter high cells and monocytes were identified as Ly6G⁻ side scatter low cells. Myeloid, neutrophil and monocyte levels were calculated as the frequency of CD45⁺ cells.

DSS (I.N. CV-6209)

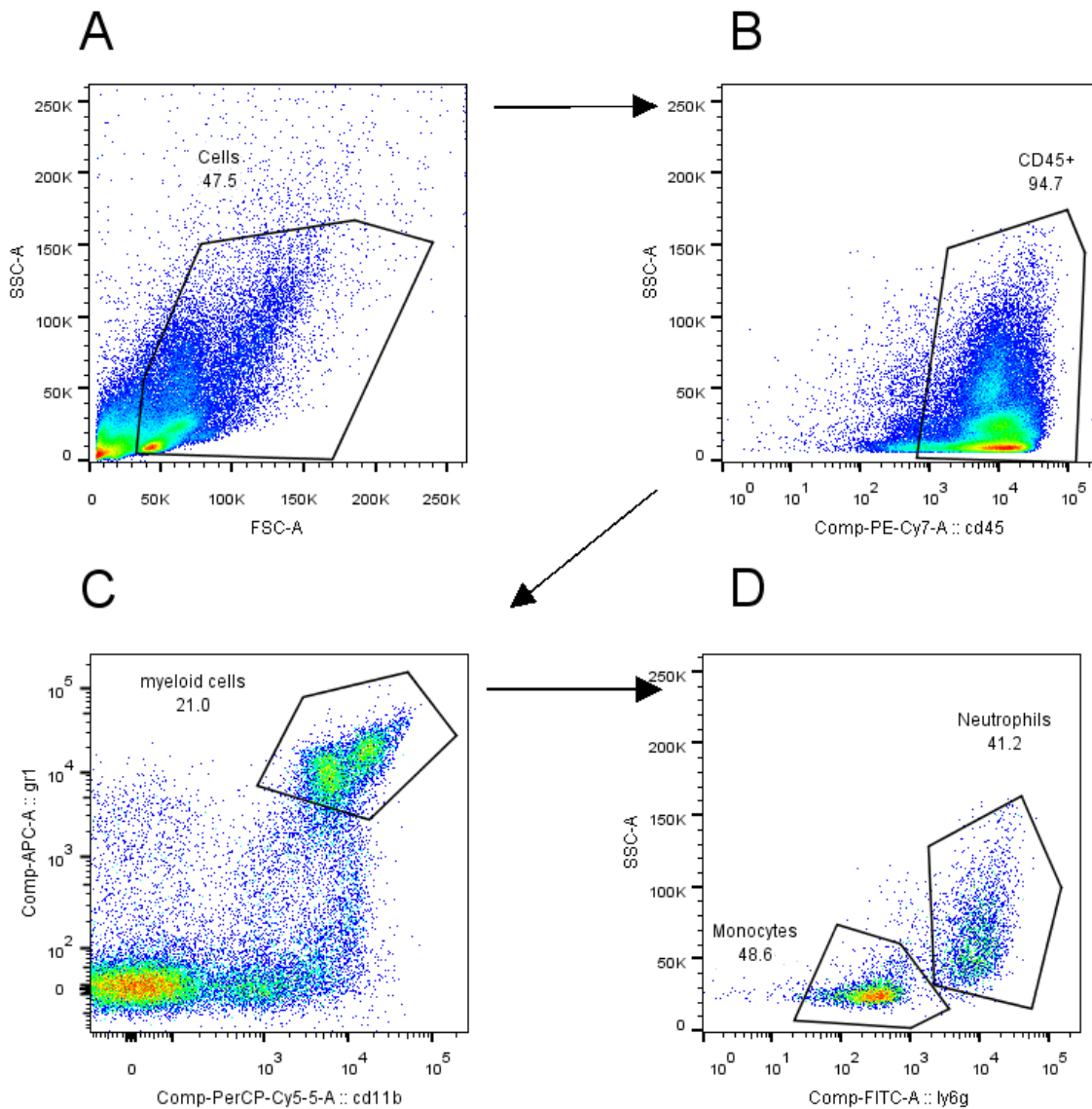


Figure 8.3.1C: Myeloid cell populations in the lungs of I.N. CV-6209 treated DSS colitis mice. Representative dot plots from the lungs of I.N. CV-6209 treated DSS colitis mice. (A) Cells were identified with a gate that excluded very low side and forward scatter events. (B) Hematopoietic cells were identified as CD45⁺ cells. (C) Myeloid cells were identified as Gr1⁺ and CD11b⁺ cells. (D) Neutrophils were identified as Ly6G⁺ side scatter high cells and monocytes were identified as Ly6G⁻ side scatter low cells. Myeloid, neutrophil and monocyte levels were calculated as the frequency of CD45⁺ cells.

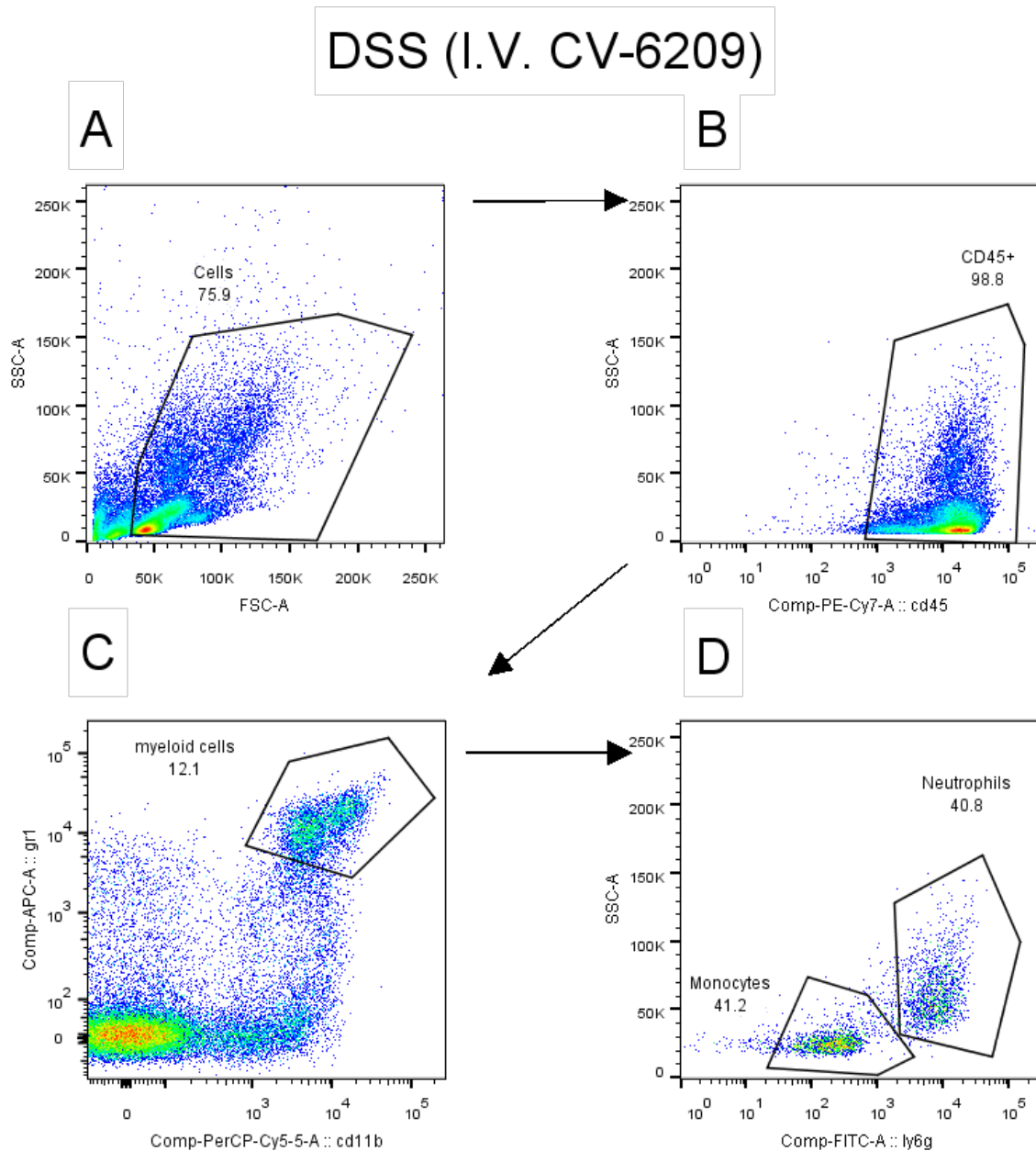


Figure 8.3.1D: Myeloid cell populations in the lungs of I.V. CV-6209 treated DSS colitis mice. Representative dot plots from the lungs of I.V. CV-6209 treated DSS colitis mice. (A) Cells were identified with a gate that excluded very low side and forward scatter events. (B) Hematopoietic cells were identified as CD45⁺ cells. (C) Myeloid cells were identified as Gr1⁺ and CD11b⁺ cells. (D) Neutrophils were identified as Ly6G⁺ side scatter high cells and monocytes were identified as Ly6G⁻ side scatter low cells. Myeloid, neutrophil and monocyte levels were calculated as the frequency of CD45⁺ cells.

8.3.2 Flow cytometry gating strategies for the quantification of myeloid cell populations in the circulatory system of CV-6209 treated DSS colitis mice.

Flow cytometry was utilized to quantify myeloid cell populations in the circulatory system of CV-6209 treated DSS colitis mice. The flow cytometry staining panel used in these experiments is described in Section 2.10. The gating strategies utilized in these experiments as well as representative dot plots from experimental groups are illustrated in Figure 8.3.2 A – D.

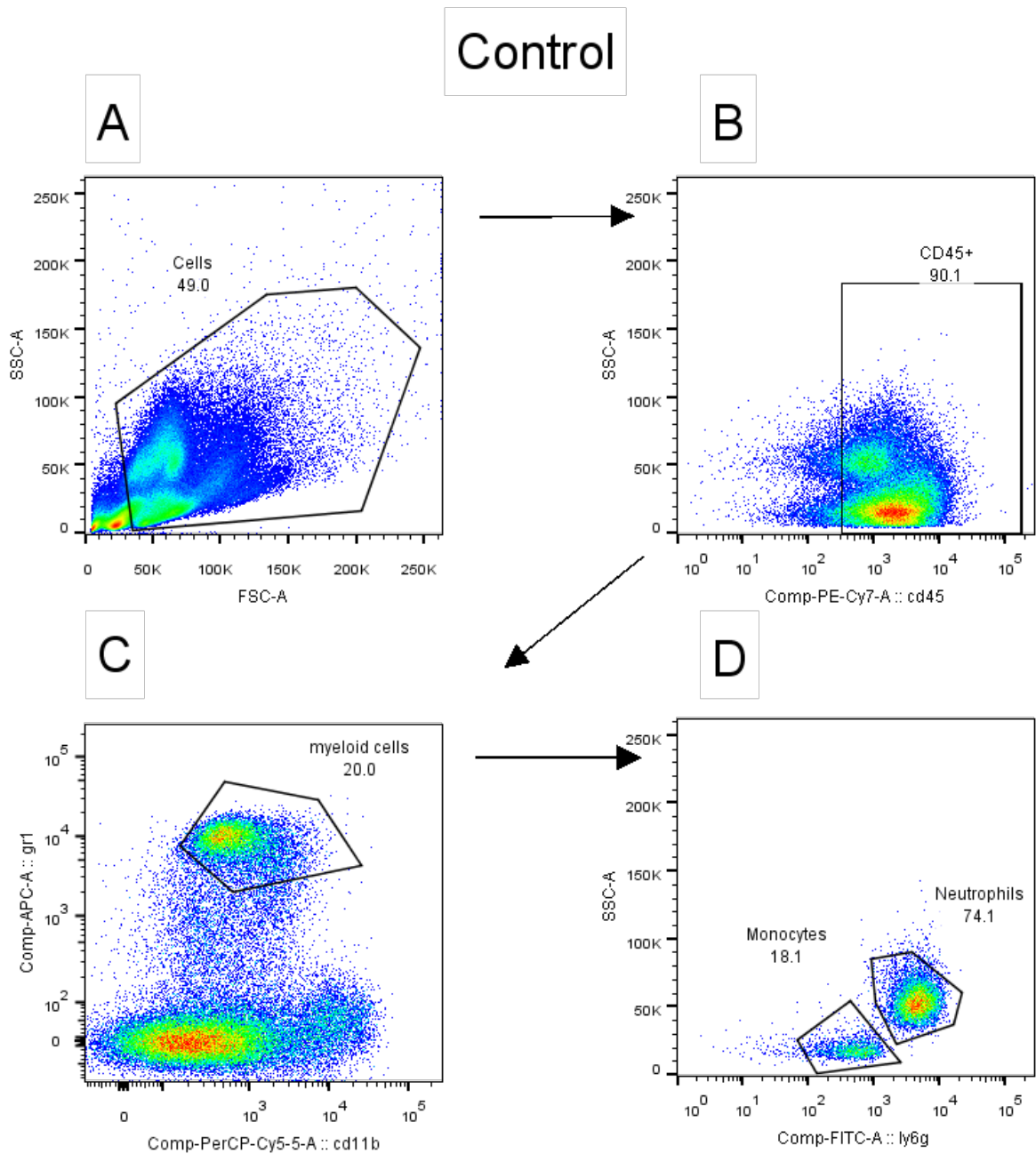


Figure 8.3.2A: Myeloid cell populations in the blood of control mice. Representative dot plots from the blood of control mice. (A) Cells were identified with a gate that excluded very low side and forward scatter events. (B) Hematopoietic cells were identified as CD45⁺ cells. (C) Myeloid cells were identified as Gr1⁺ and CD11b⁺ cells. (D) Neutrophils were identified as Ly6G⁺ side scatter high cells and monocytes were identified as Ly6G⁻ side scatter low cells. Myeloid, neutrophil and monocyte levels were calculated as the frequency of CD45⁺ cells.

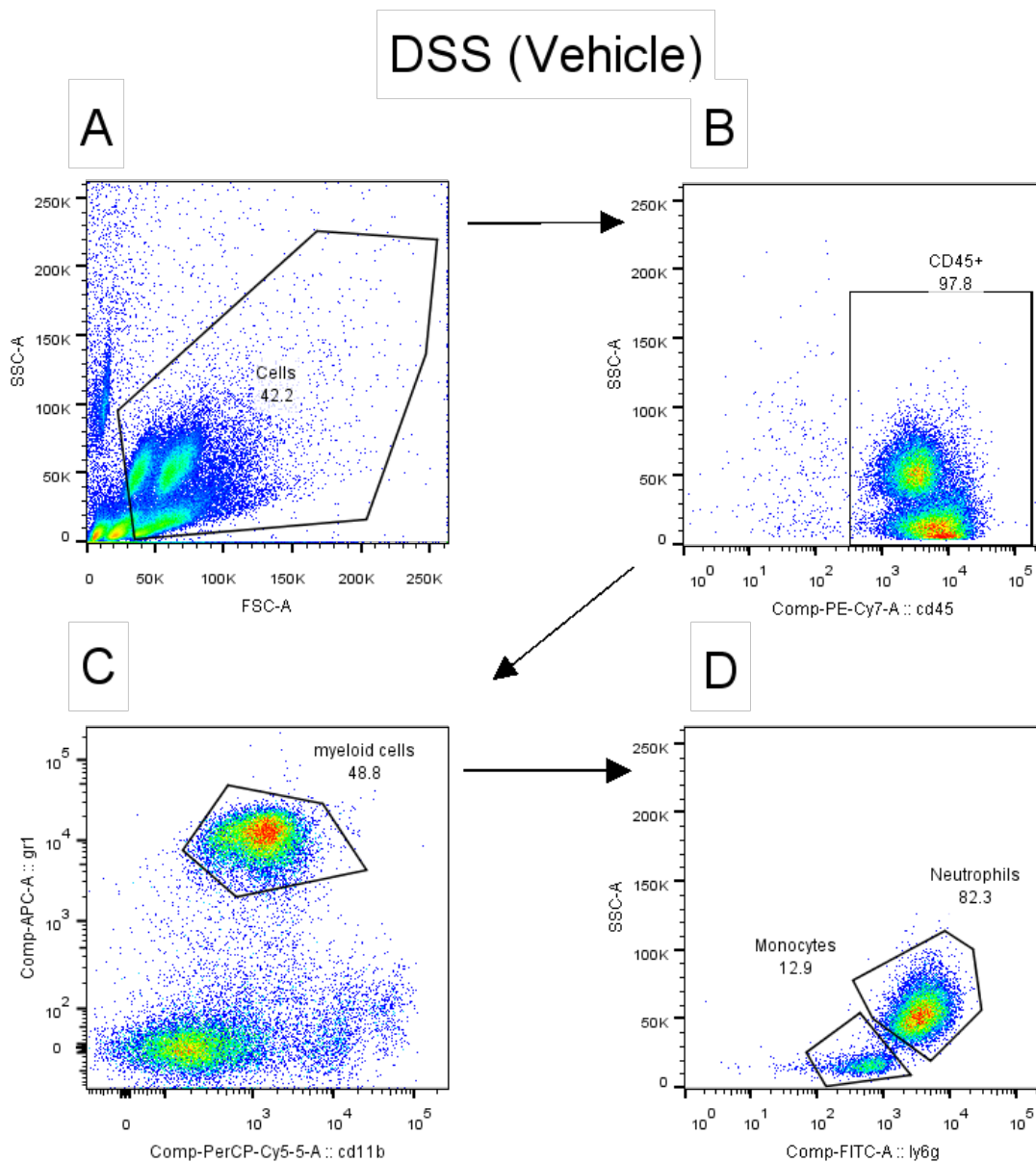


Figure 8.3.2B: Myeloid cell populations in the blood of vehicle treated DSS colitis mice.

Representative dot plots from the blood of vehicle treated DSS colitis mice. (A) Cells were identified with a gate that excluded very low side and forward scatter events. (B) Hematopoietic cells were identified as CD45⁺ cells. (C) Myeloid cells were identified as Gr1⁺ and CD11b⁺ cells. (D) Neutrophils were identified as Ly6G⁺ side scatter high cells and monocytes were identified as Ly6G⁻ side scatter low cells. Myeloid, neutrophil and monocyte levels were calculated as the frequency of CD45⁺ cells.

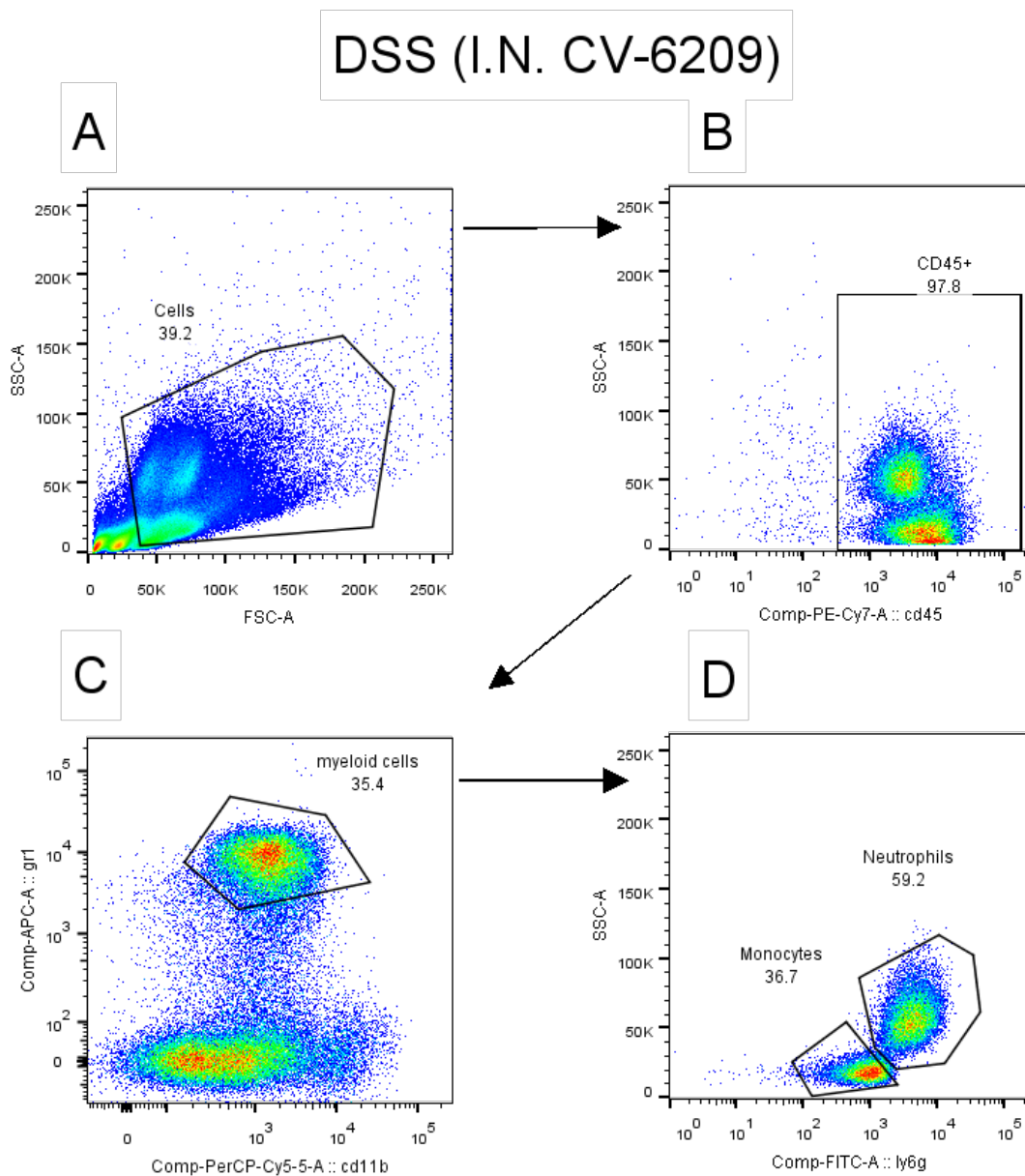


Figure 8.3.2C: Myeloid cell populations in the blood I.N. CV-6209 treated DSS colitis mice. Representative dot plots from the blood of I.N. CV-6209 treated DSS colitis mice. (A) Cells were identified with a gate that excluded very low side and forward scatter events. (B) Hematopoietic cells were identified as CD45⁺ cells. (C) Myeloid cells were identified as Gr1⁺ and CD11b⁺ cells. (D) Neutrophils were identified as Ly6G⁺ side scatter high cells and monocytes were identified as Ly6G⁻ side scatter low cells. Myeloid, neutrophil and monocyte levels were calculated as the frequency of CD45⁺ cells.

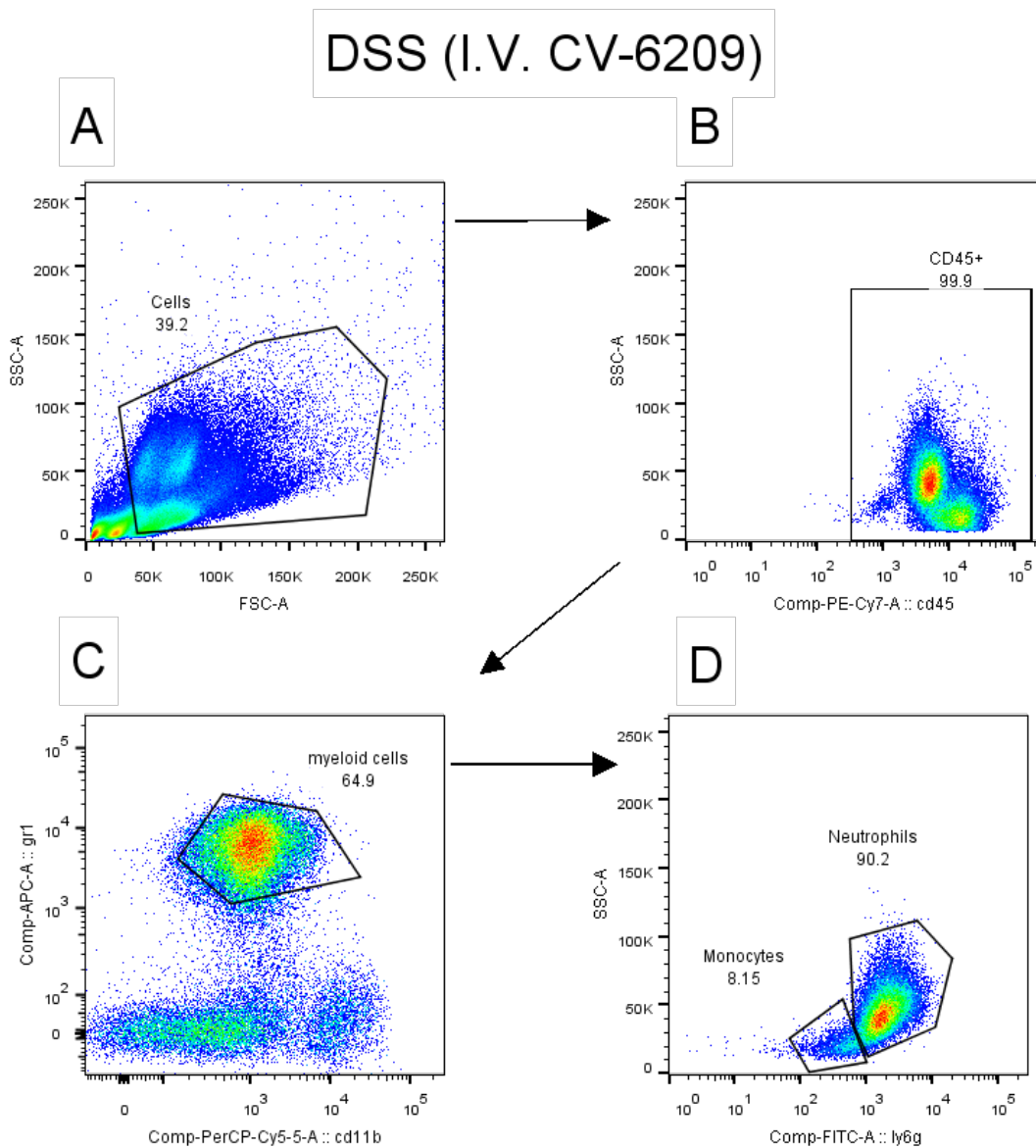
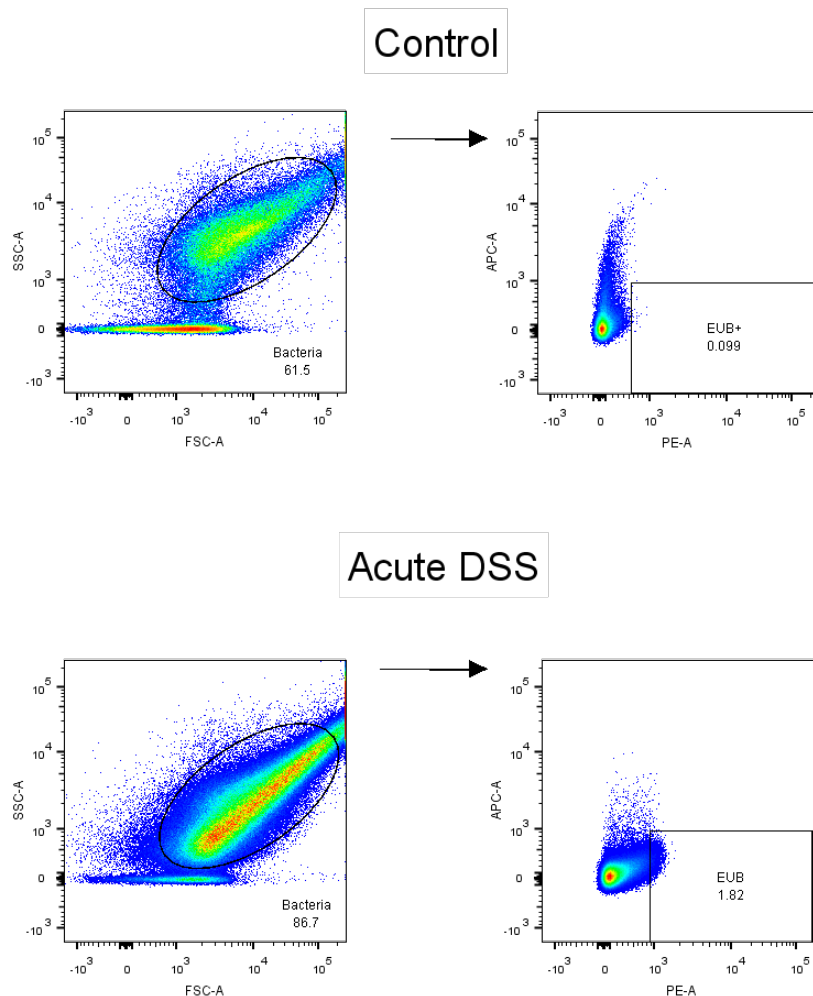


Figure 8.3.2D: Myeloid cell populations in the blood of I.V. CV-6209 treated DSS colitis mice. Representative dot plots from the blood of I.V. CV-6209 treated DSS colitis mice. (A) Cells were identified with a gate that excluded very low side and forward scatter events. (B) Hematopoietic cells were identified as CD45⁺ cells. (C) Myeloid cells were identified as Gr1⁺ and CD11b⁺ cells. (D) Neutrophils were identified as Ly6G⁺ side scatter high cells and monocytes were identified as Ly6G⁻ side scatter low cells. Myeloid, neutrophil and monocyte levels were calculated as the frequency of CD45⁺ cells.

8.4 Quantification of bacterial load in the lungs of DSS colitis mice.

Bacterial load in the lung of acute DSS colitis mice was quantified by FISH-FLOW. FISH FLOW methodology is described in section 6.2.6 and the gating strategy utilized to quantify bacteria is illustrated in Figure 8.4.



8.4 Gating strategy utilized for the quantification of bacterial load by FISH-FLOW.

Representative dot plots illustrating the gating strategy utilized to quantify bacteria by FISH-FLOW. Bacteria were gated as a medium side scatter and medium forward scatter population. EUB is the PE-conjugated oligonucleotide that is complementary to 16s rDNA. EUB⁺ positive bacteria were gated and geometric mean fluorescent intensity of EUB staining was quantified.

8.5 PAFR mediated neutrophil activation via CCL2 stimulated macrophages.

The ability of CCL2 stimulated macrophages to activate neutrophils was investigated in Section 6.3.5. It was found that the secretory factors released by CCL2 stimulated macrophages did not induce neutrophil activation. Neutrophil activation status was determined by CD11b expression and superoxide production. CD11b expression was quantified from the mean fluorescent intensity of anti-CD11b PerCP-Cy5.5 conjugated antibody staining. Superoxide production was quantified by the mean fluorescent intensity of dihydroethidium staining. Fluorescence from dihydroethidium staining was collected in the PE channel. The gating strategies utilized that identify these populations as well as representative dot plots from experiments groups are shown in figure 8.5A – D.

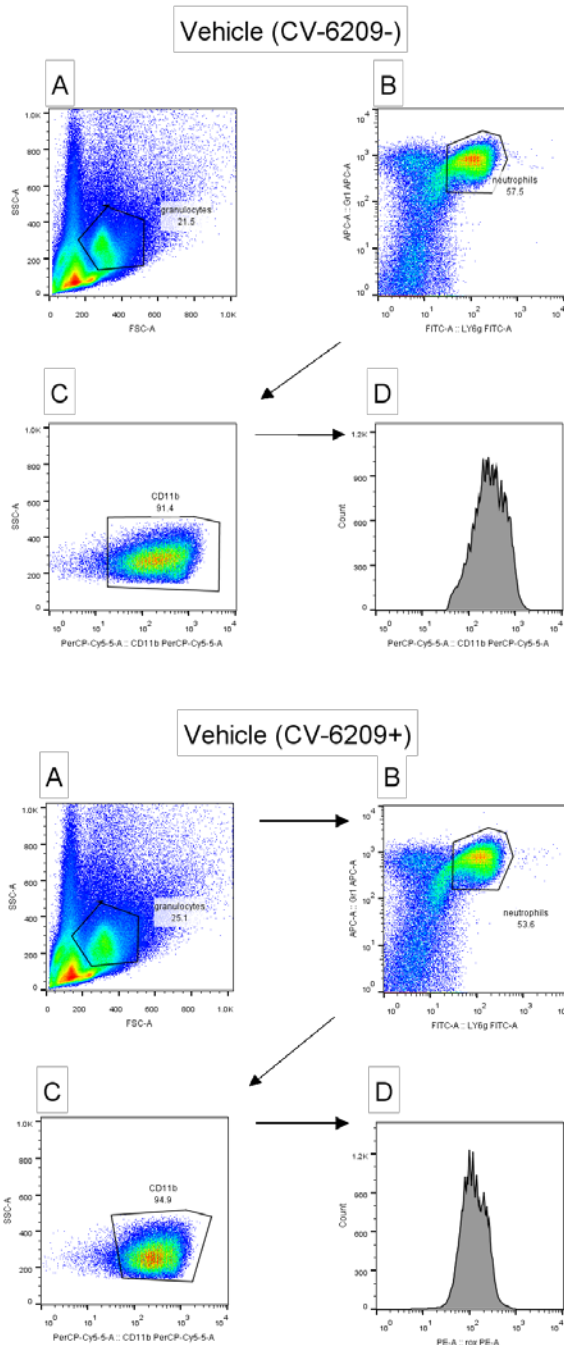


Figure 8.5A: CD11b expression on neutrophils incubated with supernatants from vehicle stimulated macrophages in the presence and absence of CV-6209. (A) Granulocytes were identified as a side scatter high forward scatter medium cell population. (B) Neutrophils were identified as Gr¹⁺ Ly6G⁺ cell population. (C) Geometric mean fluorescent intensity was calculated from the intensity of CD11b staining on neutrophils. (D) Histogram illustrating the intensity of CD11b staining on neutrophils.

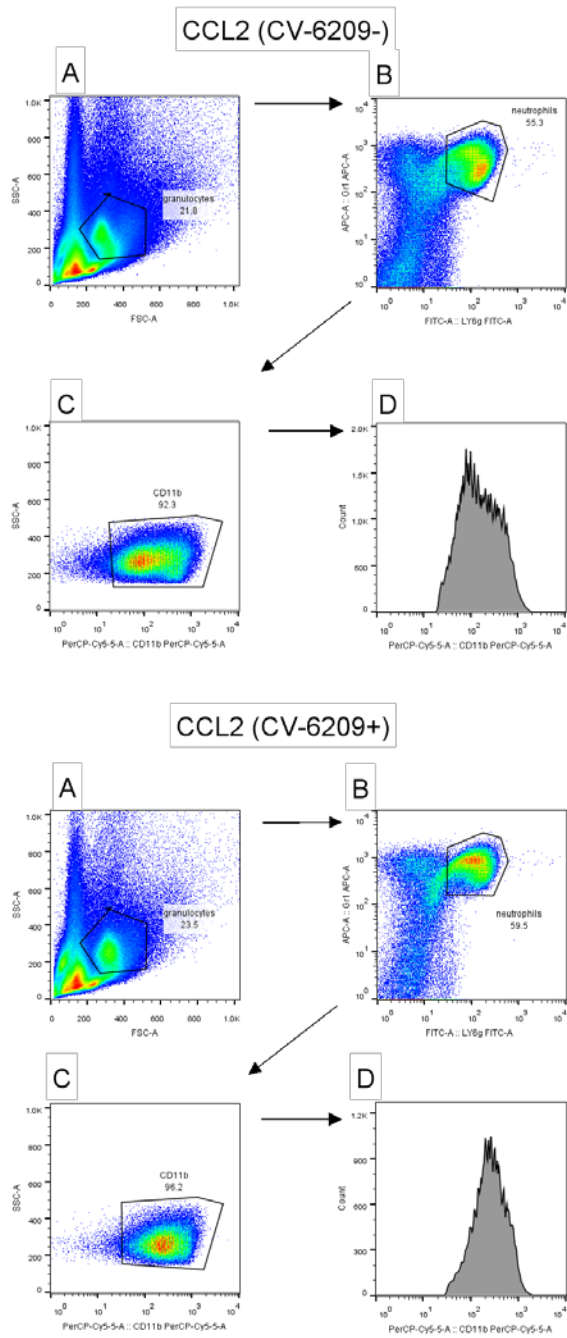


Figure 8.5B: CD11b expression on neutrophils incubated with supernatants from CCL2 stimulated macrophages in the presence and absence of CV-6209. (A) Granulocytes were identified as a side scatter high forward scatter medium cell population. (B) Neutrophils were identified as Gr1⁺ Ly6G⁺ cell population. (C) Geometric mean fluorescent intensity was calculated from the intensity of CD11b staining on neutrophils. (D) Histogram illustrating the intensity of CD11b staining on neutrophils.

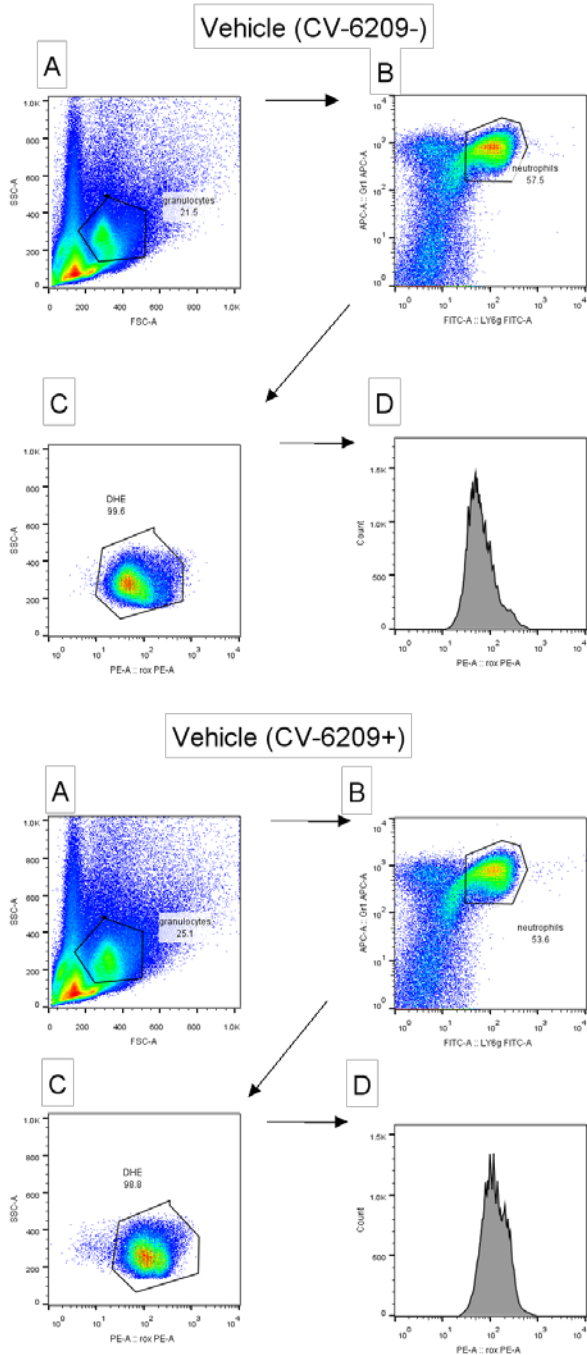


Figure 8.5C: Superoxide levels in neutrophils incubated with supernatants from vehicle stimulated macrophages in the presence and absence of CV-6209. (A) Granulocytes were identified as a side scatter high forward scatter medium cell population. (B) Neutrophils were identified as Gr1⁺ Ly6G⁺ cell population. (C) The level dihydroethidium staining was collected in the PE channel and the geometric mean fluorescent intensity of this calculated. (D) Histogram illustrating the intensity of dihydroethidium staining on neutrophils.

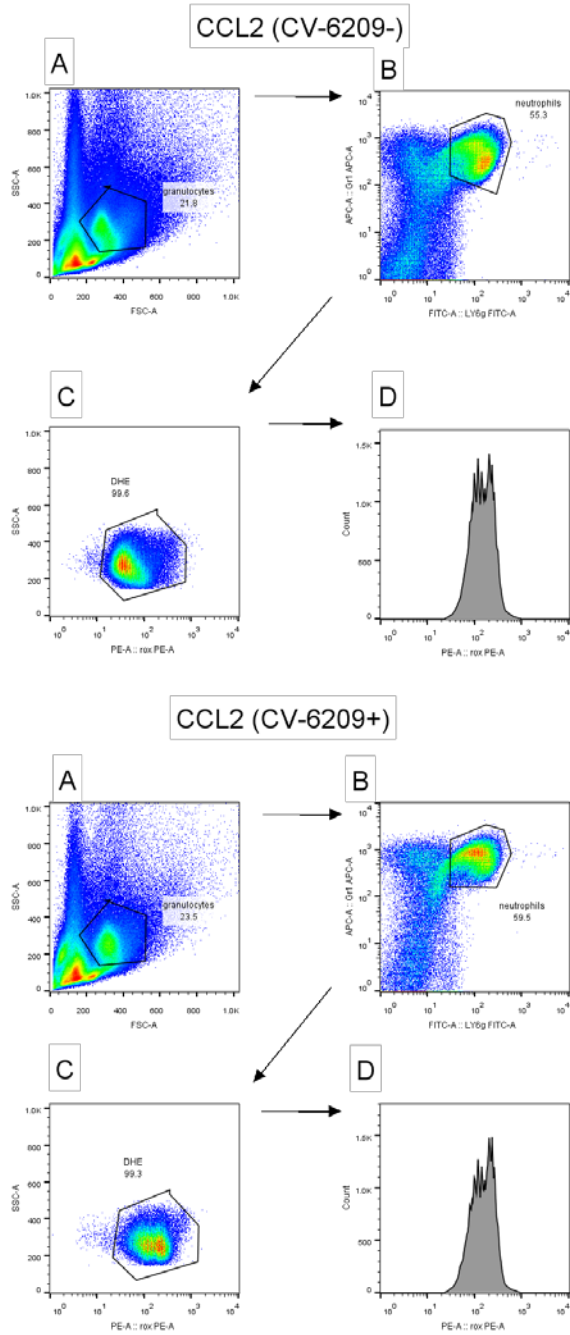


Figure 8.5D: Superoxide levels in neutrophils incubated with supernatants from vehicle stimulated macrophages in the presence and absence of CV-6209. (A) Granulocytes were identified as a side scatter high forward scatter medium cell population. (B) Neutrophils were identified as Gr1⁺ Ly6G⁺ cell population. (C) The level dihydroethidium staining was collected in the PE channel and the geometric mean fluorescent intensity of this calculated. (D) Histogram illustrating the intensity of dihydroethidium staining on neutrophils.

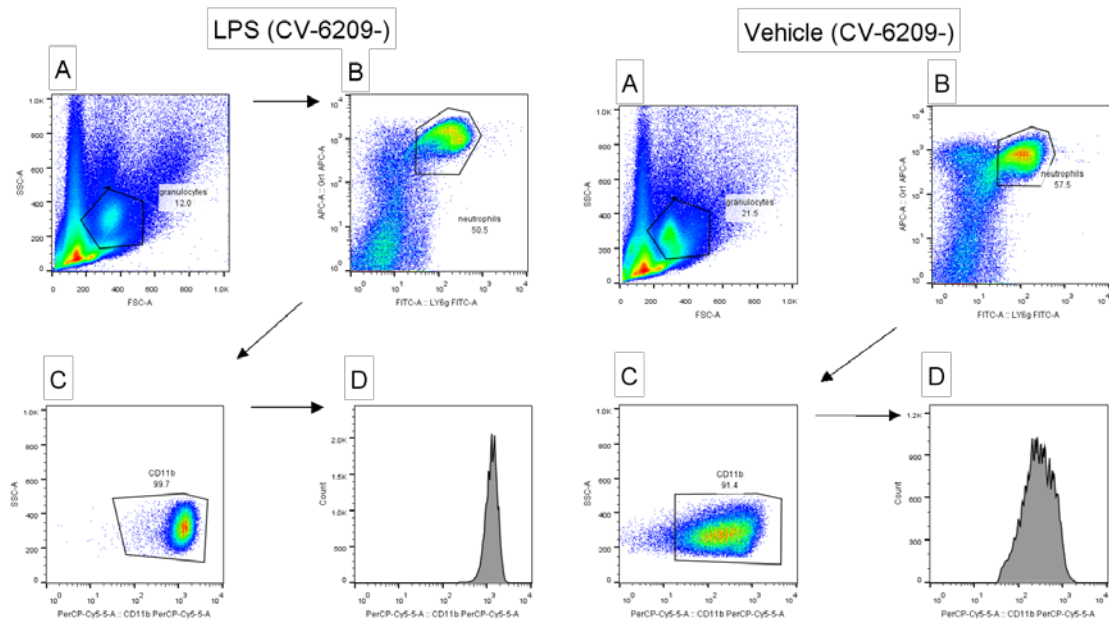


Figure 8.5E: CD11b expression on neutrophils treated directly with LPS in the absence of CV-6209. As a positive control for the experiments to determine neutrophil activation via CCL2 stimulated macrophage. Neutrophils were treated directly with LPS or the vehicle (PBS). (A) Granulocytes were identified as a side scatter high forward scatter medium cell population. (B) Neutrophils were identified as Gr1⁺ Ly6G⁺ cell population. (C) Geometric mean fluorescent intensity was calculated from the intensity of CD11b staining on neutrophils. (D) Histogram illustrating the intensity of CD11b staining on neutrophils. There is a significant increase in CD11b expression in LPS treated neutrophils, demonstrating that this assay is capable of identifying neutrophil activation.

9.0 Statement of originality

This thesis contains no material which has been accepted for the award of any degree or diploma in any university or other tertiary institution, and to the best of my knowledge and belief, contains, no material previously published or written by another person, except where due reference has been made in the text. I give consent to the final version of my thesis being made available worldwide when deposited in the University's Digital Repository **, subject to the provisions of the Copyright Act 1968.

**Unless an Embargo has been approved for a determined period

Sean William Mateer

June 2016

10.0 References

- Abraham, B. P. and J. H. Sellin (2012). "Disability in inflammatory bowel disease." Gastroenterol Clin North Am **41**(2): 429-441.
- Ajuebor, M. N., S. L. Kunkel and C. M. Hogaboam (2004). "The role of CCL3/macrophage inflammatory protein-1 α in experimental colitis." European Journal of Pharmacology **497**(3): 343-349.
- Anderson, C. A., G. Boucher, C. W. Lees, A. Franke, M. D'Amato, K. D. Taylor, J. C. Lee, P. Goyette, M. Imielinski, A. Latiano, C. Lagace, R. Scott, L. Amininejad, S. Bumpstead, L. Baidoo, R. N. Baldassano, M. Barclay, T. M. Bayless, S. Brand, C. Buning, J. F. Colombel, L. A. Denson, M. De Vos, M. Dubinsky, C. Edwards, D. Ellinghaus, R. S. Fehrmann, J. A. Floyd, T. Florin, D. Franchimont, L. Franke, M. Georges, J. Glas, N. L. Glazer, S. L. Guthery, T. Haritunians, N. K. Hayward, J. P. Hugot, G. Jobin, D. Laukens, I. Lawrance, M. Lemann, A. Levine, C. Libioulle, E. Louis, D. P. McGovern, M. Milla, G. W. Montgomery, K. I. Morley, C. Mowat, A. Ng, W. Newman, R. A. Ophoff, L. Papi, O. Palmieri, L. Peyrin-Biroulet, J. Panes, A. Phillips, N. J. Prescott, D. D. Proctor, R. Roberts, R. Russell, P. Rutgeerts, J. Sanderson, M. Sans, P. Schumm, F. Seibold, Y. Sharma, L. A. Simms, M. Seielstad, A. H. Steinhardt, S. R. Targan, L. H. van den Berg, M. Vatn, H. Verspaget, T. Walters, C. Wijmenga, D. C. Wilson, H. J. Westra, R. J. Xavier, Z. Z. Zhao, C. Y. Ponsioen, V. Andersen, L. Torkvist, M. Gazouli, N. P. Anagnou, T. H. Karlsen, L. Kupcinkas, J. Sventoraityte, J. C. Mansfield, S. Kugathasan, M. S. Silverberg, J. Halfvarson, J. I. Rotter, C. G. Mathew, A. M. Griffiths, R. Gearry, T. Ahmad, S. R. Brant, M. Chamailard, J. Satsangi, J. H. Cho, S. Schreiber, M. J. Daly, J. C. Barrett, M. Parkes, V. Annese, H. Hakonarson, G. Radford-Smith, R. H. Duerr, S. Vermeire, R. K. Weersma and J. D. Rioux (2011). "Meta-analysis identifies 29 additional ulcerative colitis risk loci, increasing the number of confirmed associations to 47." Nat Genet **43**(3): 246-252.
- Antoni, L., S. Nuding, J. Wehkamp and E. F. Stange (2014). "Intestinal barrier in inflammatory bowel disease." World Journal of Gastroenterology: WJG **20**(5): 1165-1179.
- Ardizzone, S., P. S. Puttini, A. Cassinotti and G. B. Porro (2008). "Extraintestinal manifestations of inflammatory bowel disease." Digestive and Liver Disease **40**: S253-S259.
- Arvikar, S. L. and M. C. Fisher (2011). "Inflammatory bowel disease associated arthropathy." Current Reviews in Musculoskeletal Medicine **4**(3): 123-131.
- Asensi, V., E. Valle, A. Meana, J. Fierer, A. Celada, V. Alvarez, J. Paz, E. Coto, J. A. Carton, J. A. Maradona, A. Dieguez, J. Sarasua, M. G. Ocana and J. M. Arribas (2004). "In vivo interleukin-6 protects neutrophils from apoptosis in osteomyelitis." Infect Immun **72**(7): 3823-3828.
- Ates, F., M. Karıncaoglu, S. S. Hacıevliyagil, M. Yalniz and Y. Seckin (2011). "Alterations in the pulmonary function tests of inflammatory bowel diseases." Turk J Gastroenterol **22**(3): 293-299.
- Autschbach, F., S. Eisold, U. Hinz, S. Zinser, M. Linnebacher, T. Giese, T. Loffler, M. W. Buchler and J. Schmidt (2005). "High prevalence of Mycobacterium avium subspecies paratuberculosis IS900 DNA in gut tissues from individuals with Crohn's disease." Gut **54**(7): 944-949.
- Awaya, H., Y. Takeshima, M. Yamasaki and K. Inai (2004). "Expression of MUC1, MUC2, MUC5AC, and MUC6 in atypical adenomatous hyperplasia, bronchioloalveolar carcinoma, adenocarcinoma with mixed subtypes, and mucinous bronchioloalveolar carcinoma of the lung." Am J Clin Pathol **121**(5): 644-653.
- Bailey, S. R., M. H. Nelson, R. A. Himes, Z. Li, S. Mehrotra and C. M. Paulos (2014). "Th17 cells in cancer: the ultimate identity crisis." Frontiers in Immunology **5**.
- Balamayooran, G., S. Batra, T. Balamayooran, S. Cai and S. Jeyaseelan (2011). "Monocyte chemoattractant protein 1 regulates pulmonary host defense via neutrophil recruitment during Escherichia coli infection." Infect Immun **79**(7): 2567-2577.
- Balestra, D. J., S. T. Balestra and J. H. Wasson (1988). "Ulcerative colitis and steroid-responsive, diffuse interstitial lung disease. A trial of N = 1." JAMA **260**(1): 62-64.

Barden, A., D. Graham, L. J. Beilin, J. Ritchie, R. Baker, B. N. Walters and C. A. Michael (1997). "Neutrophil CD11B expression and neutrophil activation in pre-eclampsia." Clin Sci (Lond) **92**(1): 37-44.

Barnes, T. C., M. E. Anderson and R. J. Moots (2011). "The many faces of interleukin-6: the role of IL-6 in inflammation, vasculopathy, and fibrosis in systemic sclerosis." Int J Rheumatol **2011**: 721608.

Barnich, N., T. Hisamatsu, J. E. Aguirre, R. Xavier, H. C. Reinecker and D. K. Podolsky (2005). "GRIM-19 interacts with nucleotide oligomerization domain 2 and serves as downstream effector of anti-bacterial function in intestinal epithelial cells." J Biol Chem **280**(19): 19021-19026.

Barreiro-de-Acosta, M., A. Lorenzo and J. E. Dominguez-Munoz (2012). "Efficacy of adalimumab for the treatment of extraintestinal manifestations of Crohn's disease." Rev Esp Enferm Dig **104**(9): 468-472.

Baumgart, D. C. and S. R. Carding (2007). "Inflammatory bowel disease: cause and immunobiology." Lancet **369**(9573): 1627-1640.

Berencsi, K., P. Rani, T. Zhang, L. Gross, M. Mastrangelo, N. J. Meropol, D. Herlyn and R. Somasundaram (2011). "In vitro migration of cytotoxic T lymphocyte derived from a colon carcinoma patient is dependent on CCL2 and CCR2." Journal of Translational Medicine **9**: 33-33.

Biffi, W. L., E. E. Moore, F. A. Moore, C. C. Barnett, Jr., C. C. Silliman and V. M. Peterson (1996). "Interleukin-6 stimulates neutrophil production of platelet-activating factor." J Leukoc Biol **59**(4): 569-574.

Black, H., M. Mendoza and S. Murin (2007). "Thoracic Manifestations of Inflammatory Bowel Disease." Chest **131**(2): 524-532.

Bonniere, P., B. Wallaert, A. Cortot, X. Marchandise, Y. Riou, A. B. Tonnel, J. F. Colombel, C. Voisin and J. C. Paris (1986). "Latent pulmonary involvement in Crohn's disease: biological, functional, bronchoalveolar lavage and scintigraphic studies." Gut **27**(8): 919-925.

Borish, L., R. Rosenbaum, L. Albury and S. Clark (1989). "Activation of neutrophils by recombinant interleukin 6." Cell Immunol **121**(2): 280-289.

Borthakur, A., S. Bhattacharyya, W. A. Alrefai, J. K. Tobacman, K. Ramaswamy and P. K. Dudeja (2010). "Platelet-activating factor-induced NF-kappaB activation and IL-8 production in intestinal epithelial cells are Bcl10-dependent." Inflamm Bowel Dis **16**(4): 593-603.

Broome, U. and A. Bergquist (2006). "Primary sclerosing cholangitis, inflammatory bowel disease, and colon cancer." Semin Liver Dis **26**(1): 31-41.

Budden, K. F., S. L. Gellatly, D. L. A. Wood, M. A. Cooper, M. Morrison, P. Hugenholtz and P. M. Hansbro (2017). "Emerging pathogenic links between microbiota and the gut-lung axis." Nat Rev Micro **15**(1): 55-63.

Bulger, E. M., S. Arbabi, I. Garcia and R. V. Maier (2002). "The macrophage response to endotoxin requires platelet activating factor." Shock **17**(3): 173-179.

Calkins, C. M., D. D. Bensard, B. D. Shames, E. J. Pulido, E. Abraham, N. Fernandez, X. Meng, C. A. Dinarello and R. C. McIntyre, Jr. (2002). "IL-1 regulates in vivo C-X-C chemokine induction and neutrophil sequestration following endotoxemia." J Endotoxin Res **8**(1): 59-67.

Camus, P., F. Piard, T. Ashcroft, A. A. Gal and T. V. Colby (1993). "The lung in inflammatory bowel disease." Medicine (Baltimore) **72**(3): 151-183.

Chandran, P., S. Satthaporn, A. Robins and O. Eremin (2003). "Inflammatory bowel disease: dysfunction of GALT and gut bacterial flora (II)." Surgeon **1**(3): 125-136.

Chang, S. W. (1994). "TNF potentiates PAF-induced pulmonary vasoconstriction in the rat: role of neutrophils and thromboxane A2." J Appl Physiol (1985) **77**(6): 2817-2826.

Chen, J., T. Lan, W. Zhang, L. Dong, N. Kang, S. Zhang, M. Fu, B. Liu, K. Liu and Q. Zhan (2015). "Feed-Forward Reciprocal Activation of PAFR and STAT3 Regulates Epithelial-Mesenchymal Transition in Non-Small Cell Lung Cancer." Cancer Res **75**(19): 4198-4210.

Chen, J., V. Ziboh and S. N. Giri (1997). "Up-regulation of platelet-activating factor receptors in lung and alveolar macrophages in the bleomycin-hamster model of pulmonary fibrosis." J Pharmacol Exp Ther **280**(3): 1219-1227.

Cho, J. H. (2008). "The genetics and immunopathogenesis of inflammatory bowel disease." Nat Rev Immunol **8**(6): 458-466.

Cho, J. H. and S. R. Brant (2011). "Recent insights into the genetics of inflammatory bowel disease." Gastroenterology **140**(6): 1704-1712.

Choi, J.-H., E. K. Choi, S. J. Park, H.-M. Ko, K.-J. Kim, S.-J. Han, I.-W. Choi and S.-Y. Im (2007). "Impairment of p38 MAPK-mediated cytosolic phospholipase A(2) activation in the kidneys is associated with pathogenicity of *Candida albicans*." Immunology **120**(2): 173-181.

Chou, D. B., B. Sworder, N. Bouladoux, C. N. Roy, A. M. Uchida, M. Grigg, P. G. Robey and Y. Belkaid (2012). "Stromal-derived IL-6 alters the balance of myeloerythroid progenitors during *Toxoplasma gondii* infection." J Leukoc Biol **92**(1): 123-131.

Ciccacci, C., L. Biancone, D. Di Fusco, M. Ranieri, G. Condino, E. Giardina, S. Onali, T. Lepre, F. Pallone, G. Novelli and P. Borgiani (2012). "TRAF3IP2 gene is associated with cutaneous extraintestinal manifestations in Inflammatory Bowel Disease." Journal of Crohn's and Colitis.

Ciccacci, C., L. Biancone, D. Di Fusco, M. Ranieri, G. Condino, E. Giardina, S. Onali, T. Lepre, F. Pallone, G. Novelli and P. Borgiani (2013). "TRAF3IP2 gene is associated with cutaneous extraintestinal manifestations in inflammatory bowel disease." J Crohns Colitis **7**(1): 44-52.

Clark, E., C. Hoare, J. Tanianis-Hughes, G. L. Carlson and G. Warhurst (2005). "Interferon γ Induces Translocation of Commensal *Escherichia coli* Across Gut Epithelial Cells via a Lipid Raft--Mediated Process." Gastroenterology **128**(5): 1258-1267.

Coccia, M., O. J. Harrison, C. Schiering, M. J. Asquith, B. Becher, F. Powrie and K. J. Maloy (2012). "IL-1 β mediates chronic intestinal inflammation by promoting the accumulation of IL-17A secreting innate lymphoid cells and CD4(+) Th17 cells." J Exp Med **209**(9): 1595-1609.

Corfield, A. P., H. M. Wallace and C. S. Probert (2011). "The molecular biology of inflammatory bowel diseases." Biochem Soc Trans **39**(4): 1057-1060.

Danese, S. (2005). "Chemokines in inflammatory bowel disease." Journal of Clinical Pathology **58**(10): 1025-1027.

Danese, S., S. Semeraro, A. Papa, I. Roberto, F. Scalfaferrri, G. Fedeli, G. Gasbarrini and A. Gasbarrini (2005). "Extraintestinal manifestations in inflammatory bowel disease." World J Gastroenterol **11**(46): 7227-7236.

de Souza, H. S. P. and C. Focchi (2016). "Immunopathogenesis of IBD: current state of the art." Nat Rev Gastroenterol Hepatol **13**(1): 13-27.

De Vos, M. (2009). "Joint Involvement Associated with Inflammatory Bowel Disease." Digestive Diseases **27**(4): 511-515.

Dente, F. L., M. Bilotta, M. L. Bartoli, E. Bacci, S. Cianchetti, M. Latorre, Malagrini, #xf2, L. , D. Nieri, M. A. Roggi, B. Vagaggini and P. Paggiaro (2015). "Neutrophilic Bronchial Inflammation Correlates with Clinical and Functional Findings in Patients with Noncystic Fibrosis Bronchiectasis." Mediators of Inflammation **2015**: 6.

Desai, D., S. Patil, Z. Udawadia, S. Maheshwari, P. Abraham and A. Joshi (2011). "Pulmonary manifestations in inflammatory bowel disease: a prospective study." Indian J Gastroenterol **30**(5): 225-228.

Deshmane, S. L., S. Kremlev, S. Amini and B. E. Sawaya (2009). "Monocyte Chemoattractant Protein-1 (MCP-1): An Overview." Journal of Interferon & Cytokine Research **29**(6): 313-326.

Dierkes-Globisch, A. and H. Mohr (2002). "Pulmonary function abnormalities in respiratory asymptomatic patients with inflammatory bowel disease." Eur J Intern Med **13**(6): 385.

Eade, O. E., C. L. Smith, J. R. Alexander and P. J. Whorwell (1980). "Pulmonary function in patients with inflammatory bowel disease." Am J Gastroenterol **73**(2): 154-156.

Eastaff-Leung, N., N. Mabarrack, A. Barbour, A. Cummins and S. Barry (2010). "Foxp3+ regulatory T cells, Th17 effector cells, and cytokine environment in inflammatory bowel disease." J Clin Immunol **30**(1): 80-89.

Economou, M., T. A. Trikalinos, K. T. Loizou, E. V. Tsianos and J. P. Ioannidis (2004). "Differential effects of NOD2 variants on Crohn's disease risk and phenotype in diverse populations: a metaanalysis." *Am J Gastroenterol* **99**(12): 2393-2404.

Edwards, L. J. and C. S. Constantinescu (2009). "Platelet activating factor/platelet activating factor receptor pathway as a potential therapeutic target in autoimmune diseases." *Inflamm Allergy Drug Targets* **8**(3): 182-190.

Egea, L., R. Gimenez, D. Lucia, I. Modolell, J. Badia, L. Baldoma and J. Aguilar (2008). "Increased production of the ether-lipid platelet-activating factor in intestinal epithelial cells infected by *Salmonella enteritidis*." *Biochim Biophys Acta* **1781**(5): 270-276.

Eller, J., J. R. Lapa e Silva, L. W. Poulter, H. Lode and P. J. Cole (1994). "Cells and cytokines in chronic bronchial infection." *Ann N Y Acad Sci* **725**: 331-345.

Eri, R. D., R. J. Adams, T. V. Tran, H. Tong, I. Das, D. K. Roche, I. Oancea, C. W. Png, P. L. Jeffery, G. L. Radford-Smith, M. C. Cook, T. H. Florin and M. A. McGuckin (2011). "An intestinal epithelial defect conferring ER stress results in inflammation involving both innate and adaptive immunity." *Mucosal Immunol* **4**(3): 354-364.

Farrell, K. E., R. J. Callister and S. Keely (2014). "Understanding and targeting centrally mediated visceral pain in inflammatory bowel disease." *Frontiers in Pharmacology* **5**: 27.

Forbes, E., V. E. Smart, A. D'Aprile, P. Henry, M. Yang, K. I. Matthaei, M. E. Rothenberg, P. S. Foster and S. P. Hogan (2004). "T helper-2 immunity regulates bronchial hyperresponsiveness in eosinophil-associated gastrointestinal disease in mice." *Gastroenterology* **127**(1): 105-118.

Fournier, M., F. Lebargy, F. Le Roy Ladurie, E. Lenormand and R. Pariente (1989). "Intraepithelial T-lymphocyte subsets in the airways of normal subjects and of patients with chronic bronchitis." *Am Rev Respir Dis* **140**(3): 737-742.

Franke, A., D. P. B. McGovern, J. C. Barrett, K. Wang, G. L. Radford-Smith, T. Ahmad, C. W. Lees, T. Balschun, J. Lee, R. Roberts, C. A. Anderson, J. C. Bis, S. Bumpstead, D. Ellinghaus, E. M. Festen, M. Georges, T. Green, T. Haritunians, L. Jostins, A. Latiano, C. G. Mathew, G. W. Montgomery, N. J. Prescott, S. Raychaudhuri, J. I. Rotter, P. Schumm, Y. Sharma, L. A. Simms, K. D. Taylor, D. Whiteman, C. Wijmenga, R. N. Baldassano, M. Barclay, T. M. Bayless, S. Brand, C. Buning, A. Cohen, J.-F. Colombel, M. Cottone, L. Stronati, T. Denson, M. De Vos, R. D'Inca, M. Dubinsky, C. Edwards, T. Florin, D. Franchimont, R. Geary, J. Glas, A. Van Gossum, S. L. Guthery, J. Halfvarson, H. W. Verspaget, J.-P. Hugot, A. Karban, D. Laukens, I. Lawrance, M. Lemann, A. Levine, C. Libioulle, E. Louis, C. Mowat, W. Newman, J. Panes, A. Phillips, D. D. Proctor, M. Regueiro, R. Russell, P. Rutgeerts, J. Sanderson, M. Sans, F. Seibold, A. H. Steinhardt, P. C. F. Stokkers, L. Torkvist, G. Kullak-Ublick, D. Wilson, T. Walters, S. R. Targan, S. R. Brant, J. D. Rioux, M. D'Amato, R. K. Weersma, S. Kugathasan, A. M. Griffiths, J. C. Mansfield, S. Vermeire, R. H. Duerr, M. S. Silverberg, J. Satsangi, S. Schreiber, J. H. Cho, V. Annese, H. Hakonarson, M. J. Daly and M. Parkes (2010). "Genome-wide meta-analysis increases to 71 the number of confirmed Crohn's disease susceptibility loci." *Nat Genet* **42**(12): 1118-1125.

Funderburg, N. T., S. R. Stubblefield Park, H. C. Sung, G. Hardy, B. Clagett, J. Ignatz-Hoover, C. V. Harding, P. Fu, J. A. Katz, M. M. Lederman and A. D. Levine (2013). "Circulating CD4(+) and CD8(+) T cells are activated in inflammatory bowel disease and are associated with plasma markers of inflammation." *Immunology* **140**(1): 87-97.

Fuschillo, S., A. De Felice and G. Balzano (2008). "Mucosal inflammation in idiopathic bronchiectasis: cellular and molecular mechanisms." *Eur Respir J* **31**(2): 396-406.

Fuss, I. J., M. Neurath, M. Boirivant, J. S. Klein, C. de la Motte, S. A. Strong, C. Fiocchi and W. Strober (1996). "Disparate CD4+ lamina propria (LP) lymphokine secretion profiles in inflammatory bowel disease. Crohn's disease LP cells manifest increased secretion of IFN-gamma, whereas ulcerative colitis LP cells manifest increased secretion of IL-5." *J Immunol* **157**(3): 1261-1270.

Gadek-Michalska, A., J. Tadeusz, P. Rachwalska and J. Bugajski (2013). "Cytokines, prostaglandins and nitric oxide in the regulation of stress-response systems." *Pharmacol Rep* **65**(6): 1655-1662.

Gaffen, S. L. (2008). "An Overview of IL-17 Function and Signaling." *Cytokine* **43**(3): 402-407.

Garcia, C. C., R. C. Russo, R. Guabiraba, C. T. Fagundes, R. B. Polidoro, L. P. Tavares, A. P. C. Salgado, G. D. Cassali, L. P. Sousa, A. V. Machado and M. M. Teixeira (2010). "Platelet-Activating Factor Receptor Plays a Role in Lung Injury and Death Caused by Influenza A in Mice." *PLoS Pathog* **6**(11): e1001171.

Glick, D., S. Barth and K. F. Macleod (2010). "Autophagy: cellular and molecular mechanisms." *The Journal of pathology* **221**(1): 3-12.

Graff, L. A., J. R. Walker and C. N. Bernstein (2009). "Depression and anxiety in inflammatory bowel disease: a review of comorbidity and management." *Inflamm Bowel Dis* **15**(7): 1105-1118.

Grivennikov, S., E. Karin, J. Terzic, D. Mucida, G.-Y. Yu, S. Vallabhapurapu, J. Scheller, S. Rose-John, H. Cheroutre, L. Eckmann and M. Karin (2009). "IL-6 and Stat3 Are Required for Survival of Intestinal Epithelial Cells and Development of Colitis-Associated Cancer." *Cancer Cell* **15**(2): 103-113.

Han, S. H., J. H. Kim, H. S. Seo, M. H. Martin, G.-H. Chung, S. M. Michalek and M. H. Nahm (2006). "Lipoteichoic Acid-Induced Nitric Oxide Production Depends on the Activation of Platelet-Activating Factor Receptor and Jak2." *Journal of immunology (Baltimore, Md. : 1950)* **176**(1): 573-579.

Han, S. J., H. M. Ko, J. H. Choi, K. H. Seo, H. S. Lee, E. K. Choi, I. W. Choi, H. K. Lee and S. Y. Im (2002). "Molecular mechanisms for lipopolysaccharide-induced biphasic activation of nuclear factor-kappa B (NF-kappa B)." *J Biol Chem* **277**(47): 44715-44721.

Hasegawa, S., Y. Kohro, M. Shiratori, S. Ishii, T. Shimizu, M. Tsuda and K. Inoue (2010). "Role of PAF Receptor in Proinflammatory Cytokine Expression in the Dorsal Root Ganglion and Tactile Allodynia in a Rodent Model of Neuropathic Pain." *PLoS ONE* **5**(5): e10467.

Hatoum, O. A., K. M. Gauthier, D. G. Binion, H. Miura, G. Telford, M. F. Otterson, W. B. Campbell and D. D. Gutterman (2005). "Novel mechanism of vasodilation in inflammatory bowel disease." *Arterioscler Thromb Vasc Biol* **25**(11): 2355-2361.

Head, K. A. and J. S. Jurenka (2003). "Inflammatory bowel disease Part 1: ulcerative colitis-- pathophysiology and conventional and alternative treatment options." *Altern Med Rev* **8**(3): 247-283.

Heazlewood, C. K., M. C. Cook, R. Eri, G. R. Price, S. B. Tauro, D. Taupin, D. J. Thornton, C. W. Png, T. L. Crockford, R. J. Cornall, R. Adams, M. Kato, K. A. Nelms, N. A. Hong, T. H. J. Florin, C. C. Goodnow and M. A. McGuckin (2008). "Aberrant Mucin Assembly in Mice Causes Endoplasmic Reticulum Stress and Spontaneous Inflammation Resembling Ulcerative Colitis." *PLoS Medicine* **5**(3): e54.

Heinrich, P. C., I. Behrmann, G. Müller-Newen, F. Schaper and L. Graeve (1998). "Interleukin-6-type cytokine signalling through the gp130/Jak/STAT pathway." *Biochemical Journal* **334**(Pt 2): 297-314.

Held, T. K., X. Weihua, L. Yuan, D. V. Kalvakolanu and A. S. Cross (1999). "Gamma interferon augments macrophage activation by lipopolysaccharide by two distinct mechanisms, at the signal transduction level and via an autocrine mechanism involving tumor necrosis factor alpha and interleukin-1." *Infect Immun* **67**(1): 206-212.

Hendrickson, B. A., R. Gokhale and J. H. Cho (2002). "Clinical Aspects and Pathophysiology of Inflammatory Bowel Disease." *Clinical Microbiology Reviews* **15**(1): 79-94.

Hering, N. A., M. Fromm and J. D. Schulzke (2012). "Determinants of colonic barrier function in inflammatory bowel disease and potential therapeutics." *J Physiol* **590**(Pt 5): 1035-1044.

Herrlinger, K. R., M. K. Noftz, K. Dalhoff, D. Ludwig, E. F. Stange and K. Fellermann (2002). "Alterations in pulmonary function in inflammatory bowel disease are frequent and persist during remission." *Am J Gastroenterol* **97**(2): 377-381.

Hill, A. T., D. L. Bayley, E. J. Campbell, S. L. Hill and R. A. Stockley (2000). "Airways inflammation in chronic bronchitis: the effects of smoking and alpha1-antitrypsin deficiency." *Eur Respir J* **15**(5): 886-890.

Hirayama, K., Y. Yokoi, T. Sakaguchi, T. Nakamura, H. Kashiwabara, K. Sunayama and S. Nakamura (2003). "Platelet-activating factor, a critical mediator in the pathogenesis of dextran sulfate sodium-induced colitis in rats." *Dis Colon Rectum* **46**(1): 100-110.

Hocke, M., L. Richter, H. Bosseckert and K. Eitner (1999). "Platelet activating factor in stool from patients with ulcerative colitis and Crohn's disease." *Hepatogastroenterology* **46**(28): 2333-2337.

Hogg, J. C. (2004). "Pathophysiology of airflow limitation in chronic obstructive pulmonary disease." *The Lancet* **364**(9435): 709-721.

Hogg, J. C. and C. M. Doerschuk (1995). "Leukocyte traffic in the lung." *Annu Rev Physiol* **57**: 97-114.

Hoidal, J. R. (1994). "Pathogenesis of chronic bronchitis." *Semin Respir Infect* **9**(1): 8-12.

Hooper, L. V., D. R. Littman and A. J. Macpherson (2012). "Interactions between the microbiota and the immune system." *Science* **336**(6086): 1268-1273.

Horvat, J. C., K. W. Beagley, M. A. Wade, J. A. Preston, N. G. Hansbro, D. K. Hickey, G. E. Kaiko, P. G. Gibson, P. S. Foster and P. M. Hansbro (2007). "Neonatal chlamydial infection induces mixed T-cell responses that drive allergic airway disease." *Am J Respir Crit Care Med* **176**(6): 556-564.

Hotermans, G., A. Benard, H. Guenanen, G. Demarcq-Delerue, T. Malart and B. Wallaert (1996). "Nongranulomatous interstitial lung disease in Crohn's disease." *Eur Respir J* **9**(2): 380-382.

Huang, W. C., S. J. Wu, R. S. Tu, Y. R. Lai and C. J. Liou (2015). "Phloretin inhibits interleukin-1beta-induced COX-2 and ICAM-1 expression through inhibition of MAPK, Akt, and NF-kappaB signaling in human lung epithelial cells." *Food Funct* **6**(6): 1960-1967.

Ishii, S., T. Kuwaki, T. Nagase, K. Maki, F. Tashiro, S. Sunaga, W. H. Cao, K. Kume, Y. Fukuchi, K. Ikuta, J. Miyazaki, M. Kumada and T. Shimizu (1998). "Impaired anaphylactic responses with intact sensitivity to endotoxin in mice lacking a platelet-activating factor receptor." *J Exp Med* **187**(11): 1779-1788.

Ishii, S., Y. Matsuda, M. Nakamura, I. Waga, K. Kume, T. Izumi and T. Shimizu (1996). "A murine platelet-activating factor receptor gene: cloning, chromosomal localization and up-regulation of expression by lipopolysaccharide in peritoneal resident macrophages." *Biochemical Journal* **314**(Pt 2): 671-678.

Ishii, S., T. Nagase and T. Shimizu (2002). "Platelet-activating factor receptor." *Prostaglandins Other Lipid Mediat* **68-69**: 599-609.

Ishii, S. and T. Shimizu (2000). "Platelet-activating factor (PAF) receptor and genetically engineered PAF receptor mutant mice." *Prog Lipid Res* **39**(1): 41-82.

Ito, H., M. Takazoe, Y. Fukuda, T. Hibi, K. Kusugami, A. Andoh, T. Matsumoto, T. Yamamura, J. Azuma, N. Nishimoto, K. Yoshizaki, T. Shimoyama and T. Kishimoto (2004). "A Pilot Randomized Trial of a Human Anti-Interleukin-6 Receptor Monoclonal Antibody in Active Crohn's Disease." *Gastroenterology* **126**(4): 989-996.

Jagels, M. A., J. D. Chambers, K. E. Arfors and T. E. Hugli (1995). "C5a- and tumor necrosis factor-alpha-induced leukocytosis occurs independently of beta 2 integrins and L-selectin: differential effects on neutrophil adhesion molecule expression in vivo." *Blood* **85**(10): 2900-2909.

Jagels, M. A. and T. E. Hugli (1992). "Neutrophil chemotactic factors promote leukocytosis. A common mechanism for cellular recruitment from bone marrow." *J Immunol* **148**(4): 1119-1128.

Karlinger, K., T. Gyorke, E. Mako, A. Mester and Z. Tarjan (2000). "The epidemiology and the pathogenesis of inflammatory bowel disease." *Eur J Radiol* **35**(3): 154-167.

Kawai, T. and S. Akira (2011). "Toll-like Receptors and Their Crosstalk with Other Innate Receptors in Infection and Immunity." *Immunity* **34**(5): 637-650.

Kawamoto, H. and N. Minato (2004). "Myeloid cells." *Int J Biochem Cell Biol* **36**(8): 1374-1379.

Keely, S., E. L. Campbell, A. W. Baird, P. M. Hansbro, R. A. Shalwitz, A. Kotsakis, E. N. McNamee, H. K. Eltzschig, D. J. Kominsky and S. P. Colgan (2014). "Contribution of epithelial innate immunity to systemic protection afforded by prolyl hydroxylase inhibition in murine colitis." *Mucosal Immunol* **7**(1): 114-123.

Kelly, C. J., L. Zheng, E. L. Campbell, B. Saeedi, C. C. Scholz, A. J. Bayless, K. E. Wilson, L. E. Glover, D. J. Kominsky, A. Magnuson, T. L. Weir, S. F. Ehrentraut, C. Pickel, K. A. Kuhn, J. M. Lanis, V. Nguyen, C. T. Taylor and S. P. Colgan (2015). "Crosstalk between Microbiota-Derived Short-Chain Fatty Acids and Intestinal Epithelial HIF Augments Tissue Barrier Function." *Cell Host Microbe* **17**(5): 662-671.

Kim, J. J., M. S. Shajib, M. M. Manocha and W. I. Khan (2012). "Investigating Intestinal Inflammation in DSS-induced Model of IBD." *Journal of Visualized Experiments : JoVE*(60): 3678.

Kim, Y.-G., K. G. S. Udayanga, N. Totsuka, J. B. Weinberg, G. Núñez and A. Shibuya (2014). "Gut dysbiosis promotes M2 macrophage polarization and allergic airway inflammation via fungi-induced PGE(2)." *Cell host & microbe* **15**(1): 95-102.

King, P. T. (2009). "The pathophysiology of bronchiectasis." *International Journal of Chronic Obstructive Pulmonary Disease* **4**: 411-419.

Kitajima, S., S. Takuma and M. Morimoto (1999). "Tissue distribution of dextran sulfate sodium (DSS) in the acute phase of murine DSS-induced colitis." *J Vet Med Sci* **61**(1): 67-70.

Koek, G. H., G. M. Verleden, P. Evenepoel and P. Rutgeerts (2002). "Activity related increase of exhaled nitric oxide in Crohn's disease and ulcerative colitis: a manifestation of systemic involvement?" *Respir Med* **96**(7): 530-535.

Krenke, K., J. Peradzynska, J. Lange, A. Banaszkiwicz, I. Lazowska-Przeorek, K. Grzela, A. Radzikowski and M. Kulus (2014). "Inflammatory cytokines in exhaled breath condensate in children with inflammatory bowel diseases." *Pediatr Pulmonol* **49**(12): 1190-1195.

Lakatos, P. L., T. Szamosi and L. Lakatos (2007). "Smoking in inflammatory bowel diseases: good, bad or ugly?" *World J Gastroenterol* **13**(46): 6134-6139.

Laroui, H., S. A. Ingersoll, H. C. Liu, M. T. Baker, S. Ayyadurai, M. A. Charania, F. Laroui, Y. Yan, S. V. Sitaraman and D. Merlin (2012). "Dextran Sodium Sulfate (DSS) Induces Colitis in Mice by Forming Nano-Lipocomplexes with Medium-Chain-Length Fatty Acids in the Colon." *PLoS ONE* **7**(3): e32084.

Latz, E., T. S. Xiao and A. Stutz (2013). "Activation and regulation of the inflammasomes." *Nature reviews. Immunology* **13**(6): 10.1038/nri3452.

Lee, H. Y., S. Y. Lee, S. D. Kim, J. W. Shim, H. J. Kim, Y. S. Jung, J. Y. Kwon, S. H. Baek, J. Chung and Y. S. Bae (2011). "Sphingosylphosphorylcholine stimulates CCL2 production from human umbilical vein endothelial cells." *J Immunol* **186**(7): 4347-4353.

Lee, J. S., C. M. Tato, B. Joyce-Shaikh, M. F. Gulen, C. Cayatte, Y. Chen, W. M. Blumenschein, M. Judo, G. Ayanoglu, T. K. McClanahan, X. Li and D. J. Cua (2015). "Interleukin-23-Independent IL-17 Production Regulates Intestinal Epithelial Permeability." *Immunity* **43**(4): 727-738.

Levine, J. S. and R. Burakoff (2011). "Extraintestinal manifestations of inflammatory bowel disease." *Gastroenterol Hepatol (N Y)* **7**(4): 235-241.

Liu, F., J. Poursine-Laurent, H. Y. Wu and D. C. Link (1997). "Interleukin-6 and the granulocyte colony-stimulating factor receptor are major independent regulators of granulopoiesis in vivo but are not required for lineage commitment or terminal differentiation." *Blood* **90**(7): 2583-2590.

Liu, J. Z., J. R. Hov, T. Folseraas, E. Ellinghaus, S. M. Rushbrook, N. T. Doncheva, O. A. Andreassen, R. K. Weersma, T. J. Weismuller, B. Eksteen, P. Invernizzi, G. M. Hirschfield, D. N. Gotthardt, A. Pares, D. Ellinghaus, T. Shah, B. D. Juran, P. Milkiewicz, C. Rust, C. Schramm, T. Muller, B. Srivastava, G. Dalekos, M. M. Nothen, S. Herms, J. Winkelmann, M. Mitrovic, F. Braun, C. Y. Ponsioen, P. J. Croucher, M. Sterneck, A. Teufel, A. L. Mason, J. Saarela, V. Leppa, R. Dorfman, D. Alvaro, A. Floreani, S. Onengut-Gumuscu, S. S. Rich, W. K. Thompson, A. J. Schork, S. Naess, I. Thomsen, G. Mayr, I. R. Konig, K. Hveem, I. Cleyne, J. Gutierrez-Achury, I. Ricano-Ponce, D. van Heel, E. Bjornsson, R. N. Sandford, P. R. Durie, E. Melum, M. H. Vatn, M. S. Silverberg, R. H. Duerr, L. Padyukov, S. Brand, M. Sans, V. Annesse, J. P. Achkar, K. M. Boberg, H. U. Marschall, O. Chazouilleres, C. L. Bowlus, C. Wijmenga, E. Schrupf, S. Vermeire, M. Albrecht, J. D. Rioux, G. Alexander, A. Bergquist, J. Cho, S. Schreiber, M. P. Manns, M. Farkkila, A. M. Dale, R. W. Chapman, K. N. Lazaridis, A. Franke, C. A. Anderson and T. H. Karlsen (2013). "Dense genotyping of immune-related disease regions identifies nine new risk loci for primary sclerosing cholangitis." *Nat Genet* **45**(6): 670-675.

Liu, J. Z., S. van Sommeren, H. Huang, S. C. Ng, R. Alberts, A. Takahashi, S. Ripke, J. C. Lee, L. Jostins, T. Shah, S. Abedian, J. H. Cheon, J. Cho, N. E. Daryani, L. Franke, Y. Fuyuno, A. Hart, R. C. Juyal, G. Juyal, W. H. Kim, A. P. Morris, H. Poustchi, W. G. Newman, V. Midha, T. R. Orchard, H. Vahedi, A. Sood, J. J. Sung, R. Malekzadeh, H. J. Westra, K. Yamazaki, S. K. Yang, J. C. Barrett, A. Franke, B. Z. Alizadeh, M. Parkes, K. T. B. M. J. Daly, M. Kubo, C. A. Anderson and R. K. Weersma (2015). "Association analyses identify 38 susceptibility loci for inflammatory bowel disease and highlight shared genetic risk across populations." *Nat Genet* **47**(9): 979-986.

Liu, Y., X.-Y. Wang, X. Yang, S. Jing, L. Zhu and S.-H. Gao (2013). "Lung and Intestine: A Specific Link in an Ulcerative Colitis Rat Model." Gastroenterology Research and Practice **2013**: 124530.

Loftus, E. V., G. C. Harewood, C. G. Loftus, W. J. Tremaine, W. S. Harmsen, A. R. Zinsmeister, D. A. Jewell and W. J. Sandborn (2005). "PSC-IBD: a unique form of inflammatory bowel disease associated with primary sclerosing cholangitis." Gut **54**(1): 91-96.

Loftus, E. V., Jr. (2004). "Clinical epidemiology of inflammatory bowel disease: Incidence, prevalence, and environmental influences." Gastroenterology **126**(6): 1504-1517.

Lopez-Castejon, G. and D. Brough (2011). "Understanding the mechanism of IL-1 β secretion." Cytokine & Growth Factor Reviews **22**(4): 189-195.

Lopez de Castro, J. A. (2007). "HLA-B27 and the pathogenesis of spondyloarthropathies." Immunol Lett **108**(1): 27-33.

Loukides, S., I. Horvath, T. Wodehouse, P. J. Cole and P. J. Barnes (1998). "Elevated levels of expired breath hydrogen peroxide in bronchiectasis." Am J Respir Crit Care Med **158**(3): 991-994.

Malerba, M., B. Ragnoli, L. Buffoli, A. Radaeli, C. Ricci, F. Lanzarotto and A. Lanzini (2011). "Exhaled nitric oxide as a marker of lung involvement in Crohn's disease." Int J Immunopathol Pharmacol **24**(4): 1119-1124.

Maltby, S., N. G. Hansbro, H. L. Tay, J. Stewart, M. Plank, B. Donges, H. F. Rosenberg and P. S. Foster (2014). "Production and differentiation of myeloid cells driven by proinflammatory cytokines in response to acute pneumovirus infection in mice." J Immunol **193**(8): 4072-4082.

Marks, E., B. J. Goggins, J. Cardona, S. Cole, K. Minahan, S. Mateer, M. M. Walker, R. Shalwitz and S. Keely (2015). "Oral delivery of prolyl hydroxylase inhibitor: AKB-4924 promotes localized mucosal healing in a mouse model of colitis." Inflamm Bowel Dis **21**(2): 267-275.

Marteau, P. and U. Chaput (2011). "Bacteria as trigger for chronic gastrointestinal disorders." Dig Dis **29**(2): 166-171.

Marvisi, M., P. D. Borrello, M. Brianti, G. Fornarsari, G. Marani and A. Guariglia (2000). "Changes in the carbon monoxide diffusing capacity of the lung in ulcerative colitis." Eur Respir J **16**(5): 965-968.

Matsuguchi, T., T. Musikachoen, T. Ogawa and Y. Yoshikai (2000). "Gene expressions of Toll-like receptor 2, but not Toll-like receptor 4, is induced by LPS and inflammatory cytokines in mouse macrophages." J Immunol **165**(10): 5767-5772.

Matsumura, T., A. Ito, T. Takii, H. Hayashi and K. Onozaki (2000). "Endotoxin and cytokine regulation of toll-like receptor (TLR) 2 and TLR4 gene expression in murine liver and hepatocytes." J Interferon Cytokine Res **20**(10): 915-921.

McCarthy, D. A., D. S. Rampton and Y. C. Liu (1991). "Peripheral blood neutrophils in inflammatory bowel disease: morphological evidence of in vivo activation in active disease." Clin Exp Immunol **86**(3): 489-493.

McCullers, J. A. and J. E. Rehg (2002). "Lethal synergism between influenza virus and Streptococcus pneumoniae: characterization of a mouse model and the role of platelet-activating factor receptor." J Infect Dis **186**(3): 341-350.

McLoughlin, R. M., J. Witowski, R. L. Robson, T. S. Wilkinson, S. M. Hurst, A. S. Williams, J. D. Williams, S. Rose-John, S. A. Jones and N. Topley (2003). "Interplay between IFN-gamma and IL-6 signaling governs neutrophil trafficking and apoptosis during acute inflammation." J Clin Invest **112**(4): 598-607.

Meenan, J., T. A. Grool, D. W. Hommes, S. Dijkhuizen, F. J. ten Kate, M. Wood, M. Whittaker, G. N. Tytgat and S. J. van Deventer (1996). "Lexipafant (BB-882), a platelet activating factor receptor antagonist, ameliorates mucosal inflammation in an animal model of colitis." Eur J Gastroenterol Hepatol **8**(6): 569-573.

Mitchell, Michael J., Kimberly S. Lin and Michael R. King (2014). "Fluid Shear Stress Increases Neutrophil Activation via Platelet-Activating Factor." Biophysical Journal **106**(10): 2243-2253.

Mohamed-Hussein, A. A. R., N. A. S. Mohamed and M.-E. A. R. Ibrahim (2007). "Changes in pulmonary function in patients with ulcerative colitis." Respiratory Medicine **101**(5): 977-982.

Molodecky, N. A., I. S. Soon, D. M. Rabi, W. A. Ghali, M. Ferris, G. Chernoff, E. I. Benchimol, R. Panaccione, S. Ghosh, H. W. Barkema and G. G. Kaplan (2012). "Increasing Incidence and Prevalence of the Inflammatory Bowel Diseases With Time, Based on Systematic Review." Gastroenterology **142**(1): 46-54.e42.

Molodecky, N. A., I. S. Soon, D. M. Rabi, W. A. Ghali, M. Ferris, G. Chernoff, E. I. Benchimol, R. Panaccione, S. Ghosh, H. W. Barkema and G. G. Kaplan (2012). "Increasing incidence and prevalence of the inflammatory bowel diseases with time, based on systematic review." Gastroenterology **142**(1): 46-54 e42; quiz e30.

Montrucchio, G., G. Alloatti and G. Camussi (2000). "Role of Platelet-Activating Factor in Cardiovascular Pathophysiology." Physiological Reviews **80**(4): 1669-1699.

Moreno, S. E., J. C. Alves-Filho, F. Rios-Santos, J. S. Silva, S. H. Ferreira, F. Q. Cunha and M. M. Teixeira (2006). "Signaling via platelet-activating factor receptors accounts for the impairment of neutrophil migration in polymicrobial sepsis." J Immunol **177**(2): 1264-1271.

Mosser, D. M. (2003). "The many faces of macrophage activation." Journal of Leukocyte Biology **73**(2): 209-212.

Mow, W. S., E. A. Vasiliauskas, Y. C. Lin, P. R. Fleshner, K. A. Papadakis, K. D. Taylor, C. J. Landers, M. T. Abreu-Martin, J. I. Rotter, H. Yang and S. R. Targan (2004). "Association of antibody responses to microbial antigens and complications of small bowel Crohn's disease." Gastroenterology **126**(2): 414-424.

Mowat, A. M. (2003). "Anatomical basis of tolerance and immunity to intestinal antigens." Nat Rev Immunol **3**(4): 331-341.

Munakata, M. (2012). "Exhaled Nitric Oxide (FeNO) as a Non-Invasive Marker of Airway Inflammation." Allergology International **61**(3): 365-372.

Naito, Y., T. Takagi, K. Uchiyama, M. Kuroda, S. Kokura, H. Ichikawa, R. Yanagisawa, K. Inoue, H. Takano, M. Satoh, N. Yoshida, T. Okanou and T. Yoshikawa (2004). "Reduced intestinal inflammation induced by dextran sodium sulfate in interleukin-6-deficient mice." Int J Mol Med **14**(2): 191-196.

Netea, M. G., B. J. Kullberg and J. W. M. Van der Meer (2000). "Circulating Cytokines as Mediators of Fever." Clinical Infectious Diseases **31**(Supplement 5): S178-S184.

Neurath, M. F. (2014). "Cytokines in inflammatory bowel disease." Nat Rev Immunol **14**(5): 329-342.

Neurath, M. F. and S. Finotto (2011). "IL-6 signaling in autoimmunity, chronic inflammation and inflammation-associated cancer." Cytokine Growth Factor Rev **22**(2): 83-89.

Orchard, T. R., C. N. Chua, T. Ahmad, H. Cheng, K. I. Welsh and D. P. Jewell (2002). "Uveitis and erythema nodosum in inflammatory bowel disease: clinical features and the role of HLA genes." Gastroenterology **123**(3): 714-718.

Oshikawa, K. and Y. Sugiyama (2003). "Regulation of toll-like receptor 2 and 4 gene expression in murine alveolar macrophages." Exp Lung Res **29**(6): 401-412.

Ou, M., T. Kawasaki, M. Sakon, J. Kambayashi, E. Siba, M. Yokota, K. Shinozaki and T. Mori (1991). "Simple and rapid measurement of platelet-activating factor (PAF) in whole blood." Biochem Int **24**(5): 823-831.

Ozyilmaz, E., B. Yildirim, G. Erbas, S. Akten, I. K. Oguzulgen, B. Tunc, C. Tuncer and H. Turktas (2010). "Value of fractional exhaled nitric oxide (FE NO) for the diagnosis of pulmonary involvement due to inflammatory bowel disease." Inflamm Bowel Dis **16**(4): 670-676.

Parker, T. A., H. Cheng, K. O. Willeford and S. Wu (2011). "Interleukin-6 expression in response to innate immune regulatory factor stimulation." Biomedicine & Pharmacotherapy **65**(2): 90-94.

Parkes, G. C., K. Whelan and J. O. Lindsay (2014). "Smoking in inflammatory bowel disease: impact on disease course and insights into the aetiology of its effect." J Crohns Colitis **8**(8): 717-725.

Perez-Arellano, J. L., T. Martin, J. M. Lopez-Novoa, M. L. Sanchez, A. Montero and A. Jimenez (1998). "BN 52021 (a platelet activating factor-receptor antagonist) decreases alveolar macrophage-mediated lung injury in experimental extrinsic allergic alveolitis." Mediators Inflamm **7**(3): 201-210.

Porras-Reyes, B. H. and T. A. Mustoe (1992). "Platelet-activating factor: improvement in wound healing by a chemotactic factor." Surgery **111**(4): 416-423.

Qian, Y., C. Liu, J. Hartupee, C. Z. Altuntas, M. F. Gulen, D. Jane-Wit, J. Xiao, Y. Lu, N. Giltiy, J. Liu, T. Kordula, Q. W. Zhang, B. Vallance, S. Swaidani, M. Aronica, V. K. Tuohy, T. Hamilton and X. Li (2007). "The adaptor Act1 is required for interleukin 17-dependent signaling associated with autoimmune and inflammatory disease." Nat Immunol **8**(3): 247-256.

Quinton, J. F., B. Sendid, D. Reumaux, P. Duthilleul, A. Cortot, B. Grandbastien, G. Charrier, S. R. Targan, J. F. Colombel and D. Poulain (1998). "Anti-Saccharomyces cerevisiae mannan antibodies combined with antineutrophil cytoplasmic autoantibodies in inflammatory bowel disease: prevalence and diagnostic role." Gut **42**(6): 788-791.

Ranu, H., M. Wilde and B. Madden (2011). "Pulmonary Function Tests." The Ulster Medical Journal **80**(2): 84-90.

Reichel, C. A., M. Rehberg, M. Lerchenberger, N. Berberich, P. Bihari, A. G. Khandoga, S. Zahler and F. Krombach (2009). "Ccl2 and Ccl3 mediate neutrophil recruitment via induction of protein synthesis and generation of lipid mediators." Arterioscler Thromb Vasc Biol **29**(11): 1787-1793.

Rogers, B. H., L. M. Clark and J. B. Kirsner (1971). "The epidemiologic and demographic characteristics of inflammatory bowel disease: an analysis of a computerized file of 1400 patients." J Chronic Dis **24**(12): 743-773.

Rossol, M., M. Pierer, N. Raulien, D. Quandt, U. Meusch, K. Rothe, K. Schubert, T. Schoneberg, M. Schaefer, U. Krugel, S. Smajilovic, H. Brauner-Osborne, C. Baerwald and U. Wagner (2012). "Extracellular Ca²⁺ is a danger signal activating the NLRP3 inflammasome through G protein-coupled calcium sensing receptors." Nat Commun **3**: 1329.

Saetta, M., A. Di Stefano, G. Turato, F. M. Facchini, L. Corbino, C. E. Mapp, P. Maestrelli, A. Ciaccia and L. M. Fabbri (1998). "CD8+ T-lymphocytes in peripheral airways of smokers with chronic obstructive pulmonary disease." Am J Respir Crit Care Med **157**(3 Pt 1): 822-826.

Sander, L. E., F. Obermeier, U. Dierssen, D. C. Kroy, A. K. Singh, U. Seidler, K. L. Streetz, H. H. Lutz, W. Muller, F. Tacke and C. Trautwein (2008). "Gp130 signaling promotes development of acute experimental colitis by facilitating early neutrophil/macrophage recruitment and activation." J Immunol **181**(5): 3586-3594.

Sarioglu, N., N. Turkel, A. Sakar, P. Celik, M. Saruc, M. A. Demir, C. Goktan, C. Kirmaz, H. Yuceyar and A. Yorgancioglu (2006). "Lung involvement in inflammatory bowel diseases." Ann Saudi Med **26**(5): 407-408.

Sarra, M., F. Pallone, T. T. Macdonald and G. Monteleone (2010). "IL-23/IL-17 axis in IBD." Inflamm Bowel Dis **16**(10): 1808-1813.

Sartor, R. B. (2006). "Mechanisms of disease: pathogenesis of Crohn's disease and ulcerative colitis." Nat Clin Pract Gastroenterol Hepatol **3**(7): 390-407.

Sartor, R. B. and S. K. Mazmanian (2012). "Intestinal Microbes in Inflammatory Bowel Diseases." Am J Gastroenterol Suppl **1**(1): 15-21.

Schaberg, T., H. Haller and H. Lode (1991). "Evidence for a platelet-activating factor receptor on human alveolar macrophages." Biochemical and Biophysical Research Communications **177**(2): 704-710.

Scharl, M. and G. Rogler (2012). "Inflammatory bowel disease pathogenesis: what is new?" Curr Opin Gastroenterol **28**(4): 301-309.

Scharl, M. and G. Rogler (2012). "Inflammatory bowel disease: dysfunction of autophagy?" Dig Dis **30 Suppl 3**: 12-19.

Scheffele, F. and I. J. Fuss (2002). "Induction of TNBS colitis in mice." Curr Protoc Immunol **Chapter 15**: Unit 15 19.

Scheller, J., A. Chalaris, D. Schmidt-Arras and S. Rose-John (2011). "The pro- and anti-inflammatory properties of the cytokine interleukin-6." Biochimica et Biophysica Acta (BBA) - Molecular Cell Research **1813**(5): 878-888.

Schuster, D. P., M. Metzler, S. Opal, S. Lowry, R. Balk, E. Abraham, H. Levy, G. Slotman, E. Coyne, S. Souza and J. Pribble (2003). "Recombinant platelet-activating factor acetylhydrolase to prevent acute respiratory distress syndrome and mortality in severe sepsis: Phase IIb, multicenter, randomized, placebo-controlled, clinical trial." *Crit Care Med* **31**(6): 1612-1619.

Sepper, R., Y. T. Konttinen, Y. Ding, M. Takagi and T. Sorsa (1995). "Human neutrophil collagenase (MMP-8), identified in bronchiectasis BAL fluid, correlates with severity of disease." *Chest* **107**(6): 1641-1647.

Shukla, S. D., S. S. Sohal, M. Q. Mahmood, D. Reid, H. K. Muller and E. H. Walters (2014). "Airway epithelial platelet-activating factor receptor expression is markedly upregulated in chronic obstructive pulmonary disease." *Int J Chron Obstruct Pulmon Dis* **9**: 853-861.

Siddiqi, M., Z. C. Garcia, D. S. Stein, T. N. Denny and Z. Spolarics (2001). "Relationship between oxidative burst activity and CD11b expression in neutrophils and monocytes from healthy individuals: effects of race and gender." *Cytometry* **46**(4): 243-246.

Silva, J., J. Jones, P. Cole and L. Poulter (1989). "The immunological component of the cellular inflammatory infiltrate in bronchiectasis." *Thorax* **44**(8): 668-673.

Smythies, L. E., M. Sellers, R. H. Clements, M. Mosteller-Barnum, G. Meng, W. H. Benjamin, J. M. Orenstein and P. D. Smith (2005). "Human intestinal macrophages display profound inflammatory anergy despite avid phagocytic and bacteriocidal activity." *J Clin Invest* **115**(1): 66-75.

Sommer, J., E. Engelowski, P. Baran, C. Garbers, D. M. Floss and J. Scheller (2014). "Interleukin-6, but not the interleukin-6 receptor plays a role in recovery from dextran sodium sulfate-induced colitis." *Int J Mol Med* **34**(3): 651-660.

Songur, N., Y. Songur, M. Tuzun, I. Dogan, D. Tuzun, A. Ensari and B. Hekimoglu (2003). "Pulmonary function tests and high-resolution CT in the detection of pulmonary involvement in inflammatory bowel disease." *J Clin Gastroenterol* **37**(4): 292-298.

Stephens, C. J., R. M. Graham, M. J. Sturm, M. Richardson and R. R. Taylor (1993). "Variation in plasma platelet-activating factor degradation and serum lipids after acute myocardial infarction." *Coron Artery Dis* **4**(2): 187-193.

Stone, C. D. (2012). "The economic burden of inflammatory bowel disease: clear problem, unclear solution." *Dig Dis Sci* **57**(12): 3042-3044.

Strobel, S. and A. M. Mowat (1998). "Immune responses to dietary antigens: oral tolerance." *Immunology Today* **19**(4): 173-181.

Strober, W. and I. J. Fuss (2011). "Pro-Inflammatory Cytokines in the Pathogenesis of IBD." *Gastroenterology* **140**(6): 1756-1767.

Summers, C., S. M. Rankin, A. M. Condliffe, N. Singh, A. M. Peters and E. R. Chilvers (2010). "Neutrophil kinetics in health and disease." *Trends in Immunology* **31**(8): 318-324.

Taga, T. and T. Kishimoto (1997). "Gp130 and the interleukin-6 family of cytokines." *Annu Rev Immunol* **15**: 797-819.

Thoreson, R. and J. J. Cullen (2007). "Pathophysiology of inflammatory bowel disease: an overview." *Surg Clin North Am* **87**(3): 575-585.

Thurber, S. and S. Kohler (2006). "Histopathologic spectrum of erythema nodosum." *J Cutan Pathol* **33**(1): 18-26.

Tzanakis, N., D. Bouros, M. Samiou, P. Panagou, J. Mouzas, O. Manousos and N. Siafakas (1998). "Lung function in patients with inflammatory bowel disease." *Respir Med* **92**(3): 516-522.

Uhlig, S., R. Goggel and S. Engel (2005). "Mechanisms of platelet-activating factor (PAF)-mediated responses in the lung." *Pharmacol Rep* **57** Suppl: 206-221.

Vanoirbeek, J. A. J., M. Rinaldi, V. De Vooght, S. Haenen, S. Bobic, G. Gayan-Ramirez, P. H. M. Hoet, E. Verbeken, M. Decramer, B. Nemery and W. Janssens (2010). "Noninvasive and Invasive Pulmonary Function in Mouse Models of Obstructive and Restrictive Respiratory Diseases." *American Journal of Respiratory Cell and Molecular Biology* **42**(1): 96-104.

Wallace, J. L. (1988). "Release of platelet-activating factor (PAF) and accelerated healing induced by a PAF antagonist in an animal model of chronic colitis." *Can J Physiol Pharmacol* **66**(4): 422-425.

Walsh, A., J. Mabee and K. Trivedi (2011). "Inflammatory bowel disease." Prim Care **38**(3): 415-432; vii.

Wang, Z., T. Rui, M. Yang, F. Valiyeva and P. R. Kvietys (2008). "Alveolar macrophages from septic mice promote polymorphonuclear leukocyte transendothelial migration via an endothelial cell Src kinase/NADPH oxidase pathway." J Immunol **181**(12): 8735-8744.

Wardle, T. D., L. Hall and L. A. Turnberg (1996). "Platelet activating factor: release from colonic mucosa in patients with ulcerative colitis and its effect on colonic secretion." Gut **38**(3): 355-361.

Whitwell, F. (1952). "A study of the pathology and pathogenesis of bronchiectasis." Thorax **7**(3): 213-239.

Wilson, J., C. Hair, R. Knight, A. Catto-Smith, S. Bell, M. Kamm, P. Desmond, J. McNeil and W. Connell (2010). "High incidence of inflammatory bowel disease in Australia: a prospective population-based Australian incidence study." Inflamm Bowel Dis **16**(9): 1550-1556.

Winsauer, C., A. A. Kruglov, A. A. Chashchina, M. S. Drutskaya and S. A. Nedospasov (2014). "Cellular sources of pathogenic and protective TNF and experimental strategies based on utilization of TNF humanized mice." Cytokine Growth Factor Rev **25**(2): 115-123.

Yilmaz, A. (2010). "Pulmonary involvement in inflammatory bowel disease." World Journal of Gastroenterology **16**(39): 4952.

Yilmaz, A., N. Y. Demirci, D. Hoşgün, E. Üner, Y. Erdoğan, A. Gökçek and A. Çağlar (2010). "Pulmonary involvement in inflammatory bowel disease." World Journal of Gastroenterology : WJG **16**(39): 4952-4957.

Yoshida, K., R. Kondo, Q. Wang and C. M. Doerschuk (2006). "Neutrophil cytoskeletal rearrangements during capillary sequestration in bacterial pneumonia in rats." Am J Respir Crit Care Med **174**(6): 689-698.

Zenewicz, L. A., A. Antov and R. A. Flavell (2009). "CD4 T-cell differentiation and inflammatory bowel disease." Trends in molecular medicine **15**(5): 199-207.

Zielenski, J. (2000). "Genotype and phenotype in cystic fibrosis." Respiration **67**(2): 117-133.

Zindl, C. L., J.-F. Lai, Y. K. Lee, C. L. Maynard, S. N. Harbour, W. Ouyang, D. D. Chaplin and C. T. Weaver (2013). "IL-22-producing neutrophils contribute to antimicrobial defense and restitution of colonic epithelial integrity during colitis." Proceedings of the National Academy of Sciences of the United States of America **110**(31): 12768-12773.